

26725



National Library of Canada

Bibliothèque nationale du Canada

CANADIAN THESES ON MICROFICHE

THÈSES CANADIENNES SUR MICROFICHE

NAME OF AUTHOR NOM DE L'AUTEUR \_\_\_\_\_

TITLE OF THESIS TITRE DE LA THÈSE \_\_\_\_\_

UNIVERSITY UNIVERSITÉ \_\_\_\_\_

DEGREE FOR WHICH THESIS WAS PRESENTED  
GRADE POUR LEQUEL CETTE THÈSE FUT PRÉSENTÉE \_\_\_\_\_

YEAR THIS DEGREE CONFERRED ANNÉE D'OBTENTION DE CE GRADE \_\_\_\_\_

NAME OF SUPERVISOR NOM DU DIRECTEUR DE THÈSE \_\_\_\_\_

Permission is hereby granted to the NATIONAL LIBRARY OF CANADA to microfilm this thesis and to lend or sell copies of the film.

*L'autorisation est, par la présente, accordée à la BIBLIOTHÈQUE NATIONALE DU CANADA de microfilmer cette thèse et de prêter ou de vendre des exemplaires du film.*

The author reserves other publication rights, and neither the thesis nor extensive extracts from it may be printed or otherwise reproduced without the author's written permission.

*L'auteur se réserve les autres droits de publication ni la thèse ni de longs extraits de celle-ci ne doivent être imprimés ou autrement reproduits sans l'autorisation écrite de l'auteur.*

DATED DATE \_\_\_\_\_ SIGNED SIGNÉ \_\_\_\_\_

PERMANENT ADDRESS RÉSIDENCE FIXÉE \_\_\_\_\_

\_\_\_\_\_

\_\_\_\_\_

\_\_\_\_\_

UNIVERSITY OF ALBERTA

AN APPLICATION OF  
SELF-TUNING REGULATORS

BY

FRANCIS L.Y. CHANG



A THESIS

SUBMITTED TO THE FACULTY OF GRADUATE STUDIES AND RESEARCH  
IN PARTIAL FULFILMENT OF THE REQUIREMENTS FOR THE DEGREE  
OF MASTER OF SCIENCE

IN

PROCESS CONTROL (CHEMICAL ENGINEERING)

DEPARTMENT OF CHEMICAL ENGINEERING

EDMONTON, ALBERTA

FALL, 1975

UNIVERSITY OF ALBERTA  
FACULTY OF GRADUATE STUDIES AND RESEARCH

The undersigned certify that they have read, and recommend to the Faculty of Graduate Studies and Research, for acceptance, a thesis entitled AN APPLICATION OF SELF-TUNING REGULATORS submitted by Francis L.Y. Chang, B.Sc., in partial fulfilment of the requirements for the degree of Master of Science.

*[Handwritten Signature]*  
.....  
(Supervisor)

.....

*[Handwritten Signature]*  
.....

*[Handwritten Signature]*  
.....

Date ..... 19 .....

## ABSTRACT

This thesis presents an application of a self-tuning regulator to a pilot plant double effect evaporator. A digital computer simulation study was performed to investigate the effects of several design parameters and non-ideal operating conditions on the performance of the regulator. Experimental runs were then made using an IBM 1800 process control computer to evaluate the performance of the self-tuning regulator and to verify the simulation results.

The digital simulation results revealed that the self-tuning regulator performed better than a conventional controller when process noise and unmeasured disturbances were considered. They also demonstrated that the regulator can generate a satisfactory set of control parameters even though poor initial estimates are used. The effects of using different design parameters in the self-tuning regulator were studied and the results demonstrate that the regulator gives satisfactory control even for a poor set of design parameters. It was also found that the initial values of the design parameters can often be improved after examining the output response, the control variable response, and the parameter estimates.

In general, the experimental application was successful even though some difficulties were encountered in the experimental runs for conditions that were similar to those used in the simulation study. This was due to the interactions with other control loops in the evaporator system. The controller gains in the level control loops had to be decreased before the self-tuning regulator would function properly. To summarize, the performance characteristics of the self-tuning regulator were similar in both simulation and experimental

studies and the successful application of the regulator to the  
evaporator system was demonstrated.

## ACKNOWLEDGEMENTS

The author wishes to thank his thesis supervisor, Dr. D.E. Seborg, for his guidance and assistance in this project.

Thanks also go to Dr. D.G. Fisher for his helpful suggestions and the Data Acquisition, Control, and Simulation Centre staff for their assistance in the use of their computing facilities.

The author would also like to thank his fellow control students for their advice and helpful comments throughout this study.

Financial support was generously given by the National Research Council.

## TABLE OF CONTENTS

	<u>Page</u>
CHAPTER ONE, INTRODUCTION	
1.1 Objectives of the Study	2
1.2 Structure of the Thesis	2
CHAPTER TWO, MINIMUM VARIANCE AND SELF-TUNING REGULATORS	
2.1 Introduction	4
2.2 Literature Survey	4
2.2.1 Basic Theory	6
2.2.2 Modifications and Extensions	10
2.2.3 Industrial Applications	11
2.3 Minimum Variance Regulator	12
2.4 Self-Tuning Regulator	16
2.5 Numerical Example	20
2.5.1 Derivation of Minimum Variance Regulator	21
2.5.2 Typical Simulation Results	22
CHAPTER THREE, STOCHASTIC EVAPORATOR MODELS AND DIGITAL SIMULATION STUDY	
3.1 Introduction	32
3.2 Description of the Evaporator System	32
3.2.1 Stochastic State Space Model	34
3.2.2 Derivation of the Stochastic Pulse Transfer Function Models	36
3.2.3 Minimum Variance Regulator for the Evaporator	42
3.3 Computer Program for the Simulation Study	42

	<u>Page</u>
3.4 Open Loop Results	44
3.4.1 Effect of Process Noise	46
3.4.2 Effect of Unmeasured Step Disturbances	46
3.5 Conventional Multi-loop Control	49
3.5.1 Magnitude of Proportional Gain in Steam-Product Concentration Loop	49
3.5.2 Effect of Step Disturbances	50
3.5.3 Effect of Measurement Noise	54
3.6 Conclusions	55

CHAPTER FOUR, A SELF-TUNING REGULATOR FOR THE DOUBLE EFFECT  
EVAPORATOR: SIMULATION RESULTS

4.1 Introduction	57
4.2 Base Case Conditions	59
4.3 Initial Constants and Parameters for the Self- Tuning Algorithm	66
4.3.1 Exponential Forgetting Factor $\mu$	67
4.3.2 Initial Covariance Matrix $\underline{p}(0)$ and Parameter Estimates $\{\hat{\theta}_i(0)\}$	69
4.3.3 Scaling Factor $\beta_0$	74
4.3.4 Model Order $n$	77
4.3.5 System Time Delay $k$	79
4.4 Performance of the Self-Tuning Regulator Under Non-Ideal Operating Conditions	82
4.4.1 Effect of Process Noise Level $\sigma_{PN}$	82
4.4.2 Effect of Measurement Noise	82



	<u>Page</u>
4.4.3 Effect of Unmeasured Step Disturbances	90
4.5 Practical Strategies for Implementing Self-Tuning Regulators	97
4.6 Conclusions	103
 CHAPTER FIVE, SELF-TUNING REGULATOR FOR THE DOUBLE EFFECT EVAPORATOR: EXPERIMENTAL RESULTS	
5.1 Introduction	105
5.2 Experimental Procedure	105
5.3 Computer Programs for the Experimental Study	106
5.4 Experimental Evaporator Results	107
5.4.1 Conventional Multi-loop Control	109
5.4.2 Self-tuning Regulator	115
5.4.3 Practical Strategies for Implementing the Self-Tuning Regulator	137
5.5 Conclusions	140
 CHAPTER SIX, CONCLUSIONS	
6.1 Future Work	149
 NOMENCLATURE	 151
 BIBLIOGRAPHY	 156
 APPENDICES	
Chapter Three	161
Chapter Five	163

## LIST OF TABLES

	<u>Page</u>	
 CHAPTER TWO		
TABLE 2.1	Recursive Least Squares Estimates of System Parameters After 300 Time Intervals	24
 CHAPTER THREE		
TABLE 3.1	Open Loop and Multi-loop Proportional Control Runs	45
 CHAPTER FOUR		
TABLE 4.1	Recursive Least Squares Estimates of Model Parameters After 120 Intervals (128 min)	60
TABLE 4.2	Recursive Least Squares Estimates of Model Parameters After 120 Intervals (128 min)	83
 CHAPTER FIVE		
TABLE 5.1	Experimental Results for Conventional Control Strategies	108
TABLE 5.2	Proportional Controller Gains	109
TABLE 5.3	Proportional and Integral Controller Constants	115
TABLE 5.4	Experimental Results for the Self-Tuning Regulator	118

## LIST OF FIGURES

		<u>Page</u>
CHAPTER TWO		
Figure 2.1	Basic Structure of Self-Tuning Regulator	8
Figure 2.2	Base case (Run No. 1134)	25
Figure 2.3	Base case except that $\mu = 0.98$ (Run No. 1185)	25
Figure 2.4	Base case except that $\hat{u}(0) = \underline{0}$ (Run No. 1137)	27
Figure 2.5	Base case except that $\underline{p}(0) = 1000 \underline{I}$ (Run No. 1188)	27
Figure 2.6	Base case except that $\beta_0 = 2.0$ (Run No. 1186)	28
Figure 2.7	Accumulated loss functions	28
Figure 2.8	Uncontrolled response and simulated closed loop response for different regulators	30
Figure 2.9	Input noise sequence and simulated closed loop inputs for different regulators	31
CHAPTER THREE		
Figure 3.1	Pilot plant double effect evaporator with a conventional multi-loop control system	33
Figure 3.2	Computer flow chart for program STR-2	43
Figure 3.3	Evaporator response (SIM/OL)	47

Figure 3.4	Evaporator response (SIM/-20% F, +20% F/OL)	48
Figure 3.5	Evaporator response (SIM/-30% CF/OL)	48
Figure 3.6	Evaporator response (SIM/ML), $K_{C2} = -4.89$	51
Figure 3.7	Evaporator response (SIM/ML), $K_{C2} = 0.0$	52
Figure 3.8	Evaporator response (SIM/ML), $K_{C2} = -20.0$	52
Figure 3.9	Evaporator response (SIM/-20% F, +20% F/ML)	53
Figure 3.10	Evaporator response (SIM/-30% CF/ML)	53
Figure 3.11	Evaporator response (SIM/ML), measurement noise included, $\sigma_{MN} = 0.05$ , $K_{C2} = -4.89$	55

## CHAPTER FOUR

Figure 4.1	Block diagram of the closed loop system: The self-tuning regulator is used to control C2 and conventional proportional controllers are used to control W1 and W2.	58
Figure 4.2	Evaporator response (SIM/STR), base case	62
Figure 4.3	Evaporator response (SIM/STR), $\beta_0$ estimated	63
Figure 4.4	Parameter estimates (SIM/STR), base case	64

Figure 4.5	Parameter estimates (SIM/STR), $\hat{\rho}_0$ estimated	64
Figure 4.6	Parameter estimates (SIM/STR), $\rho = 0.96$	68
Figure 4.7	Parameter estimates (SIM/STR), $\rho = 0.90$	68
Figure 4.8	Evaporator response (SIM/STR), $\underline{p}(0)=100 \underline{I}$	70
Figure 4.9	Evaporator response (SIM/STR), $\underline{p}(0) = \underline{I}$	70
Figure 4.10	Parameter estimates (SIM/STR), $\underline{p}(0)=100 \underline{I}$	71
Figure 4.11	Parameter estimates (STR/STR), $\underline{p}(0) = \underline{I}$	71
Figure 4.12	Evaporator response (SIM/STR), $\hat{\theta}_1(0) = 5$	72
Figure 4.13	Evaporator response (SIM/STR), $\hat{\theta}_1(0) = -10$	72
Figure 4.14	Parameter estimates (SIM/STR), $\hat{\theta}_1(0) = 5$	73
Figure 4.15	Parameter estimates (SIM/STR), $\hat{\theta}_1(0) = -10$	73
Figure 4.16	Evaporator response (SIM/STR), $\beta_0 = 0.1$	75
Figure 4.17	Evaporator response (SIM/STR), $\beta_0 = 0.001$	75
Figure 4.18	Parameter estimates (SIM/STR), $\beta_0 = 0.1$	76
Figure 4.19	Parameter estimates (SIM/STR), $\beta_0 = 0.001$	76
Figure 4.20	Evaporator response (SIM/STR), 2nd order model	78
Figure 4.21	Evaporator response (SIM/STR), 4th order model	78
Figure 4.22	Parameter estimates (SIM/STR), 2nd order model	80
Figure 4.23	Parameter estimates (SIM/STR), 4th order model	80
Figure 4.24	Evaporator response (SIM/STR), $k = 2$	81
Figure 4.25	Parameter estimates (SIM/STR), $k = 2$	81
Figure 4.26	Evaporator response (SIM/STR), $\sigma_{PN}=0.01$	84
Figure 4.27	Evaporator response (SIM/STR), $\sigma_{PN}=0.5$	85
Figure 4.28	Parameter estimates (SIM/STR), $\sigma_{PN}=0.01$	86
Figure 4.29	Parameter estimates (SIM/STR), $\sigma_{PN}=0.5$	86

Figure 4.30	Evaporator response (SIM/STR), measurement noise included, $\sigma_{PN} = 0.05$	87
Figure 4.31	Evaporator response (SIM/-20% F, +20% F/STR), $\sigma_{PN} = 0.01$	88
Figure 4.32	Parameter estimates (SIM/STR), $\sigma_{PN} = 0.05$	89
Figure 4.33	Parameter estimates (SIM/-20% F, +20% F/STR), $\sigma_{PN} = 0.01$	89
Figure 4.34	Evaporator response (SIM/-20% F, +20% F/STR)	92
Figure 4.35	Evaporator response (SIM/-30% CF/STR)	93
Figure 4.36	Parameter estimates (SIM/-20% F, +20% F/STR)	94
Figure 4.37	Parameter estimates (SIM/-30% CF/STR)	94
Figure 4.38	Evaporator response (SIM/-20% F, +20% F/STR), $\rho_o$ estimated	95
Figure 4.39	Evaporator response (SIM/-30% CF/STR), $\rho_o$ estimated	95
Figure 4.40	Parameter estimates (SIM/-20% F, +20% F/STR), $\rho_o$ estimated	96
Figure 4.41	Parameter estimates (SIM/-30% CF/STR), $\rho_o$ estimated	96
Figure 4.42	Evaporator response (SIM/-40% F, +40% F/STR), constant parameters in regulator	
Figure 4.43	Evaporator response (SIM/STR), re-initializing the regulator	100

Figure 4.44	Evaporator response (SIW/-20% F, +20% F/ML & STR)	101
Figure 4.45	Parameter estimates (SIW/STR), re-initializing the regulator	102
Figure 4.46	Parameter estimates (SIW/-20% F, +20% F/ML & STR)	102

## CHAPTER FIVE

Figure 5.1	Evaporator response (EXP/+20% F, -20% F/ML prop. control)	111
Figure 5.2	Evaporator response (EXP/-30% CF/ML prop. control)	112
Figure 5.3	Parameter estimates (EXP/+20% F, -20% F/ML prop. control)	112
Figure 5.4	Parameter estimates (EXP/-30% CF/ML prop. control)	113
Figure 5.5	Evaporator response (EXP/+20% F, -20% F/ML PI control)	114
Figure 5.6	Evaporator response (EXP/+20% F/ML PI control)	116
Figure 5.7	Evaporator response (EXP/-20% F/ML PI control)	117
Figure 5.8	Evaporator response (EXP/STR), $K_{W1} = 3.52$ , $K_{W2} = 15.8$	119
Figure 5.9	Evaporator response (EXP/STR), PI control of W1 and W2	121

	<u>Page</u>	
Figure 5.10	Parameter estimates (EXP/STR), $K_{W1} = 3.52$ , $K_{W2} = 15.$	122
Figure 5.11	Parameter estimates (EXP/STR), PI control of W1 and W2	122
Figure 5.12	Evaporator response (EXP/STR), $K_{W1} = 0.5$ , $K_{W2} = 3.0$	124
Figure 5.13	Evaporator response (EXP/+20% F, -20% F/STR), $K_{W1} = 0.5$ , $K_{W2} = 3.0$	125
Figure 5.14	Parameter estimates (EXP/STR), $K_{W1} = 0.5$ , $K_{W2} = 3.0$	126
Figure 5.15	Parameter estimates (EXP/+20% F, -20% F/STR), $K_{W1} = 0.5$ , $K_{W2} = 3.0$	126
Figure 5.16	Evaporator response (EXP/+20% F, -20% F/STR)	127
Figure 5.17	Evaporator response (EXP/-30% CF/STR)	128
Figure 5.18	Parameter estimates (EXP/+20% F, -20% F/STR)	130
Figure 5.19	Parameter estimates (EXP/-30% F/STR)	130
Figure 5.20	Evaporator response (EXP/STR), $\beta_0 = 0.1$	131
Figure 5.21	Evaporator response (EXP/STR), $\beta_0 = 0.001$	132
Figure 5.22	Parameter estimates (EXP/STR), $\beta_0 = 0.1$	133
Figure 5.23	Parameter estimates (EXP/STR), $\beta_0 = 0.001$	133
Figure 5.24	Evaporator response (EXP/+20% F, -20% F/ STR), 2nd order model	134
Figure 5.25	Evaporator response (EXP/+20% F, -20% F/ STR), 4th order model	135
Figure 5.26	Parameter estimates (EXP/+20% F, -20% F/ STR), 2nd order model	136



	<u>Page</u>	
Figure 5.27	Parameter estimates (EXP/+20% F, -20% F/ STR), 4th order model	136
Figure 5.28	Evaporator response (EXP/+20% F, -20% F/ STR), constant parameters	138
Figure 5.29	Evaporator response (EXP/ML prop. control & STR), $\beta_0 = 0.02$ , $\mu = 0.995$	139
Figure 5.30	Evaporator response (EXP/+20% F, -20% F/ML prop. control & STR), $K_{W1} = 3.52$ , $K_{W2} = 15.8$	141
Figure 5.31	Parameter estimates (EXP/ML prop. control & STR), $\beta_0 = 0.02$ , $\mu = 0.995$	142
Figure 5.32	Parameter estimates (EXP/+20% F, -20% F/ML prop. control & STR), $K_{W1} = 3.52$ , $K_{W2} = 15.8$	142

## CHAPTER ONE

### INTRODUCTION

Automatic control system design usually requires an accurate model of the system to be controlled before a suitable controller can be designed. However for many industrial processes, it is very difficult to get an accurate model because of changing process conditions and the disturbances in the system. Furthermore, even though identification schemes can be used to determine models for stationary processes, they may involve an excessive amount of plant experiments and off-line analysis. Thus an adaptive control system in which the parameters of a simple model are estimated on-line and subsequently used in the controller is very attractive for practical applications.

In the self-tuning regulator [1], the parameters of a single-input, single-output stochastic model are estimated on-line using a linear least squares recursive technique; the updated parameter estimates are then used in a minimum variance controller to calculate the control signal at each sampling instant. Very little a priori information about the process is required and the regulator can be easily implemented. This approach takes into account system time delays and can be used to control processes with slowly time varying parameters. The self-tuning regulator, as developed by Åström and Wittenmark [1] and Peterka [6], is the chief concern of this thesis.

This thesis presents an application of the self-tuning regulator to two systems: a simple stochastic model with constant but unknown parameters and the pilot plant double effect evaporator in the Department of Chemical Engineering at the University of Alberta. The evaporator application includes an extensive digital computer simulation.

plus experimental verification on the actual pilot plant.

### 1.1 Objectives of the Study

The chief objective of this thesis is to evaluate the utility of the self-tuning regulator for practical applications through simulation studies and experimental application to the pilot plant evaporator. The self-tuning-regulator has been previously studied in several simulations and industrial applications. However, most of the studies considered only single-input, single-output systems. In this thesis, the self-tuning regulator is used in the composition control loop of the evaporator which is an interacting multivariable system.

A second objective of this thesis is to investigate the effects of various design options on the performance of the self-tuning regulator, and also the effects of "realistic" process conditions. An on-line experimental application of the self-tuning regulator is desirable to verify the simulation results.

### 1.2 Structure of the Thesis

The thesis consists of three major sections. The first section, Chapter Two, begins with a literature survey and a derivation of the self-tuning algorithm. It also includes simulation results for a simple numerical example selected from the literature to illustrate the behaviour and characteristics of the self-tuning regulator. This simulation example also provides some familiarity with the design parameters of the regulator.

The second section, Chapters Three and Four, presents the simulation results for the evaporator system including the effects of

different choices of the design parameters that are used in the self-tuning regulator. These results were useful in developing practical guidelines for the choice of design parameters in the experimental study. This section also includes a description of the actual evaporator and the IBM 1800 process computer.

The third section describes the experimental application of the self-tuning regulator to the evaporator system and provides a verification of the simulation results. This material is presented in Chapter Five.

The general conclusions drawn from this investigation are summarized in Chapter Six.

## CHAPTER TWO

## MINIMUM VARIANCE AND SELF-TUNING REGULATORS

2.1 Introduction

For a single-input single-output stochastic system with known constant parameters, the corresponding minimum variance regulator can be easily derived. This regulator will have constant parameters and will minimize the output variance. However, in most industrial processes that can be represented by mathematical models, the parameters of the models are either not accurately known or are time varying due to changing process conditions. Consequently, in recent years there has been considerable interest in control strategies in which the regulator parameters can be automatically adjusted on-line to compensate for unknown process dynamics or changing operating conditions. Such a regulator is often referred to as an adaptive controller, and one class of such controllers that will be studied in detail in this thesis is the self-adjusting or self-tuning regulators proposed by Åström and Wittenmark [1]. This chapter presents a literature survey and the basic equations for the minimum variance and self-tuning regulators. Simulation results for a numerical example due to Åström and Wittenmark [1] are given at the end of the chapter.

2.2 Literature Survey

System identification techniques for different classes of mathematical models have been extensively studied in recent years. This interest is reflected in the survey papers by Åström and Eykhoff [2].

Nieman et. al. [3] and Gustavsson [4]. From an industrial viewpoint, a chief objective of process identification is to obtain better knowledge about existing plants so that their operation and control can be improved. Therefore, in many applications the purpose of identification is to develop a mathematical model that describes the process well, and can be used to design a control system for that process.

As noted in the previous section, there has been a large amount of interest in the development of adaptive control strategies which combine estimation and control and can be used on-line on a real-time, process control computer. The approach of interest in this thesis, self-tuning regulators, stems from stochastic optimal control theory. It can be shown that if the design of a control system is approached through identification then according to the "separation hypothesis" [2,8], the optimal regulator can be divided into two parts, identification of model parameters and their incorporation into the optimal control law.

The stochastic transfer function models and the real-time estimation techniques used in the self-tuning control strategy were first discussed by Åström and Bohlin [5]. Peterka [6] was one of the first researchers to develop the complete estimation and control algorithm. The most extensive theoretical, simulation and experimental work on the self-tuning regulator has been performed by Åström and Wittenmark [1,8], Wittenmark [7], and Åström et. al. [9].

### 2.2.1 Basic Theory

Early papers on stochastic identification and control methods were mostly concerned with separate identification and control steps. That is, generally an off-line identification scheme would be used based on experimental input/output data. The identification step would be followed by the design of a control strategy and subsequent implementation on the system. Identification problems are generally characterized by three items: the class of models to be used, the class of input signals, and a criterion for the estimation [2]. Therefore, for the identification phase, certain parametric models and the type of input signals that will generate consistent parameter estimates have to be selected. Also, the minimization of a scalar loss function is generally specified as the criterion for estimation. Once the identification phase is accomplished, the design of a suitable control strategy can be achieved using existing control theory. This type of separate estimation and control for a single input/output stochastic system has been studied by Åström and Wittenmark [8].

The idea of combining the estimation and control steps was considered by Kalman [10] in 1958; subsequently, there has been a large amount of research on this topic. The type of combined estimation and control method that is considered in this thesis is the self-tuning regulator. The regulator is designed based on the assumption that the system can be represented by a single-input single-output discrete stochastic model of the class considered by Åström and Bohlin [5], and which is generally referred to as the Åström-Bohlin model. Peterka

[6] used this model and derived an algorithm which automatically adjusted the parameters of a digital controller on-line. The basic structure of the algorithm can be seen in figure 2.1. It consists of two parts: real-time recursive least square estimation of model parameters and a minimum variance control law for the estimated model. Peterka has shown that under certain conditions, the controller is the same as the minimum variance controller that could be derived if the system parameters were known.

Åström's involvement in the development of the self-tuning regulator began quite early. He and Bohlin [5] presented a general form of stochastic models and investigated the identification of linear stochastic systems, using the maximum likelihood method. In a later paper [26], Åström examined the achievable accuracy of the parameter estimates and showed that his results can be applied to generalized least squares and model adjusting techniques. Åström and Wittenmark [8] also did a detailed study of separate and combined estimation and control; they used models with constant but unknown parameters and models in which the parameters are time varying Gauss-Markov processes. Their minimum variance control law uses previous input/output data, the estimates of the parameters and the variances of the estimation errors. This method of combining least squares estimation and minimum variance control law was simulated using models with unknown, time varying parameters by Wittenmark and Wieslander [11].

Åström and Wittenmark [1,7] then applied this type of control strategy to models with constant but unknown parameters. They assumed that the system was minimum phase with known time delay and that a



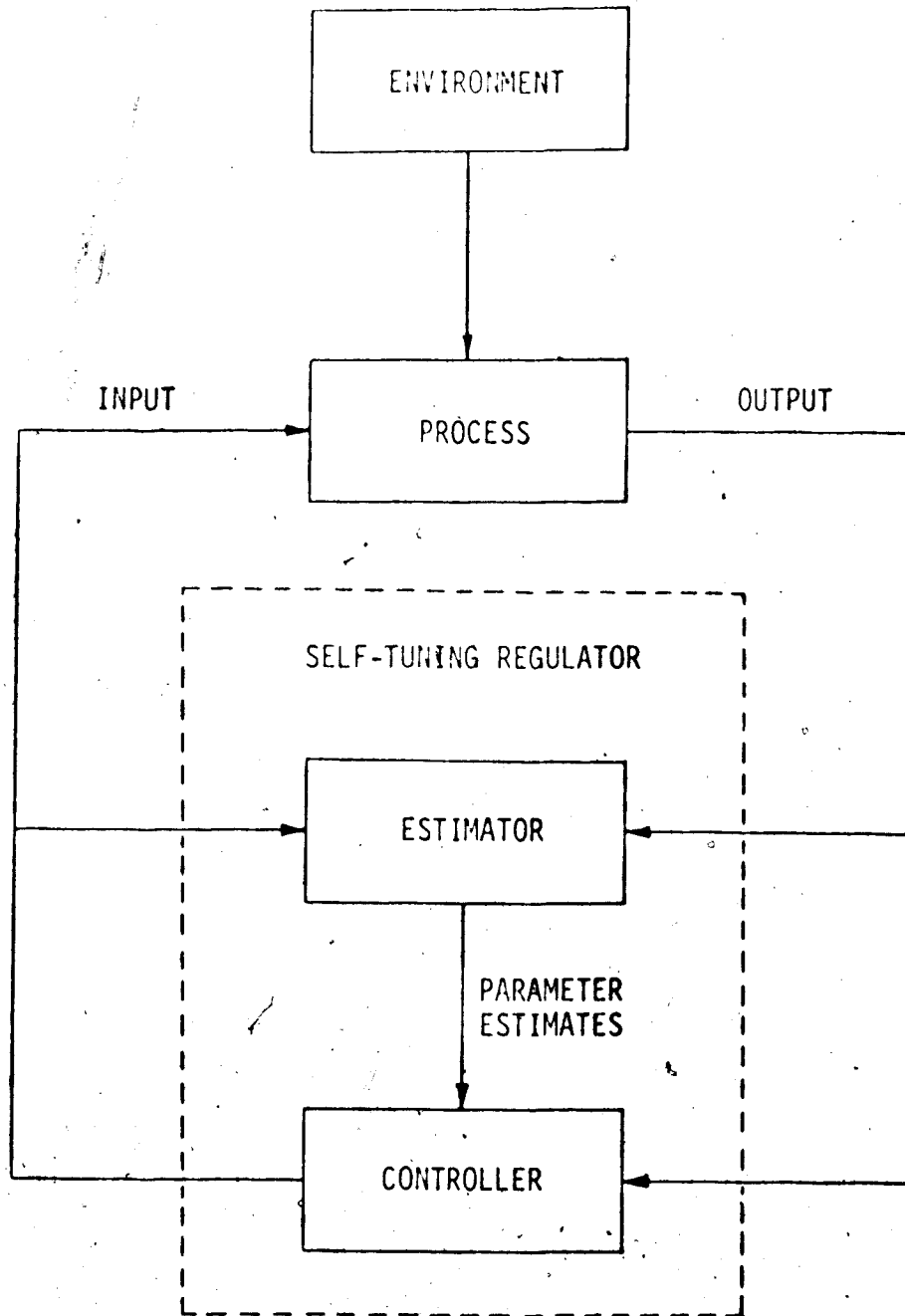


Figure 2.1 Basic structure of self-tuning regulator

bound can be given to the order of the system. They also proved two theorems for the closed-loop system that are valid if the parameter estimates converge. (Unfortunately, general conditions guaranteeing convergence have not been reported, though efforts were made in this area.) The first theorem states that under weak assumptions, the covariance of the output variable and the cross covariance of the control and the output variables are both zero. In the second theorem it is shown that the control law obtained converges to the minimum variance control law that could be derived if the constant model parameters were known.

Similar self-tuning regulators have been designed for the same stochastic model using different estimation techniques such as stochastic approximation [12] and maximum likelihood [13]. Other regulators have been investigated by retaining the least squares estimation part but using a different performance index which minimizes the output variance and penalizes the control signal. Studies on this type of regulator has been reported by Cegrell and Hedqvist [14] and Clarke and Gawthrop [15,16].

The asymptotic properties of the self-tuning regulator have been examined by Ljung and Wittenmark [17]; they have presented the techniques and basic theorems to analyse this problem. They have shown that for closed-loop systems near or outside the stability boundary, the regulator stabilizes the system even if the model noise does not agree with the true noise characteristics. They have also shown that the regulator does not converge for general noise structures, and they have constructed an example to illustrate this.

The text by Åström [13] provides an excellent introduction to stochastic control theory for linear systems with quadratic performance criteria. Its analysis of stochastic systems, parameter estimation and optimal stochastic control includes both the continuous and discrete cases.

### 2.2.2 Modification and Extensions

Wittenmark [7] has extended the self-tuning algorithm to include feedforward control for known disturbances and setpoint control of the output variable.

For non-minimum phase systems, the standard self-tuning regulator cannot be applied in general. This is because the minimum variance controller is extremely sensitive to variations in the parameters [1,13]. Several methods have been proposed to overcome this difficulty. Åström [13], Åström and Wittenmark [18], Turtle and Phillipson [19] and Peterka [6] have suggested the use of sub-optimal control strategies. Clarke and Gawthrop [15,16] claim that this problem can be easily solved by including the square of the control signal in the quadratic performance index.

An extension of the self-tuning algorithm to multi-input systems can be made quite easily by simply adding the appropriate terms to the Åström-Bohlin model and the algorithm [23]. However, an extension to multi-output systems is much more difficult since a new general structure of stochastic models has to be formulated. Furthermore, the complexity of the algorithm and the computational requirements will increase tremendously. Gustavsson, Ljung and Söderström [20] have

reported their theoretical analysis on the identification of linear multivariable process during closed-loop operation. Åström and Peterka [21] have considered the extension of the self-tuning algorithm to multivariable systems with constant but unknown parameters. However, the extensive on-line computational requirements include an orthogonal transformation and the solution of a matrix Riccati equation each time the parameters are updated. Consequently, their multivariable self-tuning regulator is not attractive for most practical applications.

### 2.2.3 Industrial Applications

Several applications of the self-tuning regulator to industrial processes in Sweden have been reported [9]. Wittenmark and Borisson [22] have used the regulator to control the moisture content of paper from a paper making machine. They reported that very good results were obtained particularly during the startup phase and for steady state control. They found that the number of the parameters in the regulator was not very crucial in their experiments since it had little influence on steady state performance. They also found that the regulator can handle non-stationary disturbances without difficulty. Feedforward compensation of a measured disturbance, couch vacuum, was included in the algorithm.

Cegrell and Hedqvist [14,23] also used the self-tuning regulator to control a different paper machine. They considered the moisture control loop of the machine which consisted of two inputs; thick stock flow and steam pressure, and one output; the moisture content. They found that replacing a conventional digital PI controller

by the self-tuning regulator resulted in a decrease in output variance and a reduction of losses during quality changes and mill setup. They also confirmed that the assumed order of the process model is not important.

The application of the self-tuning regulator on a mine ore crushing machine has been reported by Borisson and Syding [27]. For changing characteristics of the incoming ore and the crusher itself, the regulator was able to adapt to the varying situations and control the input ore flow to the crusher to maintain high production. Their results demonstrated a 10% increase in production in comparison with a fixed parameter PI controller.

### 2.3 Minimum Variance Regulator

Consider the Aström-Bohlin model which is a single-input single-output stochastic model of the form [13]:

$$y(t) + a_1 y(t-1) + \dots + a_n y(t-n) = b_1 u(t-k-1) + \dots + b_n u(t-k-n) + \lambda [e(t) + c_1 e(t-1) + \dots + c_n e(t-n)] \quad (2.1)$$

where

$y$  is the scalar output

$u$  is the scalar control

$t$  is the sampling instant

$k$  is the time delay (a non-negative integer)

$n$  is the order of the system

$\lambda$  is a constant

and  $\{e(t)\}$  is a sequence of independent, normal (0,1) random variables.

Equation (2.1) can also be expressed as:

$$A(q^{-1}) y(t) = B(q^{-1}) u(t-k-1) + \lambda C(q^{-1}) e(t) \quad (2.2)$$

or

$$y(t) = \frac{B(q^{-1})}{A(q^{-1})} u(t-k-1) + \lambda \frac{C(q^{-1})}{A(q^{-1})} e(t) \quad (2.3)$$

where  $q^{-1}$  is the backward shift operator, i.e.  $q^{-1} y(t) = y(t-1)$  and

$$A(q^{-1}) = 1 + a_1 q^{-1} + \dots + a_n q^{-n}$$

$$B(q^{-1}) = b_1 + b_2 q^{-1} + \dots + b_n q^{-n+1}$$

$$C(q^{-1}) = 1 + c_1 q^{-1} + \dots + c_n q^{-n}$$

Before the minimum variance control law can be derived, certain conditions have to be imposed on polynomials  $B(q^{-1})$  and  $C(q^{-1})$ . The polynomial  $B$  is normally assumed to have all its zeroes inside the unit circle, i.e. the system of equation (2.1) is minimum phase. Polynomial  $C$  is also assumed to have all its zeroes inside the unit circle. These conditions are explained in detail by Åström [13].

Equation (2.3) can be written as

$$y(t+k+1) = \frac{B(q^{-1})}{A(q^{-1})} u(t) + \lambda \frac{C(q^{-1})}{A(q^{-1})} e(t+k+1) \quad (2.4)$$

In order to derive a minimum variance regulator it is convenient to express  $C(q^{-1})$  as [1]:

$$C(q^{-1}) = A(q^{-1}) Z(q^{-1}) + q^{-k-1} G(q^{-1}) \quad (2.5)$$

where

$$Z(q^{-1}) = 1 + z_1 q^{-1} + \dots + z_k q^{-k} \quad (2.6)$$

$$G(q^{-1}) = g_0 + \dots + g_{n-1} q^{-n+1} \quad (2.7)$$

Introducing equation (2.5) into equation (2.4) gives

$$y(t+k+1) = \frac{B(q^{-1})}{A(q^{-1})} u(t) + \frac{\lambda [A(q^{-1}) Z(q^{-1}) + q^{-k-1} G(q^{-1})]}{A(q^{-1})} e(t+k+1) \quad (2.8)$$

or

$$y(t+k+1) = \frac{B(q^{-1})}{A(q^{-1})} u(t) + \lambda Z(q^{-1}) e(t+k+1) + \lambda \frac{G(q^{-1})}{A(q^{-1})} e(t) \quad (2.9)$$

But from equation (2.2)

$$\lambda e(t) = \frac{A(q^{-1})}{C(q^{-1})} y(t) - \frac{B(q^{-1})}{C(q^{-1})} q^{-k-1} u(t) \quad (2.10)$$

Replacing  $\lambda e(t)$  in equation (2.9) gives

$$y(t+k+1) = \lambda Z(q^{-1}) e(t+k+1) + \left[ \frac{B(q^{-1})}{A(q^{-1})} - \frac{q^{-k-1} B(q^{-1}) G(q^{-1})}{A(q^{-1}) C(q^{-1})} \right] u(t) + \frac{G(q^{-1})}{C(q^{-1})} y(t) \quad (2.11)$$

which can be simplified to,

$$y(t+k+1) = \lambda Z(q^{-1}) e(t+k+1) + \frac{B(q^{-1}) Z(q^{-1})}{C(q^{-1})} u(t) + \frac{G(q^{-1})}{C(q^{-1})} y(t) \quad (2.12)$$

A minimum variance regulator is a regulator that minimizes the output variance (or loss function)  $V$ :

$$V = E[y^2(t)] \quad (2.13)$$

where  $E$  denotes the expectation operator. Let  $u(t)$  be an arbitrary function of  $y(t), y(t-1) \dots$  and  $u(t-1), u(t-2) \dots$ . Then from equation (2.12):

$$E[y^2(t+k+1)] = E[\lambda Z(q^{-1}) e(t+k+1)]^2 + E \left[ \frac{B(q^{-1}) Z(q^{-1})}{C(q^{-1})} u(t) + \frac{G(q^{-1})}{C(q^{-1})} y(t) \right]^2 \quad (2.14)$$

Since  $e(t+1), \dots, e(t+k), e(t+k+1)$  are independent of  $y(t), y(t-1), \dots$  and  $u(t-1), u(t-2), \dots$ , hence

$$E y^2(t+k+1) \geq \lambda^2 [1 + z_1^2 + z_2^2 + \dots + z_k^2] \quad (2.15)$$

where the equality holds for

$$B(q^{-1}) Z(q^{-1}) u(t) + G(q^{-1}) y(t) = 0 \quad (2.16)$$

Re-arranging equation (2.16) gives the desired minimum variance control law:

$$u(t) = - \frac{G(q^{-1})}{B(q^{-1}) Z(q^{-1})} y(t) \quad (2.17)$$

If the minimum variance regulator is used to control the system represented by equation (2.1), the output would be a moving average process of order  $k$ , i.e.

$$y(t) = \lambda Z(q^{-1}) e(t)$$

or

$$y(t) = \lambda [e(t) + z_1 e(t-1) + \dots + z_k e(t-k)] \quad (2.18)$$



## 2.4 Self-Tuning Regulator

If a dynamic system has constant but unknown parameters, one way to formulate a control law is to first estimate the model parameters using some identification technique, and then derive the appropriate control strategy off-line by optimizing a selected performance criterion. This approach consists of separate identification and control steps.

Åström and Wittenmark [1] have proposed a type of adaptive control strategy that combines the problems of identification and control. In their self-tuning regulator, the parameters of the assumed model are updated every sampling instant using current and previous input/output data. The control signal is then calculated from a control law which utilizes the updated model. One desirable feature of the self-tuning regulator is that if the parameter estimates converge, the regulator converges to the minimum variance control law that could be derived if the model parameters were known.

In the self-tuning regulator, a recursive least squares algorithm is used to update the parameter estimates at every sampling instant, and then the control variable is calculated from a minimum variance control law which uses the updated parameter estimates as if they were the true parameters of the system. Åström and Wittenmark [1] have noted that the estimation of the model parameters in equation (2.2) can be made simpler if it is assumed that  $C(q^{-1}) = 1$ , since then the standard linear least squares analysis can be applied. Therefore, the simplified system model is written as

$$A(q^{-1})y(t) = B(q^{-1})u(t-k-1) + \lambda e(t) \quad (2.19)$$

To simplify the on-line computation of the control law, the identity in equation (2.5) is incorporated into this model. Substituting  $C(q^{-1}) = 1$  into equation (2.12) gives the "predictive model":

$$y(t+k+1) - G(q^{-1}) y(t) = B(q^{-1}) Z(q^{-1}) u(t) + \lambda Z(q^{-1}) e(t+k+1) \quad (2.20)$$

Equation (2.20) can be expanded to

$$\begin{aligned} y(t+k+1) + \alpha_1 y(t) + \dots + \alpha_n y(t-n+1) = & \beta_0 [u(t) + \beta_1 u(t-1) \\ & + \dots + \beta_\ell u(t-\ell)] + \epsilon(t+k+1) \end{aligned} \quad (2.21)$$

where  $\ell = n+k-1$  and  $\epsilon(t)$  is a moving average of order  $k$  of the driving noise  $e(t)$ . The coefficients  $\alpha_i$  and  $\beta_i$  are related to the parameters  $a_i$  and  $b_i$  in equation (2.1) through identity (2.5) and control law (2.17). If the coefficients are constant and known, then the minimum variance controller for the predictive model (2.21) is [7]:

$$u(t) = \frac{1}{\beta_0} [\alpha_1 y(t) + \dots + \alpha_n y(t-n+1)] - \beta_1 u(t-1) - \dots - \beta_\ell u(t-\ell) \quad (2.22)$$

If the parameters  $\{\alpha_i\}$  and  $\{\beta_i\}$  of the predictive model are estimated on-line and the estimates,  $\{\hat{\alpha}_i(t)\}$  and  $\{\hat{\beta}_i(t)\}$ , are used in the feedback controller (2.22), then the estimates are correlated with the disturbances  $\{\epsilon(t)\}$ . As a result, it may not be possible to accurately determine all parameters. To avoid this possible difficulty, Åström and Wittenmark assumed that parameter  $\beta_0$  is constant and given. Then equation (2.21) can be written as

$$\begin{aligned} y(t+k+1) + \hat{\alpha}_1(t) y(t) + \dots + \hat{\alpha}_n(t) y(t-n+1) = & \beta_0 [u(t) + \hat{\beta}_1(t) u(t+1) \\ & + \dots + \hat{\beta}_\ell(t) u(t-\ell)] + \epsilon(t+k+1) \end{aligned} \quad (2.23)$$

Next, introduce the column vectors,  $\underline{\psi}(t)$  and  $\underline{\hat{\theta}}(t)$ :

$$\underline{\psi}^T(t) = [-y(t) \ -y(t-1) \ \dots \ -y(t-n+1) \ \beta_0 u(t-1) \ \dots \ \beta_0 u(t-l)]$$

and

$$\underline{\hat{\theta}}^T(t) = [\hat{\alpha}_1(t) \ \hat{\alpha}_2(t) \ \dots \ \hat{\alpha}_n(t) \ \hat{\beta}_1(t) \ \dots \ \hat{\beta}_l(t)]$$

where superscript T denotes a vector transpose and the underline denotes a vector. Then equation (2.23) can be written as

$$y(t+k+1) = \beta_0 u(t) + \underline{\psi}^T(t) \underline{\hat{\theta}}(t) + \epsilon(t+k+1). \quad (2.24)$$

The least squares recursive equations that are used include exponential weighting of past data. These equations are [7]:

$$\underline{\hat{\theta}}(t) = \underline{\hat{\theta}}(t-1) + \underline{K}(t)[y(t) - \beta_0 u(t-k-1) - \underline{\psi}^T(t-k-1) \underline{\hat{\theta}}(t-1)] \quad (2.25)$$

$$\underline{K}(t) = \underline{P}(t) \underline{\psi}(t-k-1) [R + \underline{\psi}^T(t-k-1) \underline{P}(t) \underline{\psi}(t-k-1)]^{-1} \quad (2.26)$$

$$\underline{P}(t+1) = \frac{1}{\mu} (\underline{P}(t) - \underline{K}(t) [R + \underline{\psi}^T(t-k-1) \underline{P}(t) \underline{\psi}(t-k-1)] \underline{K}^T(t)) \quad (2.27)$$

where

$\underline{\hat{\theta}}(t)$  is the estimated value of  $\underline{\theta}(t)$

$\underline{K}(t)$  is the gain vector  $\{(n+l) \times 1\}$

$\underline{P}(t)$  is the covariance matrix  $\{(n+l) \times (n+l)\}$

$\mu$  is the exponential forgetting factor

$R$  is the covariance of the noise variable,  $e(t)$

The derivation of the recursive form of the least squares estimation algorithm can be found in references [6], [24] and [25].

The theoretical reasons for using the exponential forgetting factor are twofold. First, the rate of change of the parameter estimates

depends on the gain vector  $\underline{K}(t)$  in the recursive least squares equations, and after a period of time the gain vector elements may have decreased to small values before the estimates reach the true parameter values. Placing more weight on recent data and less on past data tends to prevent the elements of  $\underline{K}(t)$  from becoming too small. Second, for processes with slowly time varying parameters, it is possible to follow these parameters by using a forgetting factor of less than one.

To summarize, the self-tuning regulator estimates the unknown parameters,  $\{\alpha_i\}$  and  $\{\beta_i\}$ , on-line and these estimates,  $\{\hat{\alpha}_i(t)\}$  and  $\{\hat{\beta}_i(t)\}$ , are then used in the minimum variance controller (2.22) as if they were the true values. The following calculations are performed on-line at every sampling instant:

- (a) Parameter estimates  $\{\hat{\alpha}_i(t)\}$  and  $\{\hat{\beta}_i(t)\}$  are calculated based on input/output data using the recursive least squares algorithm in equations (2.25) to (2.27).
- (b) The control signal is calculated from:

$$u(t) = \frac{1}{\hat{\beta}_0} [\hat{\alpha}_1(t) y(t) + \dots + \hat{\alpha}_n(t) y(t-n+1)] - \hat{\beta}_1(t) u(t-1) - \dots - \hat{\beta}_2 u(t-2) \quad (2.28)$$

which can be written as

$$u(t) = \frac{1}{\hat{\beta}_0} \hat{\theta}^T(t) \underline{\psi}(t) \quad (2.29)$$

Åström and Wittenmark [1] have proved that if the parameter estimates converges, the control law converges to the minimum variance control law that can be determined if the parameters of the system are

known. This occurs despite the fact that the parameter estimates are biased due to model simplification and the correlation between parameter estimates and disturbances.

In general, the least squares estimation technique will give unbiased parameter estimates under the following conditions [1,2]: the predictive model has the correct form; the residuals  $\{e(t)\}$  are independent; the input is persistently exciting; and the input sequence  $\{u(t)\}$  is independent of the disturbance sequence  $\{e(t)\}$ . However in the self-tuning regulator several of these conditions are not satisfied since the predictive model in equation (2.20) does not have the correct form and the inputs and disturbances are correlated due to feedback control. Furthermore, the input,  $u(t)$ , is not necessarily "persistently exciting". For these reasons, the parameter estimates generated by the self-tuning regulator tend to be biased.

## 2.5 Numerical Example

Before one can use the self-tuning algorithm, several constants have to be specified for both the estimation and control parts. The constants are the exponential forgetting factor  $\mu$ , the initial covariance matrix  $\underline{P}(0)$ , and the initial parameter estimates,  $\{\hat{\alpha}_i(0)\}$  and  $\{\hat{\beta}_i(0)\}$ , the order of the predictive model  $n$ , the scaling factor  $\beta_0$ , and the assumed system time delay  $k$ .

A simple numerical example due to Åström and Wittenmark [1] was selected in order to study the effects of using different design options and initial parameter values. The example is a second order, single-input single-output stochastic system with a time delay of one

sampling interval and a noise variable of  $N(0,1)$ . The system equation is

$$\begin{aligned} y(t) - 1.9 y(t-1) + 0.9 y(t-2) \\ = u(t-2) - u(t-3) + e(t) - 0.5 e(t-1) \end{aligned} \quad (2.30)$$

The corresponding pulse transfer function model is

$$A(q^{-1}) y(t) = B(q^{-1}) u(t-2) + C(q^{-1}) e(t) \quad (2.31)$$

where

$$A(q^{-1}) = 1 - 1.9 q^{-1} + 0.9 q^{-2}$$

$$B(q^{-1}) = 1 - q^{-1}$$

$$C(q^{-1}) = 1 - 0.5 q^{-1}$$

Note that the polynomial B has a zero on the unit circle thus violating one of the assumptions in section 2.2.1. Note also that polynomial A contains a zero on the unit circle.

### 2.5.1 Derivation of Minimum Variance Regulator

The predictive model corresponding to the example of equation (2.30) is

$$\begin{aligned} y(t+2) + \alpha_1 y(t) + \alpha_2 y(t-1) = \beta_0 [u(t) + \beta_1 u(t-1) + \beta_2 u(t-2)] \\ + \epsilon(t+2) \end{aligned} \quad (2.32)$$

The identity in equation (2.5) is

$$(1 - 0.5q^{-1}) = (1 - 1.9q^{-1} + 0.9q^{-2}) Z(q^{-1}) + q^{-k-1} G(q^{-1}) \quad (2.33)$$

Solving equation (2.33) gives

$$Z(q^{-1}) = 1 + 1.4 q^{-1}$$

$$G(q^{-1}) = 1.76 - 1.26 q^{-1}$$

and substituting  $k$ , and polynomials  $B$ ,  $Z$  and  $G$  into the predictive model of equation (2.20) gives

$$\begin{aligned} y(t+2) - 1.76 y(t) + 1.26 y(t-1) &= u(t) + 0.4 u(t-1) \\ &- 1.4 u(t-2) + \epsilon(t+2) \end{aligned} \quad (2.34)$$

Comparing coefficients in equations (2.32) and (2.34) gives

$$\begin{aligned} \alpha_1 &= -1.76 & \beta_0 &= 1.0 \\ \alpha_2 &= 1.26 & \beta_1 &= 0.4 \\ & & \beta_2 &= -1.4 \end{aligned}$$

The minimum variance control law for the system of equation (2.34) is

$$u(t) = -1.76 y(t) + 1.26 y(t-1) - 0.4 u(t-1) + 1.4 u(t-2) \quad (2.35)$$

### Simulation Results

A computer program has been written to simulate the response of the system in equation (2.30) when the self-tuning regulator is used. In all the simulation runs, the noise variable was specified to be  $N(0,1)$  using the IBM 1130 random number subroutine GAUSS which is also available on the IBM 1800 computer. The same random noise sequence was used in all runs. There were no constraints applied to the control signal and  $R$  was set equal to the correct value of 1.0. For comparison purposes, the control law (2.28) was written as

$$u(t) = \hat{\alpha}_1 y(t) + \dots + \hat{\alpha}_n y(t-n+1) - \hat{\beta}_1 u(t-1) - \dots - \hat{\beta}_l u(t-l) \quad (2.36)$$

where

$$\hat{a}_i = \frac{\hat{a}_i}{\hat{\beta}_0}, \quad i = 1, 2, \dots, n$$

Typical simulation results are shown in Table 2.1 and figures 2.2 to 2.6.

Run number 1184 shown in figure 2.2 was used as a base case for purposes of comparison. For the base case, an exponential forgetting factor of  $\mu = 1.0$  was chosen so that there was no exponential weighting of data. The initial parameter estimates (at  $t=0$ ) and input/output data for  $t < 0$  were assumed to be zero. The covariance matrix was arbitrarily specified as the identity matrix. The correct scaling factor,  $\beta_0 = 1.0$ , was used and the correct system order and time delay were used as the assumed values. Figure 2.2 illustrates that the convergence properties of the parameter estimates are very good but that the final estimates are biased as expected. (The correct values of the parameters are given in Table 2.1 and the recorded parameter estimates at the end of all runs are listed both in Table 2.1 and above the estimate curves in figures 2.2 - 2.6.)

When exponential weighting of past data in the least squares estimation is introduced, the parameter estimates fluctuate more as shown in figure 2.3 and the rate of convergence is similar to that in figure 2.2. In general the proper selection of  $\mu$  can be made by examining the parameter estimate plots since too much fluctuation in the estimates implies too small a value of  $\mu$  is used, and slowly converging estimates means a smaller value of  $\mu$  should be used. In the simulation study it was found that decreasing  $\mu$  (from 1.0) resulted in



TABLE 2.1  
 RECURSIVE LEAST SQUARES ESTIMATES OF SYSTEM PARAMETERS AFTER 300 TIME INTERVALS

FIGURE	RUN NO.	$\beta_0$	$\underline{P}(0)$	$\mu$	$(\hat{\alpha}_1(0)) \& (\hat{\beta}_1(0))$	$\hat{\alpha}_1$	$\hat{\alpha}_2$	$\hat{\beta}_1$	$\hat{\beta}_2$	ACCUM. LOSS
2.2	1184	1.0	$\underline{I}$	1.0	0	-1.92	1.28	0.52	-1.51	1205
2.3	1185	1.0	$\underline{I}$	0.98	0	-1.90	1.23	0.41	-1.41	1231
2.4	1187	1.0	$\underline{I}$	1.0	1.0	-2.02	1.36	0.56	-1.56	1273
2.5	1188	1.0	1000 $\underline{I}$	1.0	0	-1.93	1.23	0.54	-1.53	1196
2.6	1186	2.0	$\underline{I}$	1.0	0	-1.76	1.23	0.26	-1.25	1367
-	1191		MINIMUM VARIANCE CONTROL		-	-	-	-	-	992
-	-		ACTUAL SYSTEM PARAMETERS		-	-1.76	1.26	0.40	-1.40	-

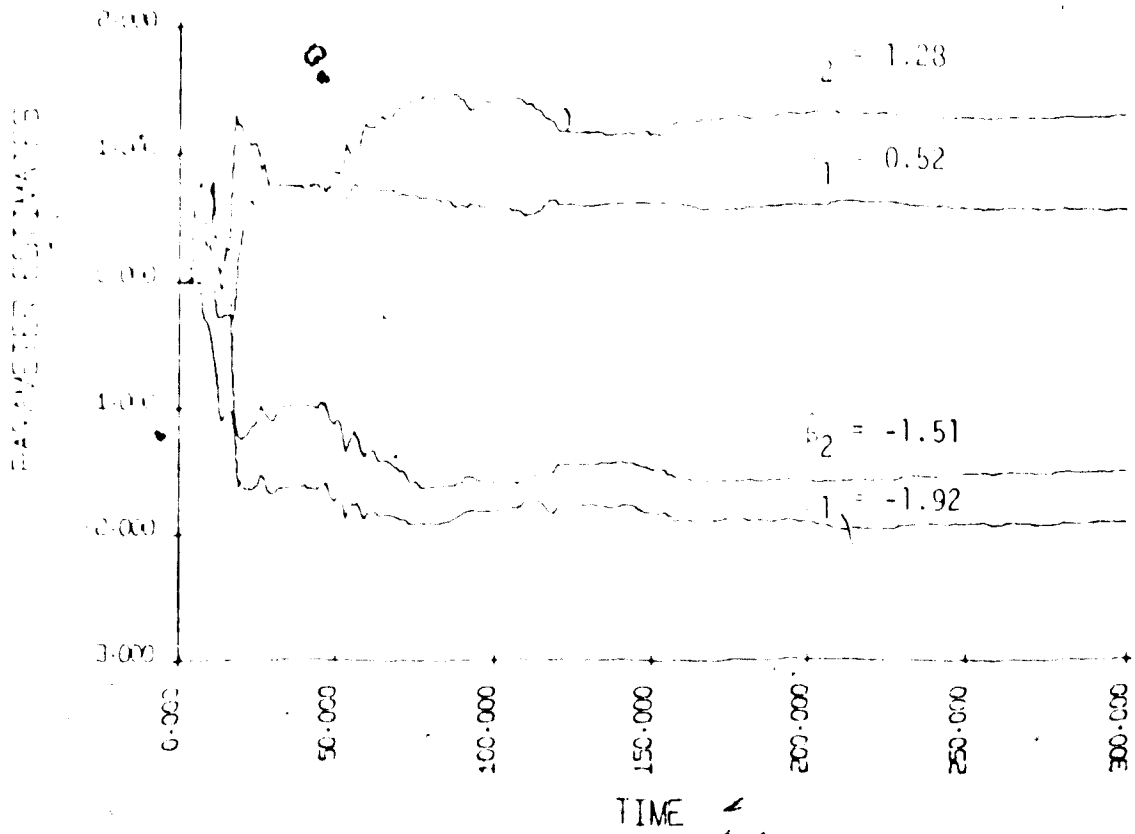


Figure 2.2 Base case (Run No. 1184)

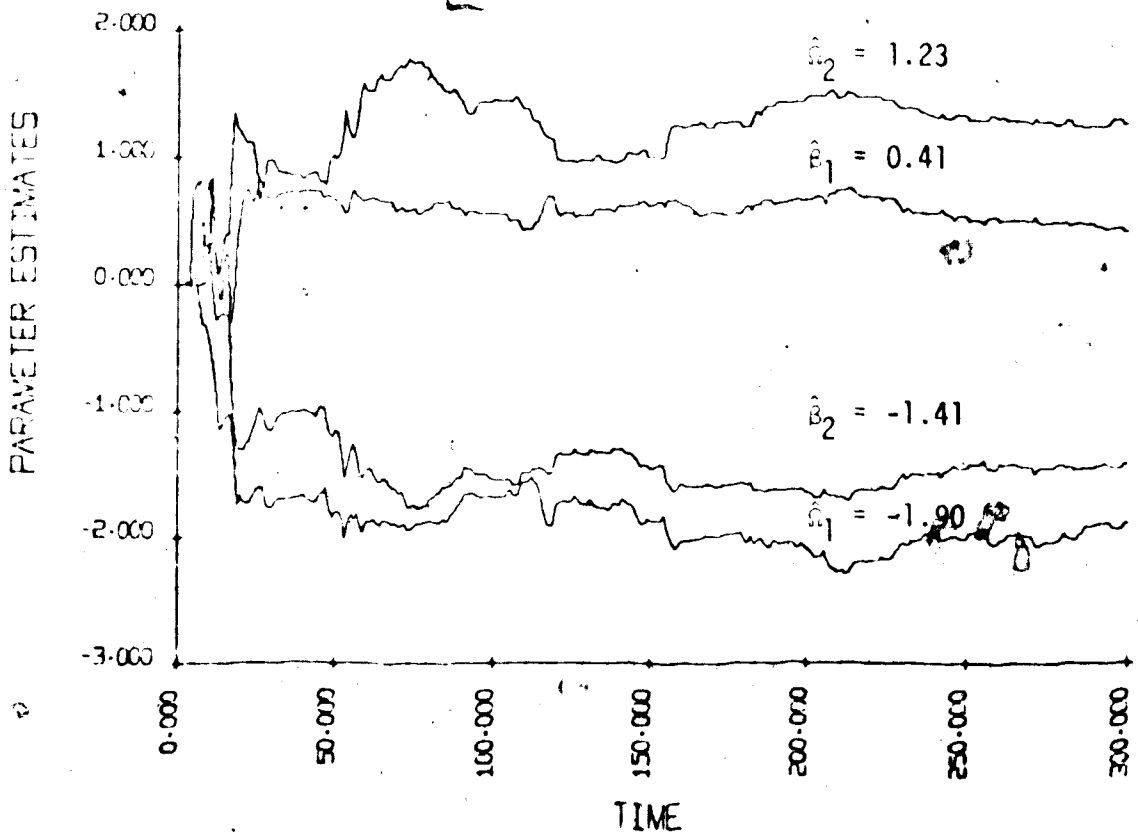


Figure 2.3 Base case except that  $\mu = 0.93$  (Run No. 1185)

increasing values of the accumulated loss. Therefore from the stand-point of control, it would be better to use a value of 1.0 for  $\mu$  in this example.

The parameter estimates converged to the true values for only a small range of initial estimates,  $\{\hat{\beta}_1(0)\}$  and  $\{\hat{\beta}_0(0)\}$ . For example, with initial parameter estimates of 2.0, the estimates converged to incorrect values which contained large biases. Figure 2.4 shows that for initial values of estimates not too far from the true values, the convergence properties are very similar to those of the base case. It seems that the best choice of the starting values is zero if there is no prior information about the actual parameter value.

Different values of the initial covariance matrix  $\underline{P}(0)$  were tried ( $\underline{I} \leq \underline{P}(0) \leq 1000 \underline{I}$ ) but there were no significant differences in the final parameter estimates. However, large initial values resulted in large initial fluctuations in the estimates as can be seen in figure 2.5. The best results were obtained with  $\underline{P}(0) = \underline{I}$ . The effect of different assumed values of  $\beta_0$  was also investigated. It was found that parameter estimates would converge for values of  $\beta_0$  which satisfied  $0.6 \leq \frac{\beta_0}{b_1} \leq 2.0$ . For  $\frac{\beta_0}{b_1} \neq 2.0$ , the estimates tended to converge slower initially than in the other runs, as shown in figure 2.6. In general, as  $\beta_0$  increases, the convergence of the parameter estimates becomes slower.

A comparison of the accumulated loss functions for the minimum variance and self-tuning regulator is shown in figure 2.7. The figure indicates that the major difference between the two curves occurs

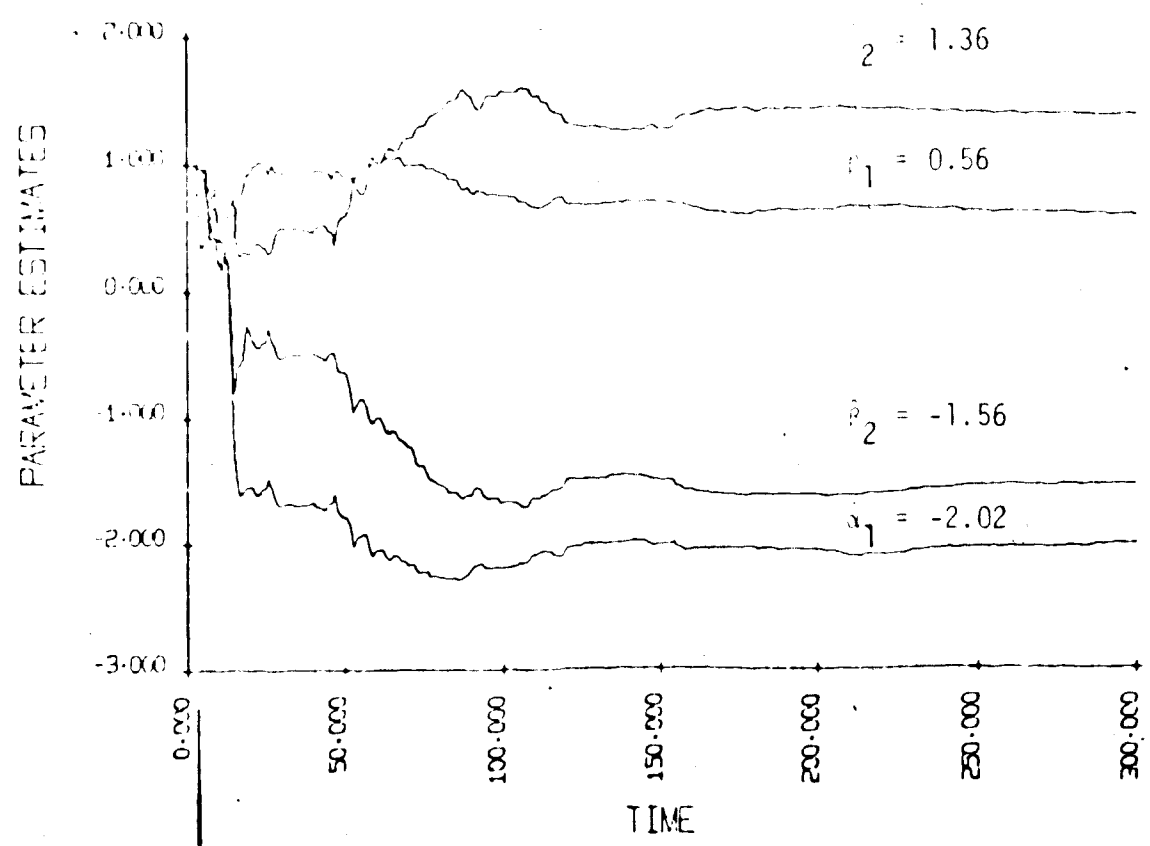


Figure 2.4 Base case, except that  $\hat{\theta}_1(0) = 1$  (Run No. 1187)

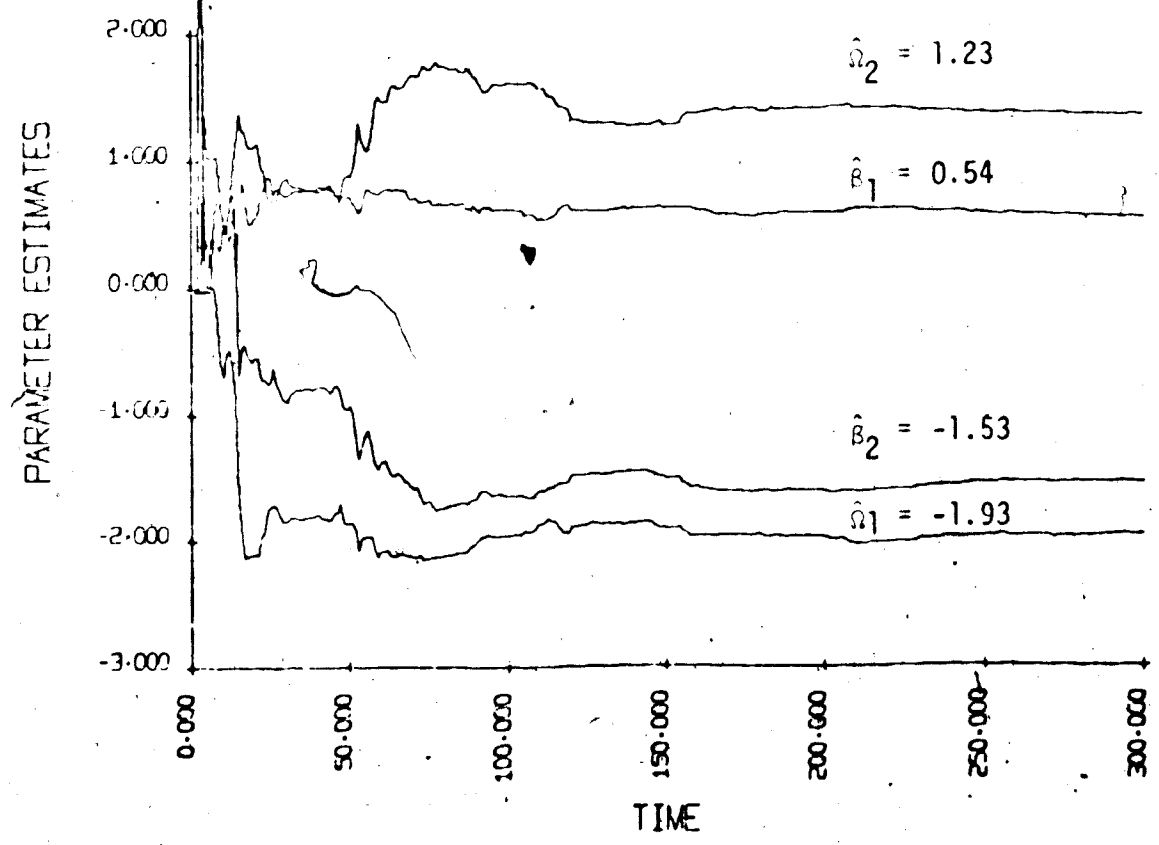


Figure 2.5 Base case except that  $\underline{p}(0) = 1000 \underline{I}$  (Run No. 1188)

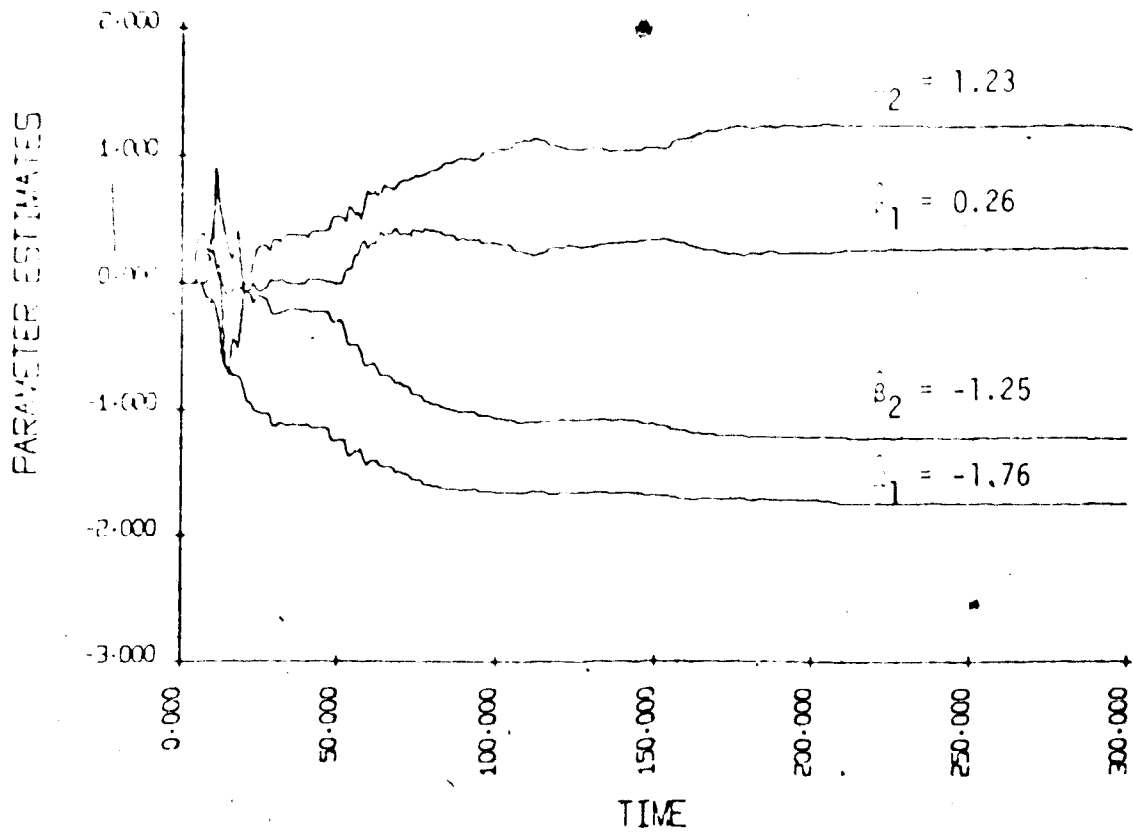


Figure 2.6 Base case except that  $\beta_0 = 2.0$  (Run No. 1186)

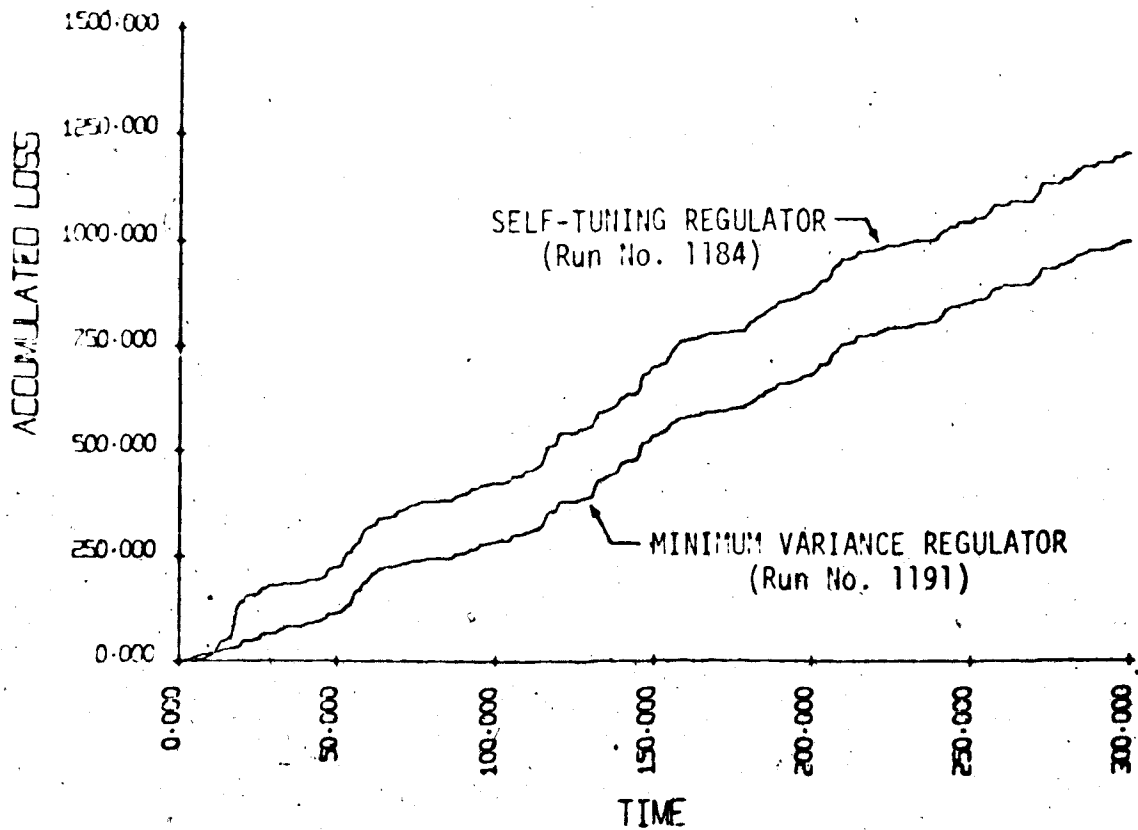


Figure 2.7 Accumulated Loss Functions

during the transient period when the parameter estimates are adjusting. After the initial period, the responses are very similar. The corresponding output variables shown in figure 2.8 also support this observation. Figure 2.8 also includes the output of the uncontrolled system. This type of drifting response can be explained by considering the uncontrolled system transfer function:

$$y(t) = \frac{1 - 0.5q^{-1}}{(1 - 0.9q^{-1})(1 - q^{-1})} e(t) \quad (2.37)$$

Since the denominator contains a root on the unit circle, this results in the integrating type of response shown in figure 2.8.

The noise variable and the two control variables for the self-tuning and minimum variance regulators are shown in figure 2.9. After the initial transient, the behaviour of the control variables for the self-tuning and minimum variance regulators are very similar.

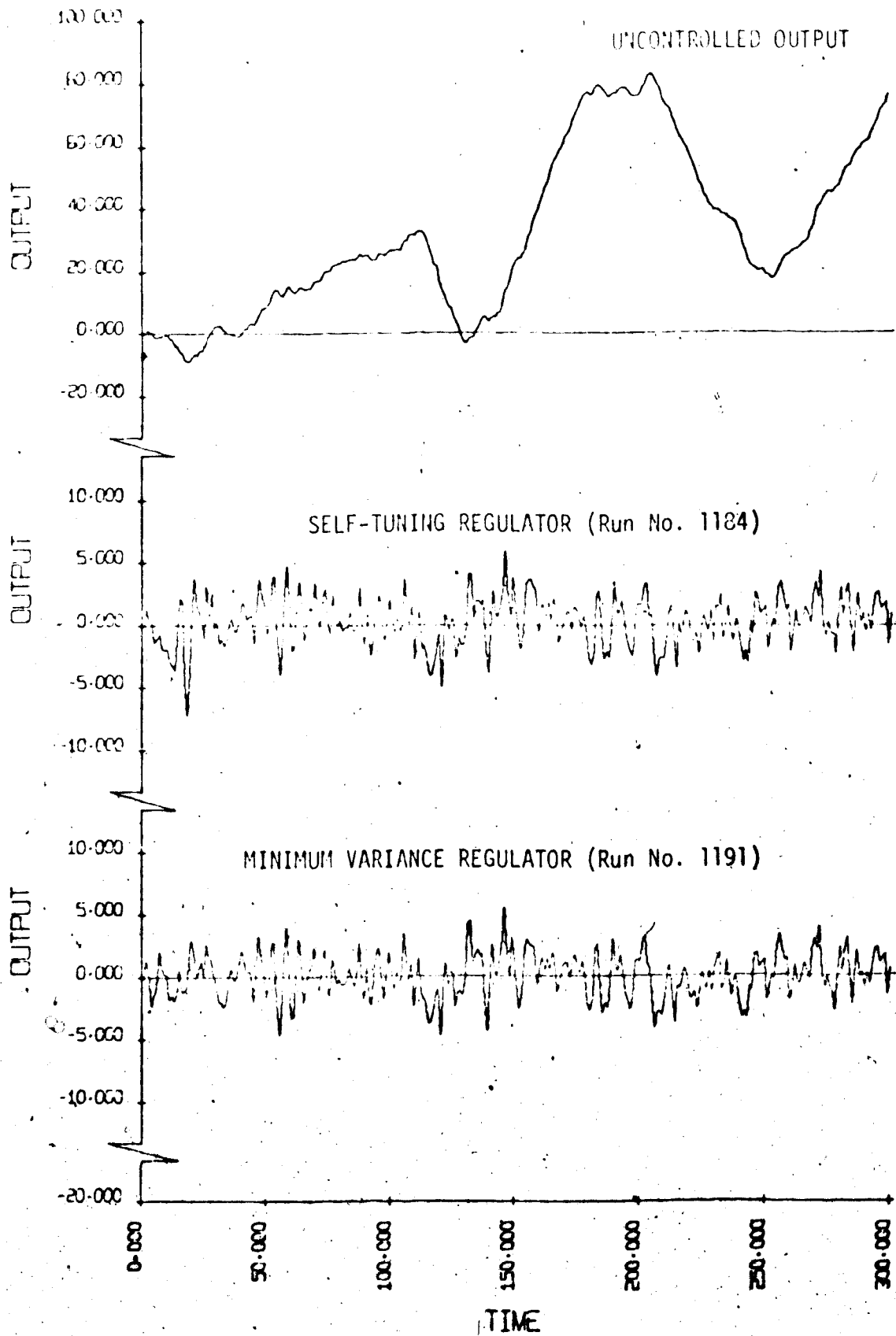


Figure 2.8 Uncontrolled response and closed loop responses for different regulators

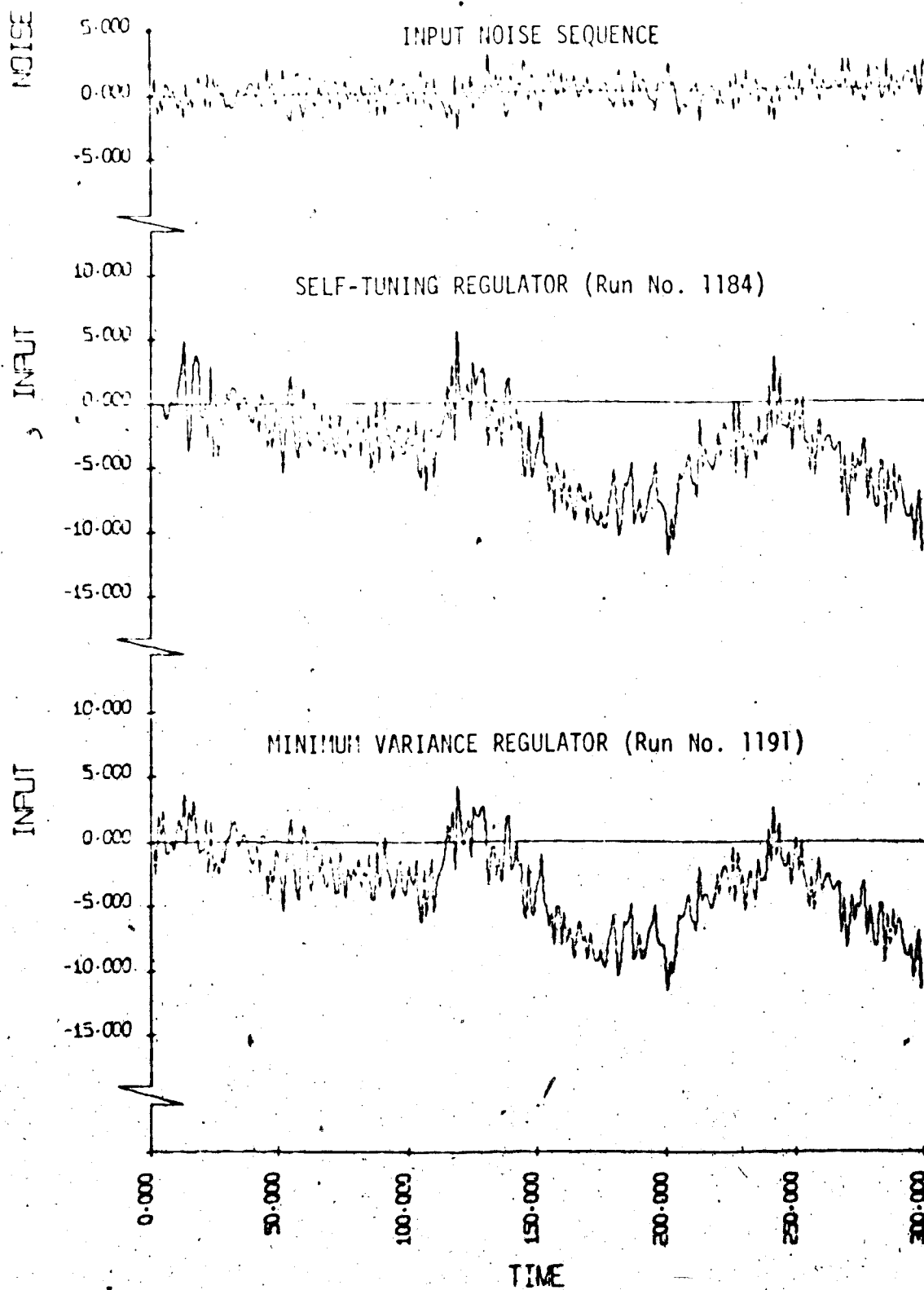


Figure 2.9 Input noise sequence and closed loop inputs for different regulators



## CHAPTER THREE

## STOCHASTIC EVAPORATOR MODELS AND DIGITAL SIMULATION STUDY

3.1. Introduction

In this chapter, several stochastic pulse transfer function models are derived starting from the fifth-order state-space evaporator model used by Hamilton [28]. The different models result from the various assumptions that can be made concerning the noise variables. The actual evaporator system and the computer program used in this simulation study are also described.

The latter part of this chapter presents the simulated responses of the double effect evaporator system when it is subjected to process and/or measurement noise and unmeasured step disturbances. In each case, the open loop response of the system is presented followed by the closed loop response when a conventional multi-loop control system is used. Finally the conclusions of the open and closed loop studies are presented.

3.2 Description of the Evaporator System

A simplified schematic flow diagram of the double effect evaporator is shown in figure 3.1. The reader is referred to the Nomenclature section for definitions of the symbols. The evaporator is a forward feed unit which operates at a nominal feed rate of 5.0 lb/min of 3.2 percent aqueous triethylene glycol and is heated by 2.0 lb/min of 250°F saturated steam. The first effect is a natural circulation calandria type unit with 32 tubes, each of which

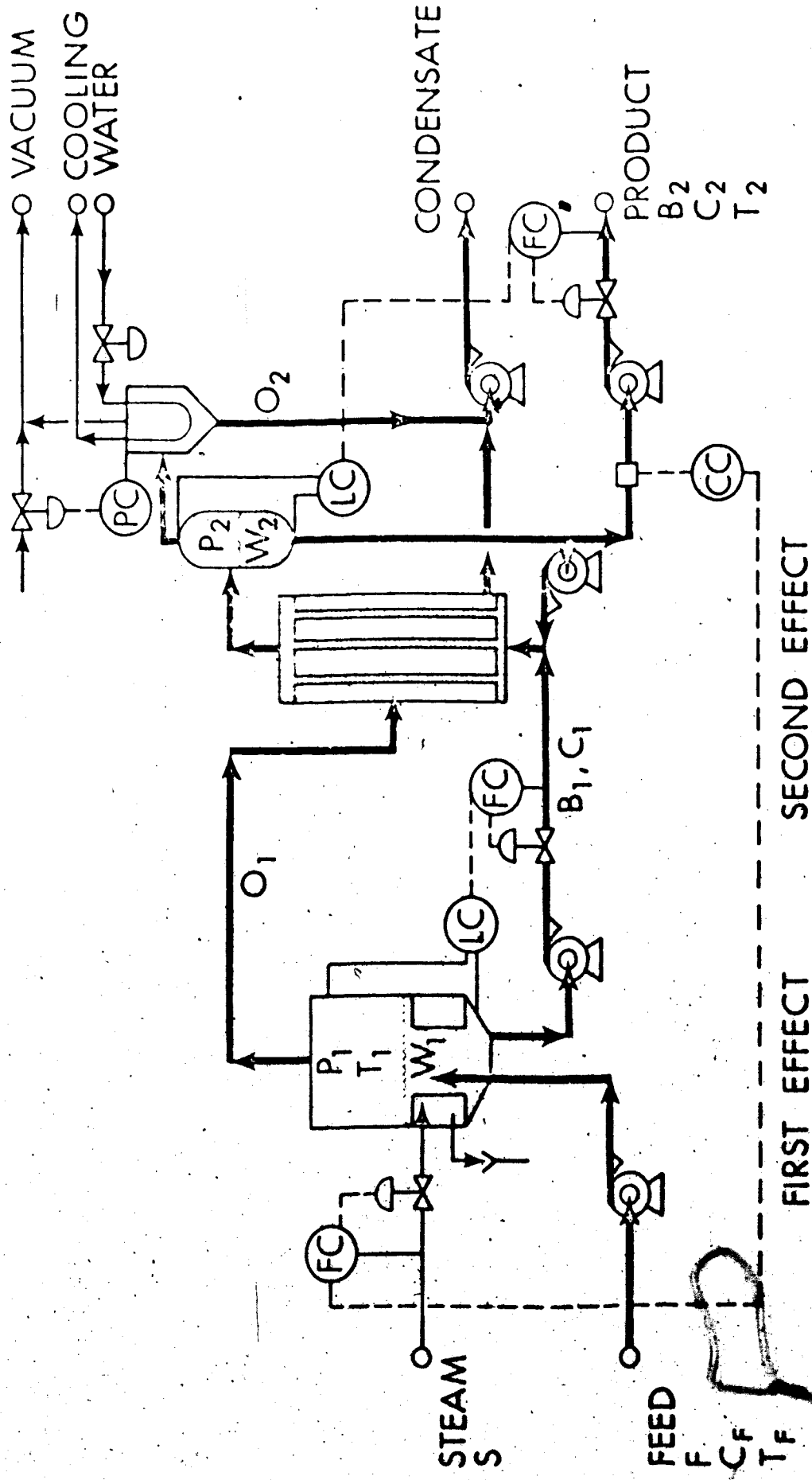


Figure 3.1 Pilot plant double effect evaporator with a conventional multi-loop control system

is eighteen inches long and has a 3/4 inch O.D. The second effect is an externally forced circulation, long tube unit with three 6 feet long, 1 inch O.D. tubes. The second effect operates under vacuum and utilizes the first effect overhead vapour to concentrate the first effect bottom stream. The final product is about 1.6 lb/min of 10 percent aqueous triethylene glycol at the normal operating conditions.

The IBM 1800 digital control computer in the Department of Chemical Engineering is interfaced to the double effect evaporator through appropriate converters and transducers. During normal operation the evaporator is controlled by means of six single control loops and four cascaded control loops. This conventional multi-loop control strategy is implemented through the standard Direct Digital Control (DDC) package. The most important controlled variable is product concentration  $C_2$  but the liquid levels,  $W_1$  and  $W_2$ , must also be controlled within operating levels. In the multi-loop control system, levels  $W_1$  and  $W_2$  are controlled by manipulating the two bottom flow rates,  $B_1$  and  $B_2$ , respectively and the product concentration  $C_2$  is controlled by adjusting the steam flow rate  $S$  into the first effect. Further details concerning the evaporator equipment, instrumentation, and control loops can be found in the theses of Newell [29] and Jacobson [30].

### 3.2.1 Stochastic State Space Model

Several models of the double effect evaporator have been developed in previous investigations by Newell [29] and Wilson [35].

They range from tenth-order non-linear state-space models to first-order transfer function models. In the simulation study, the model used is the fifth-order, linear, stochastic state-space model developed by Hamilton [28]. This theoretical model was derived from linearized material and energy balances and adequately describes the process. This discrete, stochastic model is of the form:

$$\underline{x}(t+1) = \underline{\phi}\underline{x}(t) + \underline{\Delta}u(t) + \underline{\pi}d(t) + \underline{\Gamma}w(t) \quad (3.1)$$

$$\underline{y}(t) = \underline{H}\underline{x}(t) + \underline{v}(t) \quad (3.2)$$

where

$\underline{x}$  is the state vector (5 x 1)

$\underline{u}$  is the control vector (3 x 1)

$\underline{d}$  is the disturbance vector (3 x 1)

$\underline{y}$  is the output vector (3 x 1)

$\underline{v}$  is the measurement noise vector (3 x 1)

$\underline{w}$  is the process noise vector (6 x 1)

$t$  is the sampling instant

and  $\underline{\phi}$ ,  $\underline{\Delta}$ ,  $\underline{\pi}$ ,  $\underline{\Gamma}$  and  $\underline{H}$  are constant coefficient matrices of the appropriate dimensions.

The state, control, disturbance and output vectors are defined as:

$$\underline{x} = \begin{bmatrix} W1' \\ C1' \\ H1' \\ W2' \\ C2' \end{bmatrix} \quad \underline{u} = \begin{bmatrix} S' \\ B1' \\ B2' \end{bmatrix}$$

$$\underline{d} = \begin{bmatrix} F' \\ CF' \\ HF' \end{bmatrix} \quad \underline{y} = \begin{bmatrix} W1' \\ W2' \\ C2' \end{bmatrix}$$

where  $W1'$ ,  $W2'$ , and  $C2'$  denote normalized perturbation variables, i.e.

$$\begin{matrix} \underline{ss} \\ \underline{ss} \end{matrix} \quad (\text{ss denotes the nominal steady state value})$$

The process variables are defined in the Nomenclature section and their nominal steady state values and the numerical values of the coefficient matrices are presented in the Appendix of Chapter Three.

The measurement and process noise vectors  $\underline{v}$  and  $\underline{w}$  are assumed to be zero mean, uncorrelated, Gaussian noise sequences of  $N(0, \sigma_{MN}^2)$  and  $N(0, \sigma_P^2)$  respectively. The six process noise variables in the vector  $\underline{w}$  are noise components of the three disturbance variables and the three control variables. Thus, coefficient matrix  $\underline{\Gamma}$  is specified as  $\underline{\Gamma} = [\underline{v}, \underline{\Delta}]$ .

### 3.2.2 Derivation of the Stochastic Pulse Transfer Function Models

Since the minimum variance and self-tuning regulators are based on stochastic models of the form of equation (2.1), such models will now be derived for the double effect evaporator. The starting point in the derivation is the stochastic state space model in equations (3.1) and (3.2).

In order to derive a transfer function model of the evaporator, one output, one control variable and one noise element have to be selected from the fifth-order state-space model. Then the transfer

functions relating these variables must be derived in order to determine polynomials  $A(q^{-1})$ ,  $B(q^{-1})$  and  $C(q^{-1})$ .

The pulse transfer function matrix relating the output and control variables of the state-space model is given by

$$\underline{G}_{yu}(q^{-1}) = \frac{\underline{H} \text{adj}[\underline{I} - \underline{\phi}q^{-1}]\underline{\Delta}q^{-1}}{\det |\underline{I} - \underline{\phi}q^{-1}|} \quad (3.3)$$

where "adj" denotes the adjoint matrix and "det" denotes the determinant. The pulse transfer function matrix relating the output and process noise variables is given by

$$\underline{G}_{yw}(q^{-1}) = \frac{\underline{H} \text{adj}[\underline{I} - \underline{\phi}q^{-1}]\underline{\Gamma}q^{-1}}{\det |\underline{I} - \underline{\phi}q^{-1}|} \quad (3.4)$$

Once the output, control, and process noise variables are selected, then the corresponding pulse transfer functions are the corresponding elements of the matrices in equations (3.3) and (3.4).

Let these pulse transfer functions be denoted by

$$g_{yu}(q^{-1}) = \frac{b_1q^{-1} + b_2q^{-2} + \dots + b_5q^{-5}}{1 + a_1q^{-1} + \dots + a_5q^{-5}} = \frac{q^{-1}B(q^{-1})}{A(q^{-1})} \quad (3.5)$$

and

$$g_{yw}(q^{-1}) = \frac{d_1q^{-1} + d_2q^{-2} + \dots + d_5q^{-5}}{1 + a_1q^{-1} + \dots + a_5q^{-5}} = \frac{D(q^{-1})}{A(q^{-1})} \quad (3.6)$$

Thus when measurement noise is not present (i.e.  $\underline{v} = \underline{0}$ ), the output equation will be

$$y(t) = g_{yu}(q^{-1})u(t) + g_{yw}(q^{-1})w(t) \quad (3.7)$$

or

$$y(t) = \frac{B(q^{-1})}{A(q^{-1})} u(t-1) + \frac{D(q^{-1})}{A(q^{-1})} w(t) \quad (3.8)$$

where  $y$ ,  $u$  and  $w$  are the selected elements of  $\underline{y}$ ,  $\underline{u}$  and  $\underline{w}$ , respectively.

Note that equation (3.8) is in the form of the Åström-Bohlin model in equations (2.1) and (2.3) with  $k=0$  but  $d_0 = 0$ , and  $c_0$  in equation (2.1) is equal to one. However, this difficulty can be easily resolved as shown below.

Since  $\{w(t)\}$  is a sequence of independent  $N(0, \sigma_{PN}^2)$  random variables, then it follows that the delayed sequence,  $q^{-1}w(t)$ , has the same properties and can be denoted by  $e(t)$ ; i.e.

$$q^{-1}w(t) = e(t) \quad (3.9)$$

Let  $D(q^{-1})$  in equation (3.6) be rearranged as

$$D(q^{-1}) = d_1 q^{-1} (1 + \frac{d_2}{d_1} q^{-1} + \dots + \frac{d_5}{d_1} q^{-4}) \quad (3.10)$$

Then equation (3.8) becomes

$$y(t) = \frac{B(q^{-1})}{A(q^{-1})} u(t-1) + \frac{d_1}{A(q^{-1})} (1 + \frac{d_2}{d_1} q^{-1} + \dots + \frac{d_5}{d_1} q^{-4}) q^{-1} w(t) \quad (3.11)$$

or

$$y(t) = \frac{B(q^{-1})}{A(q^{-1})} u(t-1) + \frac{d_1}{A(q^{-1})} (1 + \frac{d_2}{d_1} q^{-1} + \dots + \frac{d_5}{d_1} q^{-4}) e(t) \quad (3.12)$$

Comparing equations (3.12) and (2.3), it can be seen that a single-input, single-output stochastic model of the evaporator with only process noise has been derived with

$$\begin{aligned}
 c_1 &= \frac{d_2}{d_1} & c_3 &= \frac{d_4}{d_1} \\
 c_2 &= \frac{d_3}{d_1} & c_4 &= \frac{d_5}{d_1} \\
 & & c_5 &= 0
 \end{aligned}$$

### Alternative Models

Two alternative transfer function models can be derived for the evaporator depending on the type of noise elements which are retained from the state-space model.

In the above derivation,  $e(t)$  was specified to be an element of  $w(t)$ . However, if instead,  $e(t)$  was chosen as the element of the measurement noise vector corresponding to the chosen output, then  $A(q^{-1})$  and  $B(q^{-1})$  remain unchanged but  $C(q^{-1}) = 1$ . This model would correspond to the predictive model that was used in section 2.4.

A third type of model can be derived by retaining the appropriate element of  $v(t)$  in equation (3.2) during the derivation of the pulse transfer functions. This would give

$$y(t) = \frac{B(q^{-1})}{A(q^{-1})} u(t-1) + \frac{D(q^{-1})}{A(q^{-1})} w(t) + v(t) \quad (3.13)$$

where  $v(t)$  is the element of  $v(t)$  corresponding to the choice of  $y(t)$ . If the additional assumption is made that  $v(t) = w(t) = e(t)$ , then equation (3.13) becomes

$$y(t) = \frac{B(q^{-1})}{A(q^{-1})} u(t-1) + \frac{M(q^{-1})}{A(q^{-1})} e(t) \quad (3.14)$$

where



$$M(q^{-1}) = A(q^{-1}) + D(q^{-1}) \quad (3.15)$$

or

$$M(q^{-1}) = 1 + m_1 q^{-1} + \dots + m_5 q^{-5} \quad (3.16)$$

Equation (3.14) can be written as

$$y(t) = \frac{B(q^{-1})}{A(q^{-1})} u(t-1) + \frac{1}{A(q^{-1})} (1 + m_1 q^{-1} + \dots + m_5 q^{-5}) e(t) \quad (3.17)$$

Again comparing equations (3.17) and (2.3), it can be seen that another Åström-Bohlin model of the evaporator has been derived where

$$\lambda = 1$$

$$c_i = m_i \quad i = 1, \dots, 5$$

Note that this last model could also be derived by assuming that the original state space model is of the form

$$\underline{x}(t+1) = \underline{A}\underline{x}(t) + \underline{B}\underline{u}(t) + \underline{D}\underline{d}(t) + \underline{E}\underline{v}(t) \quad (3.18)$$

$$\underline{y}(t) = \underline{H}\underline{x}(t) + \underline{v}(t) \quad (3.19)$$

where  $\underline{E}$  is a (5 x 3) matrix. That is, by assuming that the process and measurement noise vectors are identical.

For the evaporator system, the most important control loop is the steam/product concentration loop, and the process noise variable of interest is the one corresponding to the feed flowrate since this is normally the most severe disturbance. Therefore a pulse transfer function model involving these three variables will now be derived.

The pulse transfer function relating product concentration C2 and steam S was obtained from the state-space model using the GEMSCOPE computer program [31] and the state-space model in the Appendix for Chapter Three. Since in the state space model, C2 is  $y_3$ , and S is  $u_1$ , this transfer function will be denoted by  $g_{yu_{31}}$  where:

$$g_{yu_{31}} = \frac{q^{-1}B(q^{-1})}{A(q^{-1})} = \frac{0.014q^{-1}(1-0.890q^{-1})(1+0.763q^{-1})(1-q^{-1})^2}{(1-0.439q^{-1})(1-0.922q^{-1})(1-0.960q^{-1})(1-q^{-1})^2} \quad (3.20)$$

The pulse transfer function relating product concentration C2 and  $w_1$ , the noise term corresponding to feed flow F is

$$g_{yw_{31}} = \frac{D(q^{-1})}{A(q^{-1})} = \frac{-0.002q^{-1}(1-0.712q^{-1})(1+0.879q^{-1})(1-q^{-1})^2}{(1-0.439q^{-1})(1-0.922q^{-1})(1-0.960q^{-1})(1-q^{-1})^2} \quad (3.21)$$

Therefore if measurement noise is not present, the stochastic pulse transfer function model for the evaporator is

$$y(t) = \frac{0.014 - 0.002q^{-1} - 0.009q^{-2}}{1 - 2.320q^{-1} + 1.710q^{-2} - 0.388q^{-3}} u(t-1) - \frac{0.002 + 0.0002q^{-1} - 0.001q^{-2}}{1 - 2.320q^{-1} + 1.710q^{-2} - 0.388q^{-3}} e(t) \quad (3.22)$$

Note that all three polynomials  $A(q^{-1})$ ,  $B(q^{-1})$  and  $C(q^{-1})$  in equations (3.20) and (3.21) contain a twice repeated zero of  $q=1$ . These factors cancel out and do not appear in the model of equation (3.22).

### 3.2.3 Minimum Variance Regulator for the Evaporator

For the evaporator model in the previous section, the time delay is zero. Thus equation (2.6) with  $k=0$  reduces to

$$Z(q^{-1}) = 1$$

and from the identity in equation (2.5),

$$G(q^{-1}) = 2.427 - 2.293q^{-1} + 0.388q^{-2}$$

Then the minimum variance controller for the model (3.22) is

$$u(t) = - \frac{2.427 - 2.293q^{-1} + 0.388q^{-2}}{0.014(1 - 0.127q^{-1} - 0.679q^{-2})} y(t) \quad (3.23)$$

which can be written as

$$\begin{aligned} u(t) = & -177.2 y(t) + 167.4 y(t-1) - 28.3 y(t-2) \\ & + 0.127 u(t-1) + 0.679 u(t-2) \end{aligned} \quad (3.24)$$

### 3.3 Computer Program for the Simulation Study

The objective of this simulation study was to investigate the response of the stochastic state-space evaporator model for open loop conditions and for cases when conventional multi-loop controllers were used. A computer simulation program called STR-2 was written for use on the IBM 1800 computer in the Department of Chemical Engineering. As shown in the flow chart of figure 3.2, the program begins with constant initialization and various option specifications. The outputs are calculated from the stochastic fifth-order state-space evaporator model in equations (3.1) and (3.2). Process and/or measurement noise of different noise levels can be added. Control options include no control, conventional multi-loop control, the self-tuning

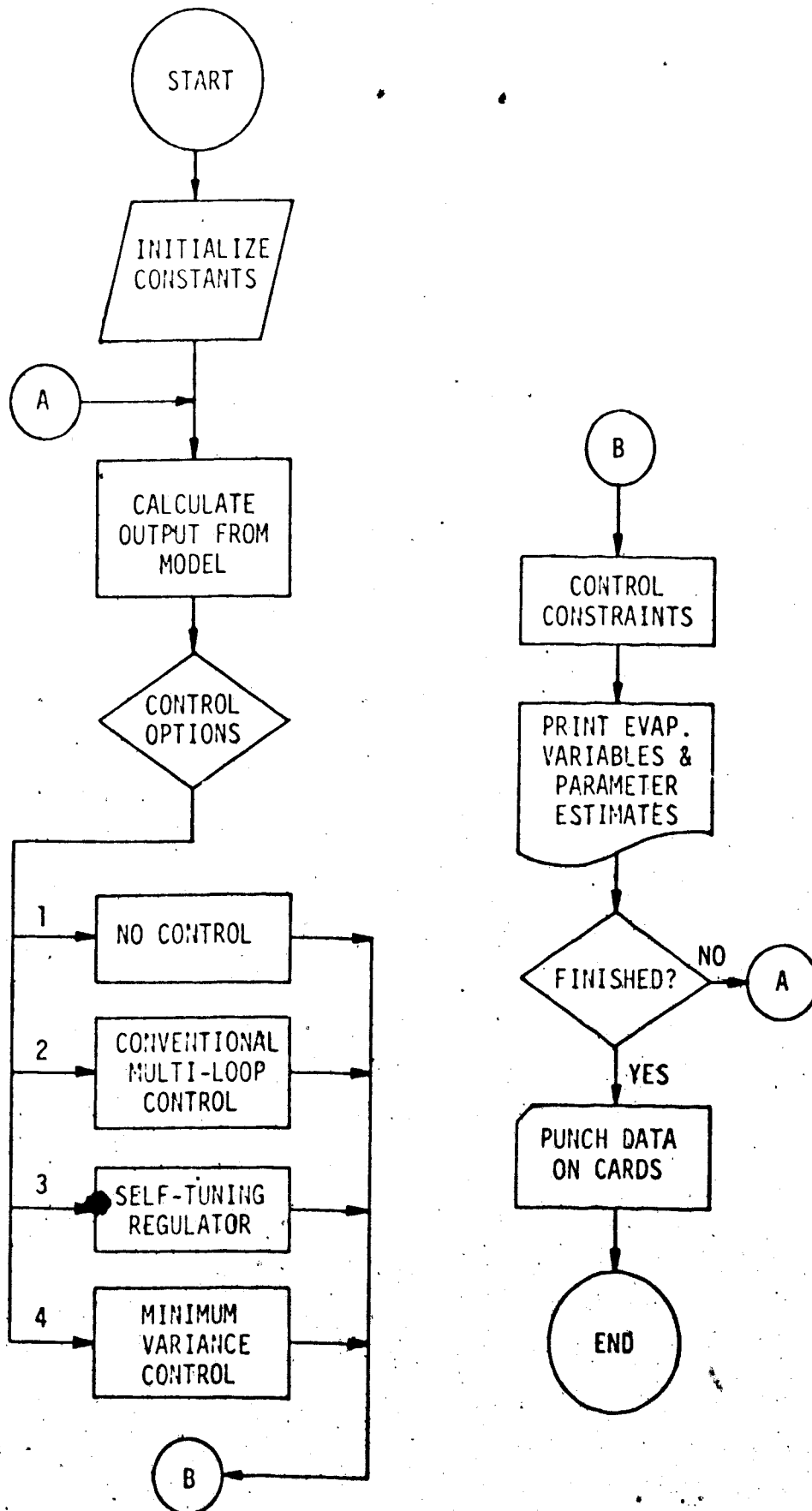


Figure 3.2 Flow chart for computer program STR-2

regulator, or minimum variance control. For all closed loop runs, the control signals are constrained to conform to the physical limitations of the actual evaporator system.

In the simulation study, evaporator variables of interest and parameter estimates of the predictive model for each run were printed. The evaporator variables and the parameter estimates were also punched on cards for the purpose of plotting. Two plotting program coreloads, RBN02 and JCH10, written by Newell [32] and modified slightly by Hamilton [33] were used to plot the evaporator variables.

### 3.4 Open Loop Results

The open loop runs were made with six process noise variables each at the 10% level (i.e.  $\sigma_{pH} = 0.1$ ) and with or without unmeasured step disturbances. These runs were made to give some indication of the fluctuations of evaporator variables. These runs were also made to serve as a comparison for the closed-loop runs. Different Gaussian random noise sequences with zero means were generated for the six process noise variables in each run and these same noise sequences were repeated for all other runs. The disturbance and manipulated variables that are plotted do not include process noise (except for the first figure), for the sake of clarity. This avoids the extensive overlapping of noisy curves that would result if the noise components were included. In all the simulation runs the system was assumed to be at the normal steady state at the start of a run. A list of the runs presented in this chapter is shown in Table 3.1.

TABLE 3.1

## OPEN LOOP AND MULTI-LOOP PROPORTIONAL CONTROL RUNS

## Note:

All runs included six process noise variables (zero mean and standard deviation of 0.1)

Run number 3259 included measurement noise in all three outputs (zero mean and standard deviation of 0.05)

FIGURE	RUN NO.	STEP DISTURBANCES	$K_{C2}$	ACCUM. LOSS (at $t=300$ )	
3.3	3107	-	-	0.0325	} OPEN LOOP
3.4	3141	(-20%F, +20%F)	-	0.3805	
3.5	3255	(-30%CF)	-	6.1353	
3.6	3137	-	-4.89	0.0325	} MULTI-LOOP PROPORTIONAL CONTROL
3.7	3136	-	0.0	0.0942	
3.8	3215	-	-20.0	0.0217	
3.9	3130	(-20%F, +20%F)	-4.89	0.1215	
3.10	3176	(-30%CF)	-4.89	0.1061	
3.11	3259	-	-4.89	0.2971	

### 3.4.1 Effect of Process Noise

As shown in figure 3.3, when the only disturbances are the six process noise variables with  $\sigma_{PN} = 0.1$ , all of the state variables remained fairly constant except for  $W_1$ , the level in the first effect. This shows that the magnitude of the process noise was not large enough to cause significant fluctuations in the evaporator variables.

The manipulated and disturbance variables (S, B1, B2, F, CF, TF) which are Gaussian random noise sequences are only shown in figure 3.3. In subsequent simulation runs, these additive noise components are omitted to avoid overlapping of curves.

### 3.4.2 Effect of Unmeasured Step Disturbances

Figures 3.4 and 3.5 illustrate the effects of unmeasured step disturbances on the open loop system. In figure 3.4, a 20% step down in feed flow followed by a 20% step up approximately 50 minutes later were applied. While most of the variables remain within reasonable limits, the first effect level was drained completely due to the integrating nature of the liquid level. (The legend for these and succeeding figures is explained in the Appendix for Chapter Three.)

In figure 3.5, a 30% step down in feed concentration was applied. As a result the concentration in the first effect dropped which in turn caused the product concentration to decrease.

Thus for the uncontrolled evaporator system, unmeasured step disturbances produce poor control.

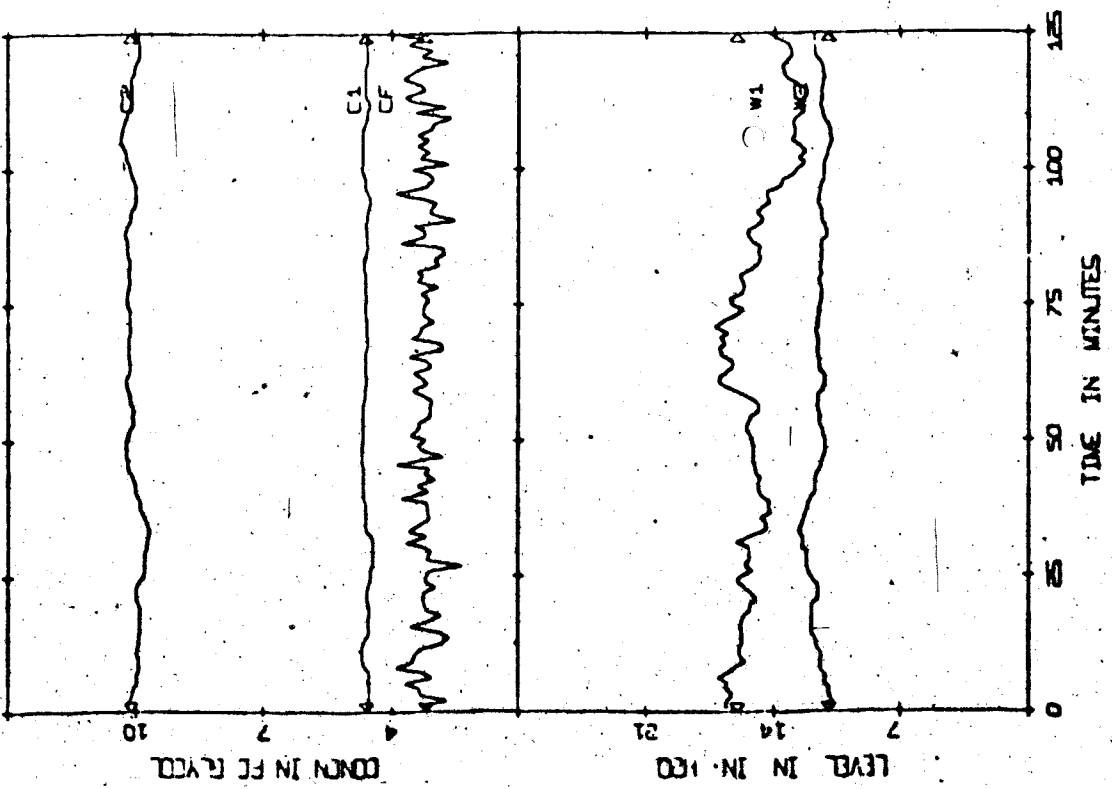
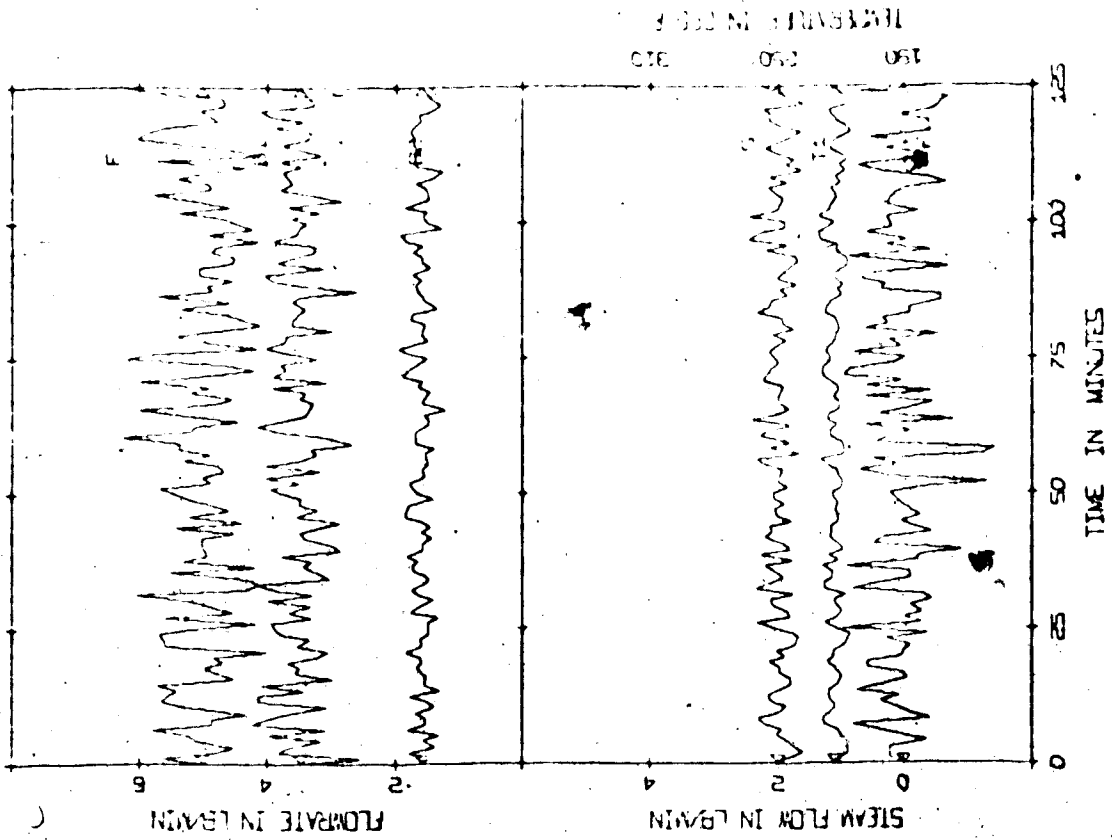


Figure 3.3 - Evaporator Response (SIM/OL)



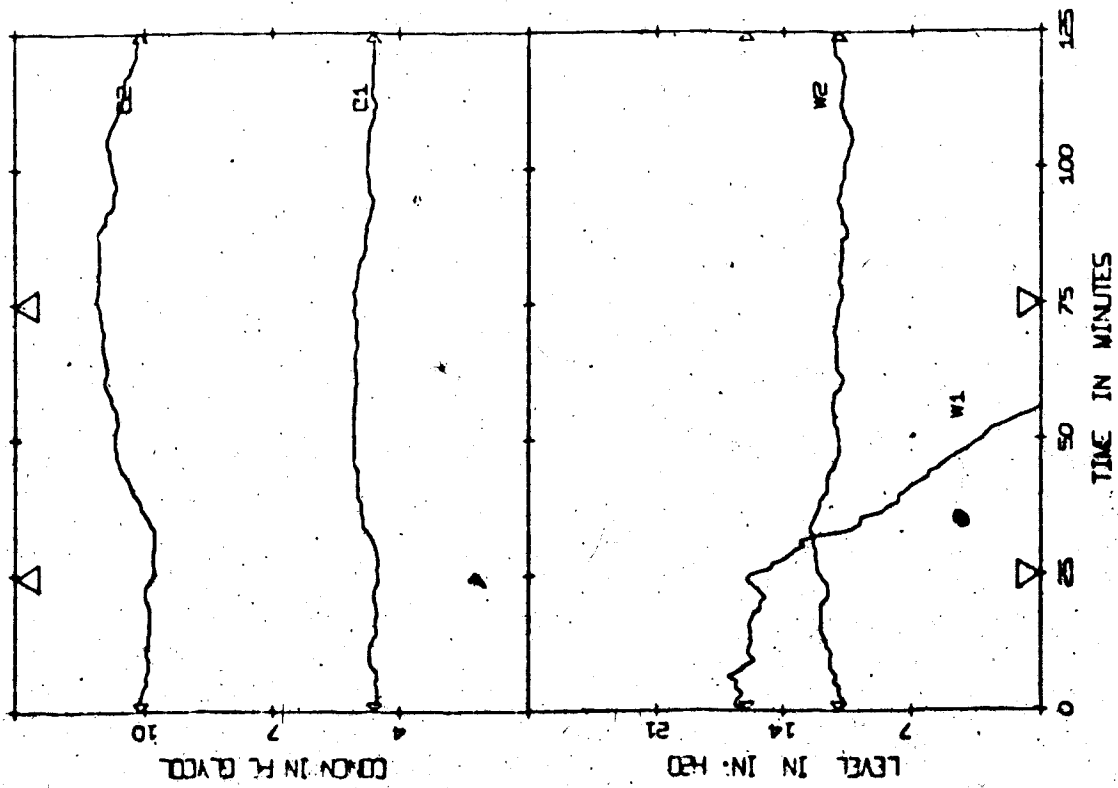


Figure 3.4 Evap. response (SIM/-20°F, +20% F/OL)

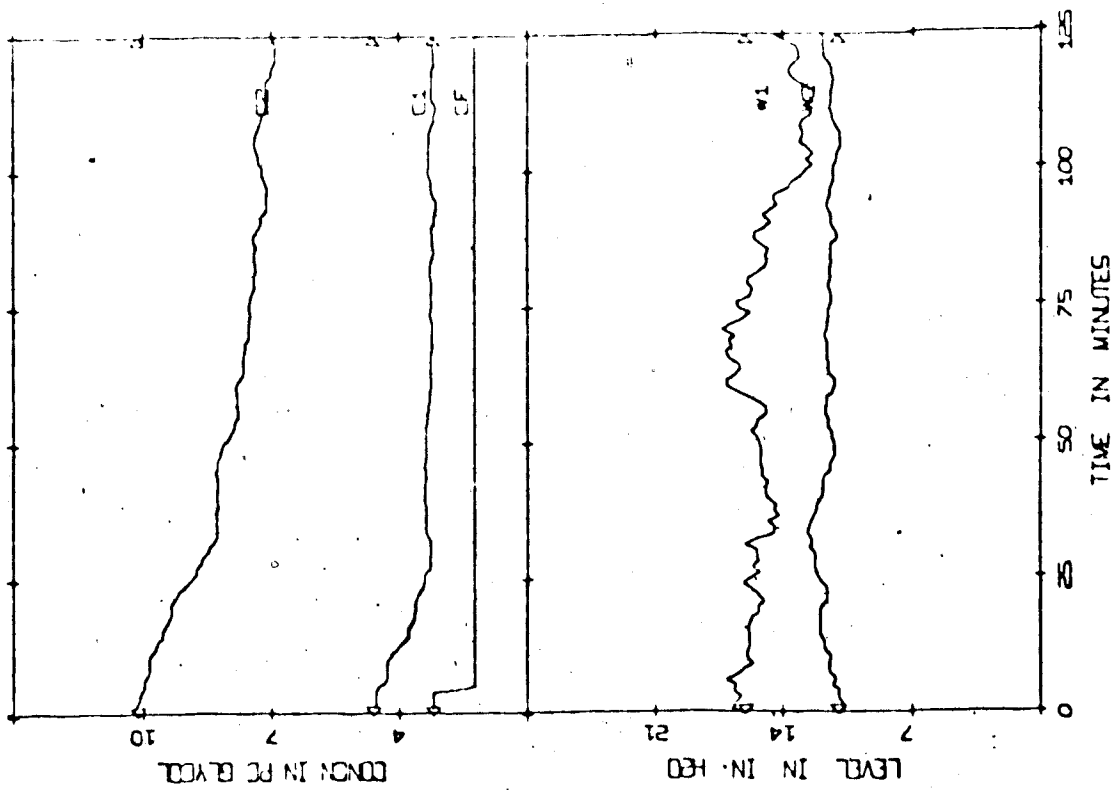


Figure 3.5 Evap. response (SIM/-30°F, CF/OL)

### 3.5 Conventional Multi-Loop Control

A simple control strategy that has been implemented on the actual evaporator system with fairly good success is multi-loop digital proportional control. As mentioned in section 3.2, the three major control loops are the two level loops and the product concentration loop. The primary control objective is to maintain product concentration at the normal steady state value.

In this section, simulation runs were made using conventional proportional controllers in the three major control loops. The purpose of these runs was to investigate the effects of process noise, process and measurement noise and also the effect of unmeasured step disturbances on the conventional control system. The nominal proportional gains were specified to be the constants used by Oliver [33]. The effect of using different proportional gains for the product concentration controller was also investigated.

#### 3.5.1 Magnitude of Proportional Gain in Steam-Product Concentration Loop

The nominal proportional gains are [34],

$$W1/B1 \text{ loop} : K_{W1} = 3.52$$

$$W2/B2 \text{ loop} : K_{W2} = 15.8$$

$$C2/S \text{ loop} : K_{C2} = -4.89$$

The control signals from the three loops were constrained to conform to the limitations of the real system. They were constrained as follows:

$$-1.0 \leq u_1 \leq +0.5$$

$$-1.0 \leq u_2 \leq +1.0$$

$$-1.0 \leq u_3 \leq +1.0$$

Figure 3.6 illustrates the response of the evaporator when multi-loop proportional control is used and six process noise variables are present. The control of C2 is fair while W1 is significantly improved over the open loop response in figure 3.3.

Figures 3.7 and 3.8 show the evaporator responses when  $K_{C2}$  is 0 and -20.0, respectively. The levels, W1 and W2, and the two bottom flow rates, B1 and B2, are omitted since they are very similar to the curves in figure 3.6. From figures 3.6 to 3.8, it appears that increasing the proportional gain  $K_{C2}$  results in higher frequency oscillations and smaller deviations in C2. However when  $K_{C2}$  is increased to -50.0 (figure not shown), the frequency of the C2 oscillations increases but the magnitude of the deviations from steady state also increases. Thus the C2 response can be improved by increasing the numerical values of the gain only up to a certain limit, beyond which the performance deteriorates.

### 3.5.2 Effect of Step Disturbances

When a disturbance of 20% step-down in feed flow followed by 20% step up in feed flow was applied, the C2 response in figure 3.9 initially increased and S decreased because of the sudden decrease in feed flow rate. This behaviour is characteristic of proportional control since there is always an offset after a step

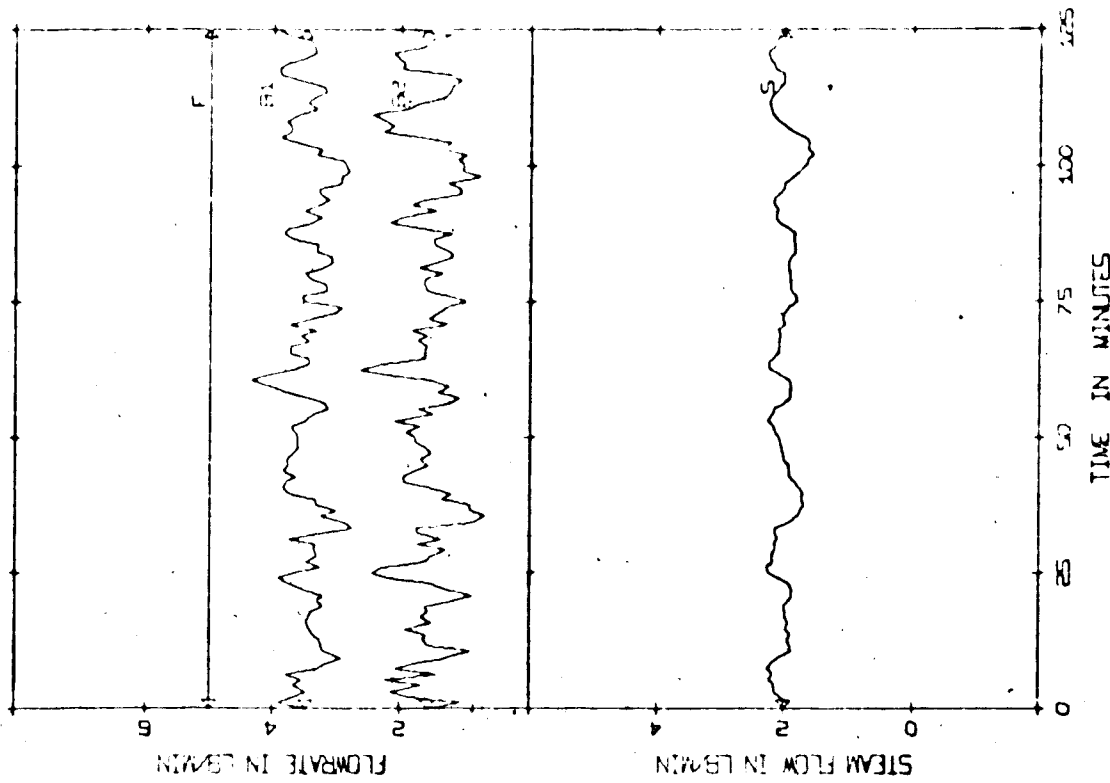
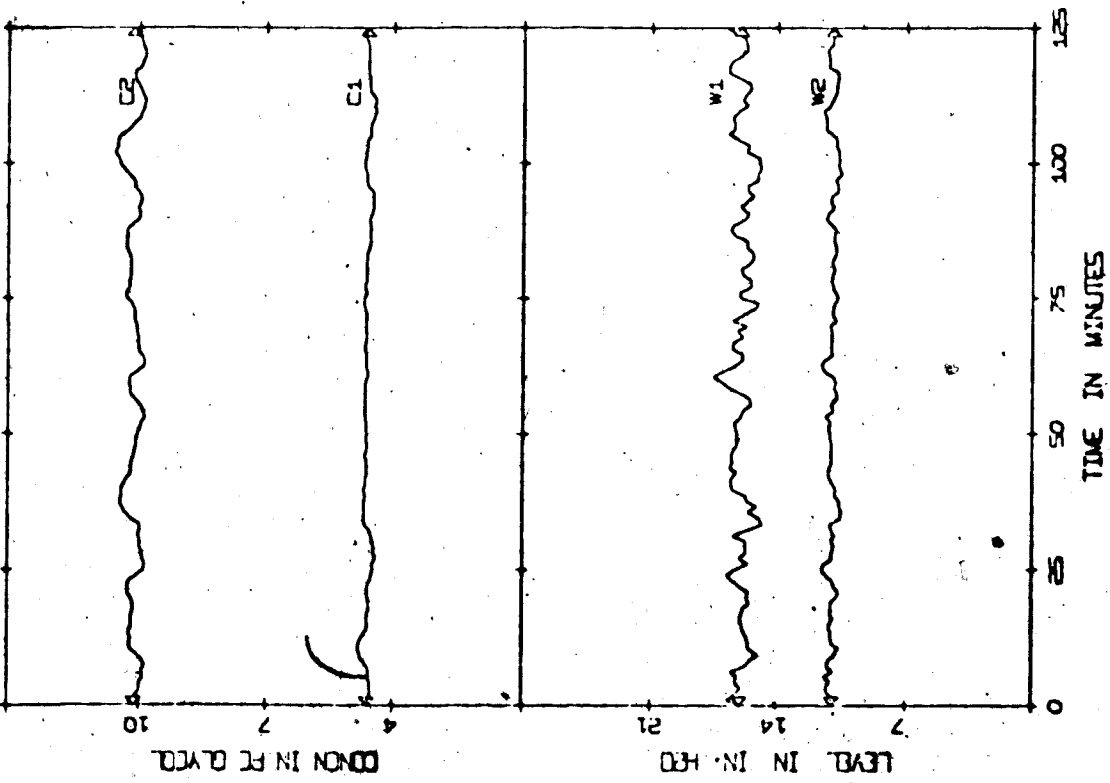


Figure 3.6 Evaporator Response (SIM/ML),  $K_{C2} = -4.89$

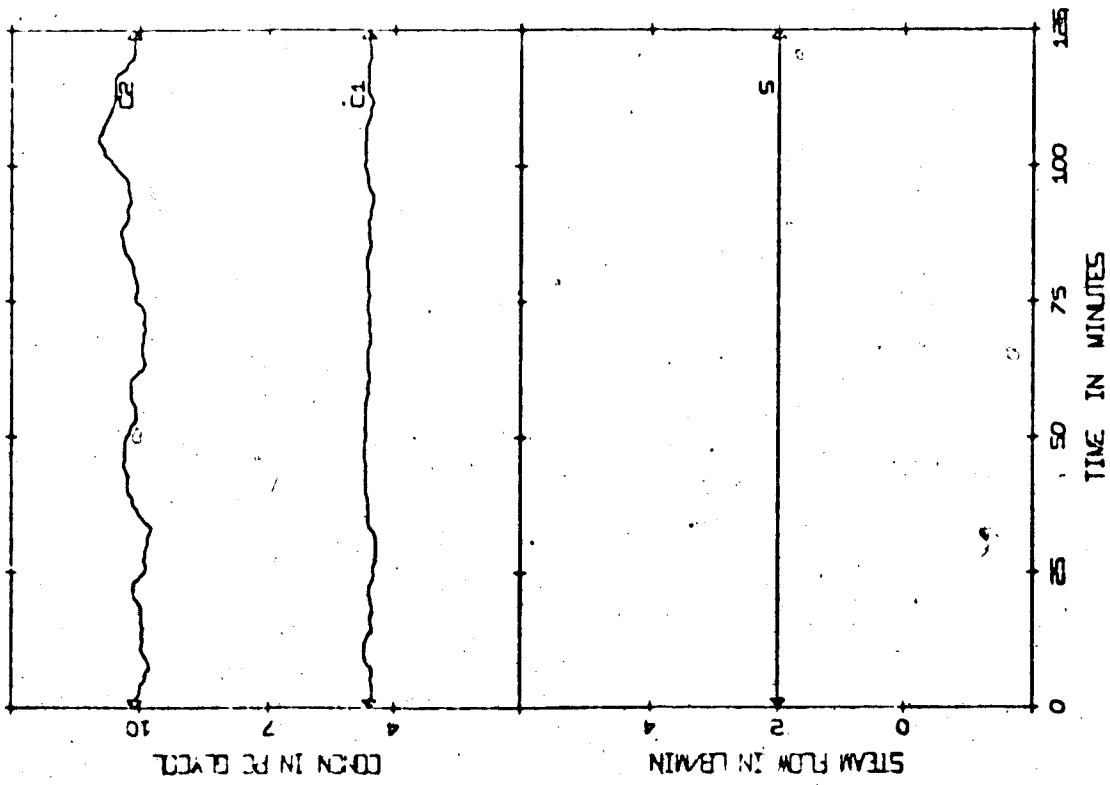


Figure 3.7 Evap. response (SIM/ML),  $K_{C2} = 0.0$

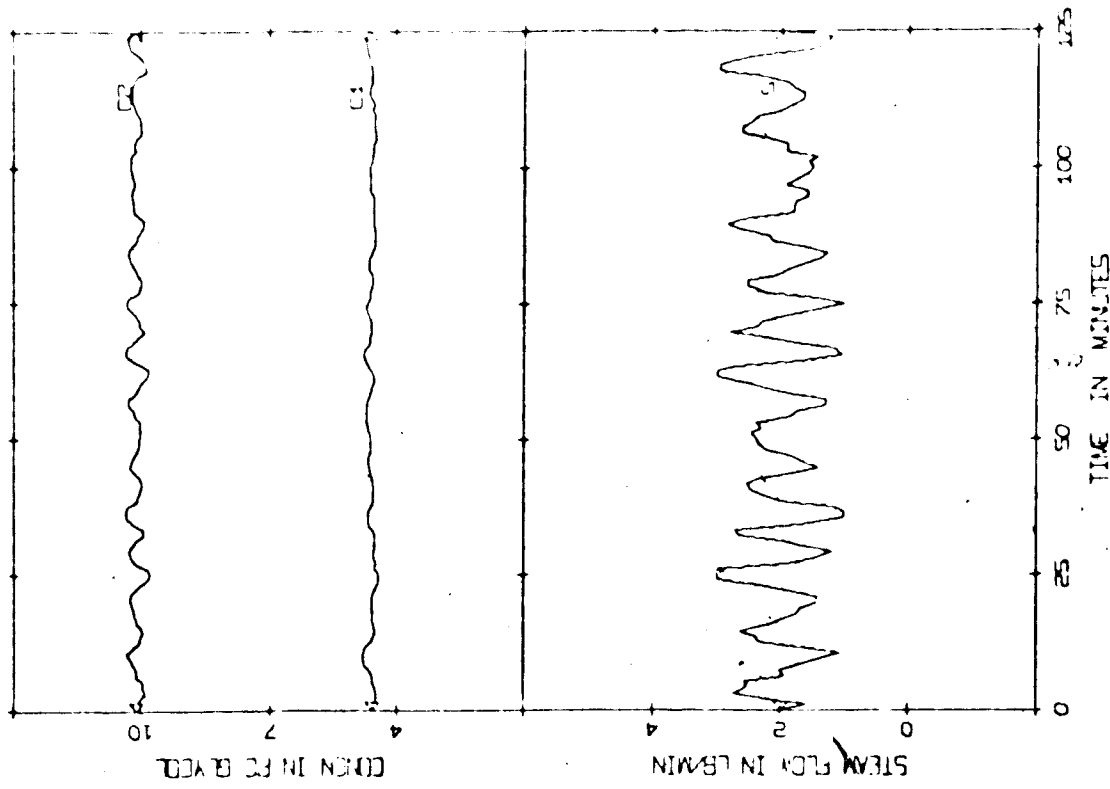


Figure 3.8 Evap. response (SIM/ML),  $K_{C2} = -20.0$

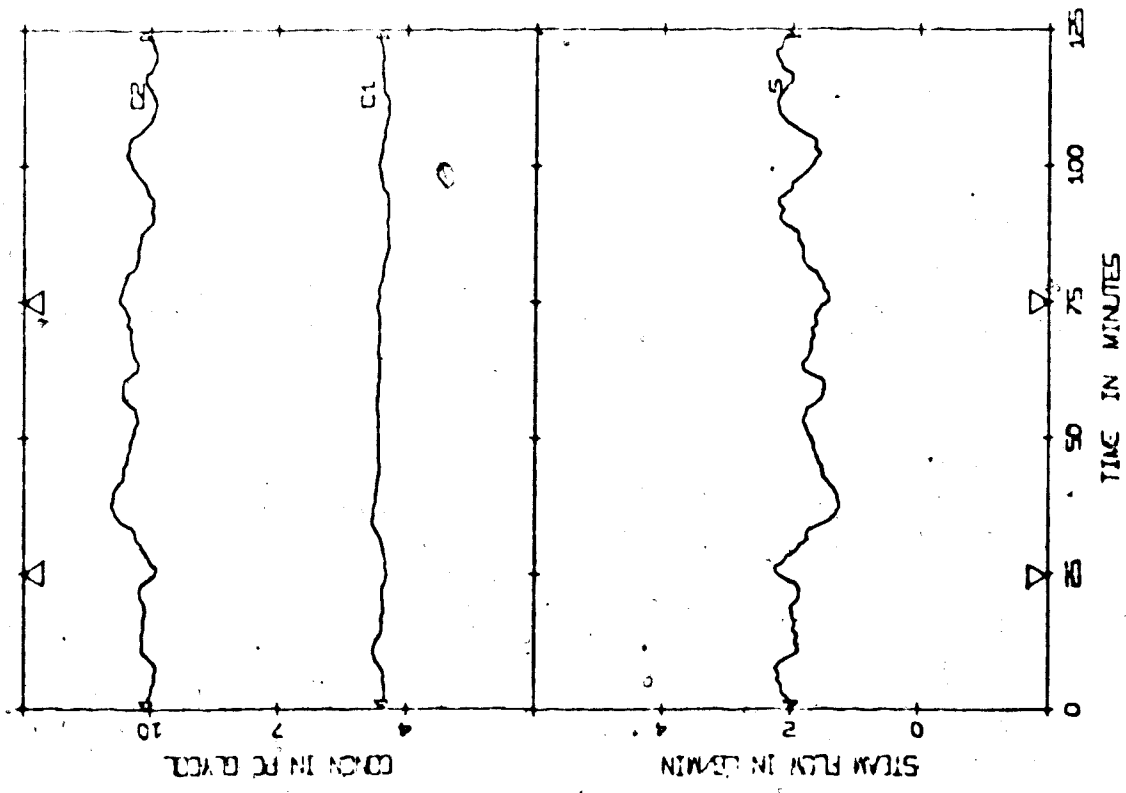


Figure 3.9 Evap. response (SIM/-20% F, +20% F/ML)

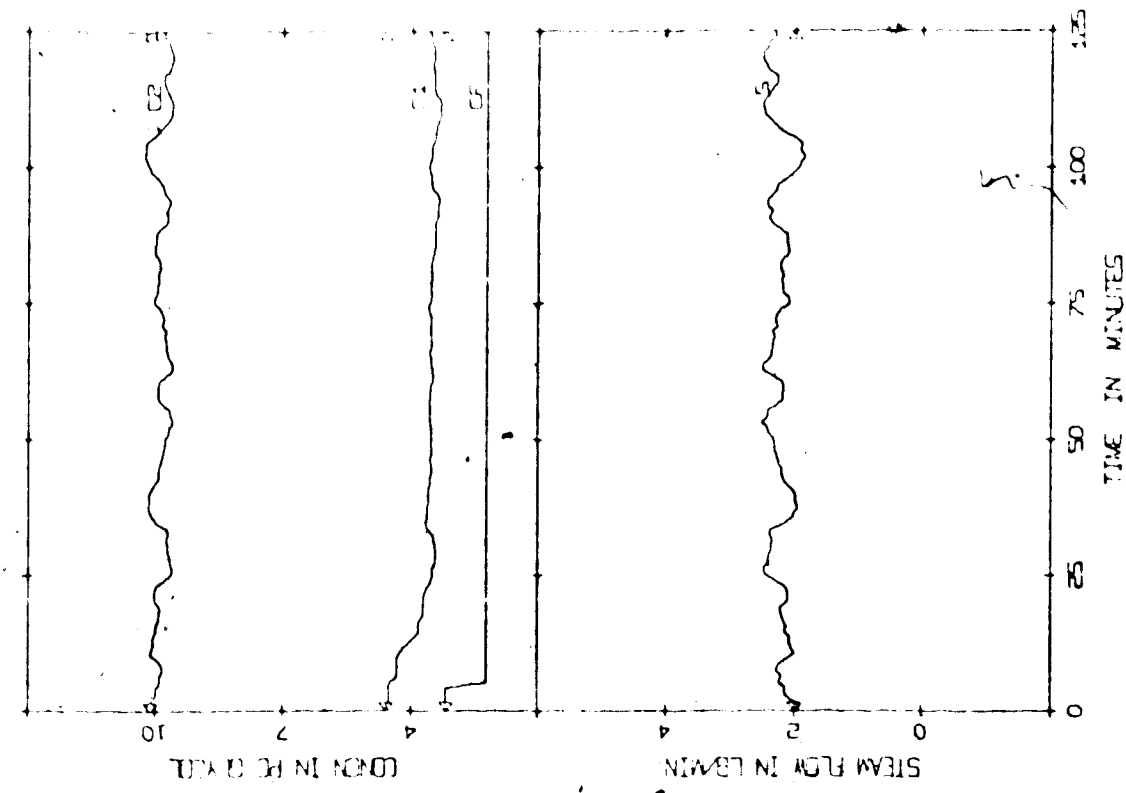


Figure 3.10 Evap. response (SIM/-30% CF/ML)

disturbance. Furthermore, since a linear model is used in the study, the effects of step disturbances and process noise are additive. This is apparent from a comparison of figures 3.6 and 3.9.

Figure 3.10 shows the evaporator response to a 30% step down in feed concentration. Once again the process noise variables give a certain pattern to the C2 curve and the step disturbance results in a general decrease in C2 and an offset.

### 3.5.3 Effect of Measurement Noise

When measurement noise with  $\sigma_{MN} = 0.05$  was added to each of the three outputs and process noise is also present; the results in figure 3.11 were quite similar to the corresponding run without the measurement noise (see figure 3.6) except there were more fluctuations in the outputs. The measurement noise also produced large fluctuations in the three control variables S, B1, and B2 as would be expected. Note that the output variables plotted in figure 3.11 do not include the additive measurement noise elements, for the sake of clarity.

Several other runs were tried using different proportional gains in the S/C2 loop. As the gain was decreased the C2 response improved. In fact, the best C2 response was obtained using zero gain in the S/C2 loop.

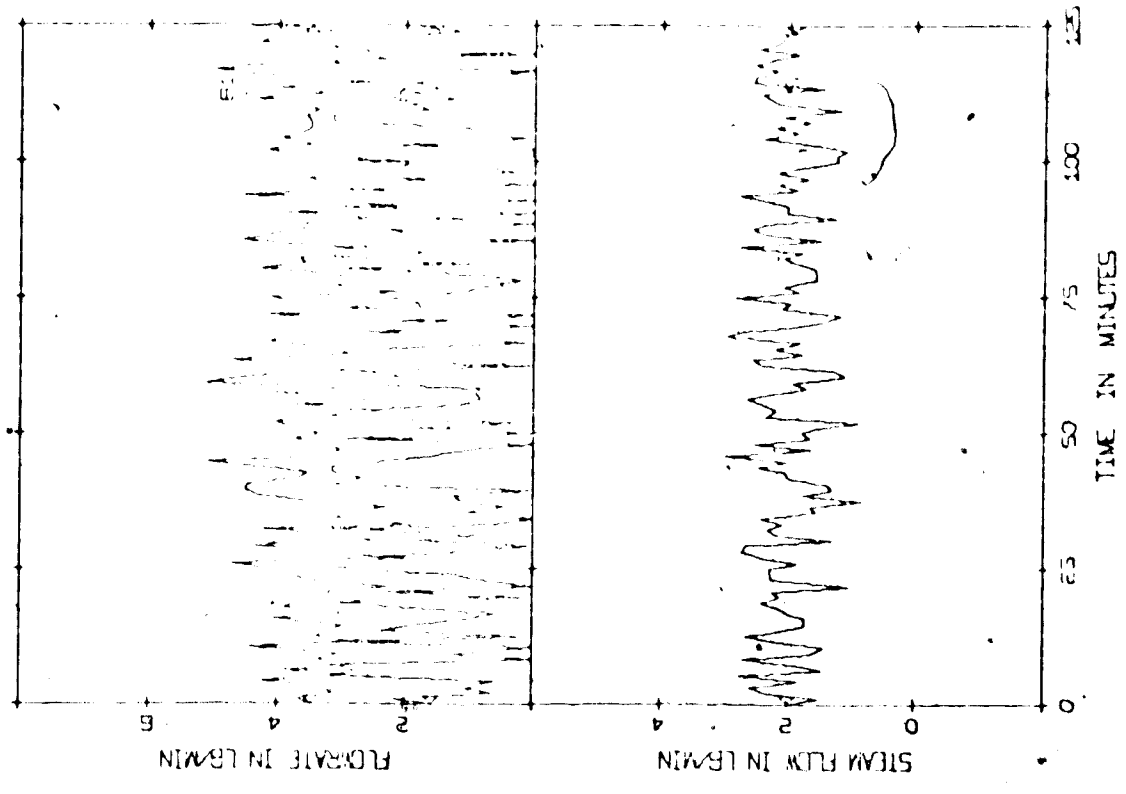
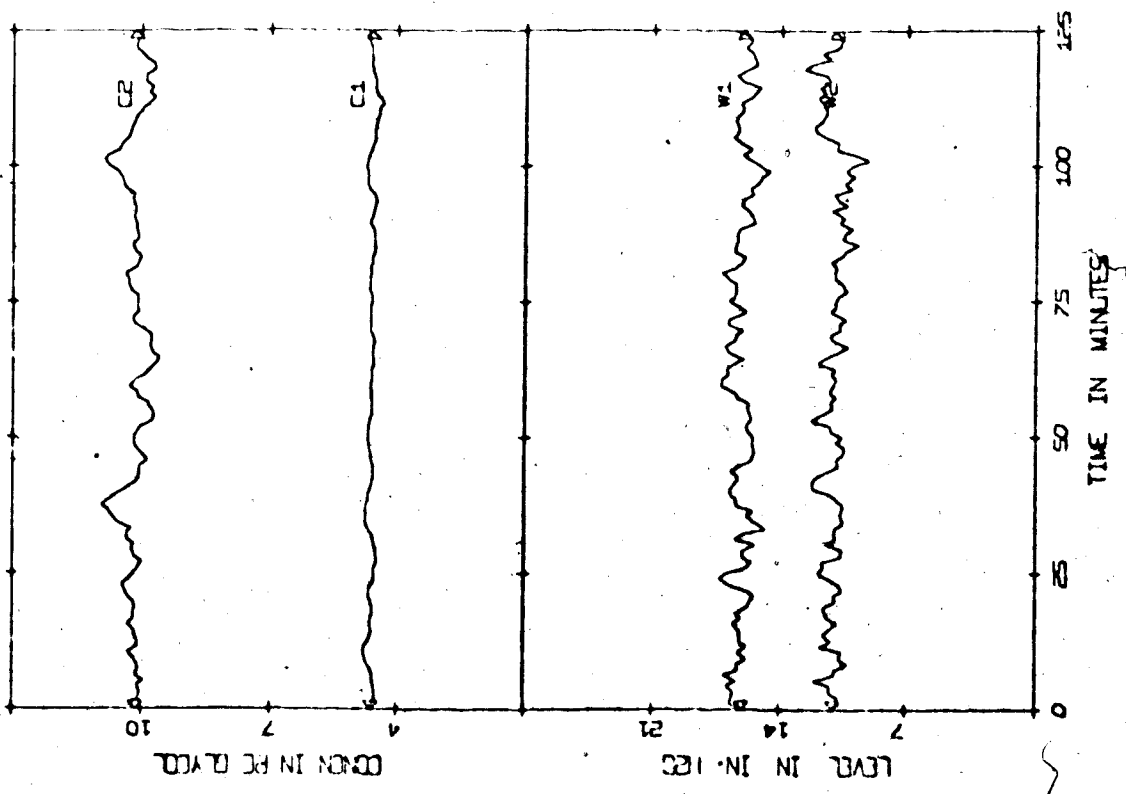


Figure 3.11 Evaporator response (SIM/ML), measurement noise included,  $c_{MN} = 0.05$ ,  $K_{C2} = -4.89$  55



### 3.6 Conclusions

Several stochastic pulse transfer function models of the evaporator have been derived starting from a stochastic state-space model. The particular form of the pulse transfer function depends on how the noise variable is specified (i.e. process noise vs measurement noise). The open loop simulation results indicate that 10% process noise in the three disturbance and three control variables does not significantly effect the evaporator. However, unmeasured step disturbances do have detrimental effects on the system. For example, a 20% step down in feed flow causes the first effect to drain completely.

When conventional multi-loop proportional control is used, the process noise caused small fluctuations in all three outputs. With the addition of a step disturbance, larger offsets occurred. When measurement noise is added, the fluctuations in the actual product concentration increase while the three control signals exhibited much larger fluctuations. Increasing the proportional gain of the product concentration controller results in increased oscillations but smaller amplitude fluctuations in product concentration. However, this is only true up to a certain point, beyond which the control of C2 deteriorates.

## CHAPTER FOUR

A SELF-TUNING REGULATOR FOR THE DOUBLE EFFECT EVAPORATOR:  
SIMULATION RESULTS4.1 Introduction

This chapter presents simulation results for the evaporator when the self-tuning regulator (STR) is used to control product concentration  $C_2$ . It was mentioned in the previous chapter that it would be more realistic to use the fifth-order state-space model in the simulation rather than the pulse transfer function model because the actual evaporator is an interacting multivariable system. Therefore it would not be realistic to consider only a single-output, a single-input, and one noise variable and neglect their interactions with the other evaporator variables.

For purpose of comparison with the conventional multi-loop control scheme, the two level control loops were left unchanged but the proportional controller for the  $S/C_2$  control loop was replaced by the self-tuning regulator. Thus the input variable of the predictive model is steam flow rate, the output variable is the product concentration, and the noise variable is in effect a combination of all process noise and measurement noise variables plus the disturbances due to interactions between the evaporator variables. A block diagram showing the implementation of a self-tuning regulator in the multi-variable evaporator system is shown in figure 4.1.

This chapter investigates the various design options that are available in the self-tuning regulator and its operation under

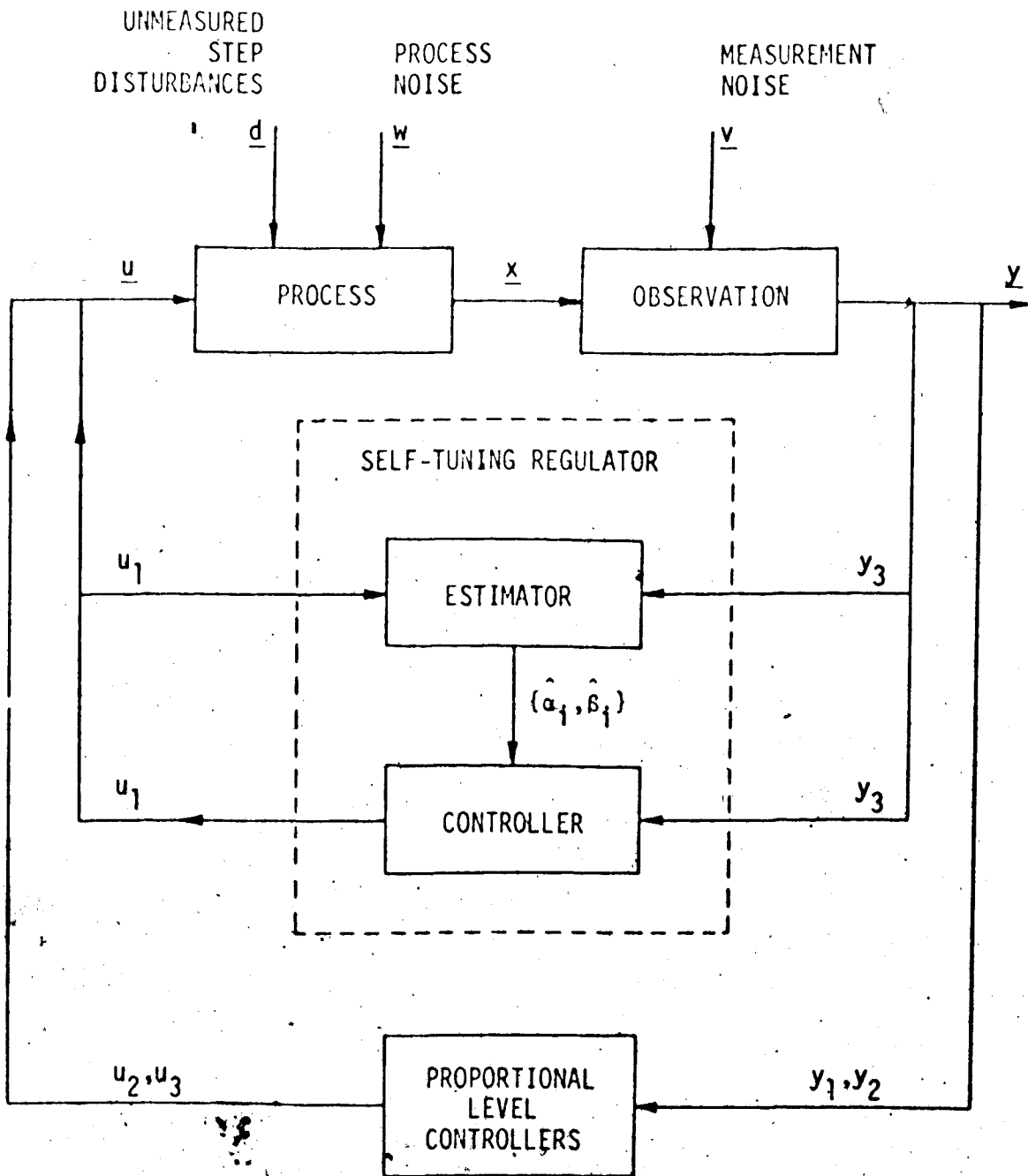


Figure 4.1 Block diagram of the closed loop system: the self-tuning regulator is used to control C2 and conventional proportional controllers are used to control W1 and W2

realistic conditions. Practical considerations in applying the self-tuning regulator and the conclusions of the simulation study are presented at the end of the chapter. A list of simulation runs for sections 4.2, 4.3 and 4.4 is shown in Table 4.1.

#### 4.2 Base Case Conditions

The self-tuning algorithm has been explained in detail in section 2.4. Basically the algorithm can be divided into two parts at every sampling instant: estimation and control. Before the self-tuning algorithm can be used, the constants and initial values listed below must be specified:

Exponential forgetting factor  $\mu$

Initial covariance matrix  $\underline{P}(0)$

Initial parameter estimates  $\underline{\hat{\theta}}(0)$

Scaling factor  $\beta_0$

Model order  $n$

Time delay  $k$

The simulation study of the second order numerical example in section 2.5 has provided experience in the selection of these factors. Based on this experience a set of constants and initial parameters was selected for the base case run and served as a basis of comparison for the other runs.

The exponential forgetting factor  $\mu$  was chosen to be 1.0 so that there would be no exponential weighting of past data. The initial parameter estimates,  $\{\hat{\theta}_i(0)\}$ , were chosen to be zero based on the assumption that prior information about the evaporator system

TABLE 4.1

RECURSIVE LEAST SQUARE ESTIMATES OF MODEL PARAMETERS AFTER 120 INTERVALS (128 MIN)

Note: Six process noise variables are used, each is an independent Gaussian noise sequence with zero mean and  $\sigma_{PN} = 0.1$   
 The base case conditions are:  $\mu = 1.0$ ,  $P(0) = 10,000 I$ ,  $\hat{\theta}(0) = 0$   
 $\beta_0 = 0.014$ ,  $n = 3$ ,  $k = 0$

FIGURES	RUN NO.	BASE CASE CONDITIONS	PARAMETER ESTIMATES (at t = 128 min)						ACCU. LOSS (at t = 128 min)
			$\hat{\alpha}_1$	$\hat{\alpha}_2$	$\hat{\alpha}_3$	$\hat{\beta}_1$	$\hat{\beta}_2$		
4.2, 4.4	3109	-	-1.258	0.102	0.172	1.076	0.183	0.1224	
4.3, 4.5	3224*	$\beta_0$ estimated	-1.264	0.078	0.238	0.013	0.002	0.0293	
4.6	3143	$\mu = 0.96$	-1.357	0.234	0.120	0.884	-0.007	0.1228	
4.7	3189	$\mu = 0.90$	-1.330	0.043	0.225	0.766	0.092	0.1224	
4.8, 4.10	3151	$P(0) = 100 I$	-1.252	0.108	0.182	1.068	0.238	0.0265	
4.9, 4.11	3152	$\hat{\theta}(0) = I$	-0.732	0.027	0.244	0.208	0.200	0.0242	
4.12, 4.14	3171	$\hat{\theta}_1(0) = 5$	-1.271	0.081	0.181	1.047	0.179	0.0349	
4.13, 4.15	3172	$\hat{\theta}_1(0) = -10$	-1.271	0.081	0.206	1.056	0.194	0.1104	
4.16, 4.18	3148	$\beta_0 = 0.1$	-0.270	-2.080	1.240	-0.102	0.170	0.1833	
4.17, 4.19	3149	$\beta_0 = 0.001$	-0.917	-0.105	0.193	10.700	4.300	0.1235	
4.20, 4.22	3178	$n = 2$	-1.415	-0.454	-	0.757	-	0.0482	
4.21, 4.23	3179**	$n = 4$	-1.213	0.084	0.140	1.100	0.240	0.7985	
4.24, 4.25	3188***	$k = 2$	-0.744	-0.221	0.242	1.700	0.860	0.1223	

\*  $\hat{\beta}_0 = 0.0148$   
 \*\*  $\hat{\alpha}_4 = 0.043$ ,  $\hat{\beta}_3 = -0.110$   
 \*\*\*  $\hat{\beta}_3 = -0.660$ ,  $\hat{\beta}_4 = -0.490$

was unknown. An initial covariance matrix of  $\underline{P}(0) = 10,000 \underline{I}$  was used since there was little confidence in the initial parameter estimates. Results obtained from the derivation of the pulse transfer function model were used to select the other constants for the base case run. The correct order of the predictive model and the correct time delay were used, that is,  $n=3$  and  $k=0$ . Also the correct scaling factor,  $\beta_0 = 0.014$ , was used. In the simulation runs, the noise covariance was assumed to be the correct value, i.e.  $R = \sigma_{PN}^2$ . This choice was made since preliminary runs indicated that the value of  $R$  was not critical. For example,  $R=1$  and  $R=0.01$  gave almost identical results for the case when  $\sigma_{PN}^2 = 0.01$ . Wittenmark and Wieslander [11] have recommended using  $R=1$  if the actual noise covariance is not known.

The base case run was carried out using these constants and initial parameters. The response of the system and the parameter estimates when process noise is present are shown in figures 4.2 and 4.4, respectively. The large "bump" at the beginning of the  $C_2$  curve can be explained as follows. Since zero initial parameter estimates were used, it takes several sampling intervals before the recursive least squares estimates have numerical values other than zero, and several more intervals before the estimates are near their final values (see figure 4.4). Therefore during this initial transient period, the control of  $C_2$  may not be good, which is the case in this run. The algorithm was able to adapt fairly rapidly, and after about 20 minutes, the control of  $C_2$  was quite good. The control variable  $S$  exhibits bang-bang behaviour due to the large parameter values used in the control law. In figure 4.4 and succeeding plots of

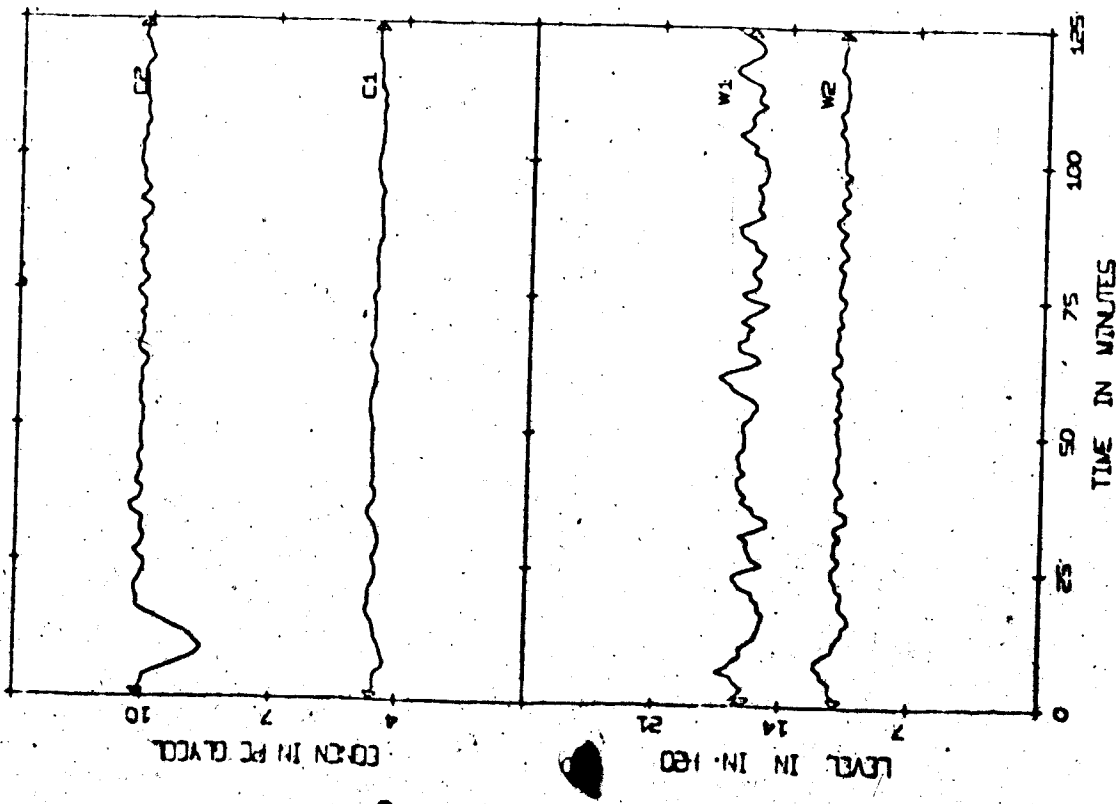
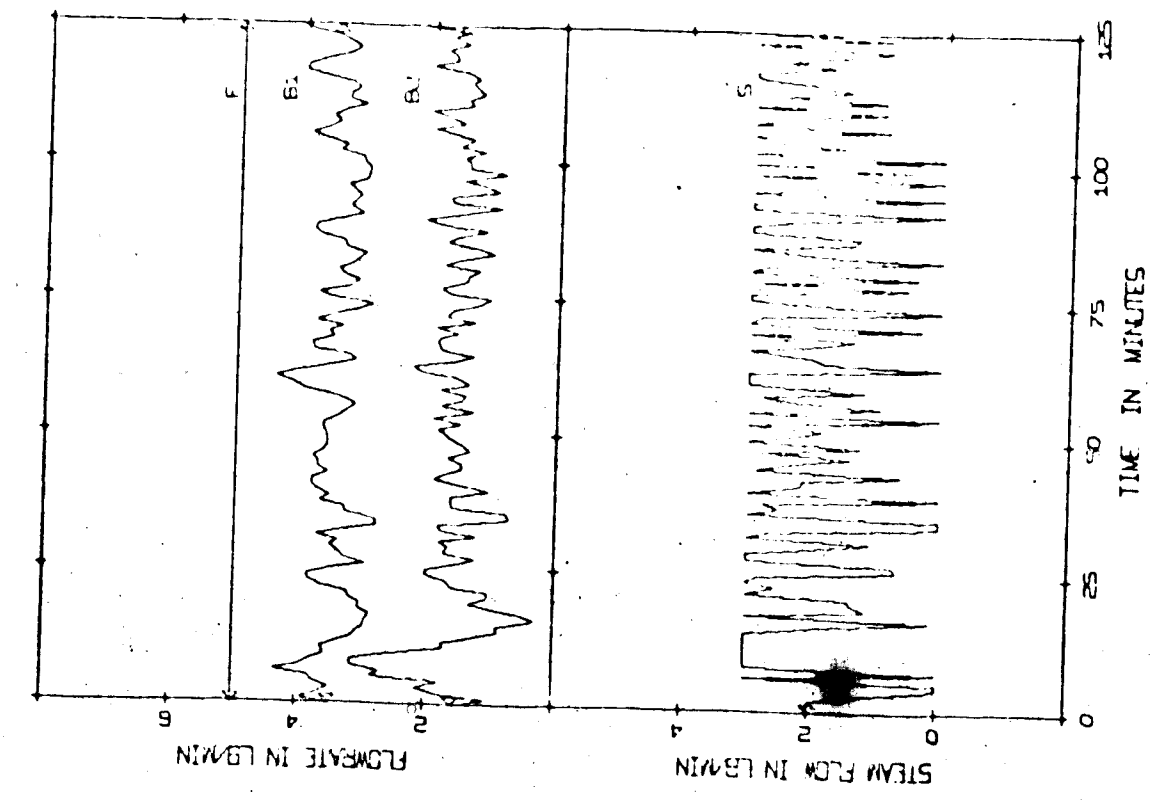


Figure 4.2 Evaporator response (SIM/STR), base case

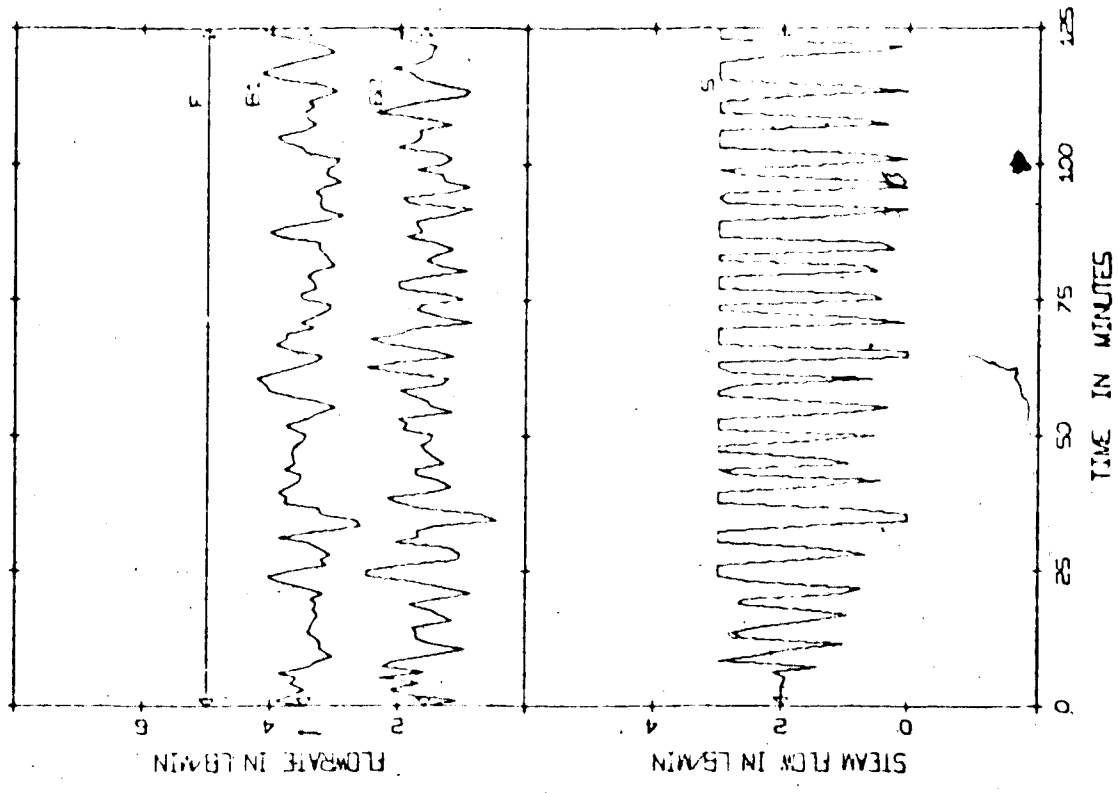
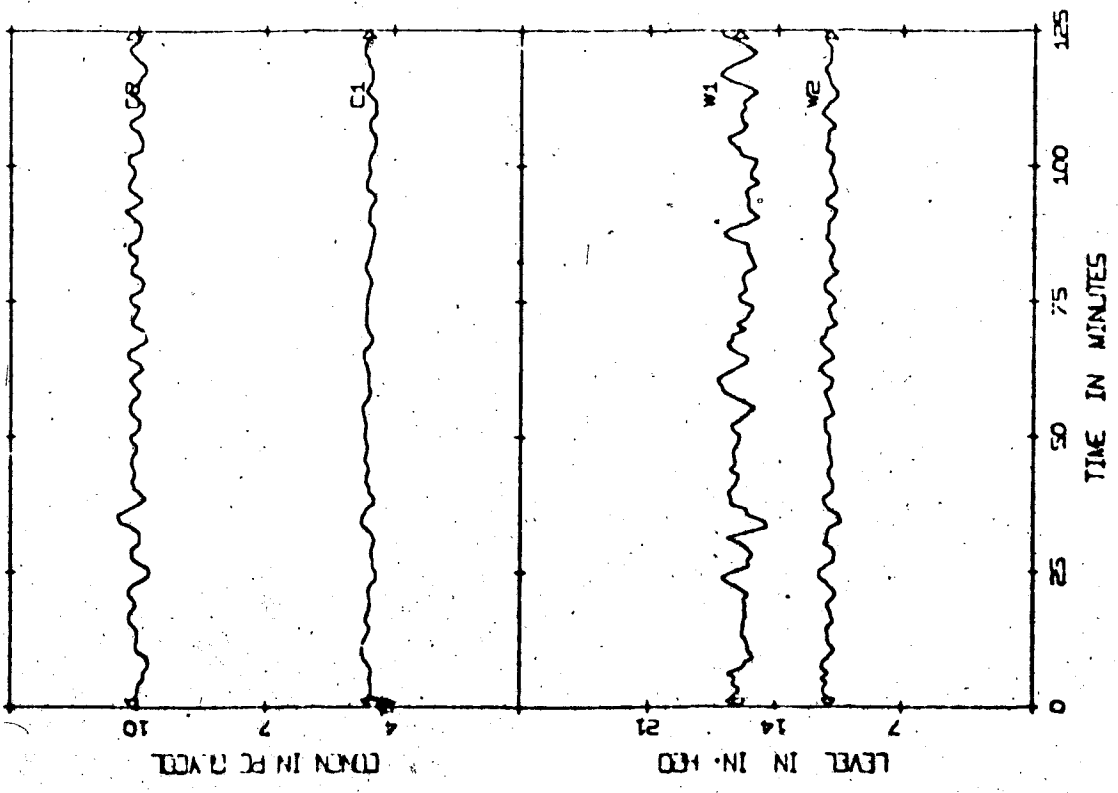


Figure 4.3. Evaporator response (SIM/STR),  $\beta_0$  estimated



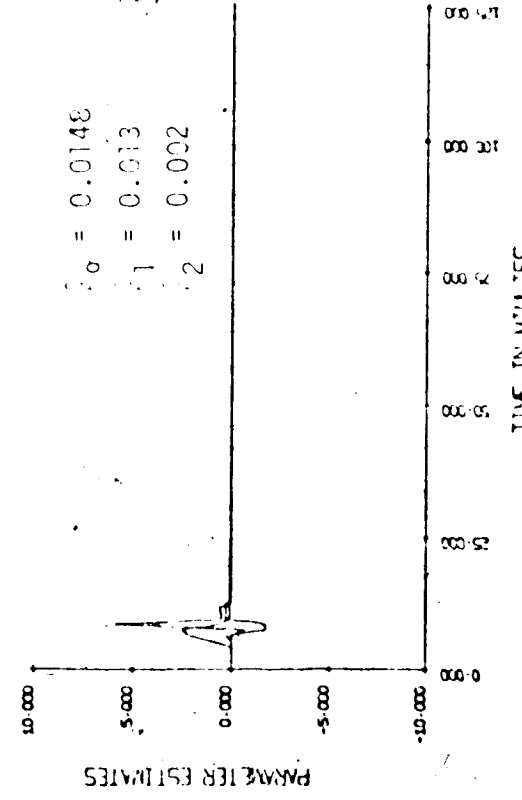
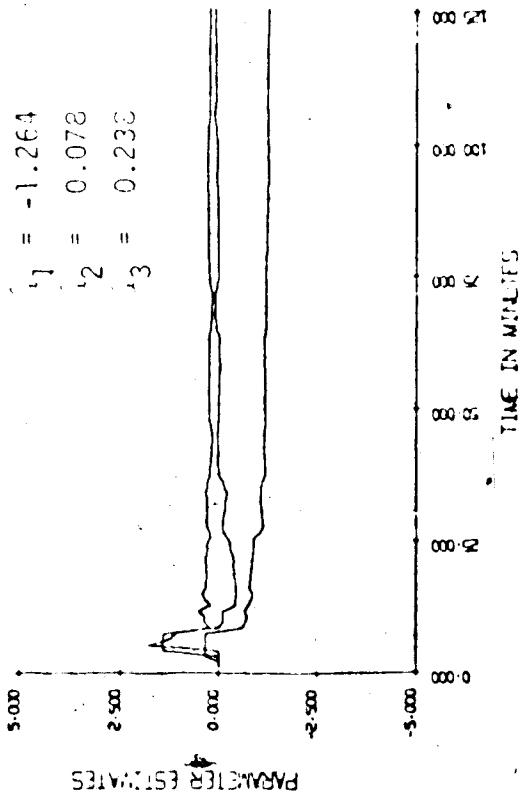
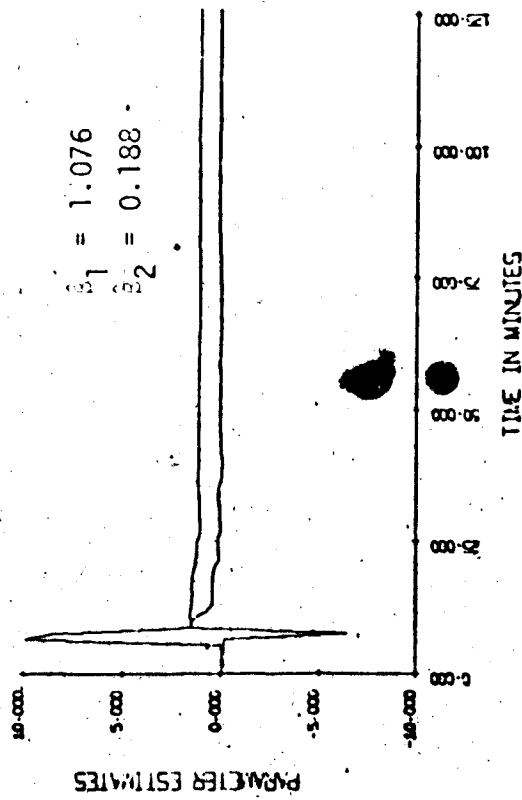
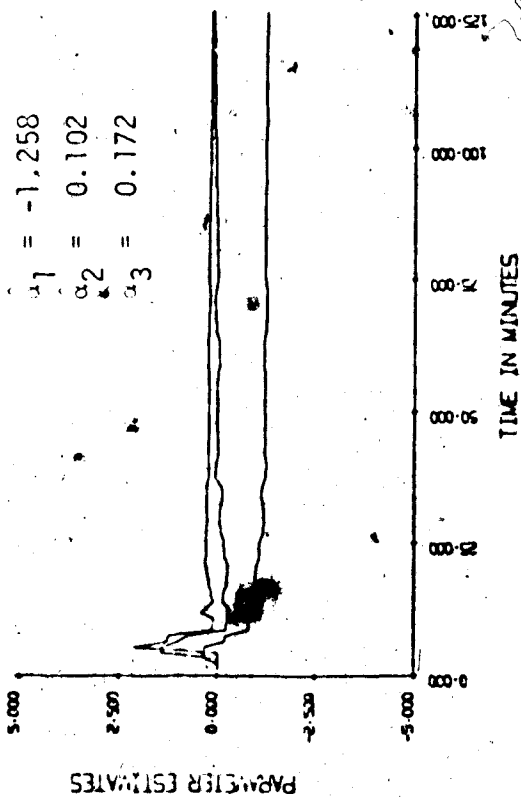


Figure 4.4 Parameter estimates (SIM/STR), base case

Figure 4.5 Parameter estimates (SIM/STR),  $\alpha_0$  estimated

parameter estimates. The final values of the parameter estimates are noted in the figures.

The parameter estimates in figure 4.4 of the base case run show large adjustments during the transient period. This was due to the large diagonal elements in the initial covariance matrix  $\underline{P}(0)$ . The rate of convergence of the parameter estimates was quite fast. Since the evaporator variables were generated from a fifth-order state-space model with six process noise variables, therefore, not only are the parameter estimates biased, they are also be different from the transfer function parameters derived in section 3.2.2. Thus it is impossible to compare the estimated parameters from different runs with the derived parameters. Note also that different operating conditions or use of different initial parameters in the self-tuning regulator resulted in different parameter estimates at the end of each of the runs.

Several different sets of process noise sequences were tried for the same base case run to check the randomness of the noise sequences. The evaporator responses (figures not shown) were very similar except for the initial "bump" of the C2 curves. Different process noise sequences appear to effect the size of the initial "bump" of the C2 curve and the one shown in figure 4.2 is the worst one. The final parameter estimates for different noise sequences were very similar.

It was explained in section 2.4 that it may not be possible to estimate all the model parameters under closed loop conditions. To avoid this difficulty,  $\beta_0$  is usually assumed to be a known constant

as suggested by Åström and Wittenmark [1]. Figure 4.3 shows a run in which all of the parameters, including  $\beta_0$  were estimated. The evaporator response of this run is very similar to the base case run except the C2 curve contains no initial "bump" and has small sustained oscillations. The parameter estimates in figure 4.5 show that the  $\{\hat{\theta}_i\}$  are very close to those obtained in the base case run and  $\hat{\beta}_0$  is very close to the derived value in the pulse transfer function evaporator model in section 3.2.2. However,  $\hat{\beta}_1$ , and  $\hat{\beta}_2$  converge to very small values. Therefore it appears that even though the control of C2 is not very good,  $\hat{\beta}_0$  can be estimated fairly accurately. Thus for some systems, on-line estimation during closed-loop conditions is one way of getting an initial value of  $\beta_0$  that can then be held constant for later runs. When successful, this approach eliminates the need for a priori specification of  $\beta_0$ .

#### 4.3 Initial Constants and Parameters for the Self-Tuning Algorithm

The purpose of the simulation runs in this section is to study the response of the system when different initial values are specified for the self-tuning algorithm. The range of initial values which can be used without unduly upsetting the system or resulting in unstable behaviour was also determined. This is quite important because unless the self-tuning regulator can be used for a relatively wide range of constants and parameters, it will not be that attractive as a control strategy for use in industrial processes.

In general, the selection of  $\mu$ ,  $\underline{p}(0)$ , and  $\{\hat{\theta}_i(0)\}$  is not very difficult. Based on his simulation and experimental experience,

Wittenmark [7] has reported some guidelines on their selection. The value of  $\lambda$  should be chosen to be between 0.99 and 1.0, and unless there is prior information available,  $\hat{\theta}_i(0) = 0$  should be used. If  $\hat{\theta}_i(0) \neq 0$  is used, this means large elements of  $\underline{P}(0)$  should be used because of the low confidence in  $\hat{\theta}_i(0)$ . A range ( $10I \leq \underline{P}(0) \leq 10,000 I$ ) is recommended by Wittenmark [7]. These three parameters can be further adjusted by examining the response of the controlled system and the parameter estimate curves. The effect of different choices of these parameters are examined in sections 4.3.1 and 4.3.2.

The selection of the constants for the regulator is more difficult since this depends on the user's knowledge of the physical system to be controlled. Therefore, before the self-tuning regulator can be used, a rough idea of the system order and the process time delay should be known. As for  $\beta_0$ , according to Wittenmark [7] a wider range of values can be used if the control signal is constrained as was the case in the evaporator simulation. In sections 4.3.3 to 4.3.5, the performance of the self-tuning regulator is evaluated for conditions where the system order, time delay and values of  $\beta_0$  are only approximately known.

#### 4.3.1 Exponential Forgetting Factor $\mu$

The evaporator responses remained relatively unchanged for values of  $\mu$  in the range,  $1.0 \geq \mu \geq 0.9$ , but the parameter estimates in figures 4.6 and 4.7 become more oscillatory as  $\mu$  decreases. When  $\mu$  is decreased to 0.8, (figure not shown) the parameter estimates fluctuated widely and the evaporator response showed signs of becoming

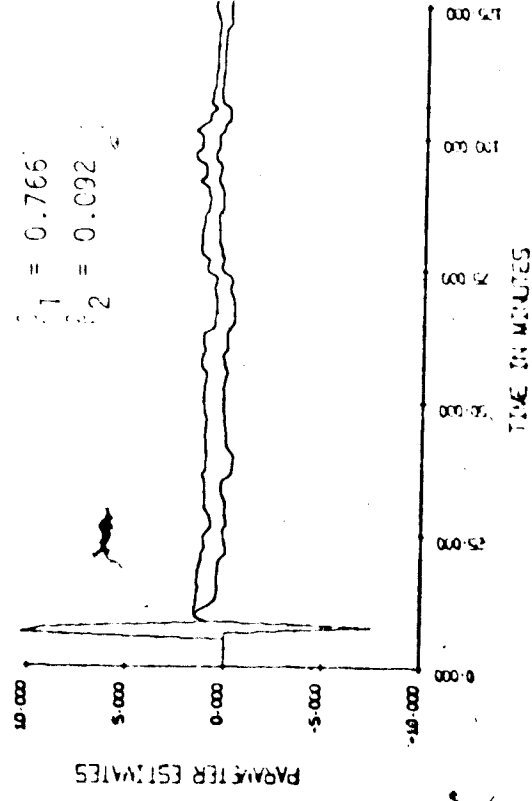
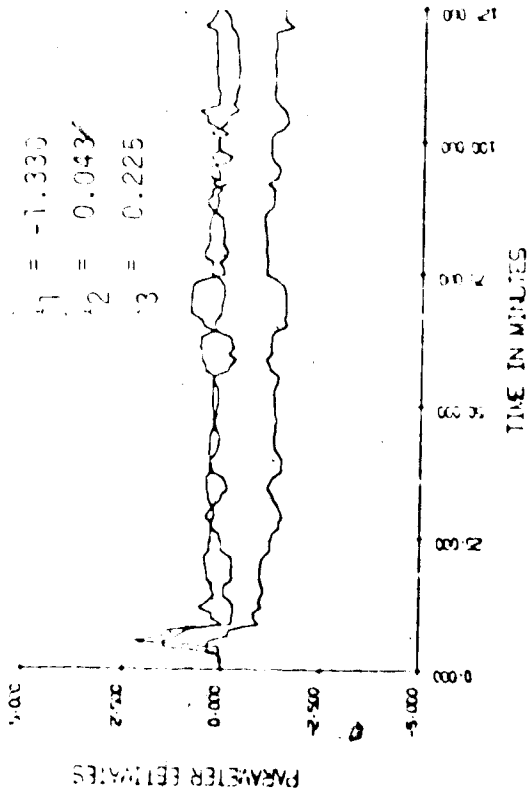
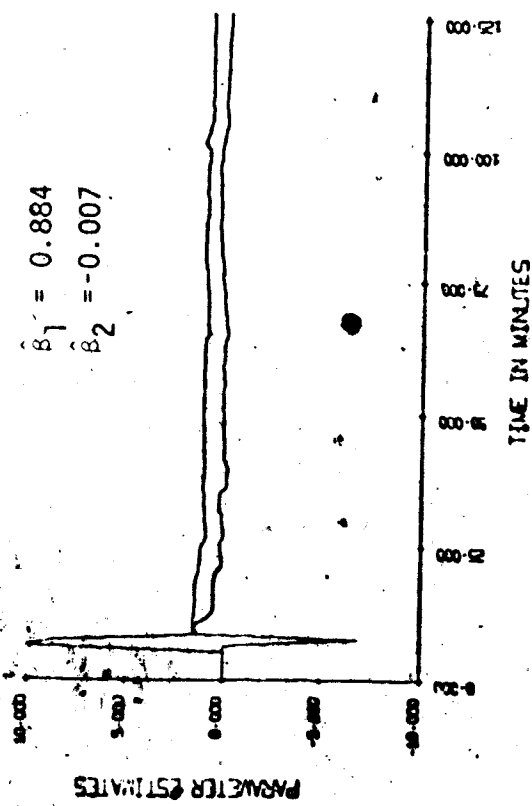
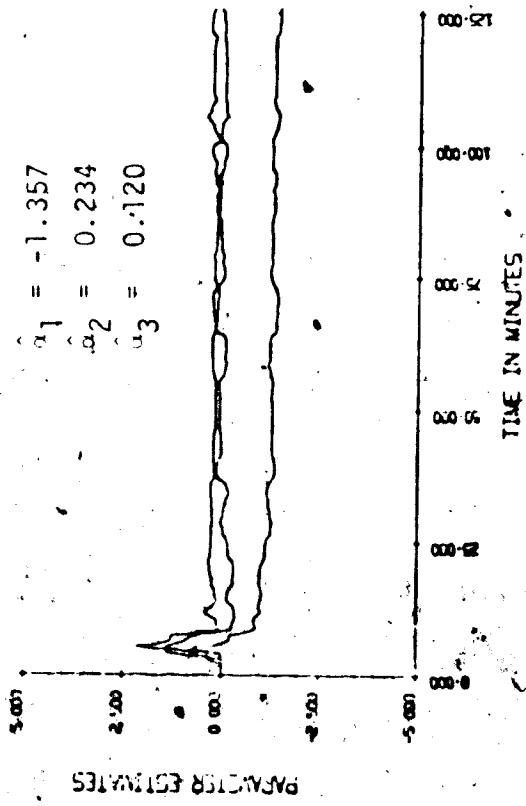


Figure 4.6 Parameter estimates (SIM/STR),  $\mu = 0.96$

Figure 4.7 Parameter estimates (SIM/STR),  $\mu = 0.90$

unstable. In general, it is advisable to use a value slightly less than one for  $\mu$  [7]. This would ensure better tracking of model parameters especially parameters that are slowly time varying. Therefore the ability to track parameters and the quality of steady state control would depend on the user's choice of  $\mu$ .

#### 4.3.2 Initial Covariance Matrix $\underline{P}(0)$ and Parameter Estimates

$\{\hat{\theta}_i(0)\}$

The choice of the initial covariance matrix  $\underline{P}(0)$  depends on the user's confidence in the initial parameter estimates  $\{\hat{\theta}_i(0)\}$ . For  $\hat{\theta}_i(0) = 0$ , several values of  $\underline{P}(0)$  were tried ( $10,000 \underline{I} \geq \underline{P}(0) \geq 0.001 \underline{I}$ ). Typical evaporator responses are shown in figures 4.8 to 4.11. Reducing the elements of  $\underline{P}(0)$  results in smaller elements in the gain vector  $\underline{K}(t)$  which in turn causes smaller changes (per step) in the parameter estimates (see equations 2.25 to 2.27). This is quite evident when the two estimates plots are compared with the base case. For  $\underline{P}(0) = 100 \underline{I}$ , the "bump" at the beginning of the C2 curve in figure 4.8 was reduced due to the smaller diagonal elements, but these elements were still large enough to ensure convergence of the estimates. For  $\underline{P}(0) = \underline{I}$ , the parameter estimates converged much slower and at the end of the run, the gain vector  $\underline{K}(t)$  was too small to cause further changes in the estimates. Consequently, the control of C2 was not as good.

The performance of the self-tuning regulator when non-zero initial parameter estimates and  $\underline{P}(0) = 10,000 \underline{I}$  are used is shown in figures 4.12 to 4.15. For both  $\hat{\theta}_i(0) = 5$ , and  $\hat{\theta}_i(0) = -10$ , the

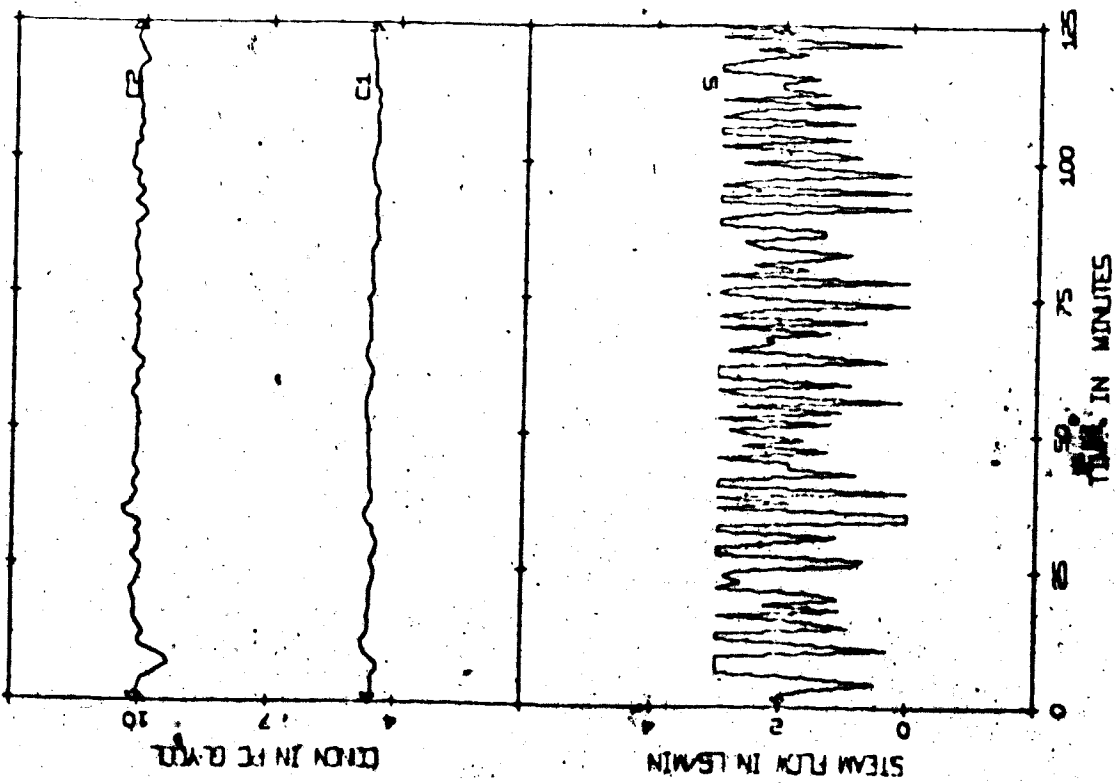


Figure 4.8 Evap. response (SIM/STR),  $P(0) = 100$

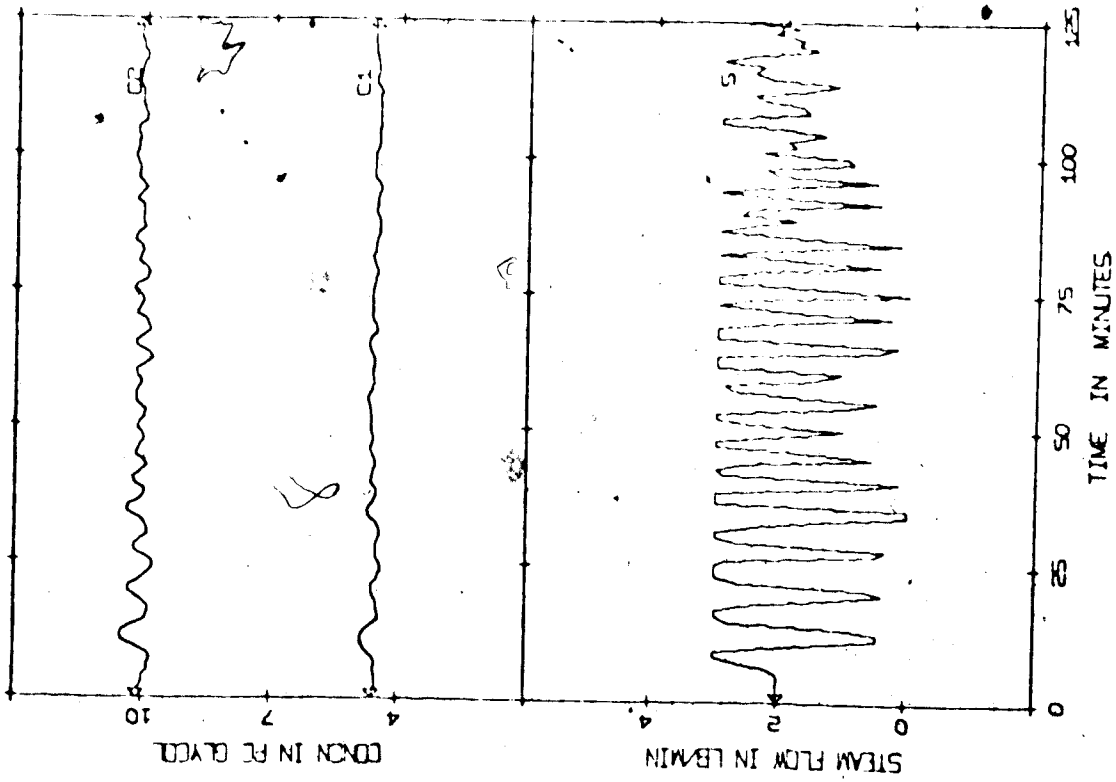


Figure 4.9 Evap. response (SIM/STR),  $P(0) = 1$

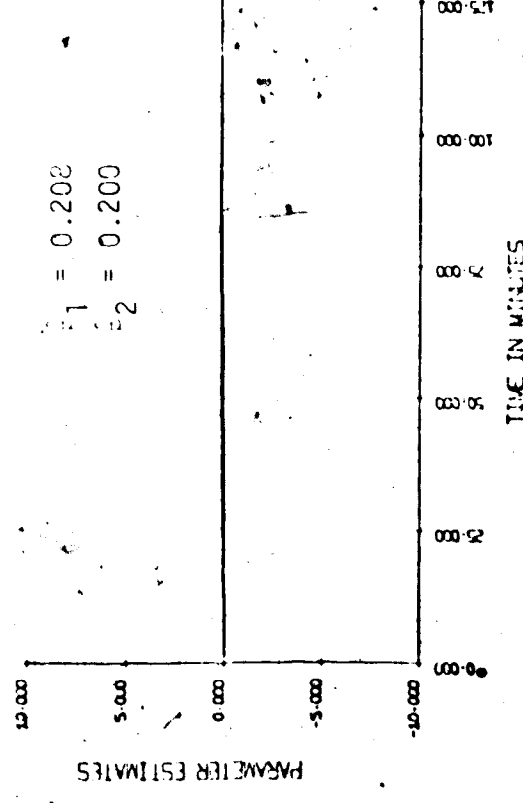
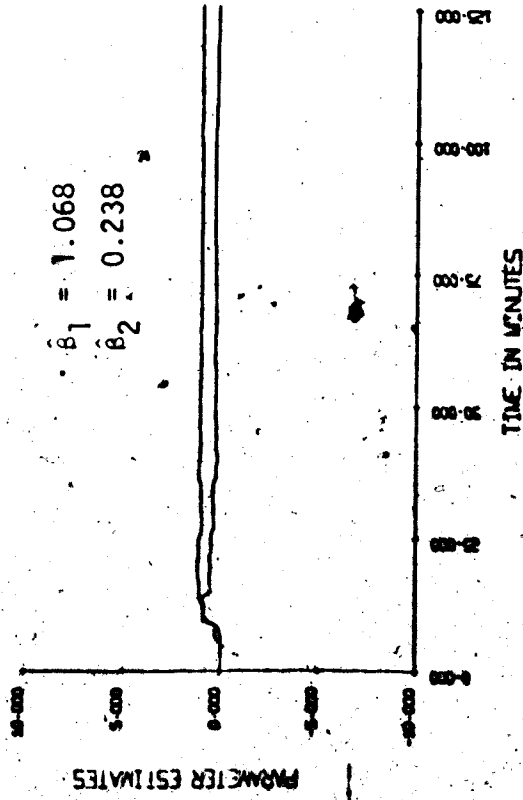
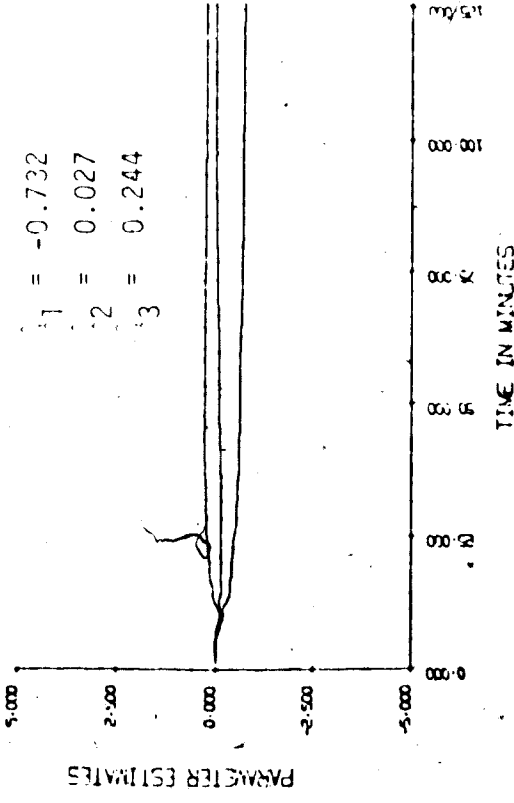
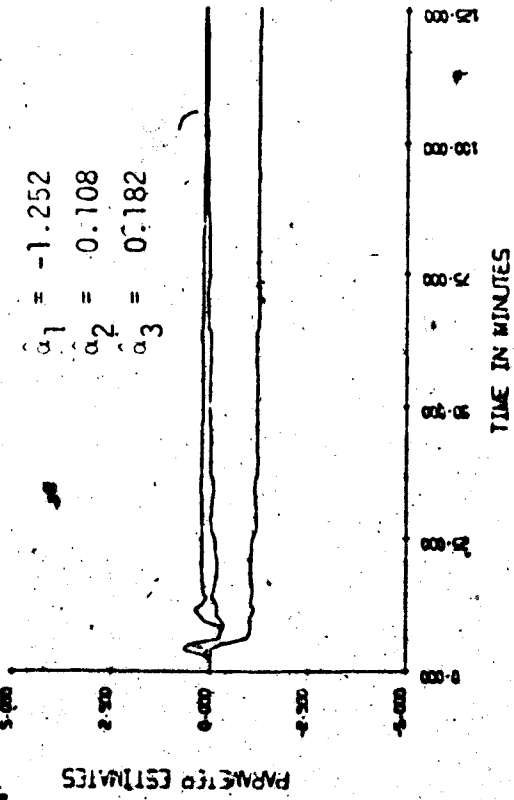


Figure 4.10 Parameter estimates (SIM/STR),  $\underline{p}(0) = 100\mathbf{I}$  Parameter estimates (SIM/STR),  $\underline{p}(0) = \mathbf{I}$



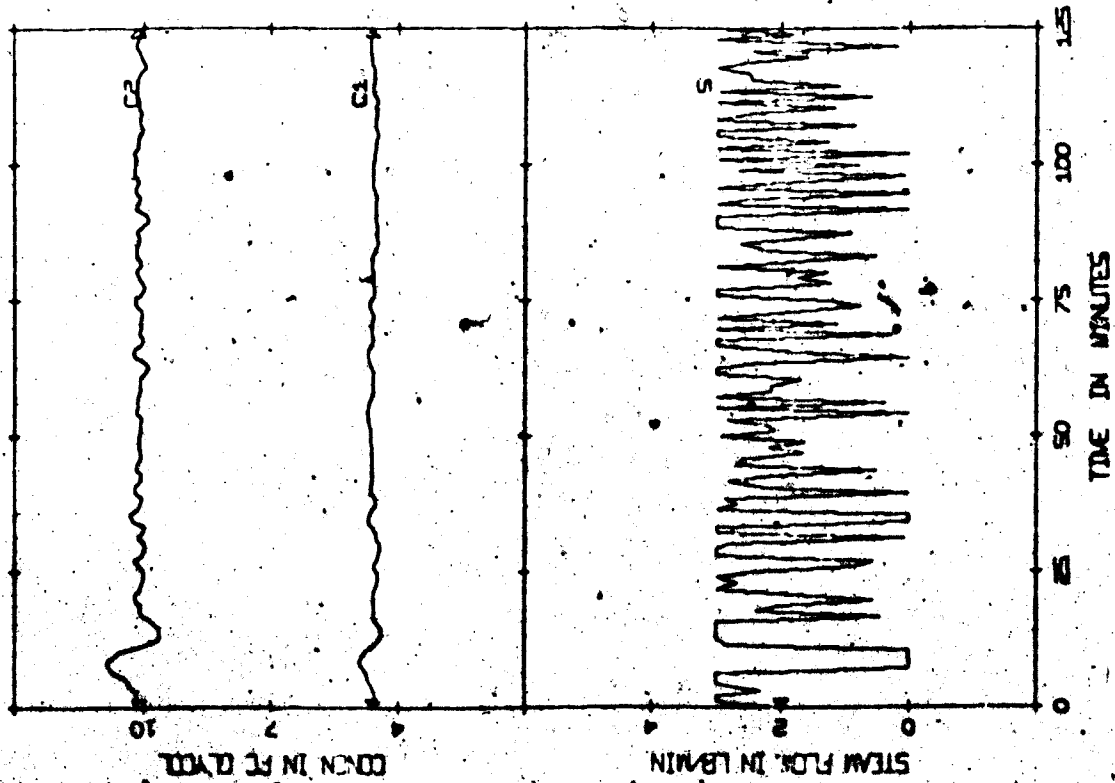


Figure 4.12 Evap. response (SIM/STR),  $\theta_i(0) = 5$

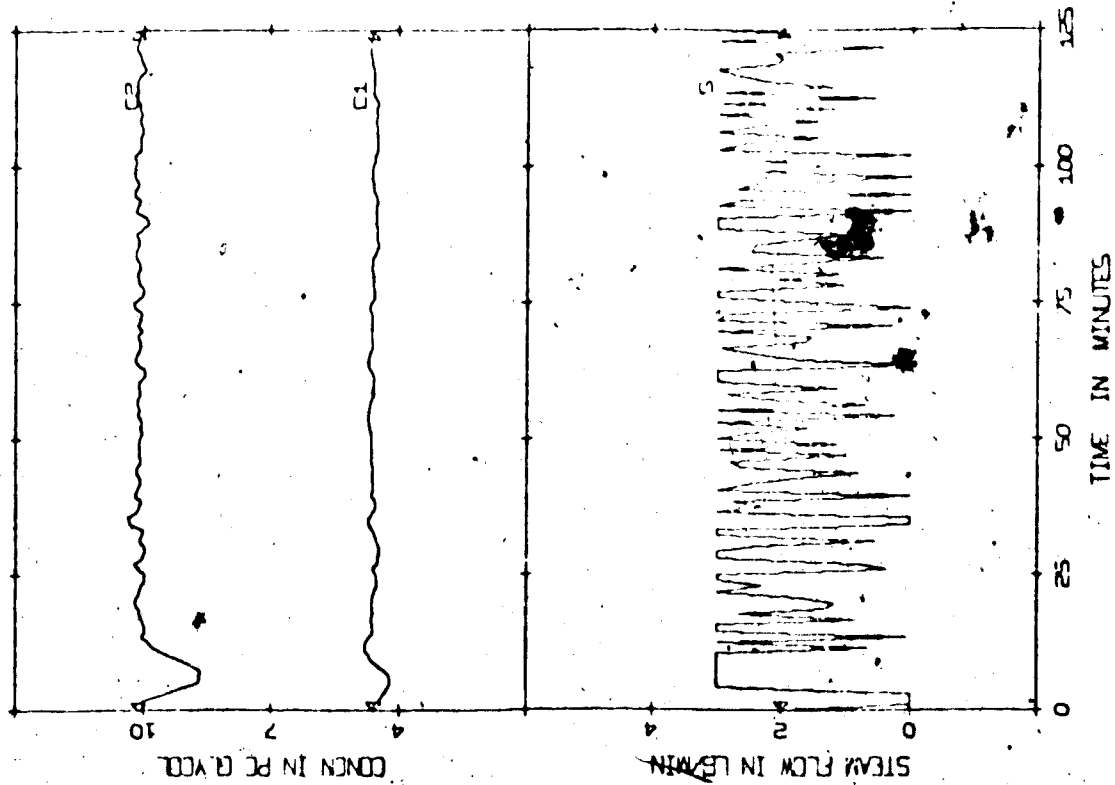


Figure 4.13 Evap. response (SIM/STR),  $\theta_i(0) = -10$

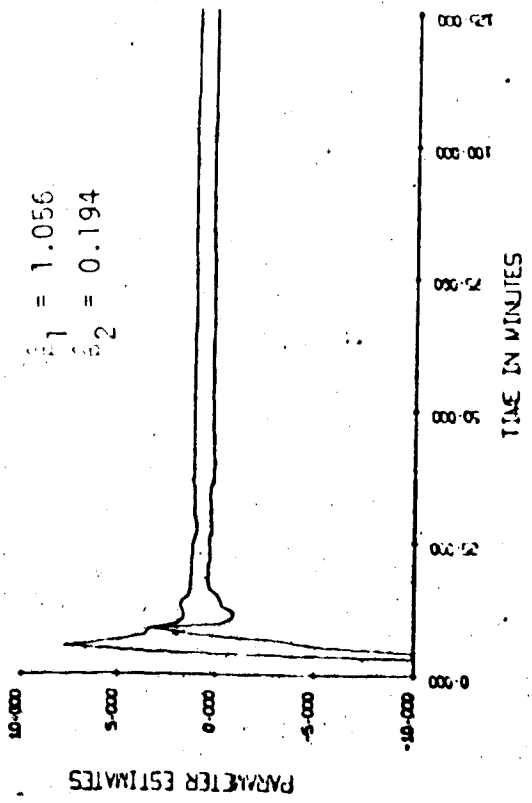
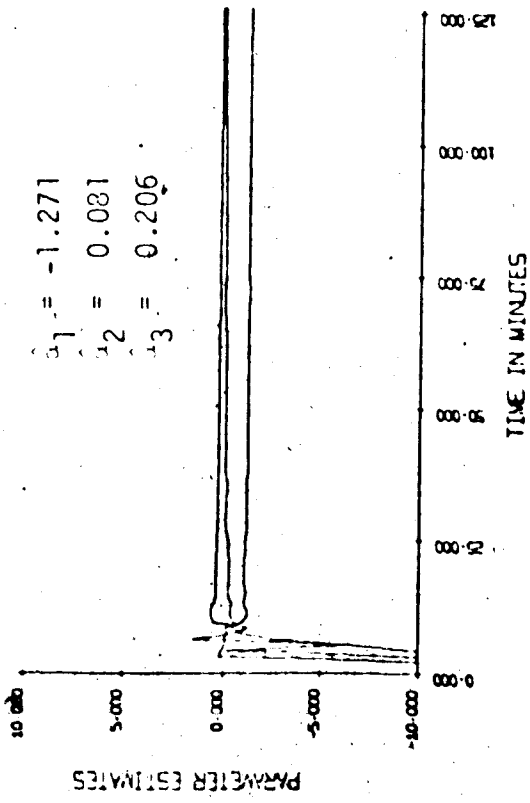
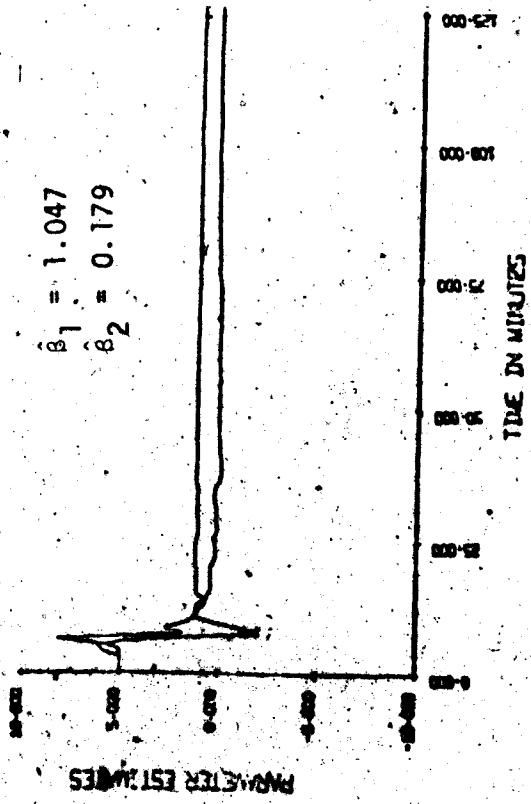
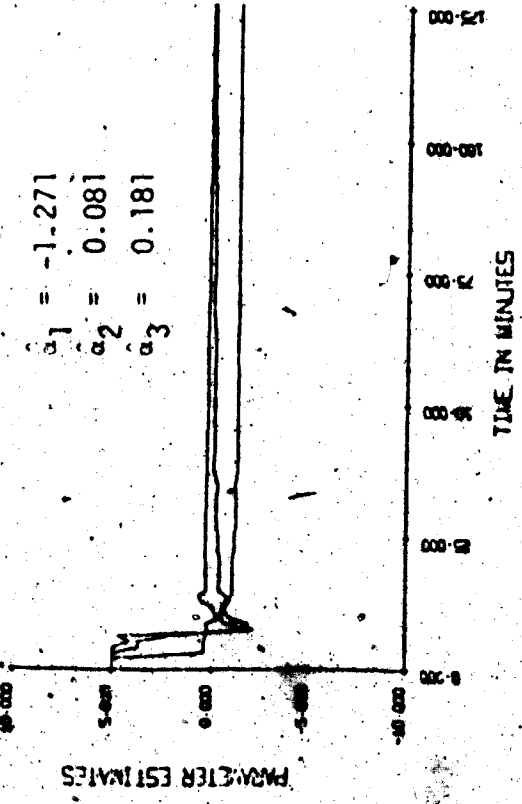


Figure 4.14 Parameter estimates (SIM/STR),  $\hat{\theta}_i(0) = 5$  Figure 4.15 Parameter estimates (SIM/STR),  $\hat{\theta}_i(0) = -10$

convergence properties were very good due to the large value of  $\underline{p}(0)$ . The C2 responses of the two runs were different during the initial transient due to the different signs and magnitudes of the initial parameters estimates. After the initial period, the control of C2 was quite good in both cases. (Note that the scale of the  $\hat{a}_i$  plot in figures 4.14 and 4.15 was increased by a factor of two in comparison with previous figures.)

#### 4.3.3 Scaling Factor $\beta_0$

A large range of  $\beta_0$  values varying from 0.00001 to 1.0 were considered. For  $0.1 \geq \beta_0 \geq 0.00001$ , the product concentration was maintained within acceptable limits although the control of C2 deteriorated at the two extremes, 0.1 and 0.00001, and there appears to be an optimum value of  $\beta_0$  in between. For  $\beta_0$  values outside this range, large sustained oscillations in C2 occur. When values close to  $\beta_0 = 0.014$  were tried, the C2 responses were good and were very similar except for the initial "bump". Though a detailed search for the optimum value of  $\beta_0$  was not performed, the best run, in terms of accumulated loss was observed when  $\beta_0 = 0.03$ . Again, the lower accumulated loss is primarily due to the smaller initial "bump".

In general, for relatively large values of  $\beta_0$ , the  $\hat{a}_i$  curves had large fluctuations and were still adjusting at the end of the run but the  $\hat{\beta}_i$  curves converged quickly. The opposite situation occurred for relatively small values of  $\beta_0$ : the  $\hat{a}_i$  curves converged but the  $\hat{\beta}_i$  curves fluctuated. Typical results are shown in figures 4.16 to 4.19.

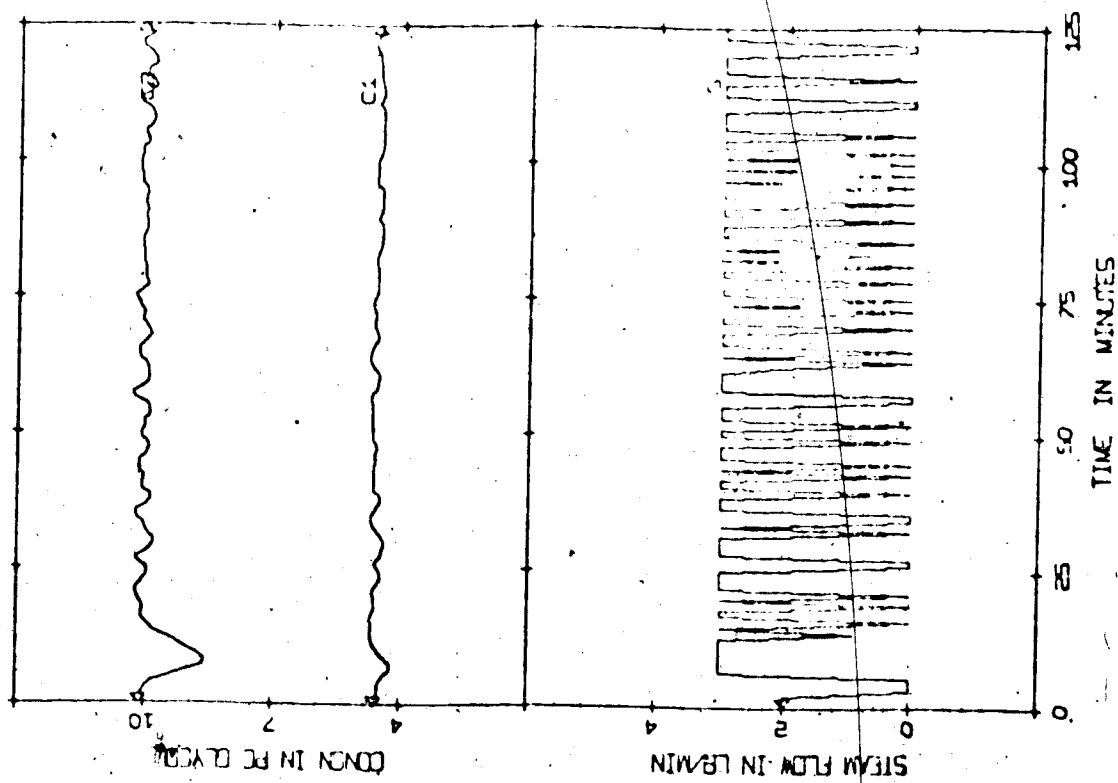


Figure 4.17 Evap. response (SIM/STR),  $\beta_0 = 0.001$

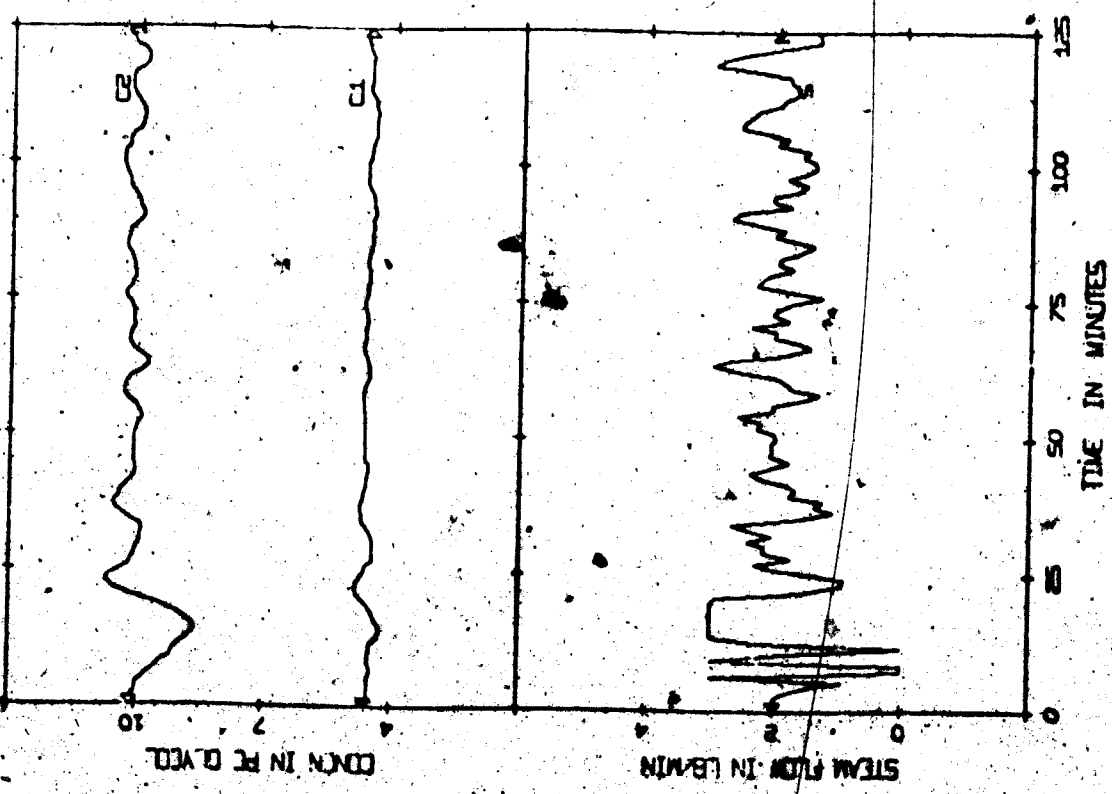


Figure 4.16 Evap. response (SIM/STR),  $\beta_0 = 0.1$

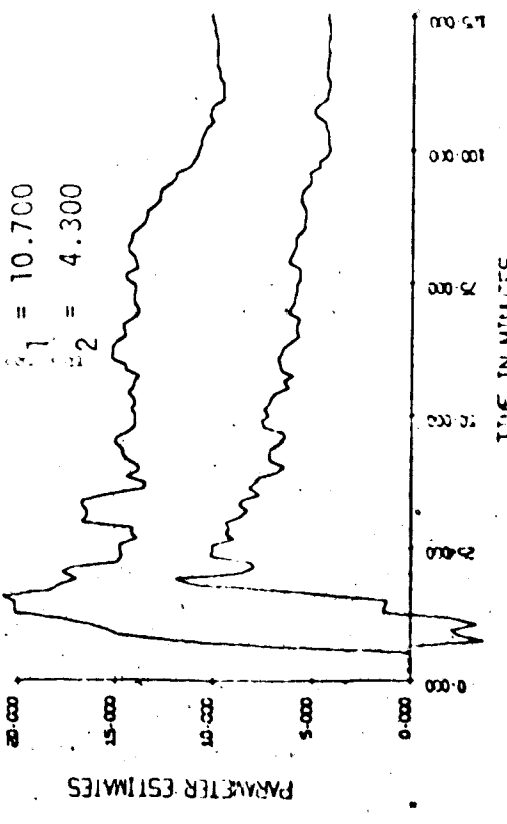
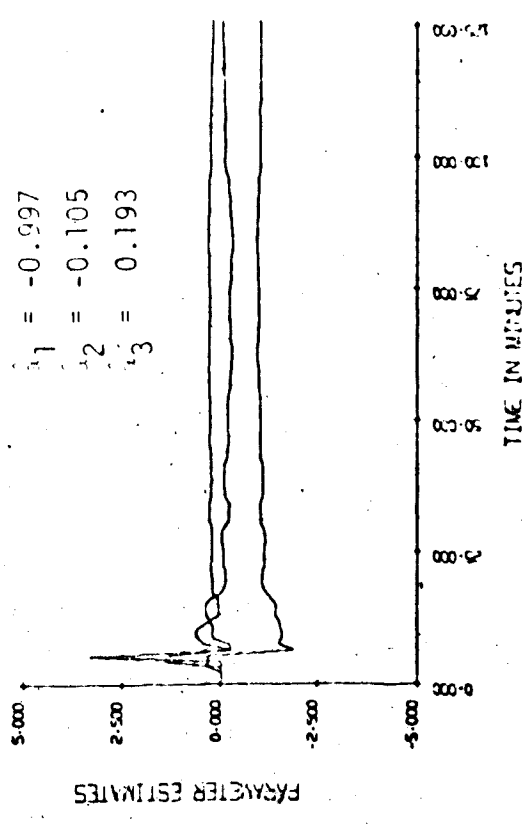
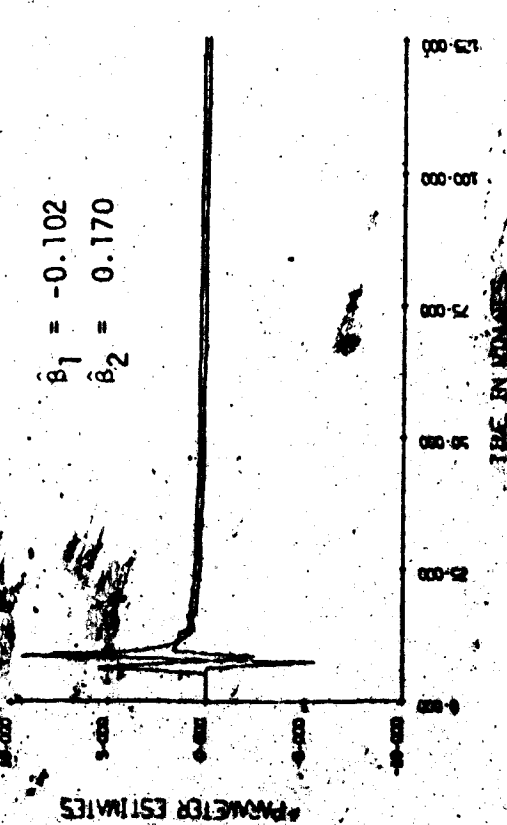
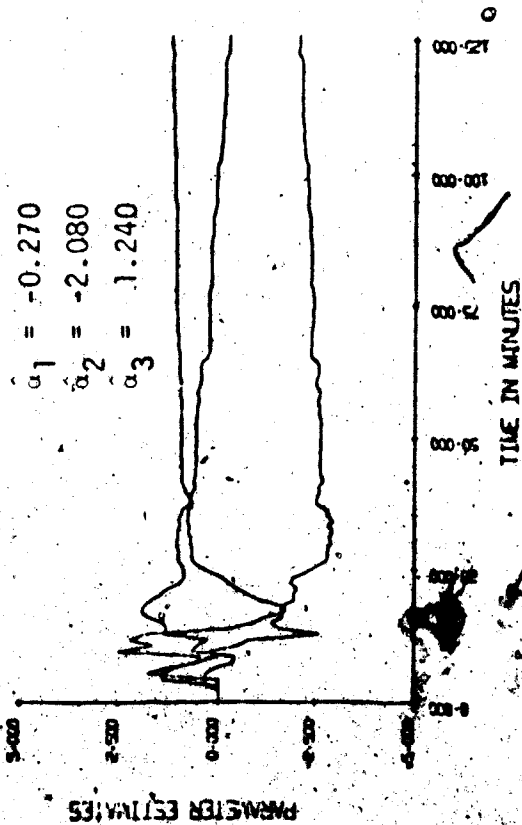


Figure 4.18 Parameter estimates (SIM/STR),  $\beta_0 = 0.1$

Figure 4.19 Parameter Estimates (SIM/STR),  $\beta_0 = 0.001$

Wittenmark [7] has suggested that the user can examine the response of the control variable to find out if a good choice of  $\beta_0$  has been made. If the control signal is hitting the constrained limits too often, this means that  $\beta_0$  is too small; if the control signal is not hitting the constrained limits at all, this means that  $\beta_0$  should be decreased. These situations were observed by Wittenmark [7] in his simulation study and are also illustrated by the steam response in figures 4.16 and 4.17. Different values of  $\beta_0$  were also tried for smaller elements in  $\underline{P}(0)$  and similar results were obtained.

If no control constraints are applied, a value of  $\beta_0 = 0.02$  results in unstable responses. This supports Wittenmark's comment [7] concerning the effect of control constraints on the operable range of  $\beta_0$ .

#### 4.3.4 Model Order n

In the base case run, the correct model order of  $n=3$  was specified (see figure 4.2). Figures 4.20 and 4.21 show evaporator responses when  $n=2$  and  $n=4$  were used as the assumed model orders. The order of the predictive model did not seem to influence the C2 response very much after the initial transient period. Note that the "bump" in the initial part of the C2 response increases as the assumed model order increases. This can be explained as follows. When a higher order model is used, more parameters have to be estimated and since zero initial conditions were assumed, the information vector  $\underline{y}$  contains only zero elements initially. If the recursive least squares algorithm in section 2.4 is examined closely, it can be seen that the elements of

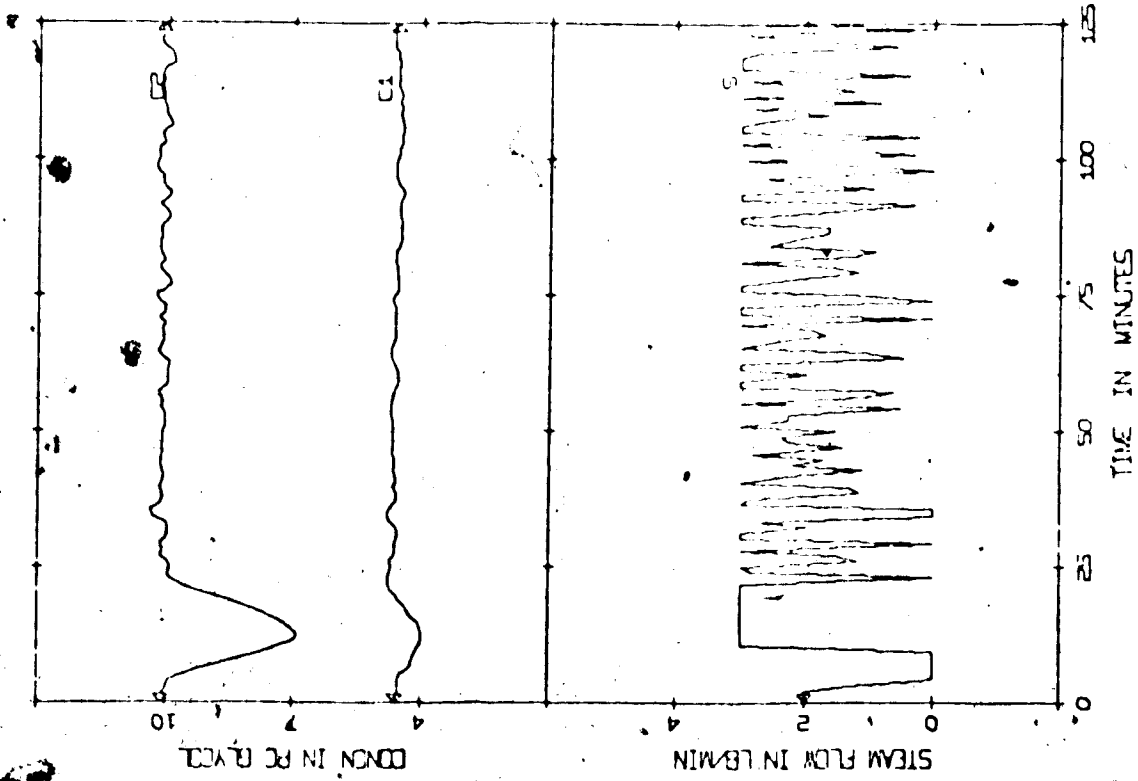


Figure 4.21 Evap. response (SIM/STR), 4<sup>th</sup> order model

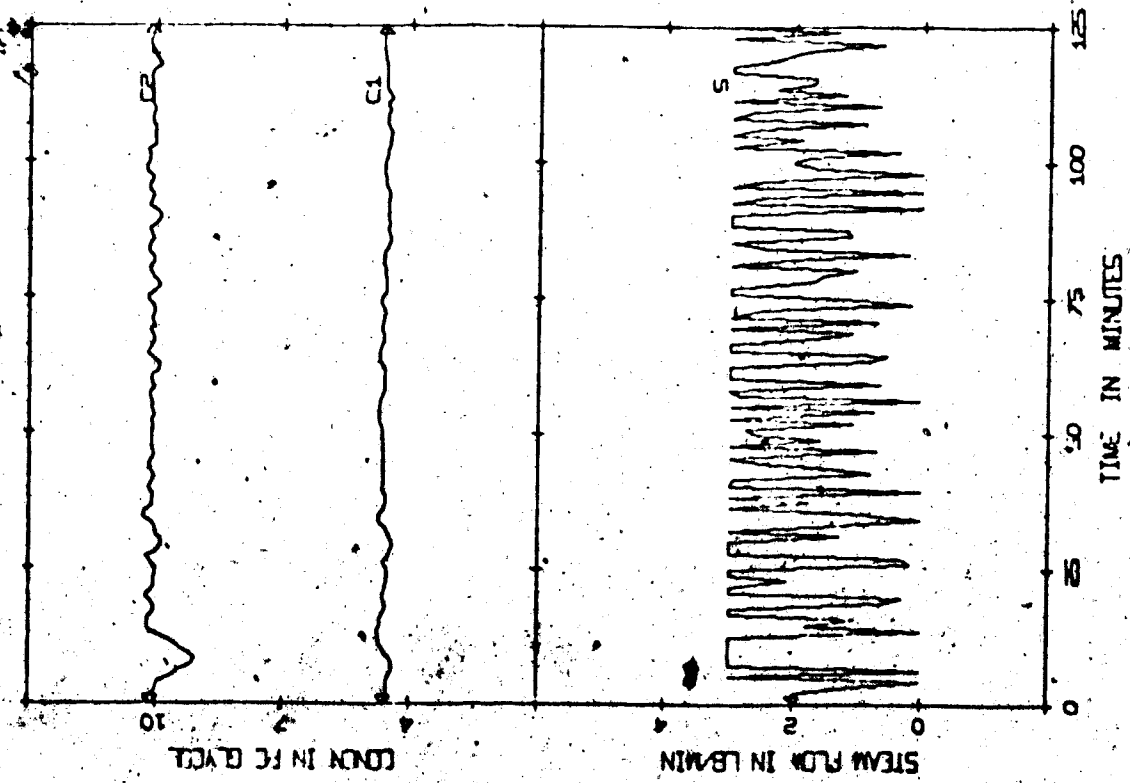


Figure 4.20 Evap. response (SIM/STR), 2<sup>nd</sup> order model

the parameter vector have non-zero values only if the corresponding information vector also has non-zero elements. Therefore, for higher order models, it takes more sampling intervals before the information vector and the parameter vector have non-zero elements. As a result, higher order models will generally give poorer control during the initial transient period.

Additional runs were performed with  $n=1$  and  $n=5$  (figures not shown). For  $n=1$ , the regulator has only one parameter and is actually a proportional controller; the evaporator response was similar to those shown in section 3.5. For  $n=5$ , the evaporator response was similar to the run where  $n=4$ . The parameter estimates for the runs where  $1 \leq n \leq 5$  all had good convergence properties. Figures 4.22 and 4.23 show the parameter estimates plots for  $n=2$  and  $n=4$ , respectively.

#### 4.3.5 System Time Delay k

Simulation runs were also made using assumed time delays of  $k=1$  and  $k=2$ . Since the actual time delay in the derived pulse transfer function model is  $k=0$ , control of C2 became worse as  $k$  increased, as would be expected. However, for  $k=2$  the control was still satisfactory which suggests that overestimating the delay may not degrade the performance of this system too much. Figures 4.24 and 4.25 show the evaporator response and the parameter estimates for  $k=2$ .



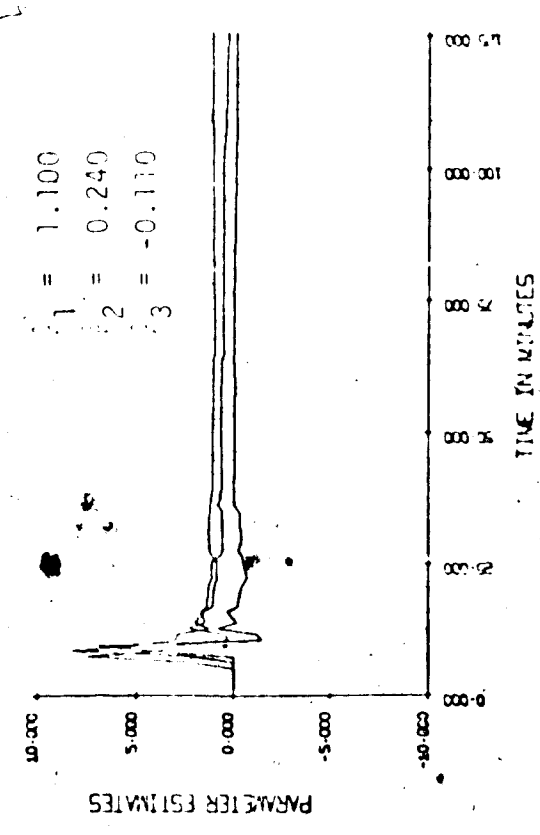
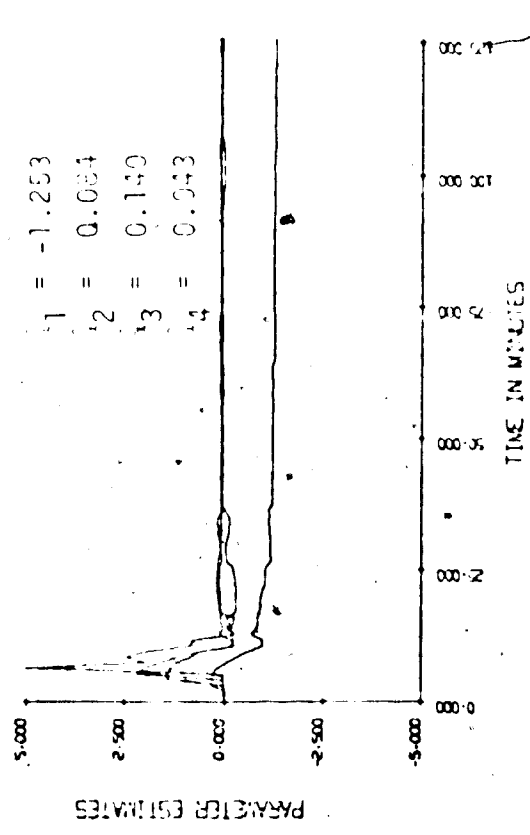
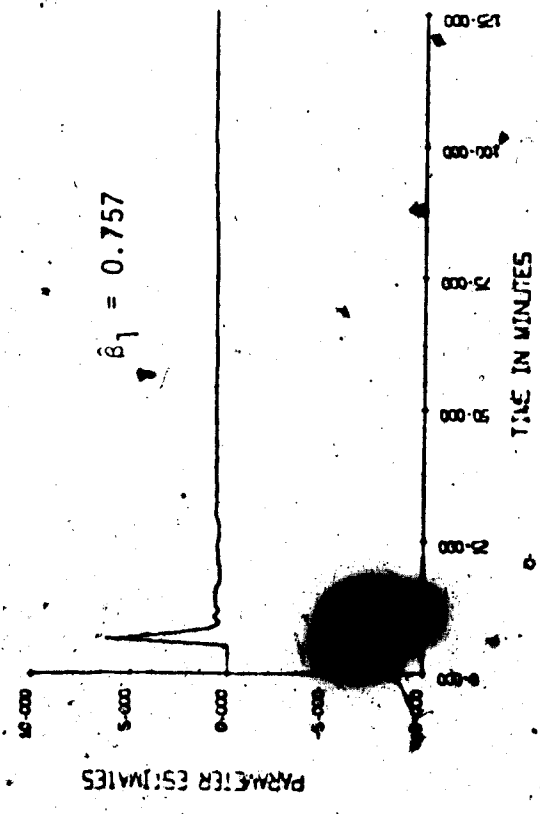
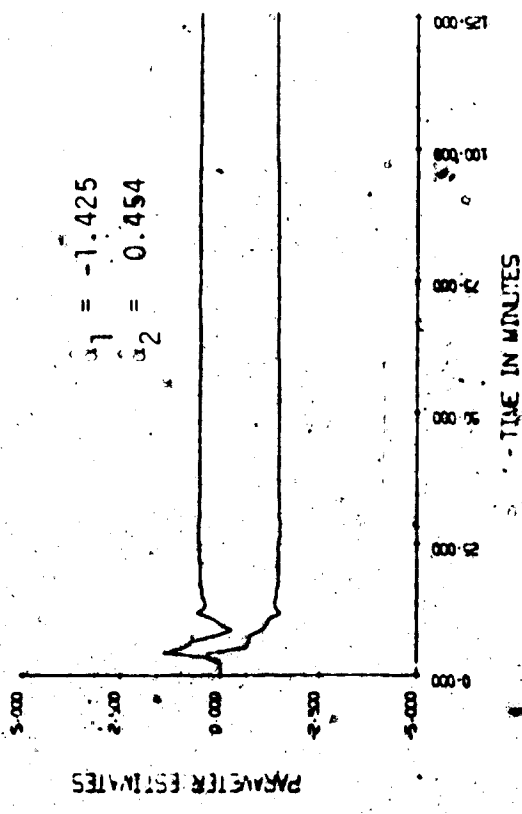


Figure 4.22 Parameter estimates (SIM/STR), 4<sup>th</sup> order model

Figure 4.23 Parameter estimates (SIM/STR), 4<sup>th</sup> order model

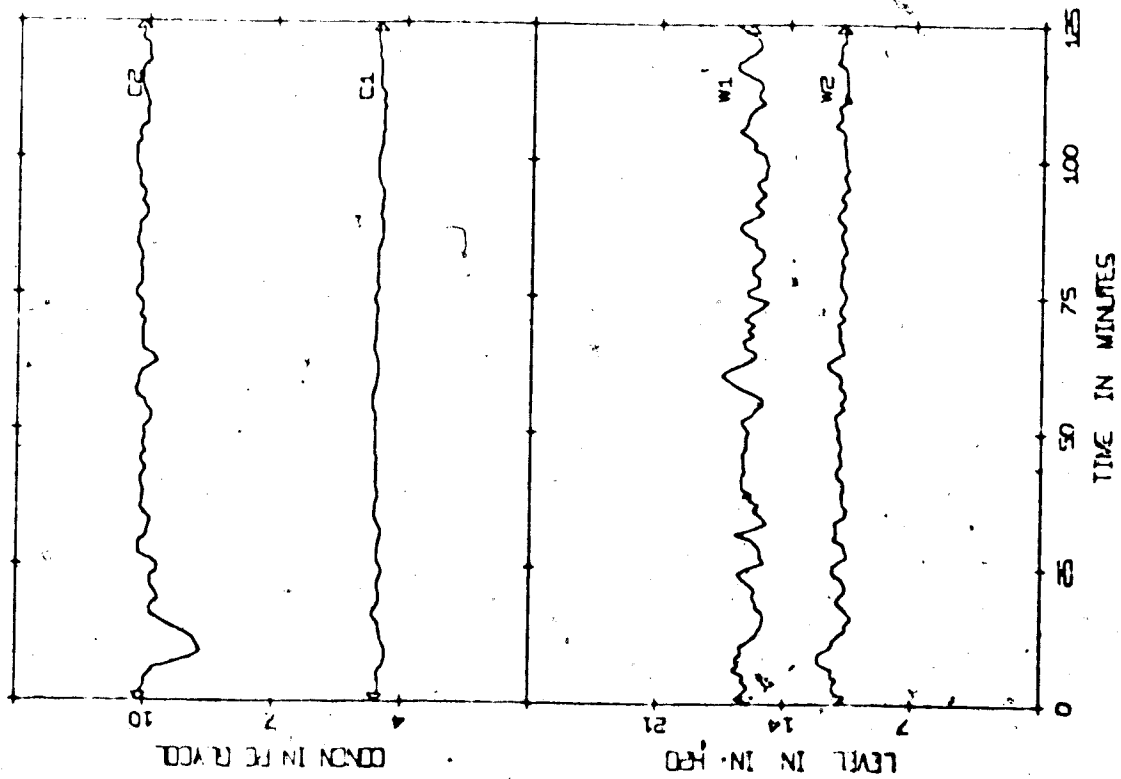


Figure 4.24 Evaporator response (SIM/STR),  
k = 2

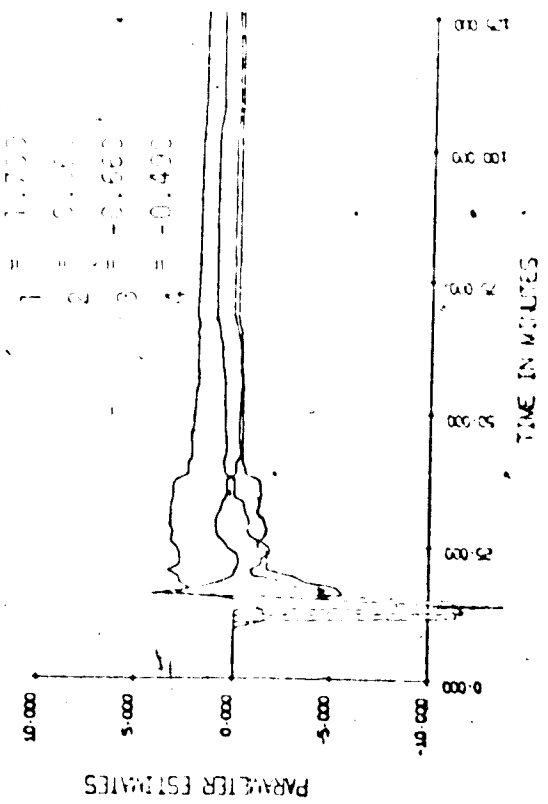
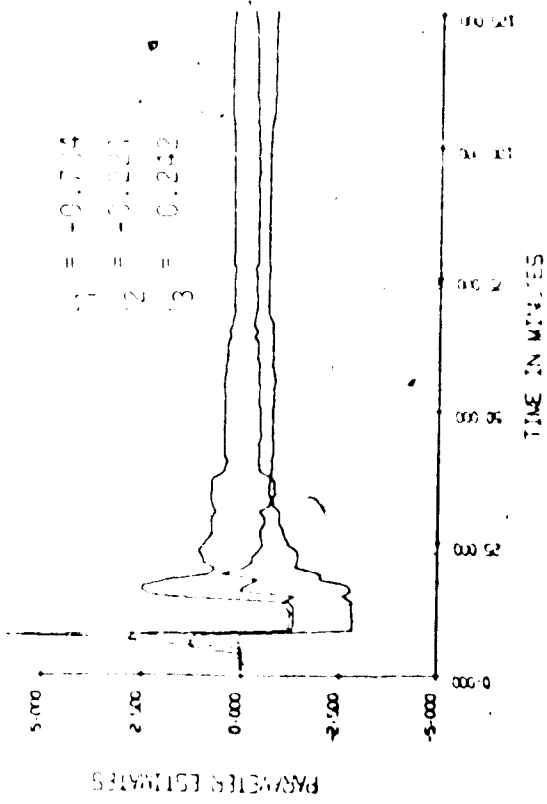


Figure 4.25 Parameter estimates (SIM/STR),  
k = 2

#### 4.4 Performance of the Self-Tuning Regulator Under Non-Ideal Operating Conditions

An evaluation of the performance of the self-tuning regulator for a variety of operating conditions was a prime objective of the simulation study. In this section the effects of process noise level and the inclusion of measurement noise and unmeasured step disturbances are described. A list of simulated runs for this section is shown in Table 4.2.

##### 4.4.1 Effect of Process Noise Level, $\sigma_{PN}$

In the base case run, a 10% process noise level was used (i.e.  $\sigma_{PN} = 0.1$ ). Figure 4.26 and 4.27 show evaporator responses when 1% and 50% process noise levels are used, respectively. Increasing the noise level resulted in an increase in output variance and large fluctuations in all the other evaporator variables, as would be expected. Note that the parameter estimates in figure 4.28 and 4.29 are quite similar although increasing the noise level results in more fluctuations.

##### 4.4.2 Effect of Measurement Noise

Addition of 5% measurement noise to the three evaporator outputs resulted in poor control of C2 as shown in figure 4.30. The corresponding parameter estimates are shown in figure 4.32. A run with only measurement noise and no process noise (not shown) gave results similar to figures 4.30 and 4.32. These results indicate that 5% measurement noise is more significant than 10% process noise.

TABLE 4.2  
 RECURSIVE LEAST SQUARE ESTIMATES OF THE MODEL PARAMETERS AFTER 120 SAMPLING INTERVALS (128 MIN)

Note: Six process noise variables, each has zero mean and standard deviation of 0.1 are used except as noted. Three measurement noise, each with zero mean and standard deviation of 0.05 are used in run 3258.

Base case conditions:  $\mu = 1.0$  ,  $P(0) = 10,000 I$  ,  $\hat{e}(0) = 0$   
 $\beta_0 = 0.014$  ,  $n = 3$  ,  $k = 0$

FIGURES	RUN NO.	BASE CASE CONDITIONS EXCEPT	UNMEASURED STEP DISTURBANCE	PARAMETER ESTIMATES (at t=128 min)			ACCUM. LOSS (at t=128 min)		
				$\hat{\alpha}_1$	$\hat{\alpha}_2$	$\hat{\alpha}_3$			
4.26, 4.28	3193	$\sigma_{PN} = 0.01$	-	-1.271	0.087	0.196	1.022	0.175	0.0357
4.27, 4.29	3257	$\sigma_{PN} = 0.5$	-	-1.256	0.053	0.232	1.151	0.128	1.1314
4.30, 4.32	3258	Meas. noise added	-	-0.400	-0.379	-0.101	1.707	0.128	0.7112
4.31, 4.33	3194	$\sigma_{PN} = 0.01$	(-20%F, +20%F)	-2.416	1.873	-0.444	-0.163	-0.731	0.0359
4.34, 4.36	3125	-	(-20%F, +20%F)	-1.502	0.458	0.057	0.654	-0.155	0.1253
4.35, 4.37	3174	-	(-30%CF)	-1.453	0.378	0.064	0.745	-0.047	0.1641
4.38, 4.40	3225*	$\beta_0$ estimated	(-20%F, +20%F)	-2.662	0.766	0.182	0.011	-0.002	0.0302
4.39, 4.41	3226**	$\beta_0$ estimated	(-30%CF)	-1.356	0.151	0.088	0.015	0.093	0.0152
4.42	3207	constant $\hat{e}(t)$	(-40%F, +40%F)	-1.258	0.102	0.172	1.076	0.188	0.0221
4.43, 4.45	3209	-	-	-1.266	0.013	0.263	1.195	0.302	0.0176
4.44, 4.46	3212	-	(-20%F, +20%F)	-1.481	0.480	-0.062	0.665	-0.072	0.0147

\*  $\beta_0 = 0.0097$   
 \*\*  $\beta_0 = 0.0128$

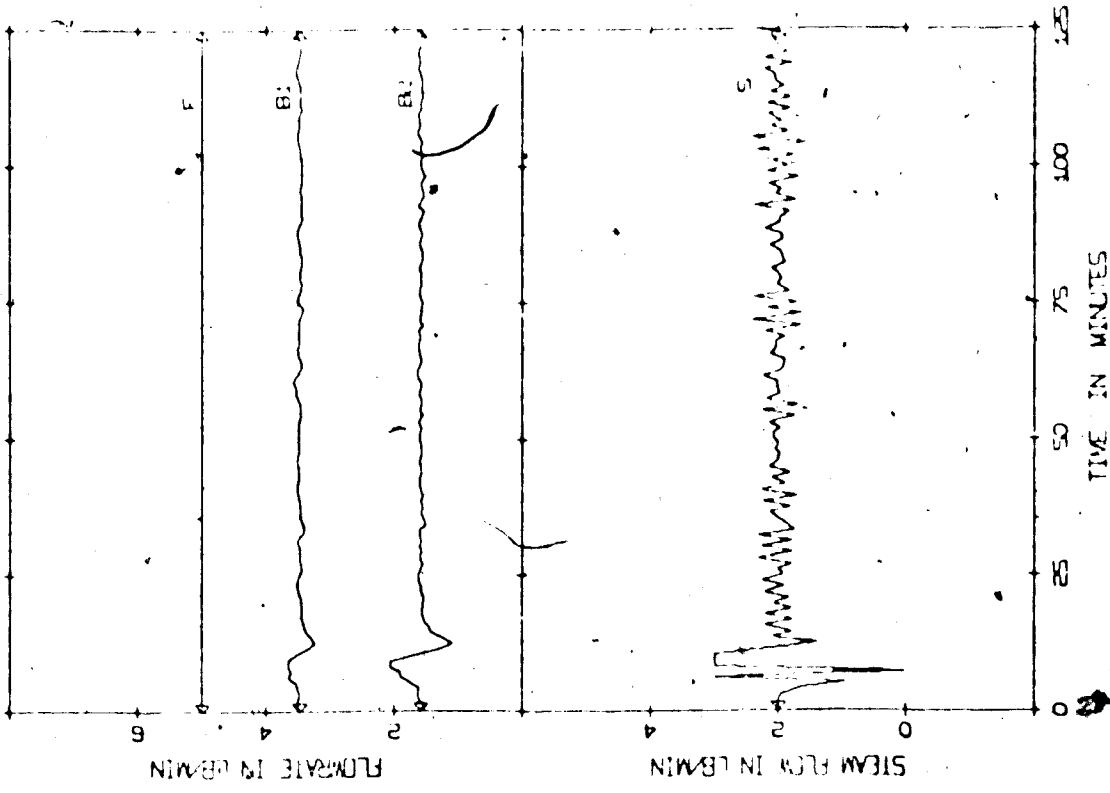
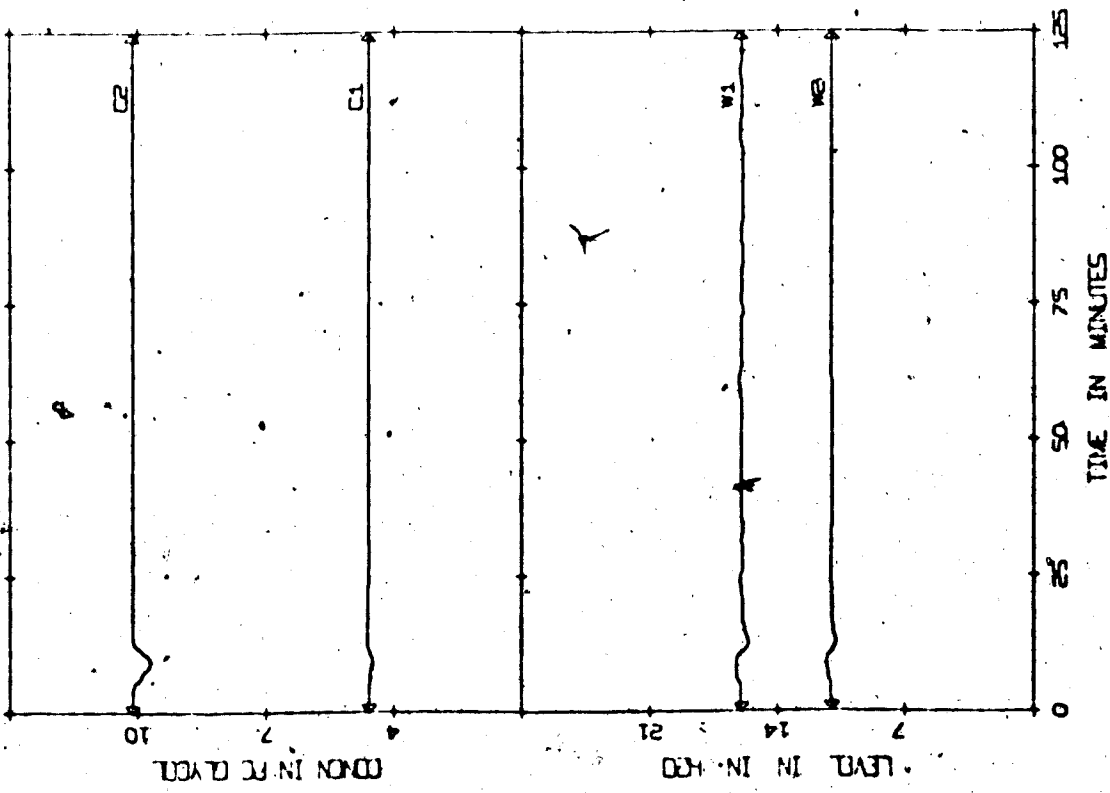


Figure 4.26 Evaporator response (SIM/STR),  $c_{PN} = 0.01$

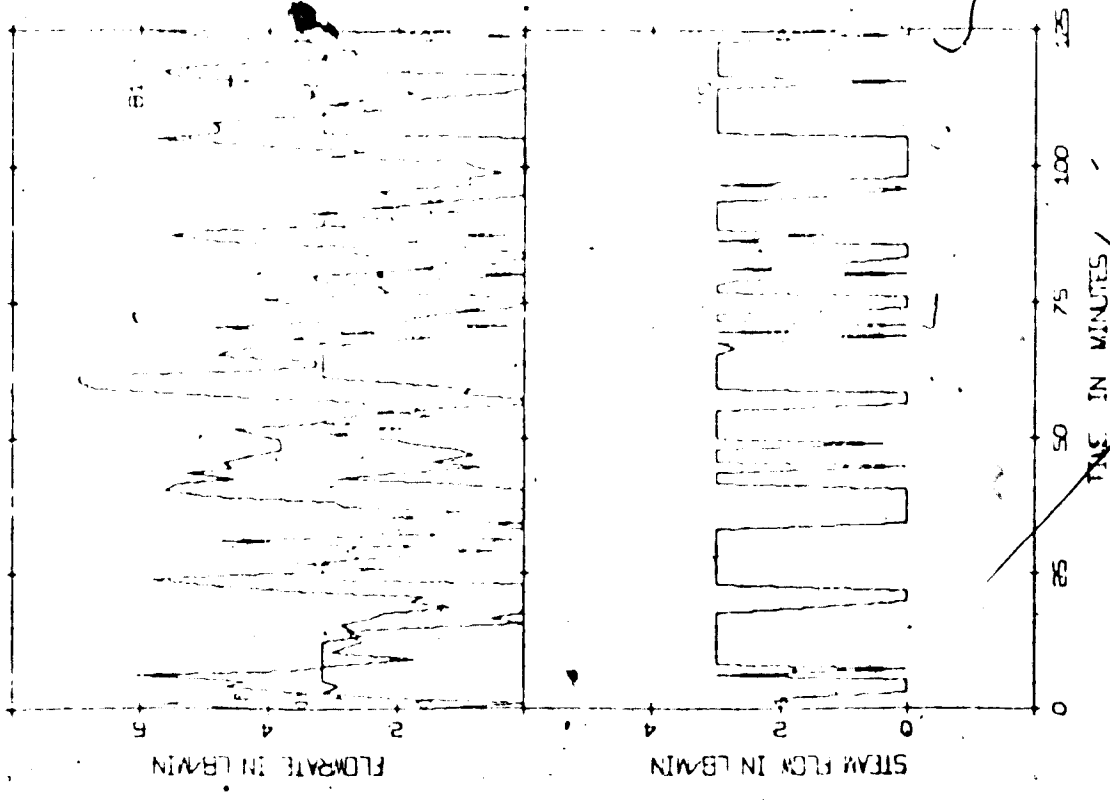
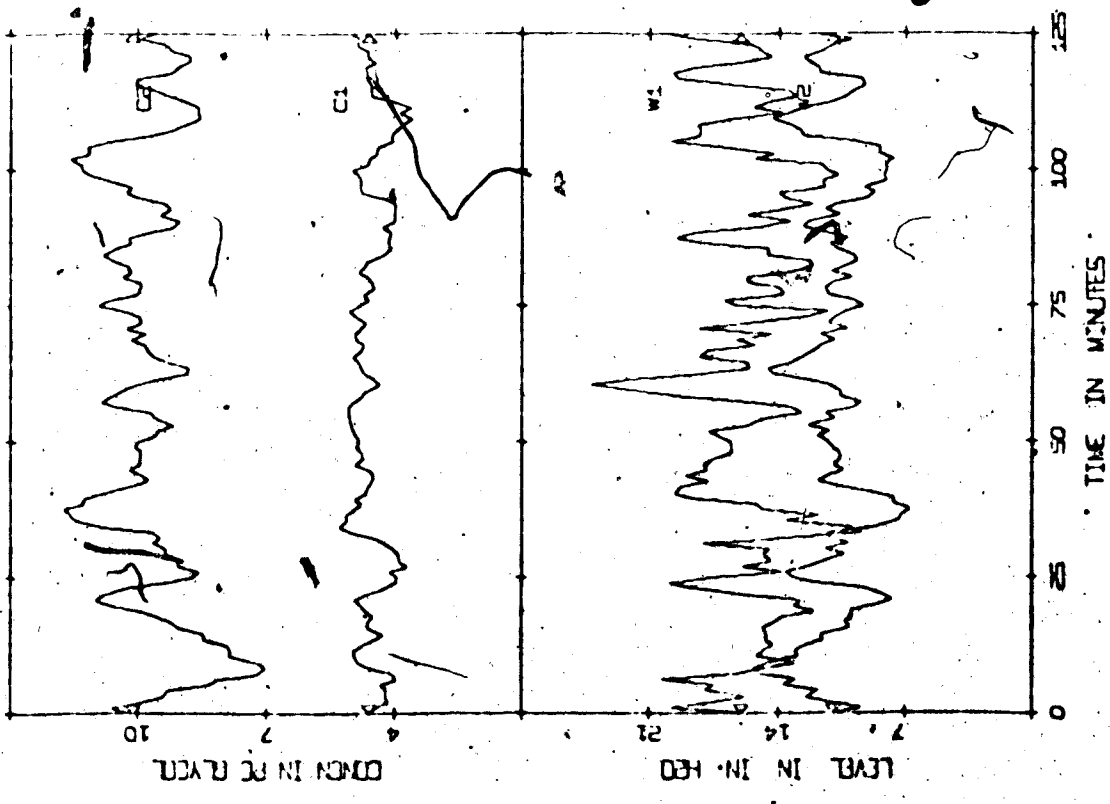


Figure 4.27 Evaporator response (SIM/STR),  $\sigma_{PN} = 0.5$

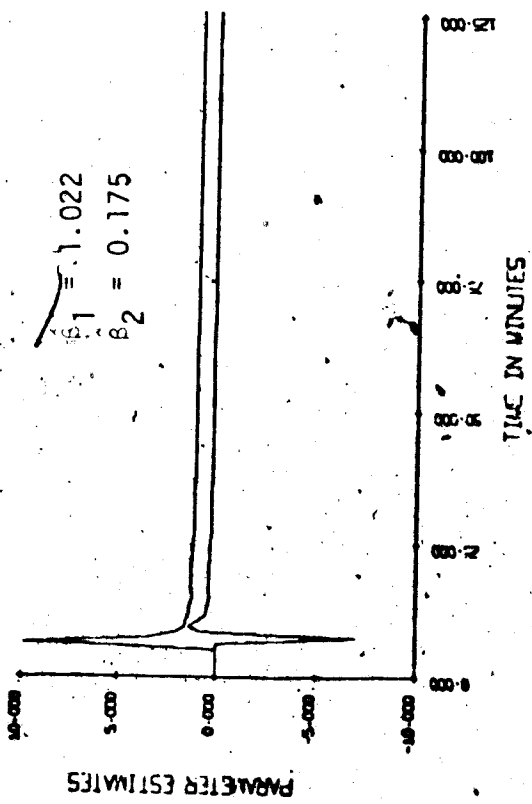
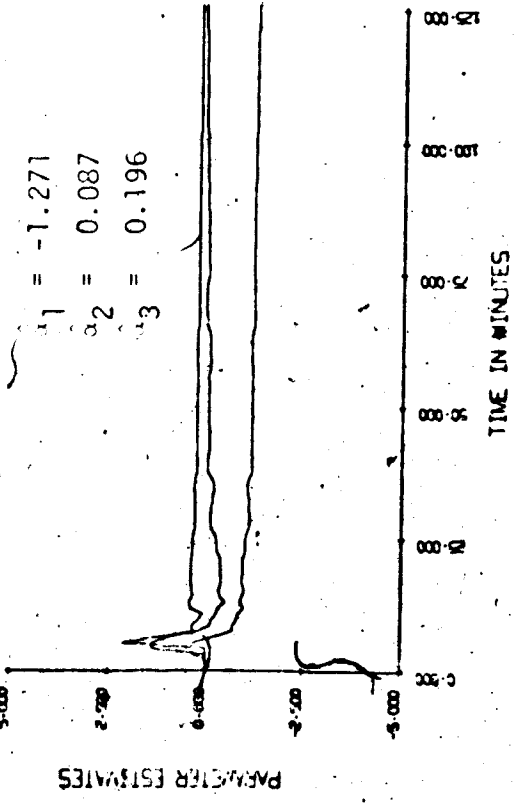


Figure 4.28 Parameter estimates (SIM/STR),  $\sigma_{PN} = 0.01$

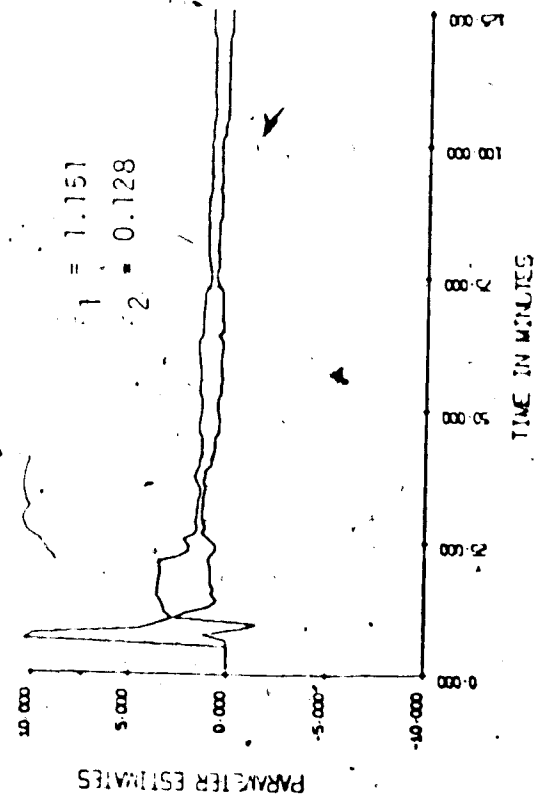
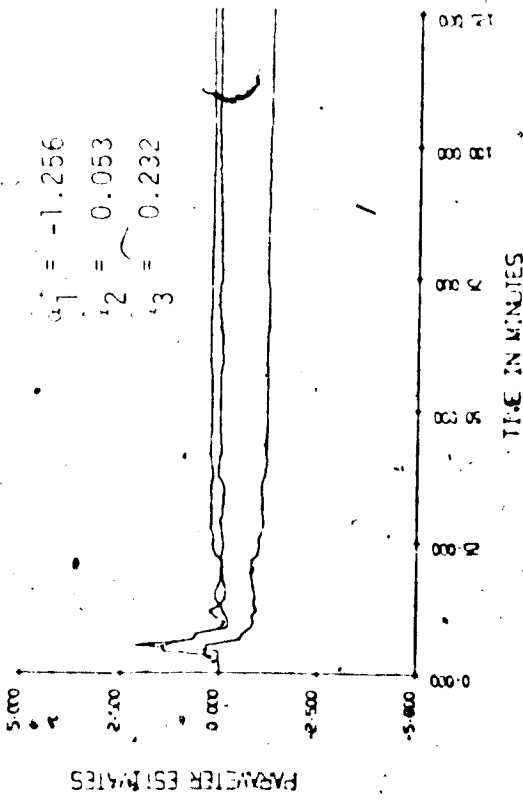


Figure 4.29 Parameter estimates (SIM/STR),  $\sigma_{PN} = 0.5$

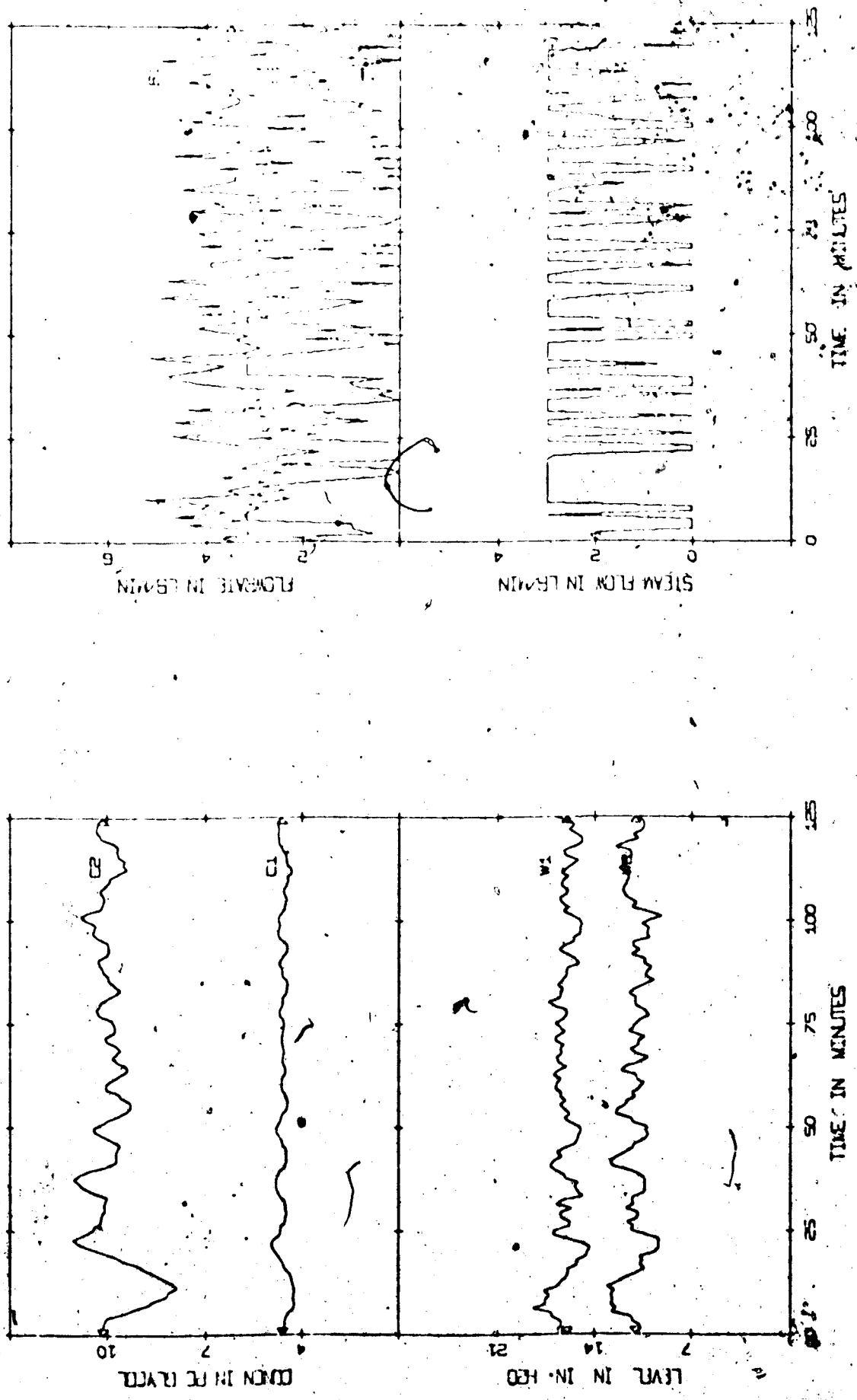


Figure 4.30 Evaporator response (SIM/STR), measurement noise included,  $\sigma_{MN} = 0.05$



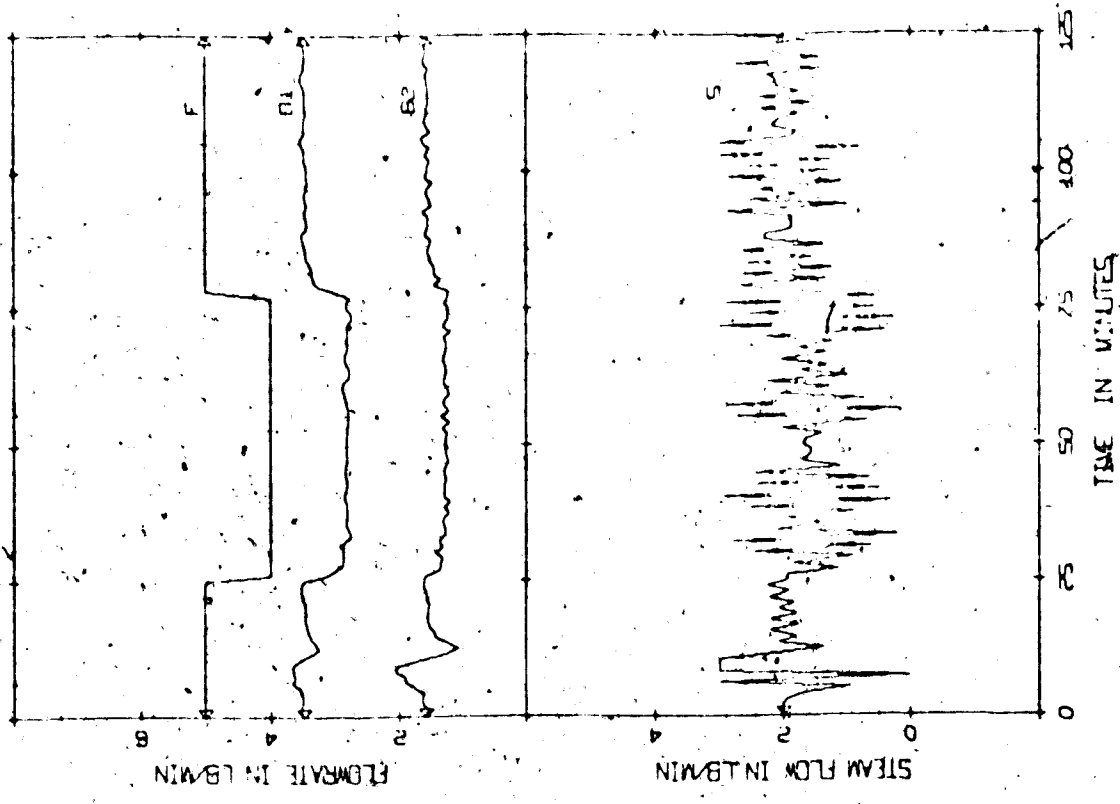
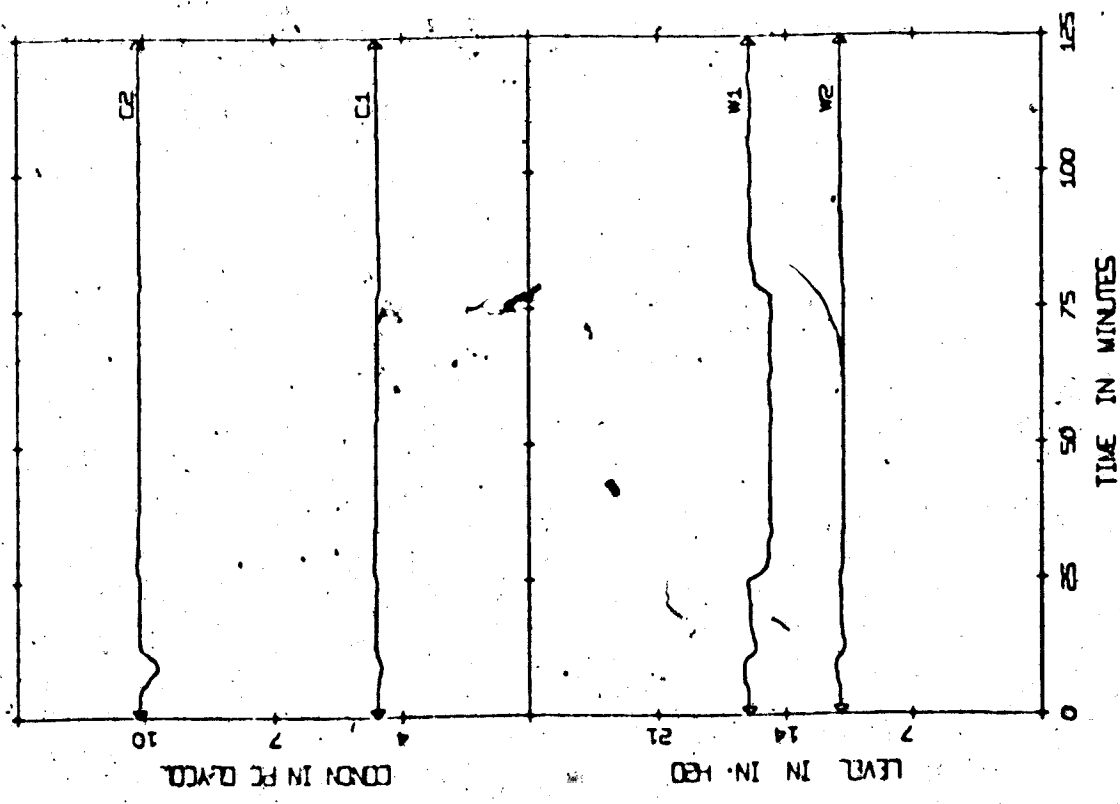


Figure 4.31 Evaporator response (SIM/-20% F, +20% F/STR),  $c_{PN} = 0.01$

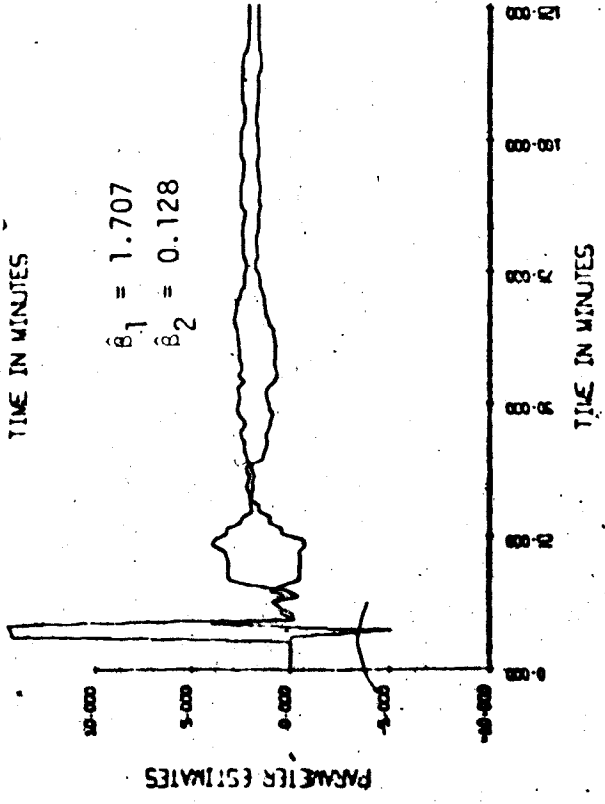
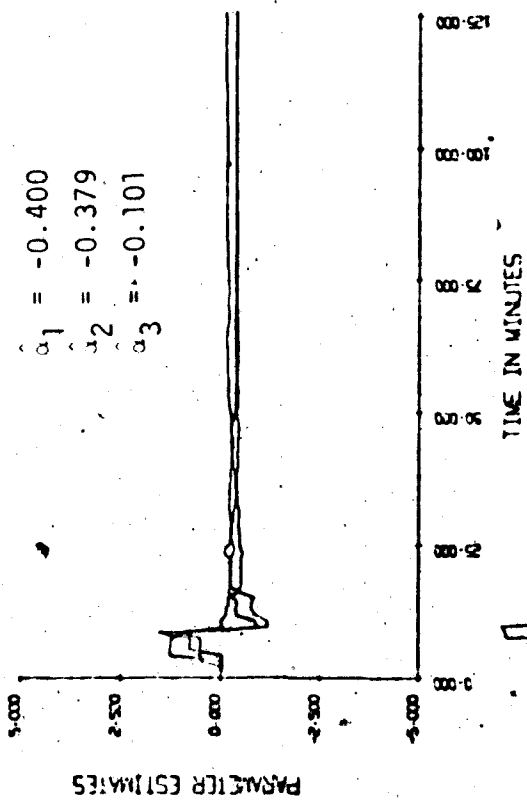


Figure 4.32 Parameter estimates (SIM/STR)  $\sigma_{MN} = 0.05$

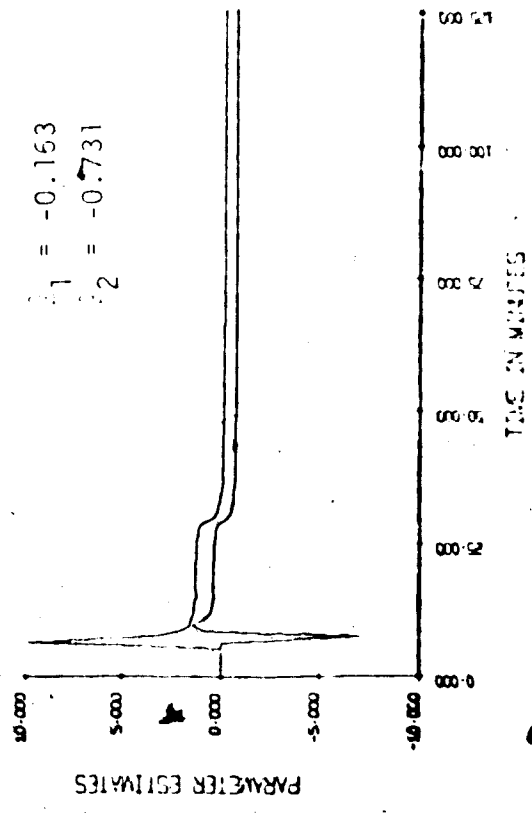
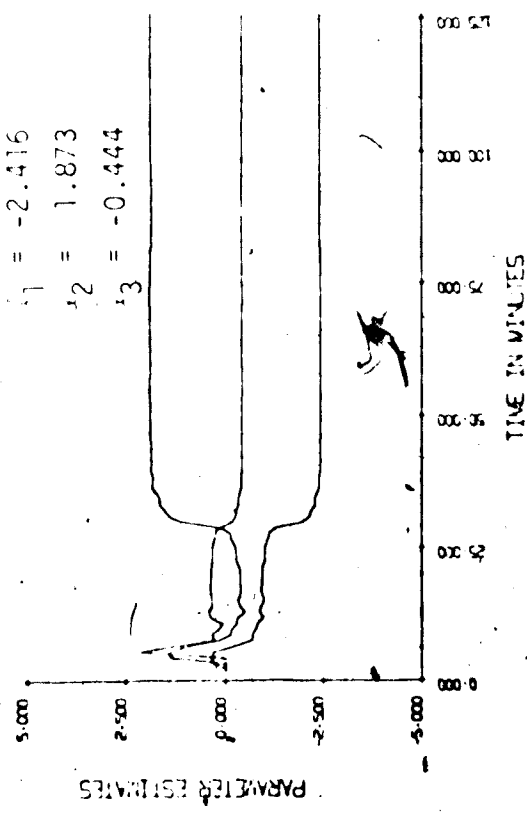


Figure 4.33 Parameter estimates (SIM/-20% F, +20% F/STR),  $\sigma_{PN} = 0.01$

It is interesting to note that the latter part of the C2 response in figure 4.30 is worse than the response in figure 3.11 where proportional control is used with  $K_{C2} = -4.89$  for the same process conditions.

#### 4.4.3 Effect of Unmeasured Step Disturbances

In practical applications it is seldom feasible to measure all possible disturbance variables. Consequently, the performance of the self-tuning regulator when unmeasured, non-zero mean disturbances occur is quite important.

For a low process noise level of  $\sigma_{PN} = 0.01$  and two step disturbances in feed flow, the self-tuning regulator results in satisfactory control as shown in figure 4.31. The corresponding parameter estimates in figure 4.33 show that the estimates change rapidly after the first step disturbance, but not after the second step change. This somewhat unexpected behaviour can be explained as follows. After the first step down in feed flow, the product concentration increases slightly (this can not be observed in figure 4.33 but can be clearly seen in the computer printout). Therefore, the output elements in the information vector  $\underline{\psi}(t)$  are above their steady state values, and this causes the elements in the covariance matrix  $\underline{P}(t)$  to change. This adjustment in  $\underline{P}(t)$  results in larger elements in the gain vector  $\underline{K}(t)$  which in turn causes some adjustment of the parameter estimates. These changes in the estimates when used in the control law seem to have the same effect as increasing the gain in a proportional controller. This can be observed by comparing the steam

flow rate in figures 4.26 and 4.31.

The set of parameter estimates at  $t = 75$  min were able to handle the second step disturbance quite well. As a consequence, the product concentration, covariance matrix and gain vector were all observed to undergo much smaller changes which meant there was little change in the estimates.

Figures 4.34 and 4.35 show the evaporator response for 10% process noise and step disturbances in feed flow and feed composition respectively. The C2 responses in both runs are very similar to the response for the base case conditions (see figure 4.2). These results indicate that the self-tuning regulator can handle unmeasured step disturbances quite well. The corresponding parameter estimates are shown in figures 4.36 and 4.37. Note that the estimates in figure 4.36 do not undergo sudden changes after the first step change at  $t = 25$  min, as was the case in figure 4.33. This was attributed to the higher process noise level in figure 4.36 since the 10% noise level tended to reduce the effect of the 20% step changes in feed flow rate. It is interesting to note that C2 in figure 4.35 does not have an offset.

When, all the parameters of the predictive model (including  $\beta_0$ ) were estimated, and unmeasured step disturbances were applied, the control of C2 was not very good. Figures 4.38 and 4.39 show two cases where feed flow and feed concentration disturbances occur. The two C2 responses were significantly worse than the same case without the step disturbances (see figure 4.3). This illustrates that poor C2 responses, can result if all parameters are estimated during closed loop operation. The corresponding parameter estimates plots are shown in figures 4.40

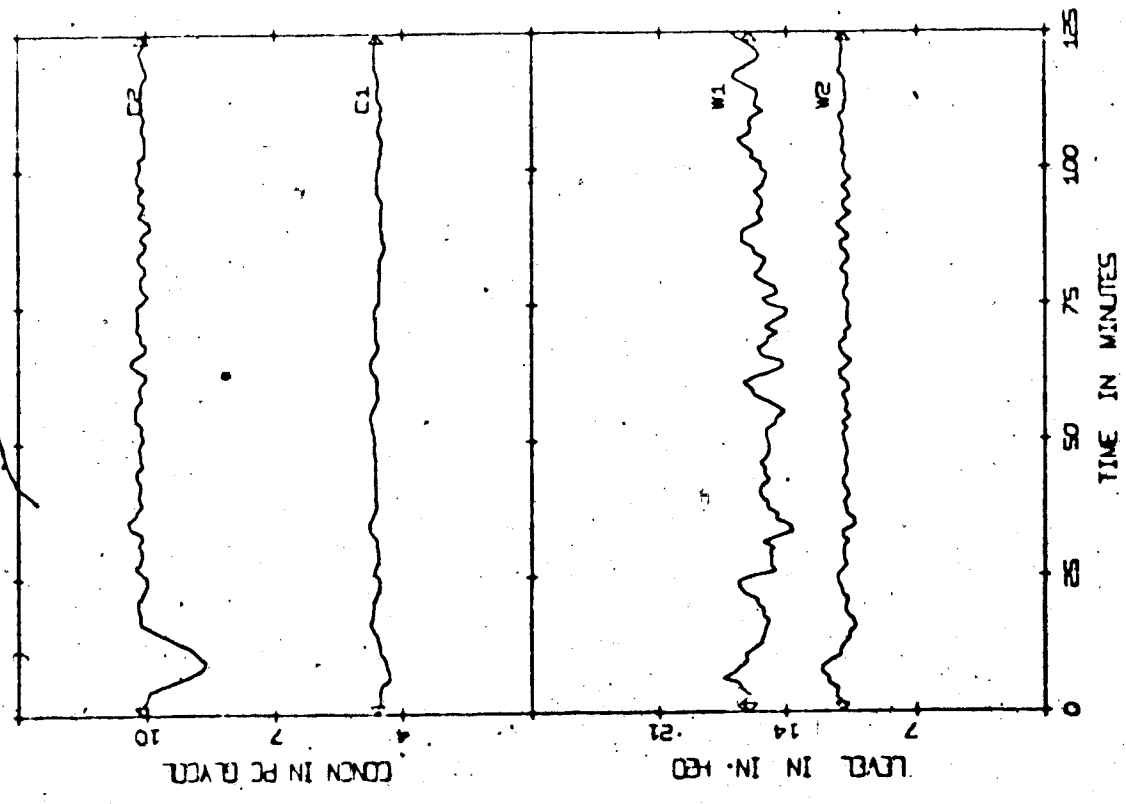
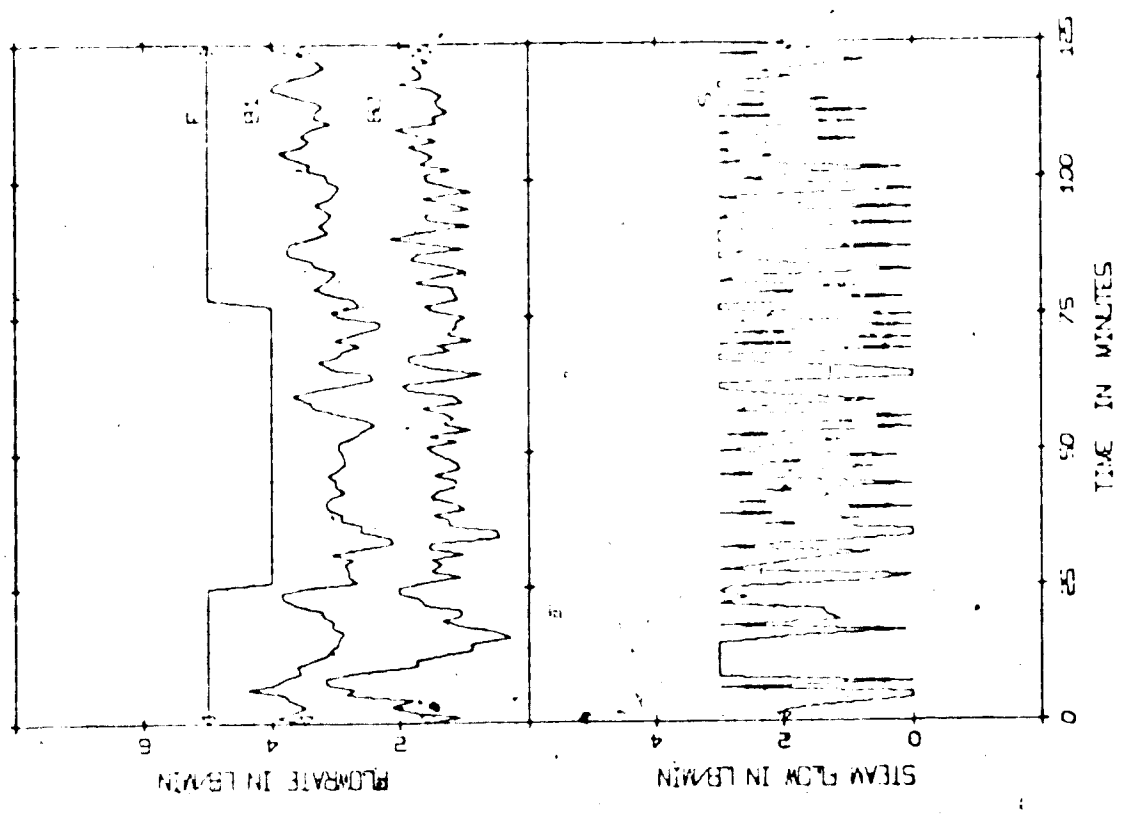


Figure 4.34 Evaporator response (SIM/-20% F, +20% F/STR)

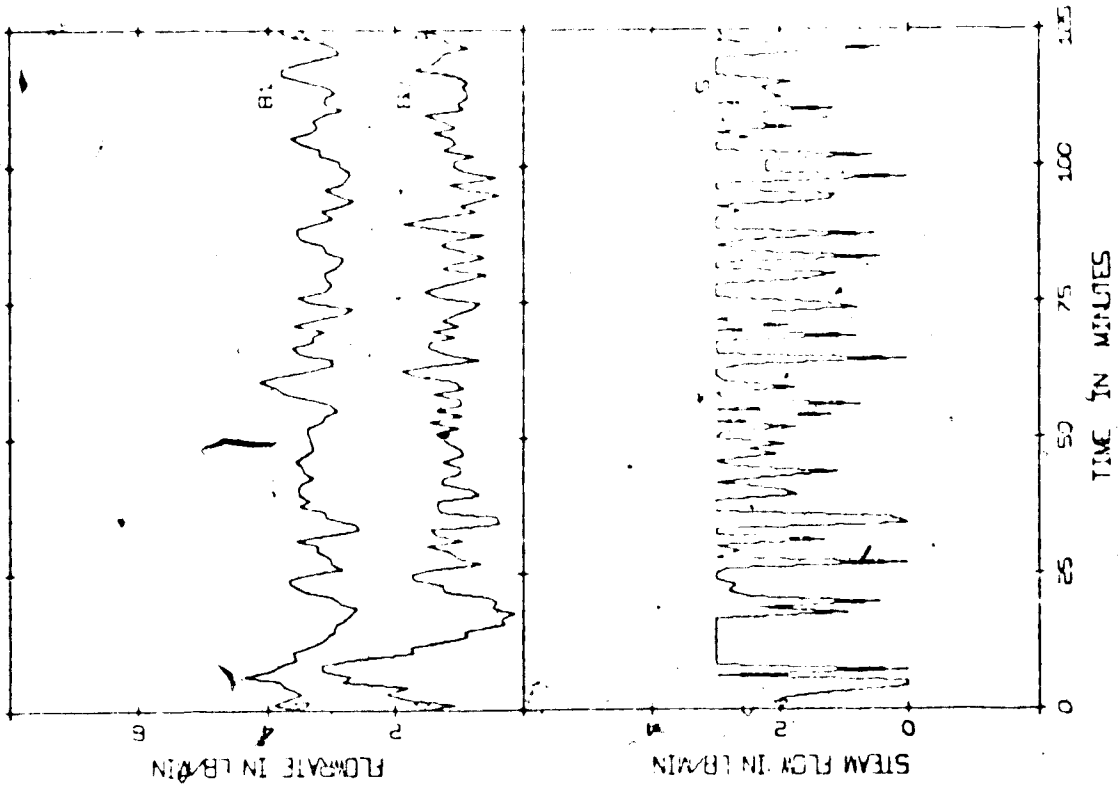
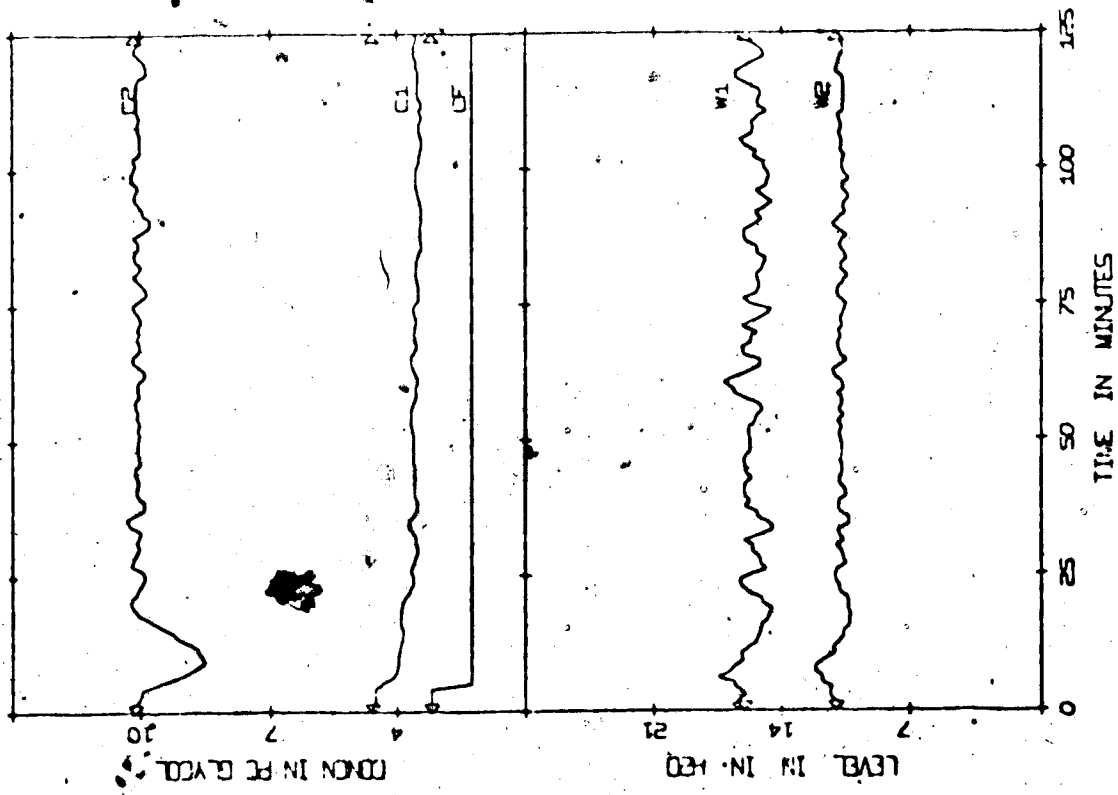


Figure 4.35 Evaporator response (SIM/-30% CF/STR)

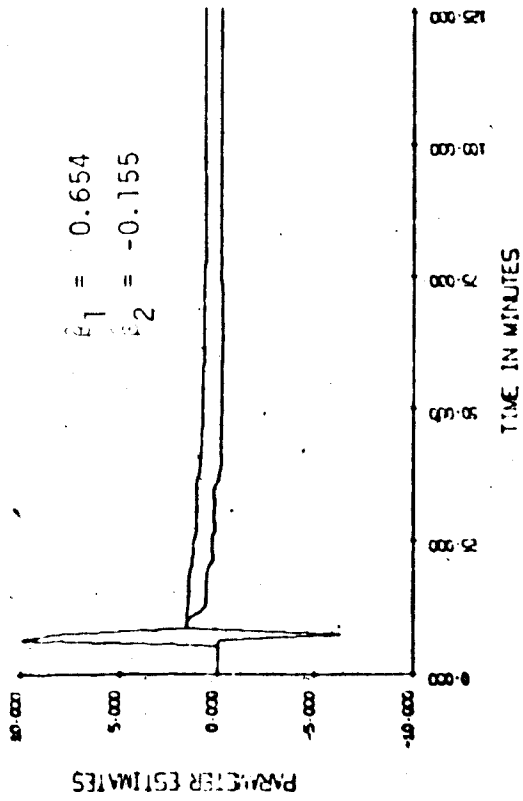
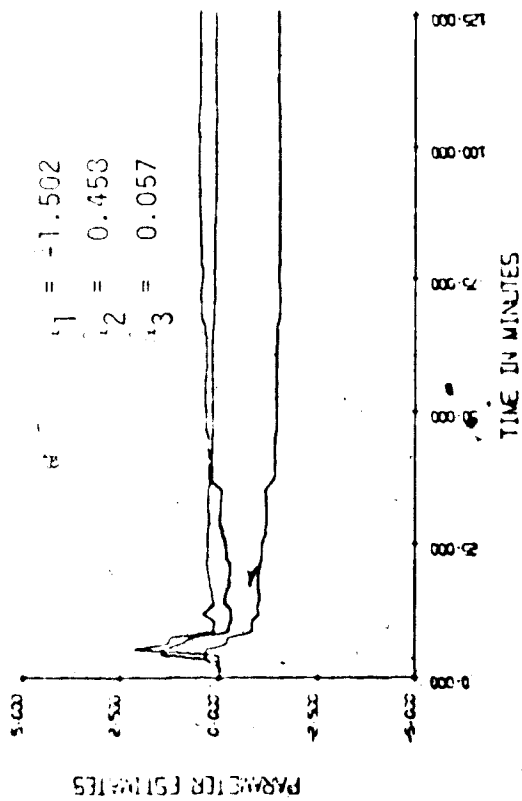


Figure 4.36 Parameter estimates (SIM/-20% F, +20% F/STR)

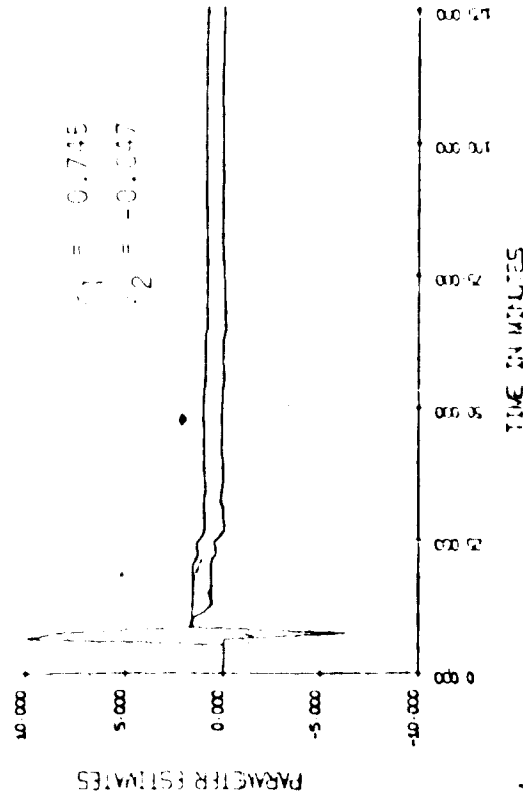
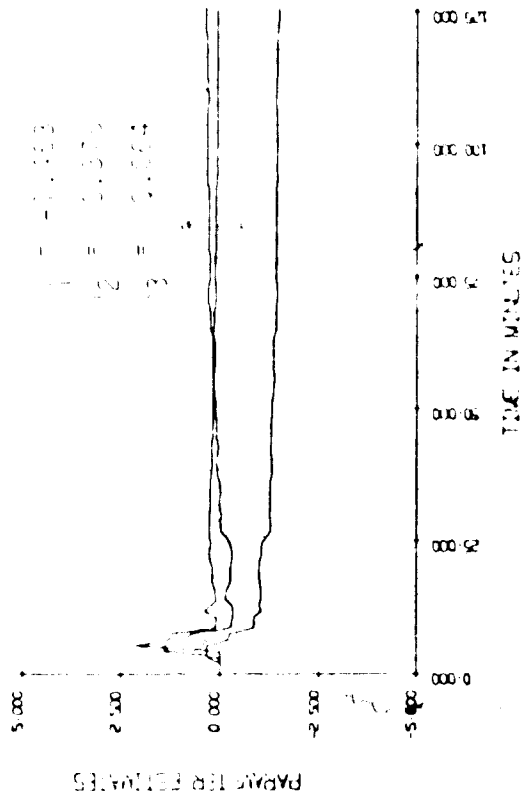


Figure 4.37 Parameter estimates (SIM/-30% CF, STR)

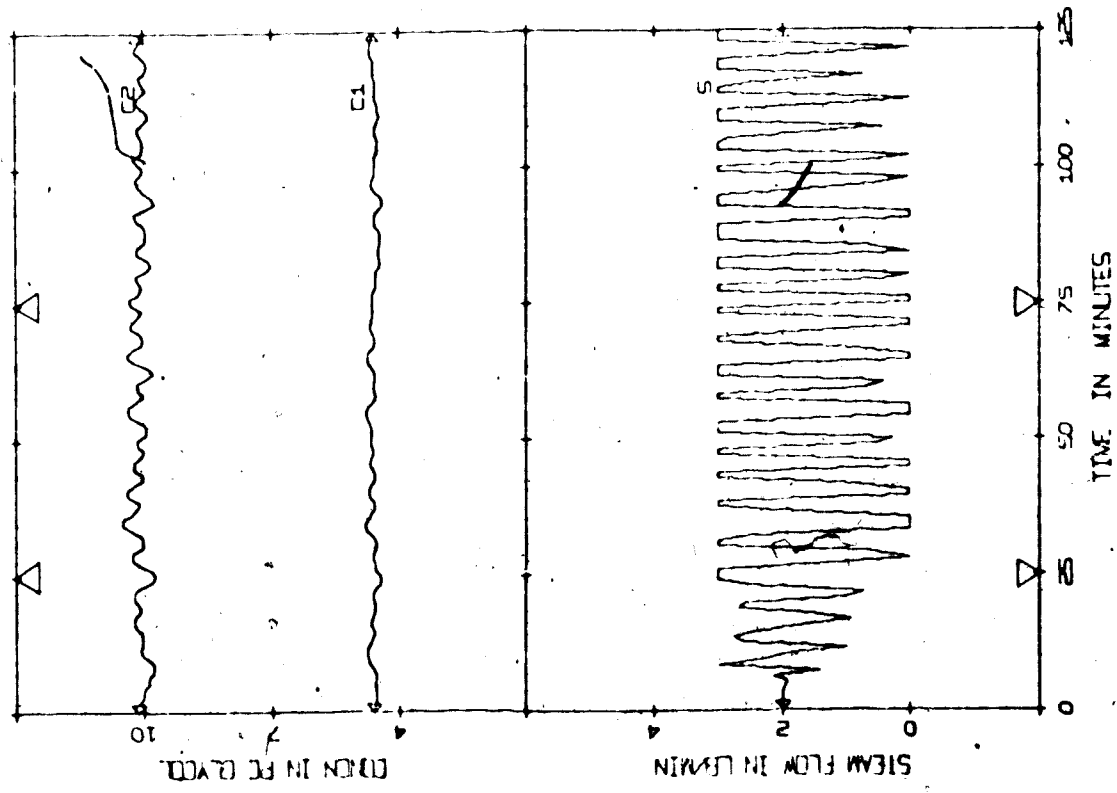


Figure 4.38 Evap. response (SIM/-20% F, +20% F/STR),  $\beta_0$  estimated

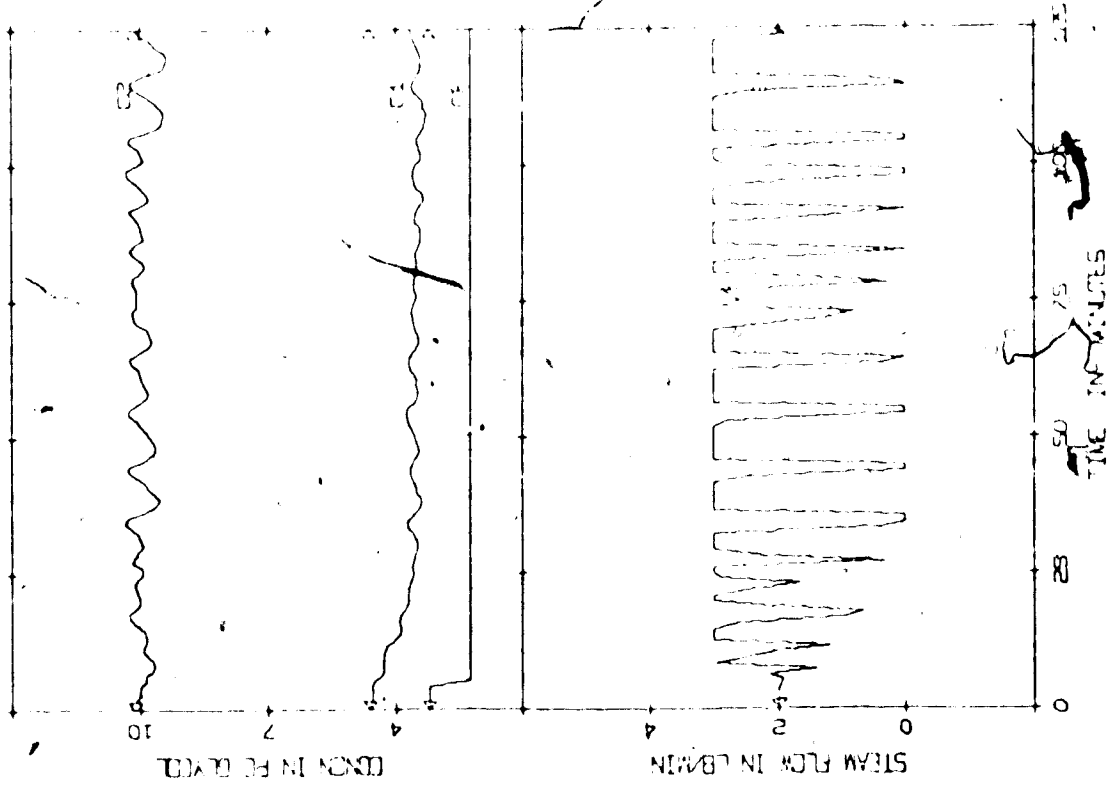


Figure 4.39 Evap. response (SIM/30% CF/STR),  $\beta_0$  estimated



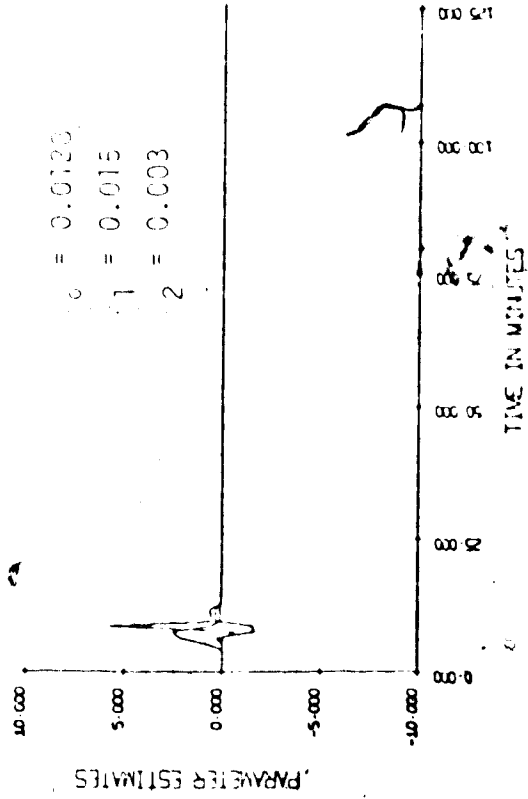
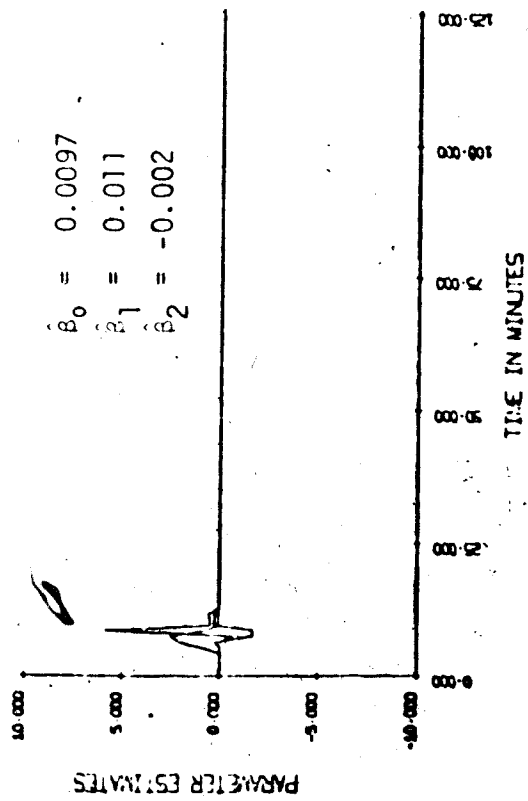
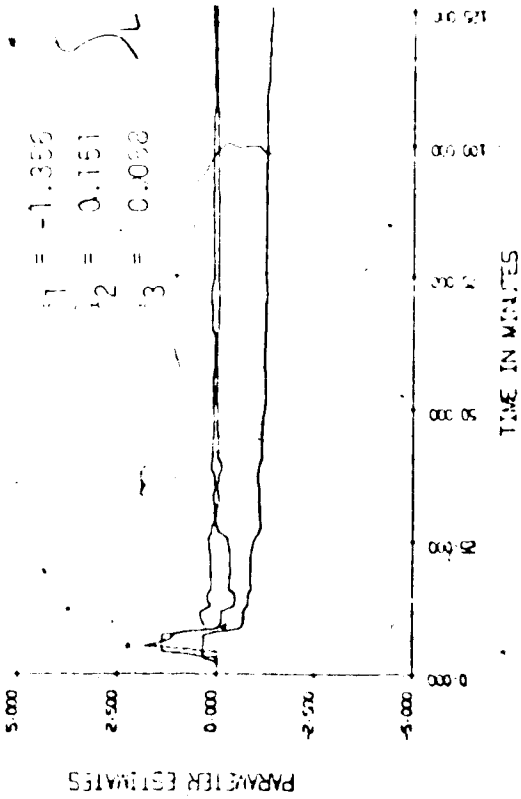
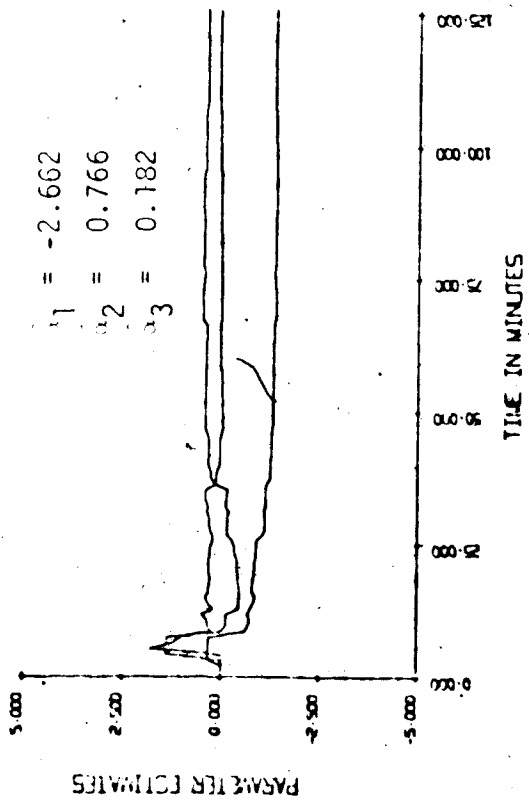


Figure 4.40 Parameter estimates (SIM/-20%, +20% F/STR), Figure 4.41 Parameter estimates (SIM/-30% CF/STR),  $\beta_0$  estimated.

and 4.41. For all runs where  $\hat{\theta}$  is estimated, the  $\hat{\theta}$  converged to values very close to zero.

#### 4.5 Practical Strategy for Implementing Self-Tuning Regulator

When a process control computer is used to control an industrial process, it will probably not be economical to replace most of the conventional digital controllers in individual loops with self-tuning regulators. This is because self-tuning regulators require more execution time due to the recursive least squares equations and they also require more storage space for input/output data. The process computer might not be able to handle the extra work load or have sufficient storage space for the extra data. One way of getting around this problem is to use the self-tuning regulator only on important control loops and/or after process conditions have experienced a significant change. Furthermore, the self-tuning regulator need only be applied until good parameter estimates and a satisfactory controller have been obtained. Then the estimation step can be bypassed and the now constant parameter estimates can be used in the control calculations (i.e. a controller with constant coefficients in the control law).

Figure 4.42 shows a run in which the controller had constant parameters which were obtained from the final parameter estimates at the end of the base case run. Even when two 40% step disturbances in feed flow were applied, the controller was able to control C2 quite well.

Theoretically, if the estimator is being used for very long periods of time the elements in both the covariance matrix and the gain

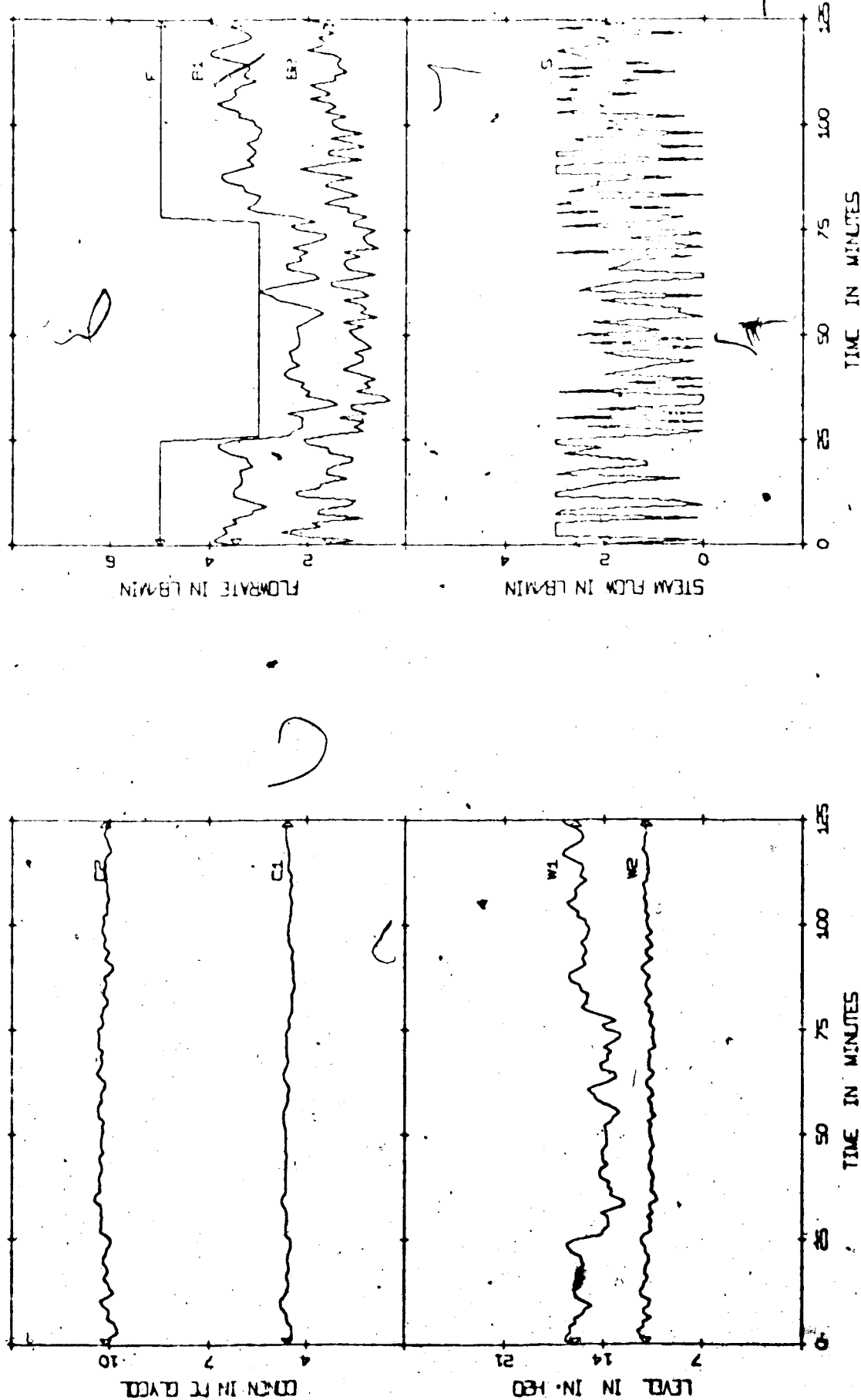


Figure 4.42 Evaporator response (SIM/-40% F, +40% F/STR), constant parameters in regulator

vector in the algorithm decrease as the parameter estimates converge. This is satisfactory as long as process conditions do not change. But if the process conditions do change, the elements of the gain vector are now too small to be of any effective use in updating the parameter estimates. To avoid this type of situation, the regulator should be re-initialized periodically. This can be done by re-initializing the covariance matrix. Figure 4.43 shows a run in which the initial parameter estimates were the final estimates obtained from the base case run and  $\underline{P}(0) = 100 \underline{I}$  was employed at the beginning of the run. The corresponding parameter estimates are shown in figure 4.45. Note that the estimates deviate from the initial values at the beginning of the run but gradually approach these values towards the end of the run.

One way of avoiding the problem of poor estimates and poor control during the transient period has been suggested by Wittenmark [7] and is as follows. Suppose a well-tuned conventional controller is used initially and least square estimation is performed to determine the parameters of the predictive model. Then the switch to the self-tuning regulator can be made after the parameter estimates have become fairly constant.

Figures 4.44 and 4.46 show a run in which a proportional controller was used in the S/C2 loop for the first 14 minutes with  $K_{C2} = -4.89$ . The self-tuning regulator was then substituted for the proportional controller at the 15 minute mark. Note that the initial "bump" in previous C2 curves is eliminated since the self-tuning regulator starts with better initial parameter estimates, namely, those that were generated during proportional control. Thus

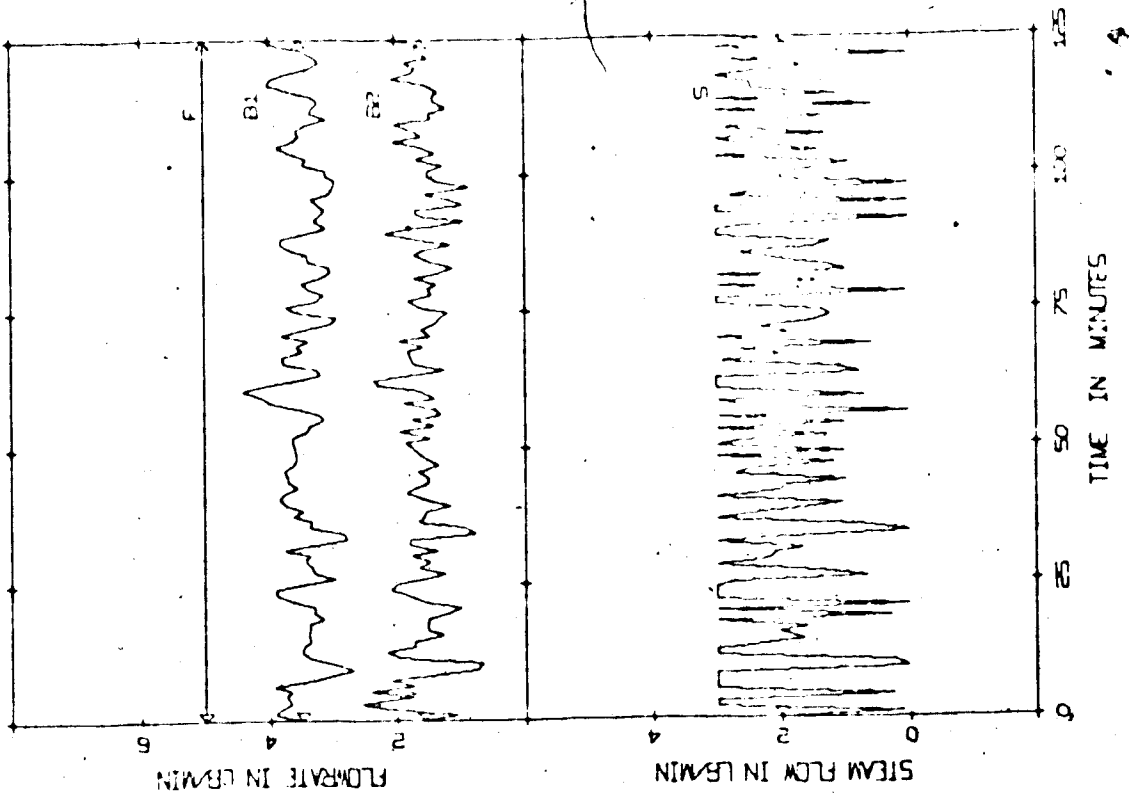
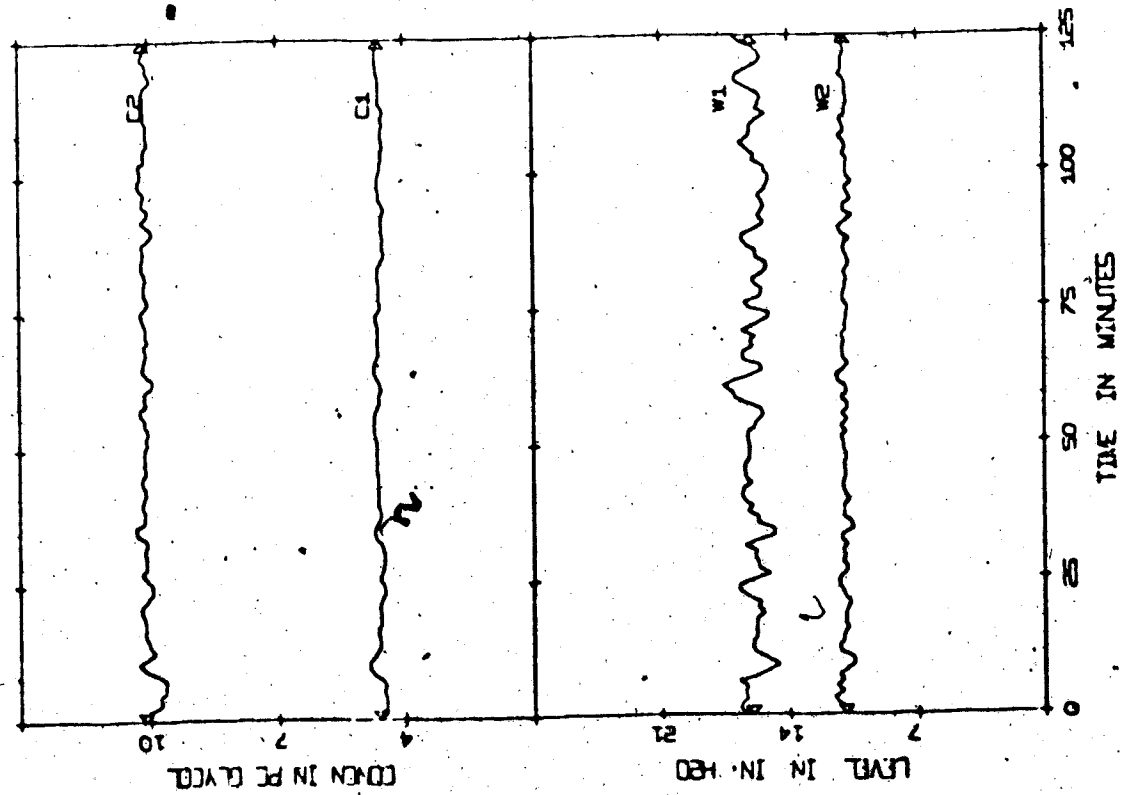


Figure 4.43 Evaporator response (SIM/STR), re-initializing the regulator

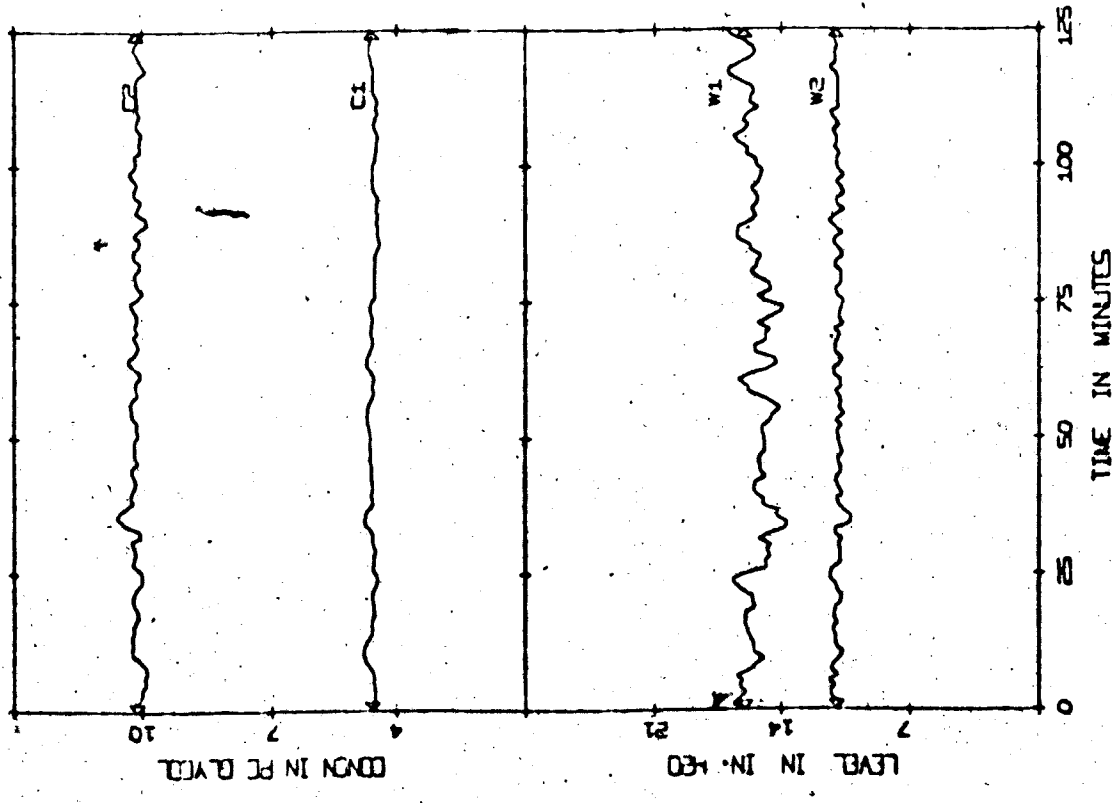
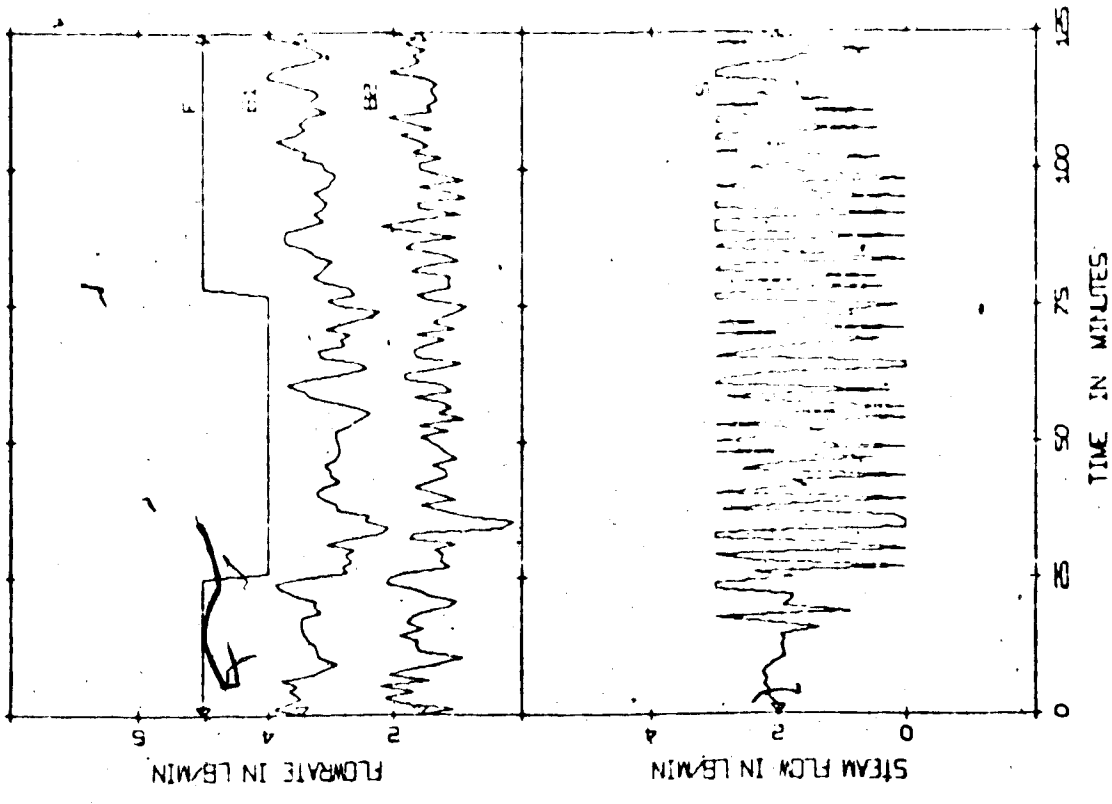


Figure 4.44 Evaporator response (SIM/-20% F, +20% F/ML & STR)

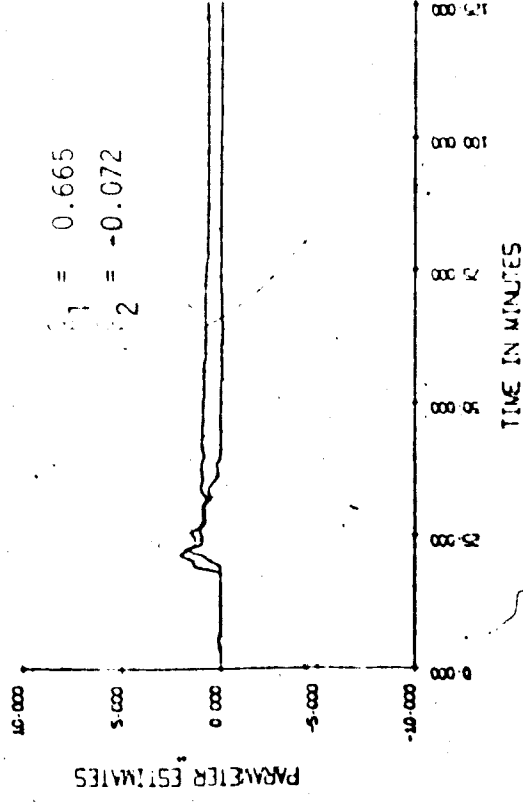
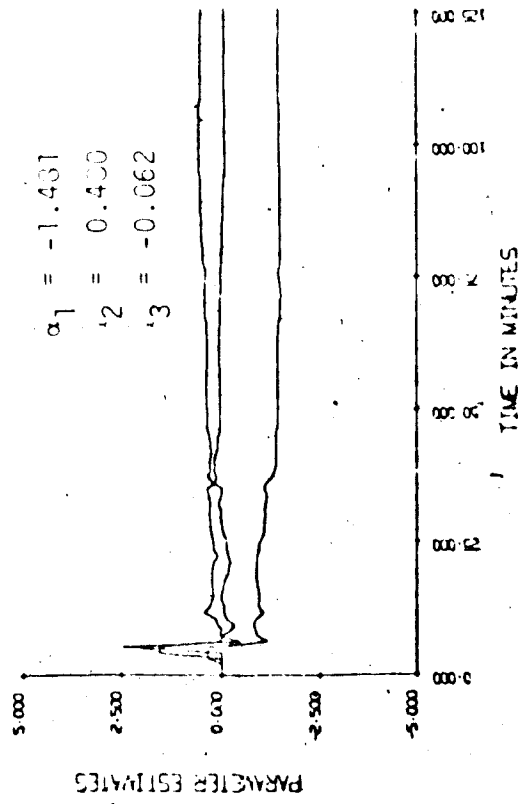
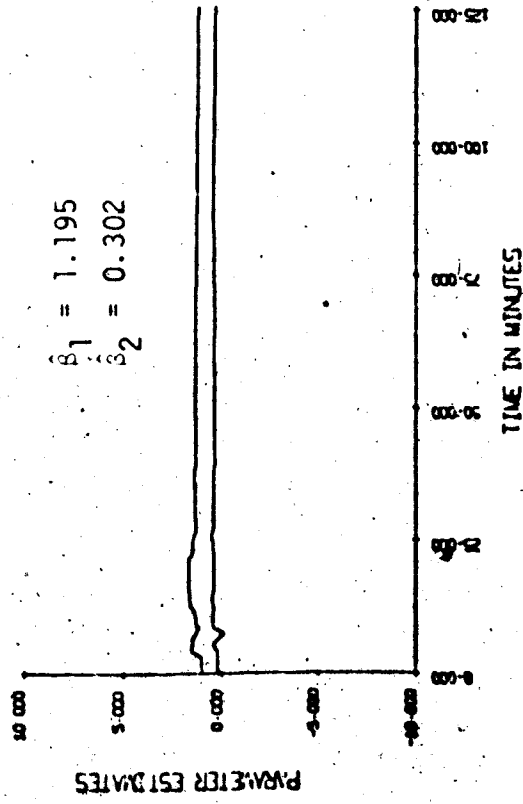
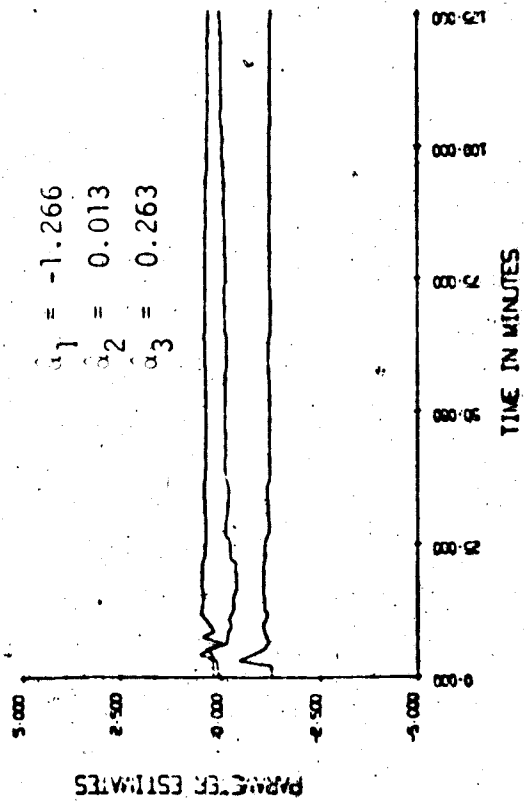


Figure 4.45 Parameter estimates (SIM/STR), re-initializing the regulator

Figure 4.46 Parameter estimates (SIM/-20%F, +20% F/ML & STR)

this strategy provides a systematic technique for a bumpless transfer from a conventional control strategy to the self-tuning regulator.

#### 4.6 Conclusions

From the extensive simulation study of the double effect evaporator model, it can be observed that the self-tuning regulator is very simple to use. The initial choice of constants and parameters required for the regulator can be made without detailed knowledge of the process to be controlled and the regulator performs fairly well, even for poor choices. Once the regulator is operational, these constants can be adjusted to better values by examining the process data and the parameter estimates.

The self-tuning regulator also performed well when different unmeasured disturbances of relatively large magnitude were applied, but did not fare as well when 5% measurement noise was added.

Practical ways of implementing the self-tuning regulator were suggested in section 4.5. These methods tend to ensure good performance of the regulator when it is used periodically on a long term basis.

In general, the self-tuning regulator definitely performed better than the conventional proportional controller in the simulation study. This success results because the algorithm is designed to minimize the output variance in the presence of noise.

The simulation results showed the good convergence properties of the self-tuning algorithm. The system was stable unless very poor constants were used in the algorithm. The algorithm itself is very



simple and there are no complex mathematical operations involved. The compactness and the simplicity of the algorithm plus its ability to handle relatively large process noise levels and unmeasured disturbances make it very attractive for industrial applications.

## CHAPTER FIVE

## SELF-TUNING REGULATOR FOR THE DOUBLE EFFECT EVAPORATOR:

## EXPERIMENTAL RESULTS

5.1 Introduction

This chapter presents experimental results of the application of conventional multi-loop control and the self-tuning regulator to the double effect evaporator. The pilot plant evaporator that is interfaced to the IBM 1800 process control computer has been described in Chapter Three. The simulation results for the evaporator have been presented in Chapters Three and Four. This chapter also includes a brief description of the control computer program that was used. The experimental results are then presented and compared with the simulation results. Finally, conclusions on the practical uses of the self-tuning regulator in industry are given.

5.2 Experimental Procedure

In order to compare the simulated and experimental results, a similar set of runs was performed on the actual evaporator system. Initial conditions were maintained close to those used in the simulation runs. Prior to the start of each experimental run, the evaporator was brought to the nominal steady state conditions by means of multi-loop digital proportional-integral controllers (the nominal steady state values are shown in the Appendix for Chapter Three). The control program was then initiated and the evaporator data were collected via individual DDC (Direct Digital Control) loops at every sampling interval and were stored on disk files. The control and sampling periods were specified to be 64 seconds as in the simulation runs. The control

signals calculated from the control algorithms were set as setpoints to the individual DDC control loops. At the end of each run, all the collected data were printed and also punched on computer cards. Documentation of a typical experimentation run is shown in the Appendix for Chapter Five, including heat and material balances and a log of pressures, temperatures and flow rates etc. These records plus the computer print-out of the evaporator variables and parameter estimates, and the recorder charts for each run have been compiled in an "Experimental Data Book".

A statistical analysis of normal steady state experimental data has been performed by Hamilton [28] to estimate the actual process and measurement noise levels. These estimates were found to be much less than the 10% and 5% levels used for process noise and measurement noise, respectively, in the simulation study. The actual estimates calculated by Hamilton were 0.1% to 5% for the process noise and 0.1% to 2% for the measurement noise. In all the runs, the evaporator variables were filtered by simple filters such as exponential or Union filters so that smooth and accurate data would be used and recorded. The three output variables were filtered by exponential filters with filter constants of 0.75.

### 5.3 Computer Programs for the Experimental Study

The real-time computer programs that were used in the closed-loop experimental study were basically the ones developed by Newell [36]. Program coreloads RBN30, RBN31, RBN32 and RBN33 were modified so that three different control strategies could be used: multi-loop proportional control, the self-tuning regulator and minimum variance control.

To avoid confusion with the original program coreloads, these modified coreloads were re-named, FLC30 to FLC33. The initialization procedures of these control programs are essentially the same as those used by Newell and these procedures can be found in Newell's "User's Manual" [36]. Programs RBN19 and RBN20, used to print and punch the accumulated experimental data, were also modified to include the parameter estimates and were re-named as FLC19 and FLC20. Plotting programs RBN01 and RBN02 [32] were used to plot the evaporator variables.

#### 5.4 Experimental Evaporator Results

To verify the main results of the simulation study, a similar set of experimental runs were performed. Again, conventional multi-loop control techniques such as digital proportional control and proportional plus integral control were applied. Then the self-tuning regulator was used in the steam/product concentration control loop and the effects of various design decisions and parameter values were investigated, as in the simulation study.

In addition to the lower process noise levels in the actual evaporator system, several other changes had to be made for the experimental runs. First, tighter constraints were placed on the steam flow rate which was limited to between 0.5 and 2.5 lb/min. The upper bound was chosen to limit the pressure in the first effect to a safe operating level. The lower bound was chosen to be 0.5 lb/min instead of zero to prevent negative pressure in the first effect as a result of stoppage of boiling and condensation of overhead vapour. Second, the proportional gains in the two level control loops had to be reduced to less than half the normal values which were used in the simulation study. The

TABLE 5.1  
EXPERIMENTAL RESULTS FOR CONVENTIONAL CONTROL STRATEGIES

FIGURES	RUN NO.	TYPE OF CONTROL	STEP DISTURBANCES
5.1, 5.3	26	ML prop. control	(+20% F, -20% F)
5.2, 5.4	27	ML prop. control	(-30% CF)
5.5	21	ML PI control	(+20% F, -20% F)
5.6	24	ML PI control	(+20% F)
5.7	25	ML PI control	(-20% F)

reason for reducing the gains was that the bang-bang characteristics of the steam signal resulted in large fluctuations in the first effect pressure and the first effect level measurements, which in turn affected the first effect bottom flow rate, and the second effect level and bottom flow rate. These interactions between process variables resulted in poor control of product concentration. To avoid this undesirable situation, the proportional gains in the two level control loops were decreased in order to reduce the interactions.

These differences in operating conditions should be kept in mind when the simulation results are compared with the experimental results. The experimental runs for conventional multi-loop control and the self-tuning regulator are shown in Tables 5.1 and 5.4, respectively. Since the experimental runs were performed for different periods of time, the parameter estimates listed in Table 5.4 and in the figures were those recorded at the end of the runs.

#### 5.4.1 Conventional Multi-Loop Control

Conventional multi-loop proportional control using the modified version of the multivariable control programs [36] was applied with the following proportional gains for the three control loops.

TABLE 5.2

PROPORTIONAL CONTROLLER GAINS

S/C2	loop	,	$K_{C2} = -4.89$
W1/B1	loop	.	$K_{W1} = 1.5$
W2/B2	loop	.	$K_{W2} = 6.5$

Note that the proportional gains in the two level control loops are lower than those used in the simulated study of Section 3.5.

The evaporator responses for feed flow and feed composition step disturbances are shown in Figures 5.1 and 5.2. The C2 responses and the two effect levels and bottom flow rates in both figures are less oscillatory than those in the simulation results. This is due to the lower process noise level and lower gains in the level control loops. Both the feed and first effect concentrations (CF and C1) were only measured before, but not during, the experimental runs, thus, the C1 curves are not shown and CF is a straight line in Figure 5.1.

During these closed loop runs, the least squares estimator in the self-tuning algorithm was used to estimate the parameters of the predictive model. The initial constants and parameters specified for the algorithm were those used in the base case run in Section 4.2. The parameter estimates for these two runs are shown in Figures 5.3 and 5.4. The convergence of the estimates is not very good because the evaporator variables undergo little excitation.

The DDC version of multi-loop proportional plus integral control was also applied since this is a widely used conventional control technique. The closed-loop response of the evaporator to two 20% step disturbances in feed flow for King and McNeill's DDC controller constants [37] in Table 5.3 is shown in Figure 5.5. (KP and KI are the proportional and integral constants, respectively, readers are referred to the DDC Manual [39] for more information on DDC control loops).

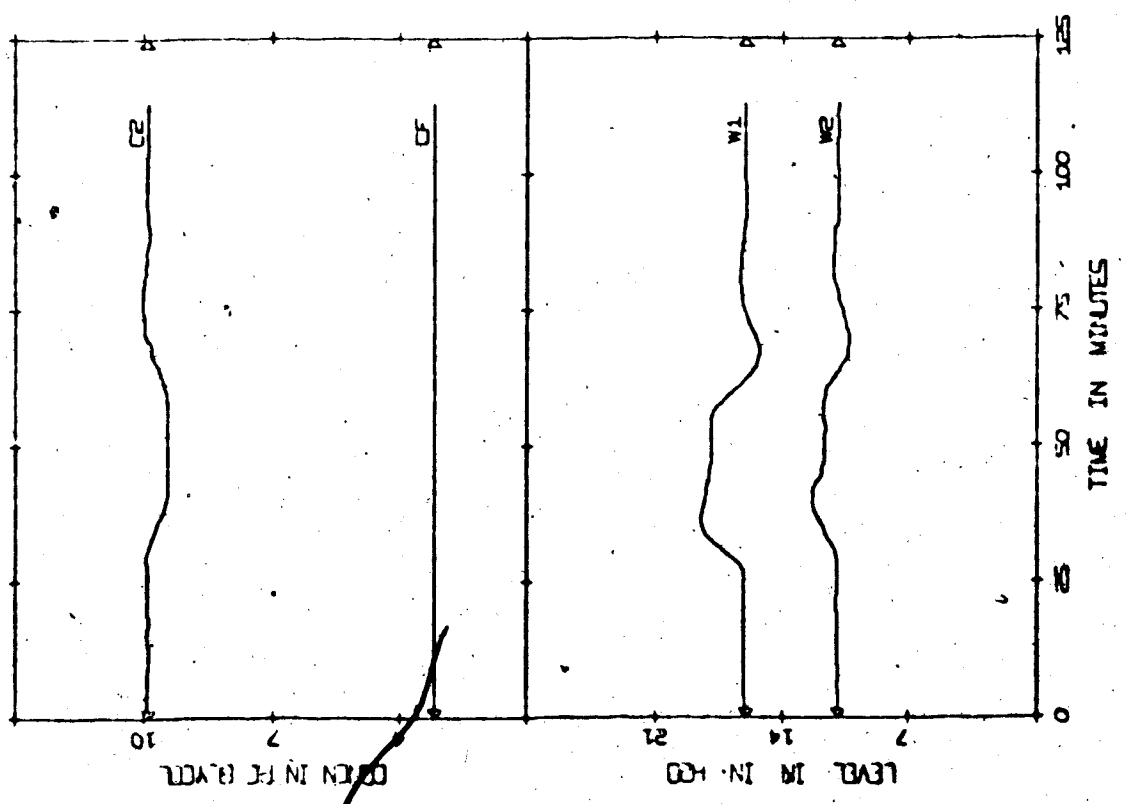
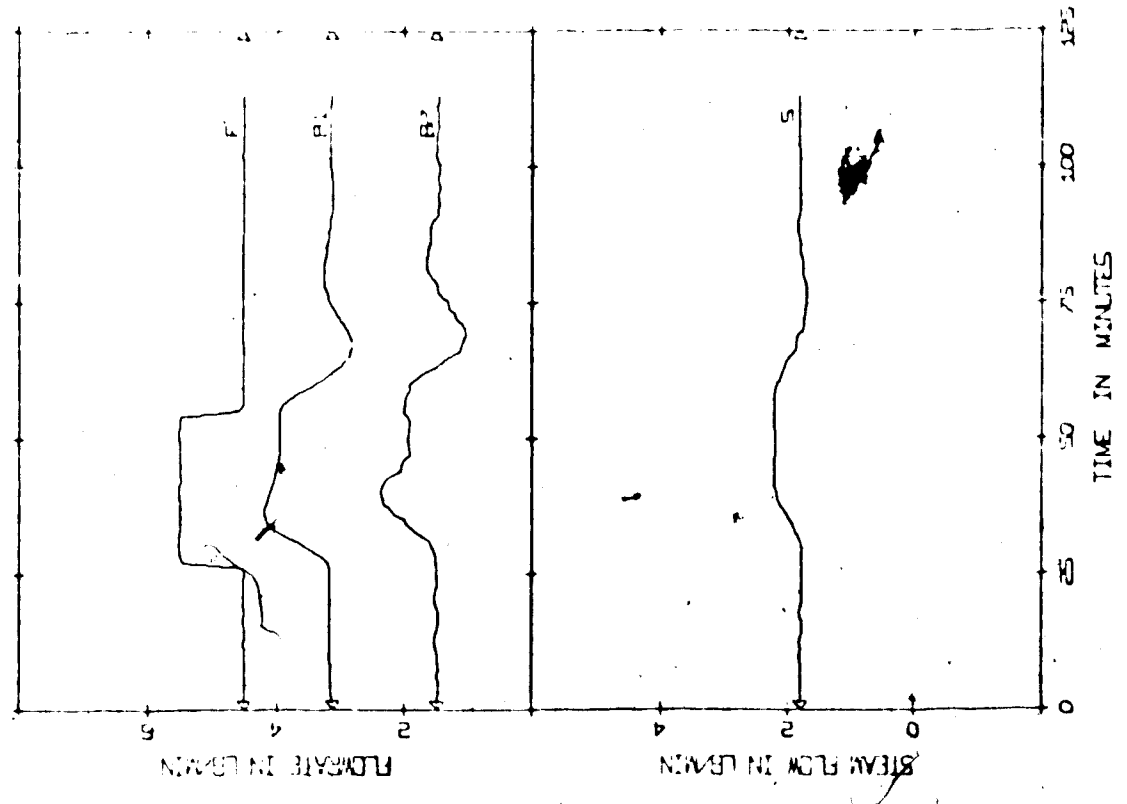


Figure 5.1 Evaporator response (EXP/+20% F, -20% F/ML prop. control)



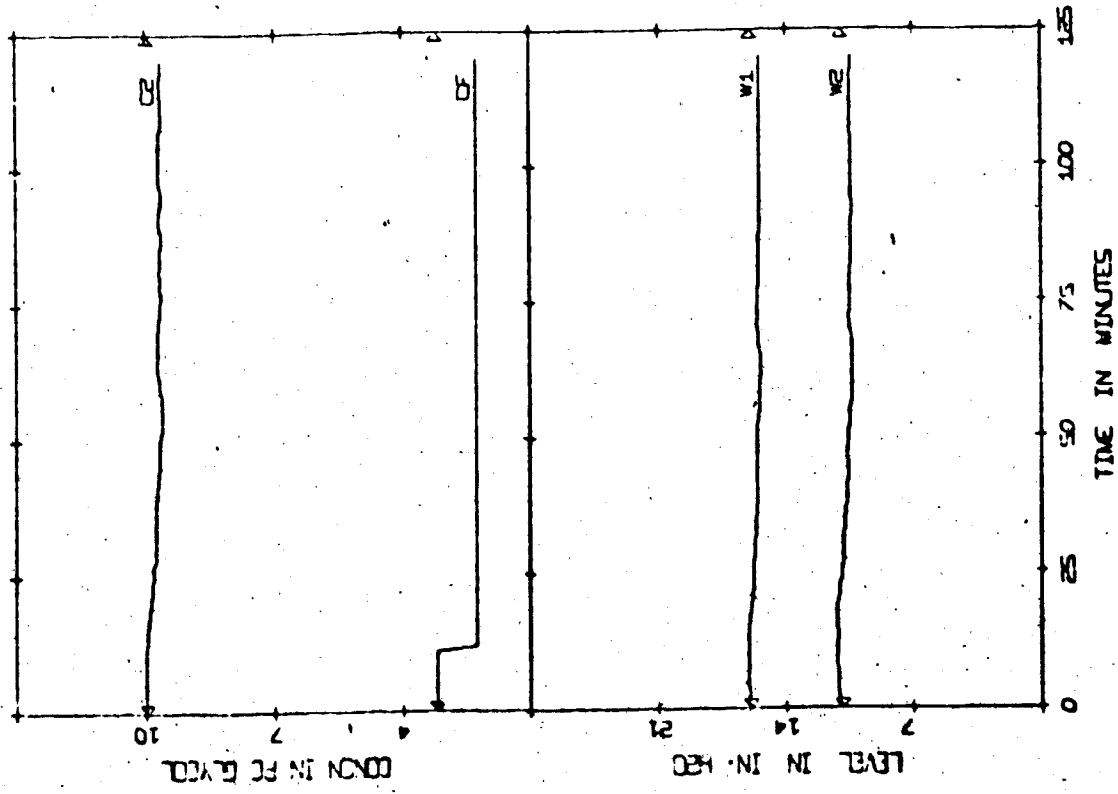
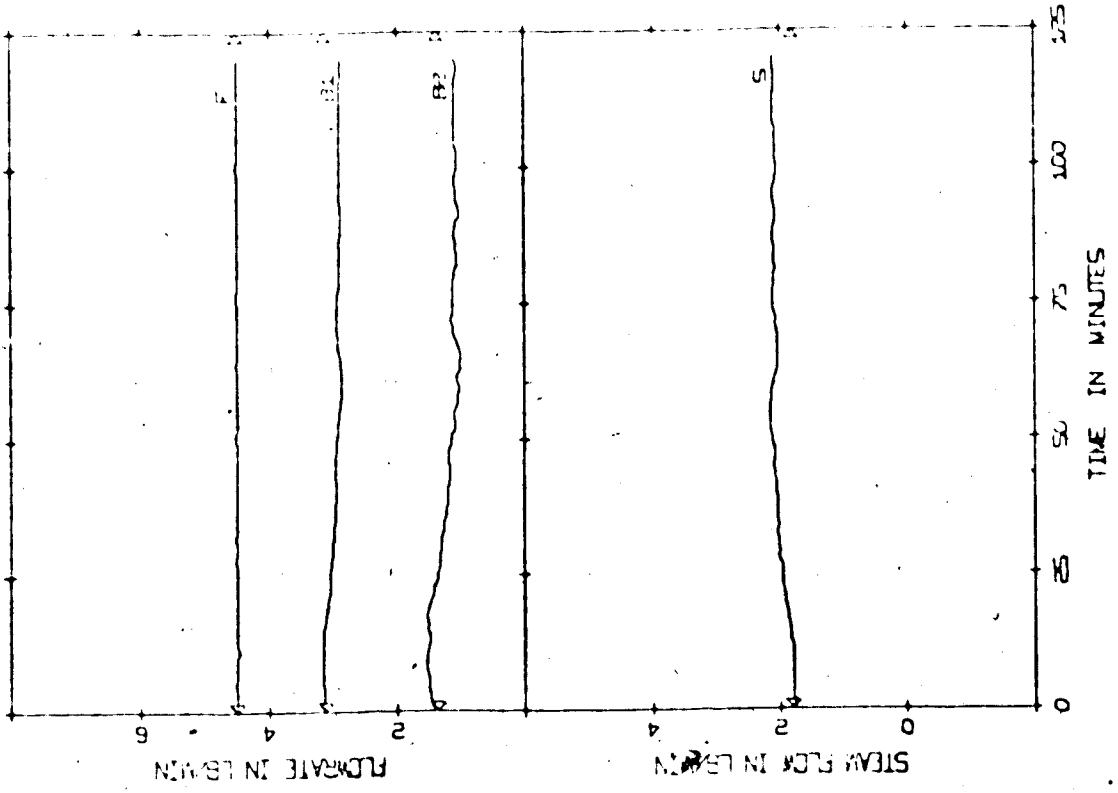


Figure 5.2 Evaporator response (EXP/-30% CF/ML prop. control)

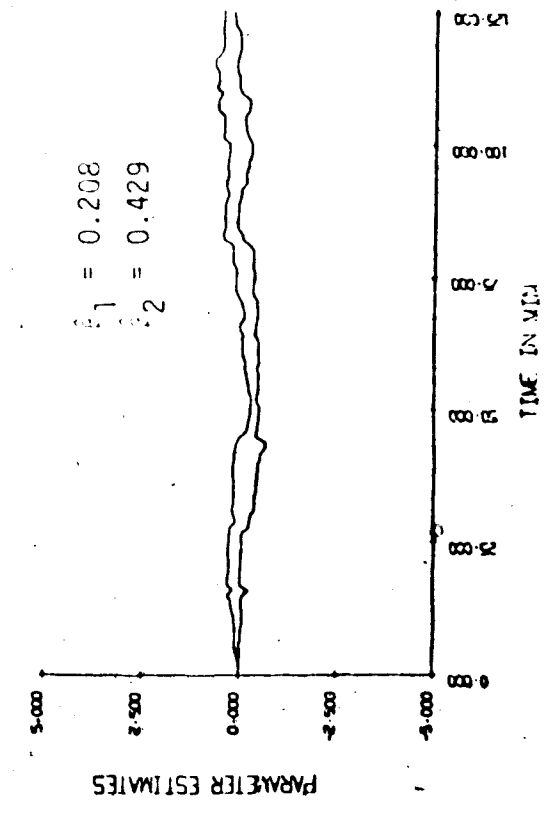
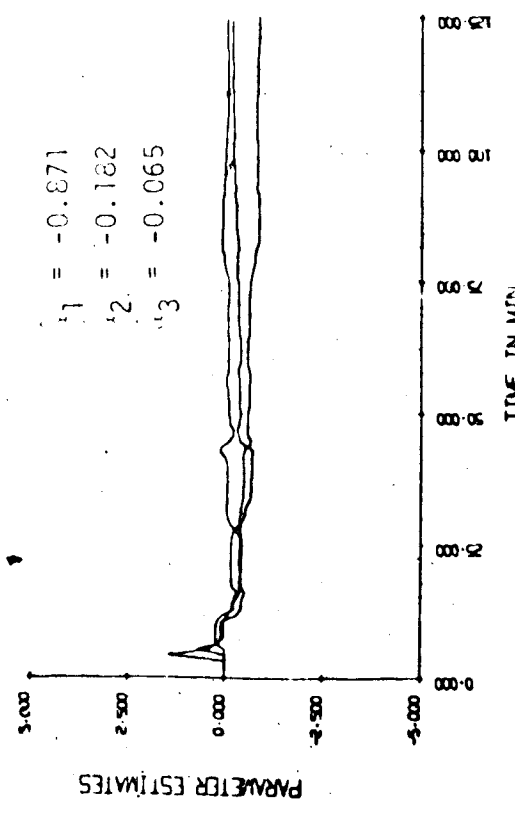
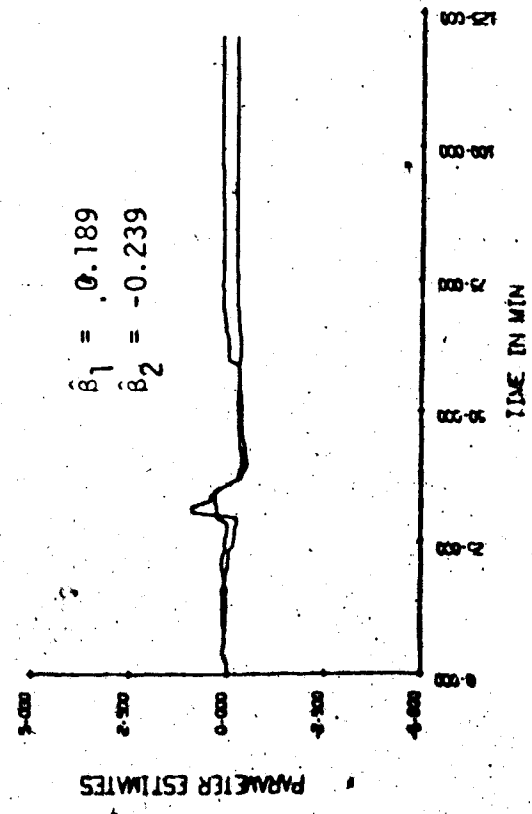
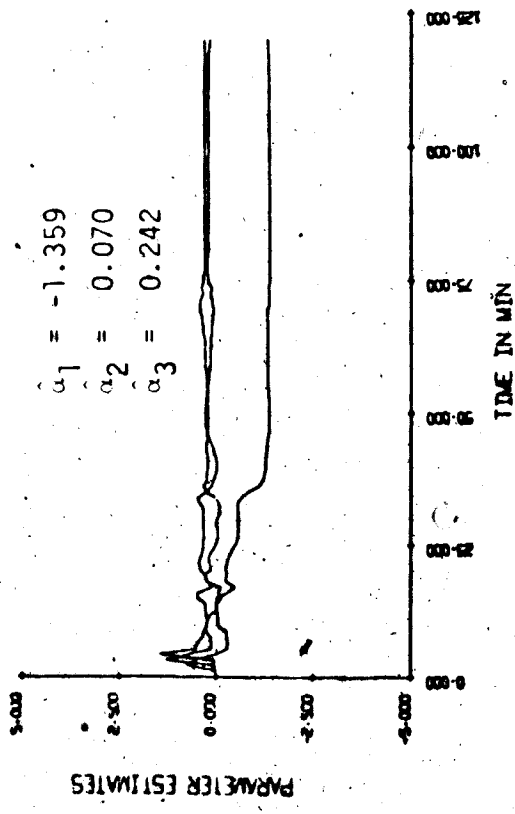


Figure 5.3 Parameter estimates (EXP/+20% F, -20% F/ML prop. control)

Figure 5.4 Parameter estimates (EXP/-30% CF/ ML prop. control)

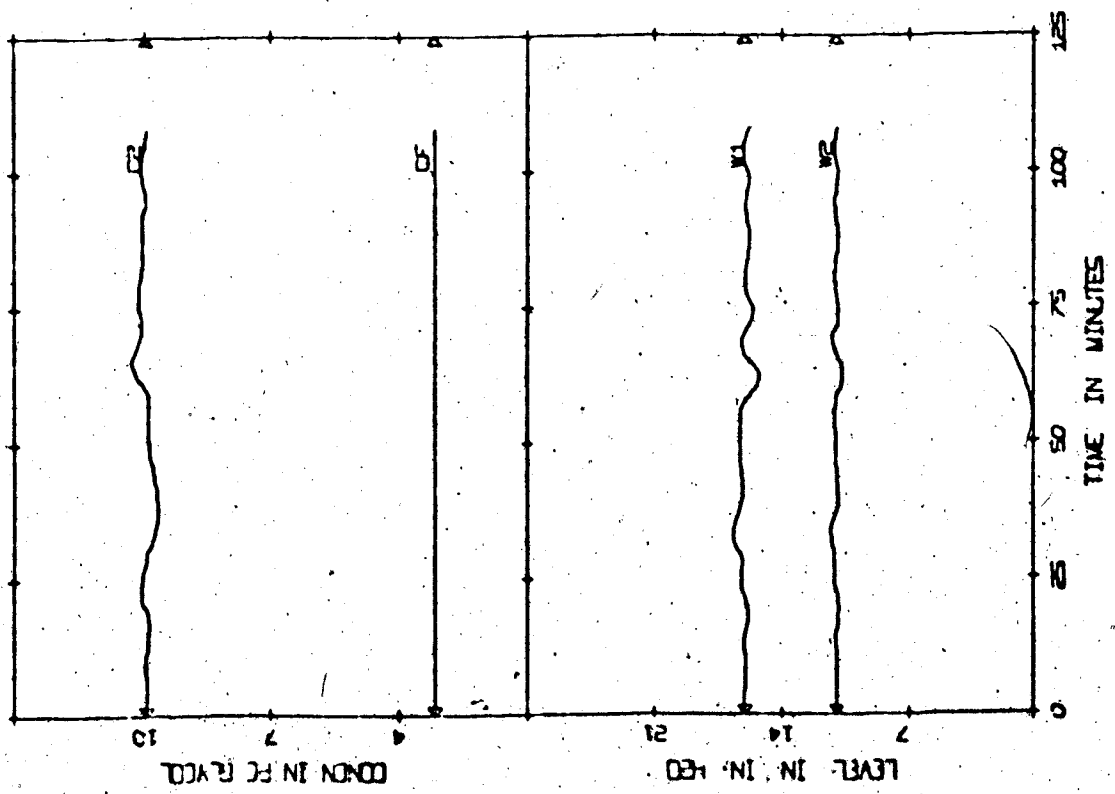
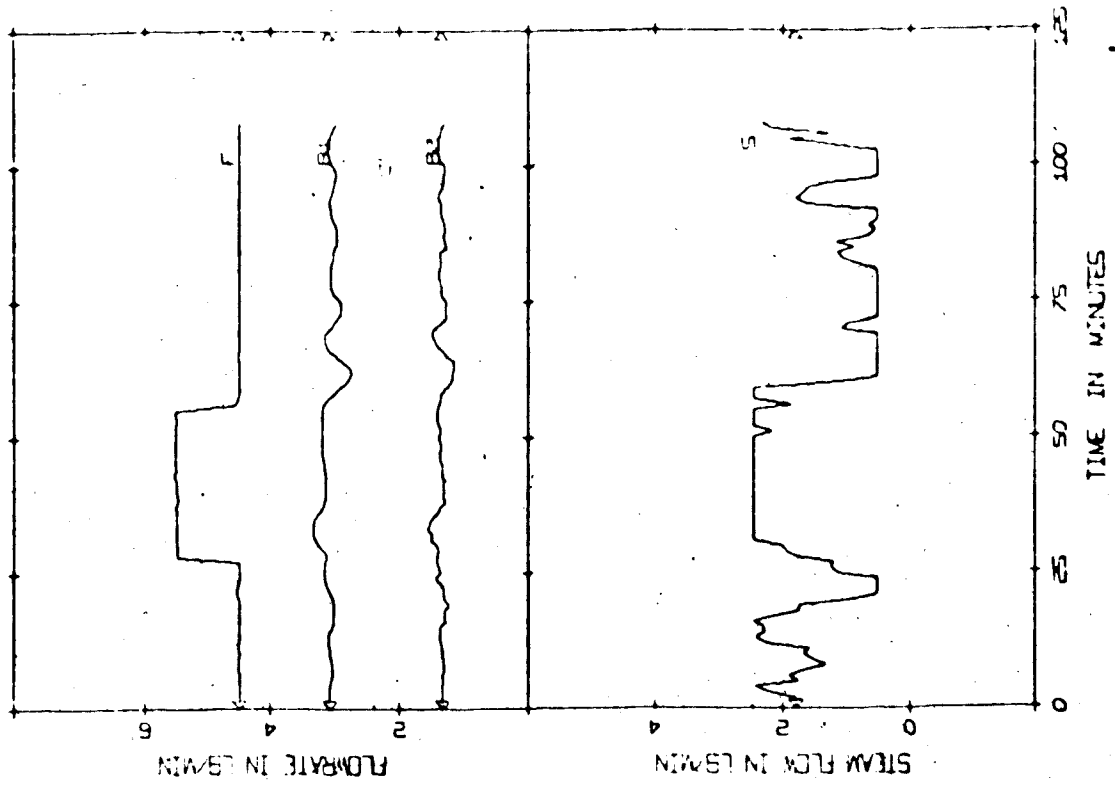


Figure 5.5 Evaporator response (EXP/+20% F, -20% F/ML PI control)

TABLE 5.3  
PROPORTIONAL AND INTEGRAL CONTROLLER CONSTANTS

CONTROL LOOP	KING & MCNEILL [37]		HAMILTON [38]		CONTROL INTERVAL
	KP	KI	KP	KI	
S/C2	3.5	0.04	3.125	0.0234	64 sec
W1/B1	6.0	0.009	6.0	0.009	2 sec
W2/B2	32.0	0.009	32.0	0.009	2 sec

The control of C2 was better than in Figure 5.1 as expected, and the level control was also improved. The DDC controller constants used by Hamilton [38], shown in Table 5.3 were also tried and the resulting evaporator responses are shown in Figures 5.6 and 5.7. Comparing Figures 5.5 and 5.6, it can be seen that King and McNeill's constants resulted in smaller fluctuations in B1 and B2 but larger fluctuations in S. Also the control of C2 after the first step disturbance was better.

From these runs, it appears that conventional multi-loop strategies provide fairly good control of C2 and also keep the two levels near their steady state values even when step disturbances are applied.

#### 5.4.2 Self-Tuning Regulator

The experimental runs for the self-tuning regulator are summarized in Table 5.4.

The base case run in Section 4.2 was also tried experimentally and the response is shown in Figure 5.8. Process variables C2, W1, W2, B1, B2 and S all have sustained oscillations even though no step disturbance was applied. This can be explained as follows. At about

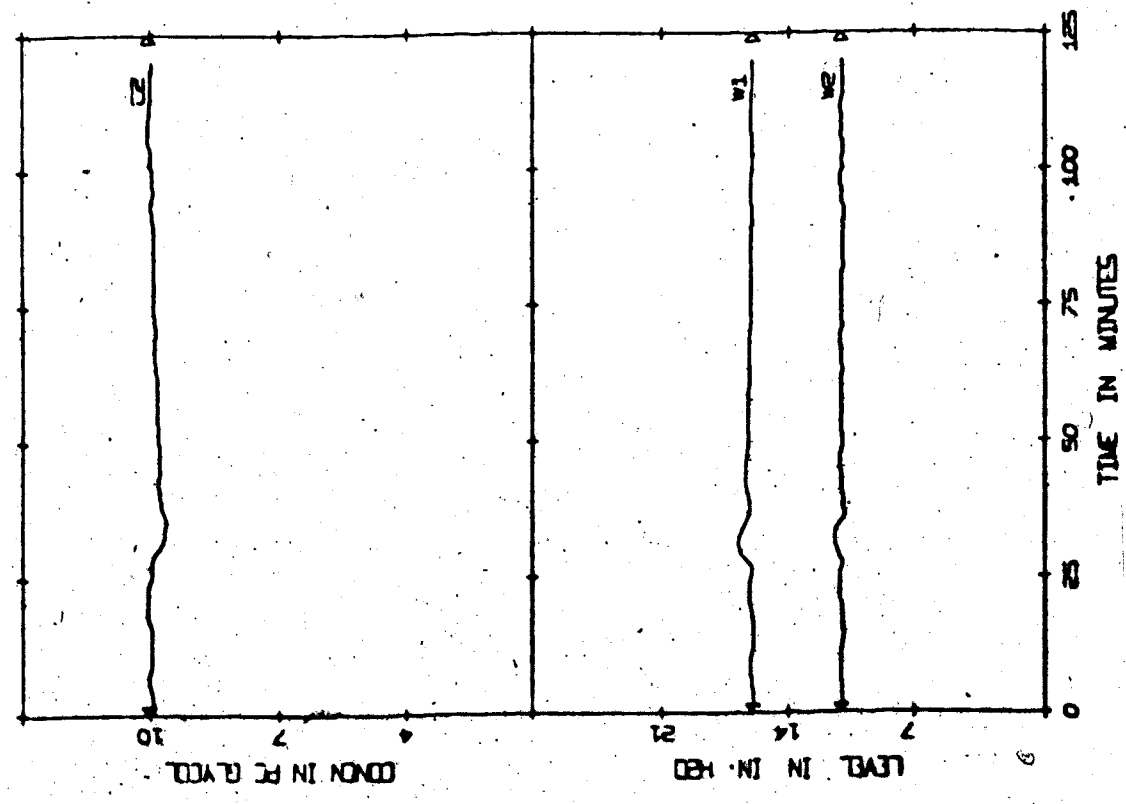
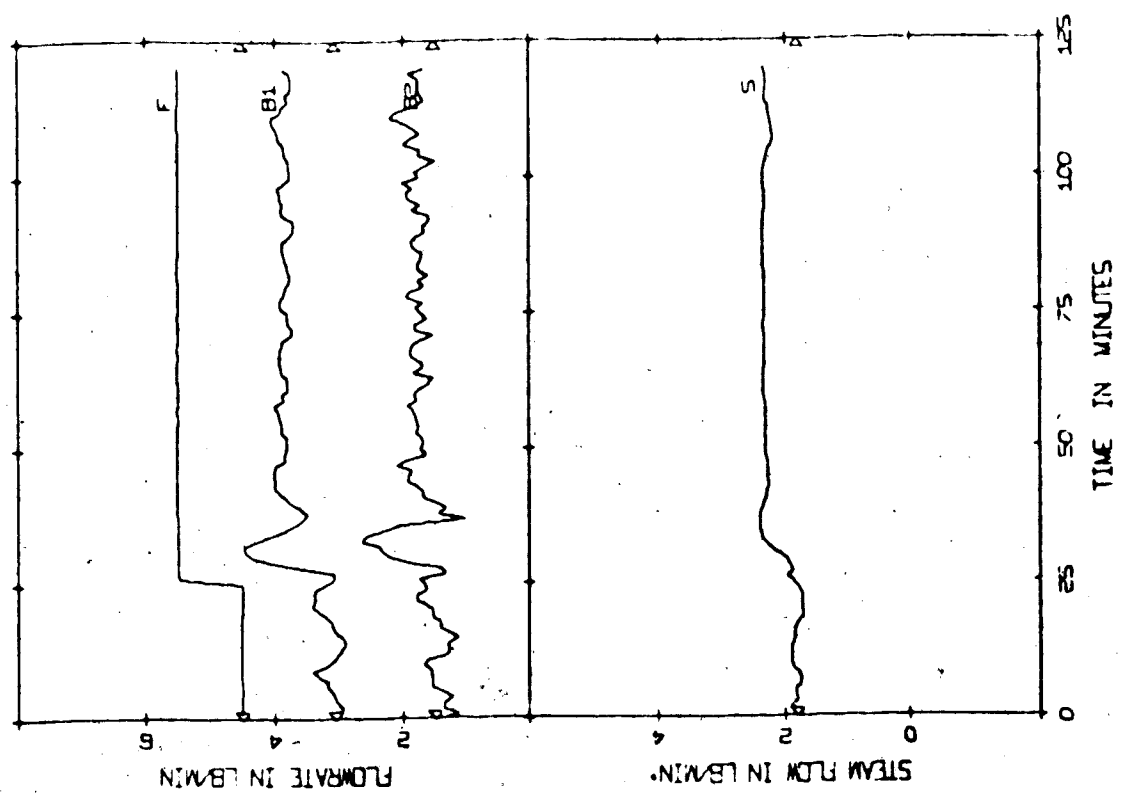


Figure 5.6 Evaporator response (EXP/+20% F/ML PI control)

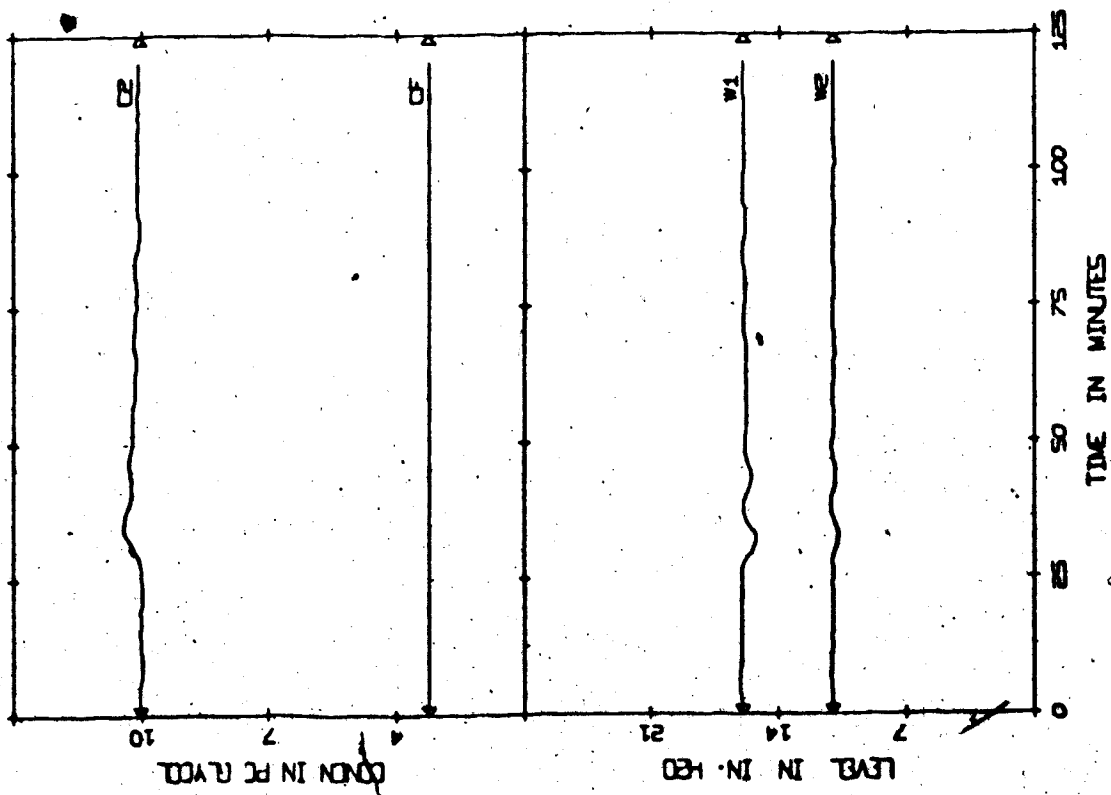
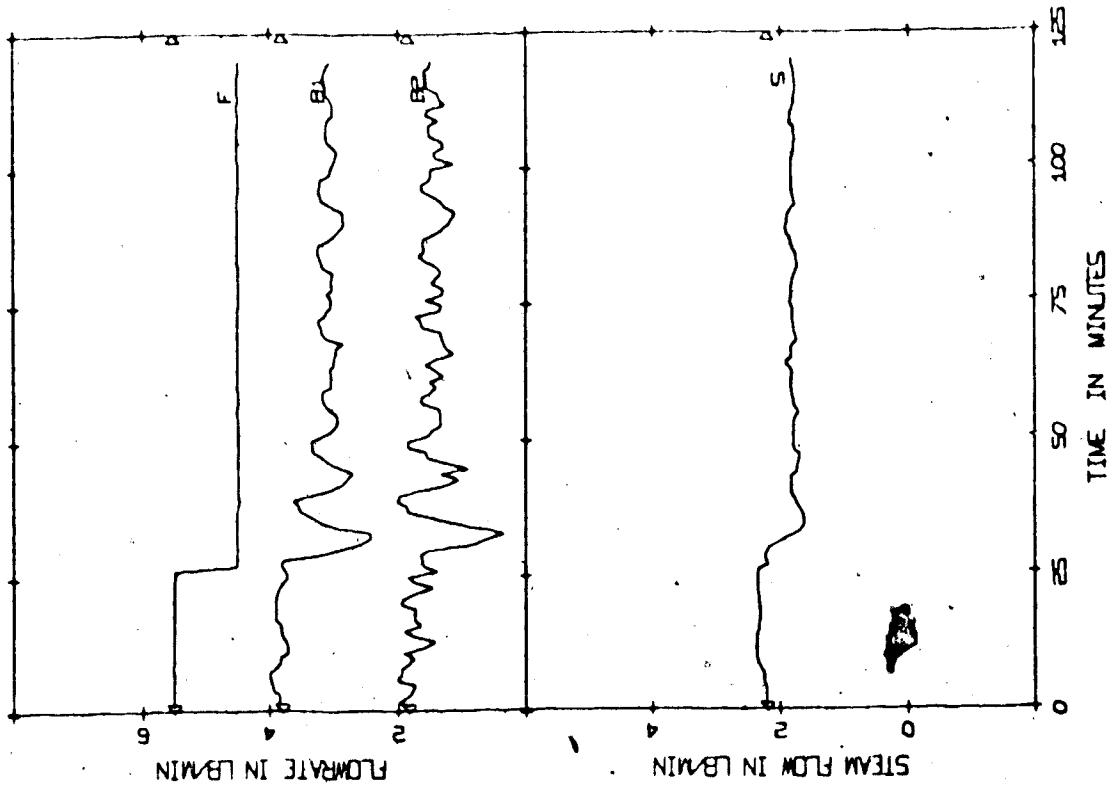


Figure 5.7 Evaporator response (EXP/-20% F/ML PI control)

TABLE 5.4  
EXPERIMENTAL RESULTS FOR THE SELF-TUNING REGULATOR

Note: The proportional gains used in the two level control loops are:  $K_{W1} = 1.5, K_{W2} = 6.5$ .  
 The base case conditions are:  $\mu = 1.0, \hat{p}(0) = 10,000 \text{ J}, \hat{e}(0) = 0$   
 $\beta_0 = 0.014, n = 3, k = 0$

FIGURES	RUN NO.	BASE CASE CONDITIONS EXCEPT STEP DISTURBANCE	FINAL PARAMETER ESTIMATES			
			$\hat{a}_1$	$\hat{a}_2$	$\hat{a}_3$	$\hat{p}_2$
5.8, 5.10	29	$K_{W1} = 3.52, K_{W2} = 15.8$	-1.694	0.192	0.447	0.105
5.9, 5.11	20	ML PI control on level loops	-1.545	0.037	0.491	0.252
5.12, 5.14	10	$K_{W1} = 0.5, K_{W2} = 3.0$	-1.840	-0.297	0.209	0.622
5.13, 5.15	11	$K_{W1} = 0.5, K_{W2} = 3.0$	-1.880	-0.048	0.322	0.458
5.16, 5.18	12	(-20% F, +20% F)	-2.218	0.967	-0.131	0.093
5.17, 5.19	13	(-20% F, +20% F)	-1.928	0.269	0.155	0.479
5.20, 5.22	14	(-30% CF)	-2.008	-0.398	-0.154	-0.992
5.21, 5.23	15	$\beta_0 = 0.1$	-1.201	-0.129	0.333	7.733
5.24, 5.26	17	$\beta_0 = 0.001$	-2.401	0.969	-	0.361
5.25, 5.27	19*	$n = 2$	-1.644	0.416	-0.226	-0.052
5.28	18	$n = 4$	-1.840	-0.297	0.809	0.622
5.29, 5.31	23	constant parameter in STR ML prop. control & STR, $\beta_0 = 0.02, \mu = 0.995$	-1.765	0.257	0.315	0.044
5.30, 5.32	22	ML prop. control & STR	-2.043	0.166	0.509	0.538

\*  $\hat{a}_4 = 0.276, \hat{p}_3 = 0.138$

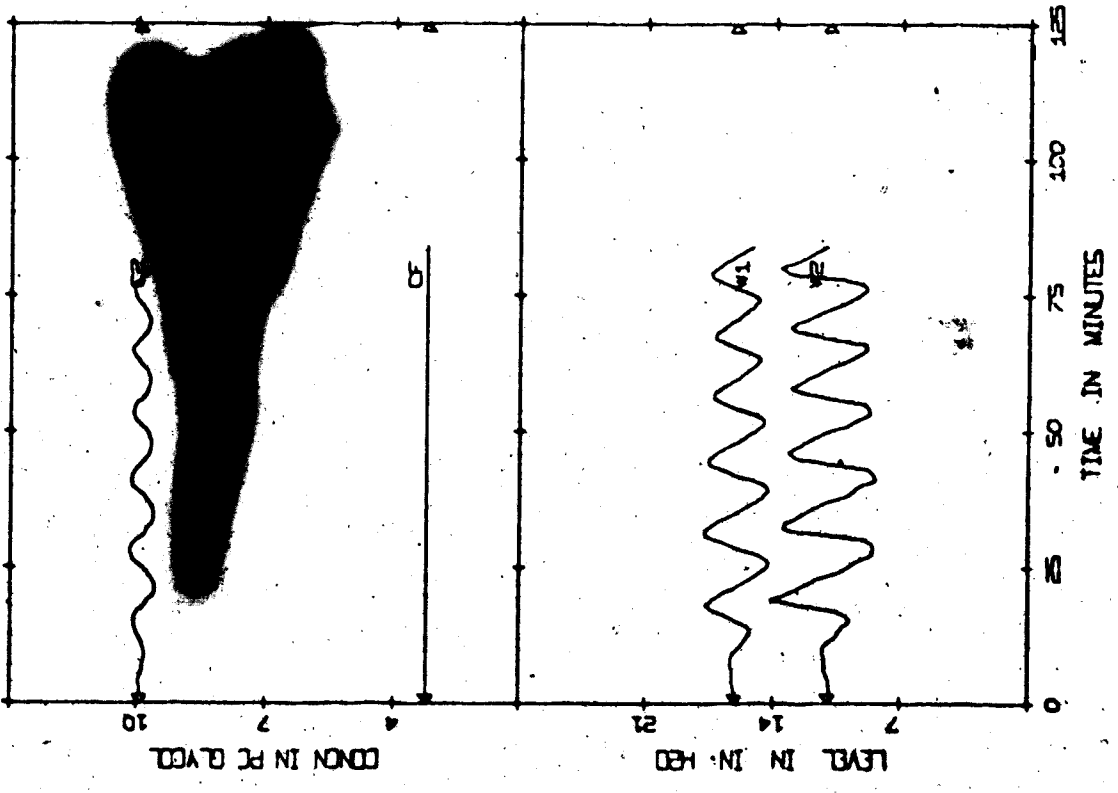
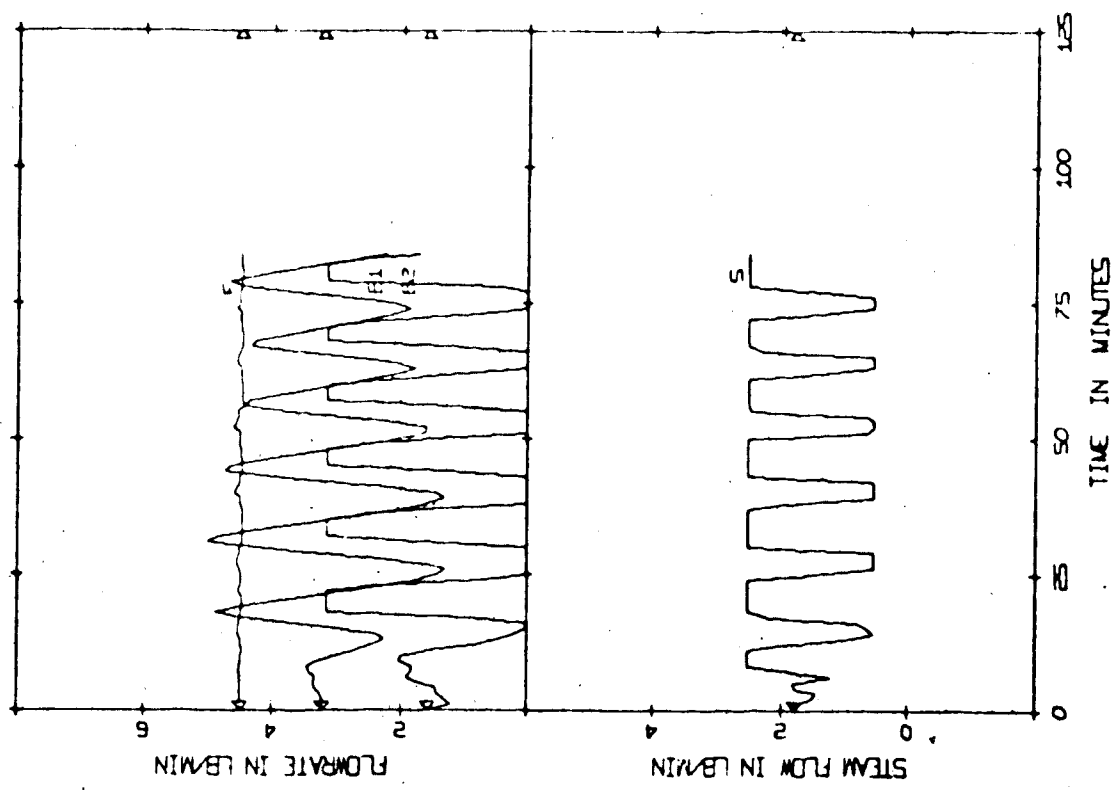


Figure 5.8 Evaporator response (EXP/STR),  $K_{W1} = 3.52$ ,  $K_{W2} = 15.8$



the 10 minute mark, C2 decreases because of the lower steam flow. As a result, the steam flowrate increases and boils off more water from the first effect thus lowering W1. Because of the decrease in W1, B1 decreases (due to the W1/B1 control loop) which in turn causes W2 and B2 to decrease. C2 increases due to S and B1, and the self-tuning regulator then reduces the steam flow rate to compensate for this. When the steam signal drops, the whole procedure is repeated but in the opposite direction. From that point onwards, all the key variables have sustained oscillations. The corresponding parameter estimates plots are shown in Figure 5.10 and all have good convergence properties. Again, the final parameter estimates are listed in the figure.

Several unsuccessful attempts were made to eliminate these oscillations. Values of  $\delta_0$  of 0.03, 0.05, and 0.005 were tried but the results were similar to those in Figure 5.8. Then the control and sampling periods were reduced by half but the oscillations still occurred. The two level proportional controllers were then replaced by the standard PI controllers (with Hamilton's constants), but this did not provide any improvement as can be seen from Figure 5.9. The corresponding parameter estimates are shown in Figure 5.11.

By examining the results obtained when self-tuning regulator was used, it seemed that the strong interaction initiated by the bang-bang behaviour of steam could be reduced by reducing the proportional gains in the level control loops. Thus, a run was tried using zero gains in the level controllers. The result was that B1 and B2 were held constant and the control of C2 was good (figure not shown), but the two levels dropped below their operating ranges due to the integrating nature of the two holdups. To avoid this situation, another run was tried

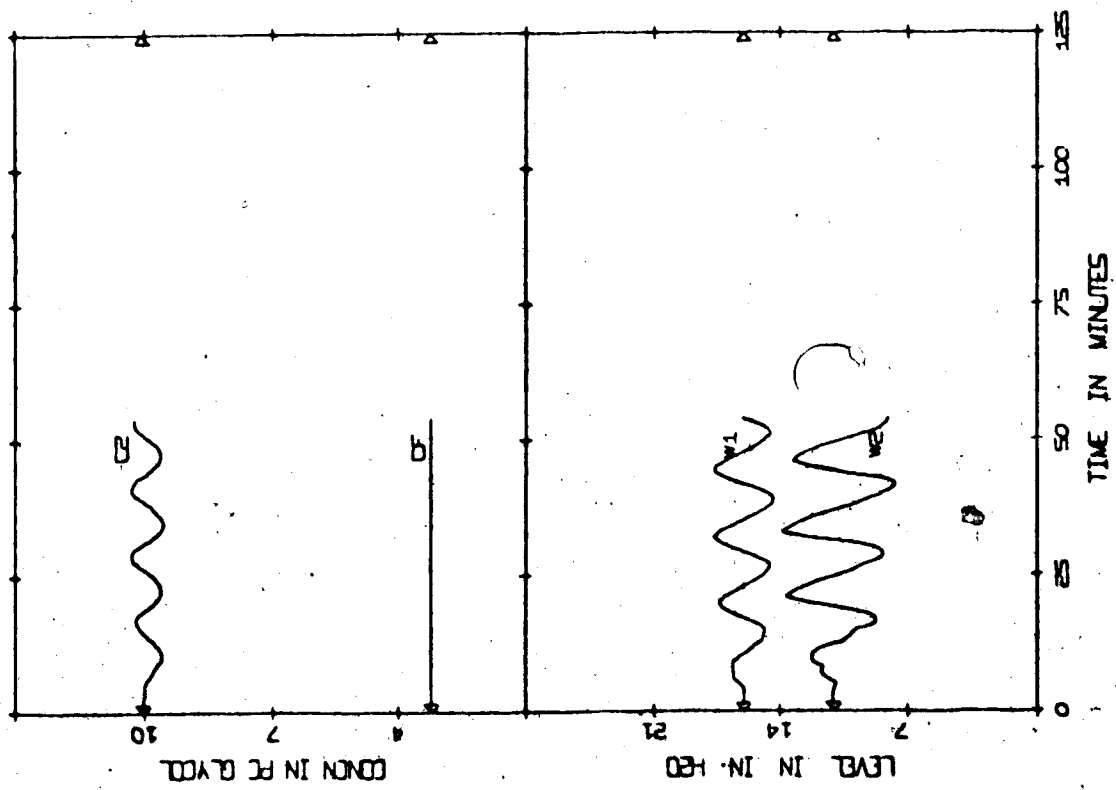
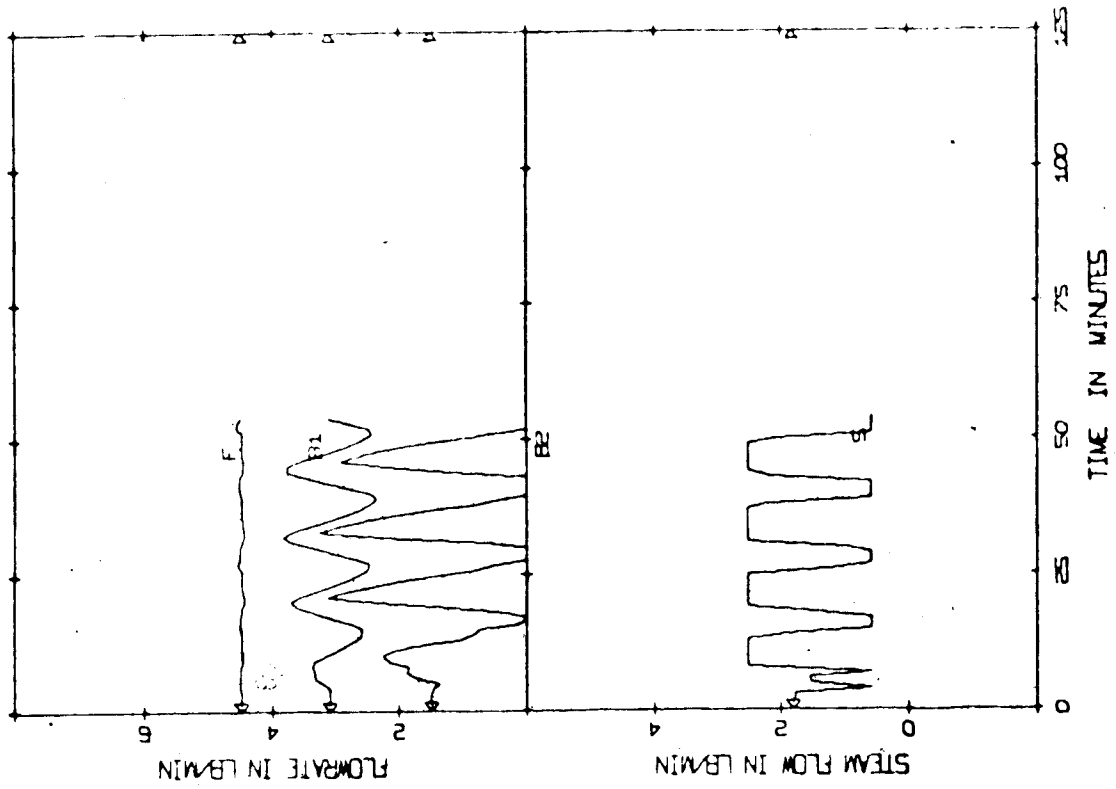


Figure 5.9 Evaporator response (EXP/STR), PI control of W1 and W2

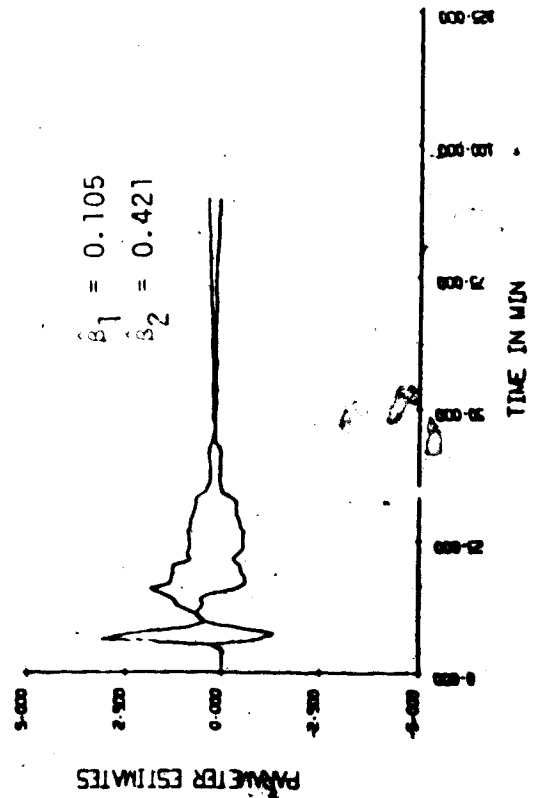
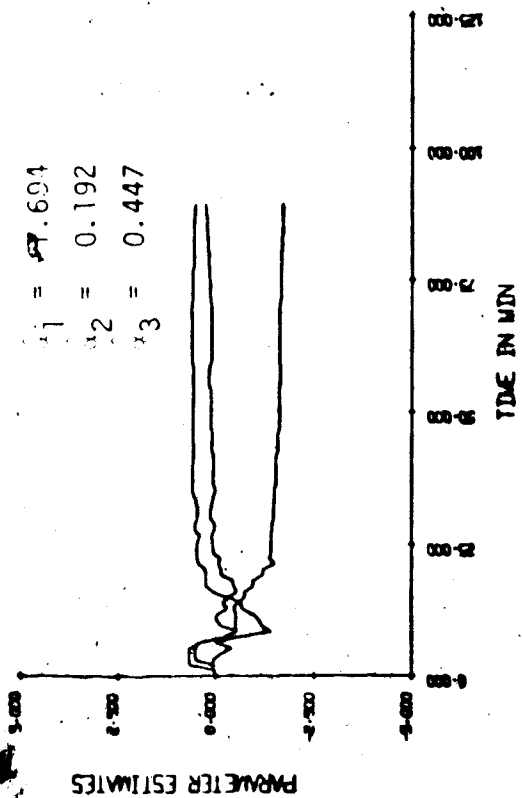


Figure 5.10 Parameter estimates (EXP/STR),  $K_{W1} = 3.52$ ,  $K_{W2} = 15.8$

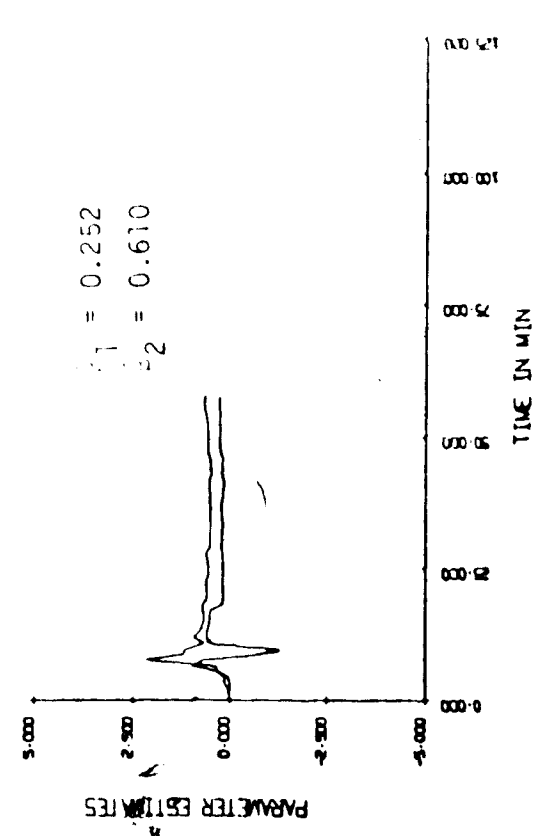
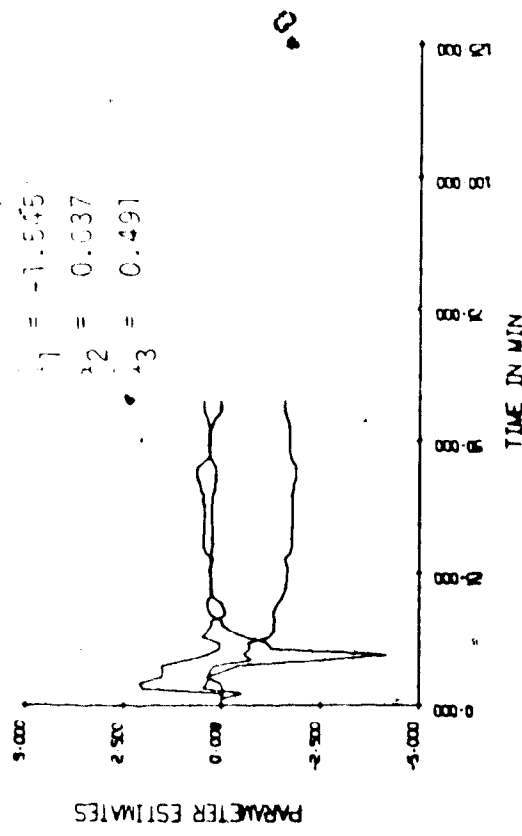


Figure 5.11 Parameter estimates (EXP/STR), PI control of  $W1$  and  $W2$

using very small gains in the two level control loops. The self-tuning regulator was able to keep the evaporator at the nominal steady state as shown in Figure 5.12. When 20% step disturbances in feed flow were applied, the self-tuning regulator was able to handle the disturbances without difficulty as shown in Figure 5.13. Note that with the low gains used in the level loops, the increase in feed flow resulted in a large upsurge in the first effect level. The corresponding parameter estimate plots for these two runs are shown in Figures 5.14 and 5.15. The convergence of the estimates was quite good.

In order to prevent large offsets in  $W1$  after a step disturbance in feed flow, the proportional gains in the level loops were increased to the values shown in Table 5.4. These gains which are about half the values used in the simulation study were also used in the remaining experimental runs. Two runs were performed using the base case parameters in the self-tuning algorithm with two different types of step disturbances as shown in Figures 5.16 and 5.17. In Figure 5.16 the  $C2$  response was good and the regulator was able to handle the two 20% step disturbances in feed flow quite well. With the larger gains in the level control loops, the levels were controlled much better. The  $C2$  performance was comparable to the analogous run in the simulation study (see Figure 4.34). In comparison with the conventional P and PI controllers (see fig. 5.1 and 5.5) the self-tuning regulator produces smaller deviations in  $C2$  but resulted in small sustained oscillations towards the end of the run. In Figure 5.17, the 30% step disturbance in feed concentration had little offset on  $C2$  as compared to the proportional control run in Figure 5.2. The strong influence of  $S$  on the levels and the bottom flow rates is again apparent in Figures 5.17. The correspond-

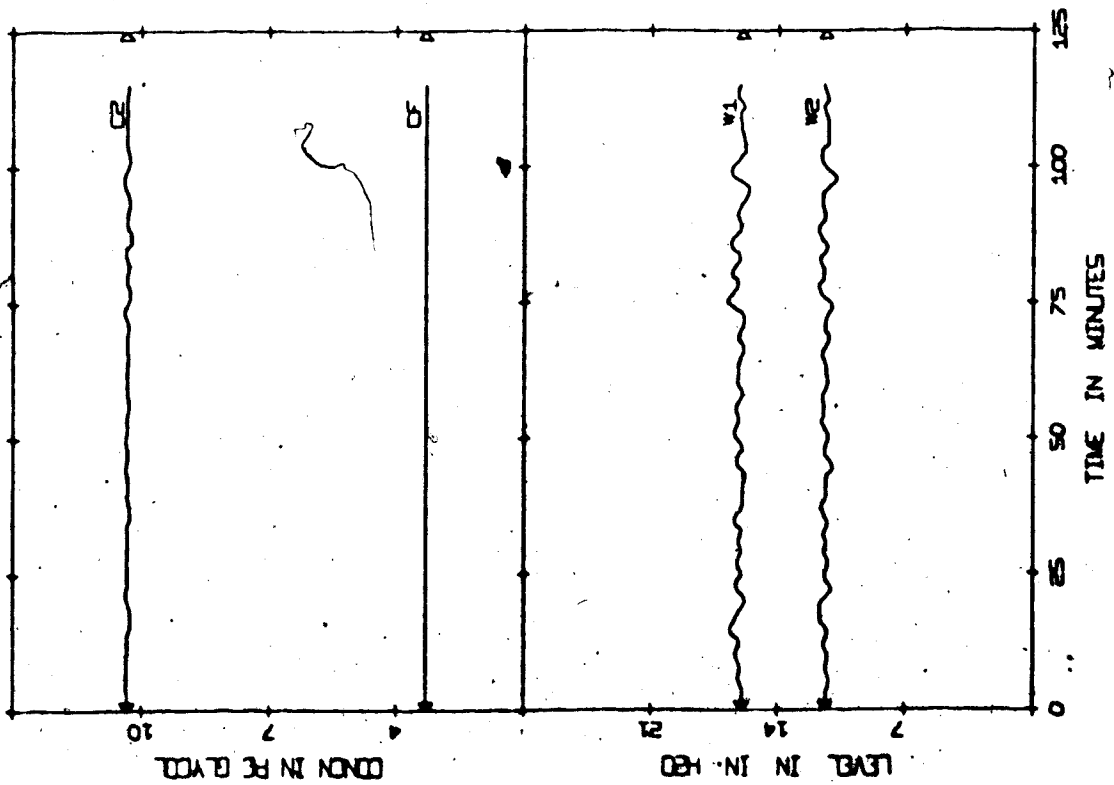
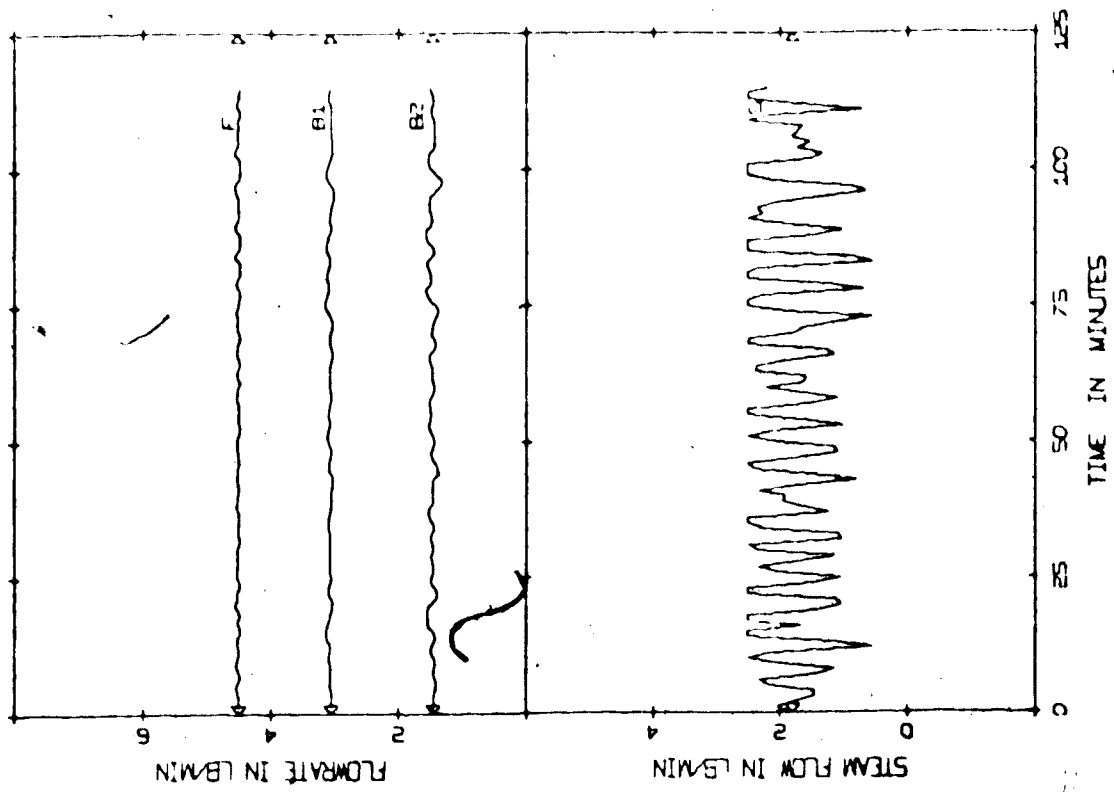


Figure 5.12 Evaporator response (EXP/STR),  $K_{W1} = 0.5$ ,  $K_{W2} = 3.0$

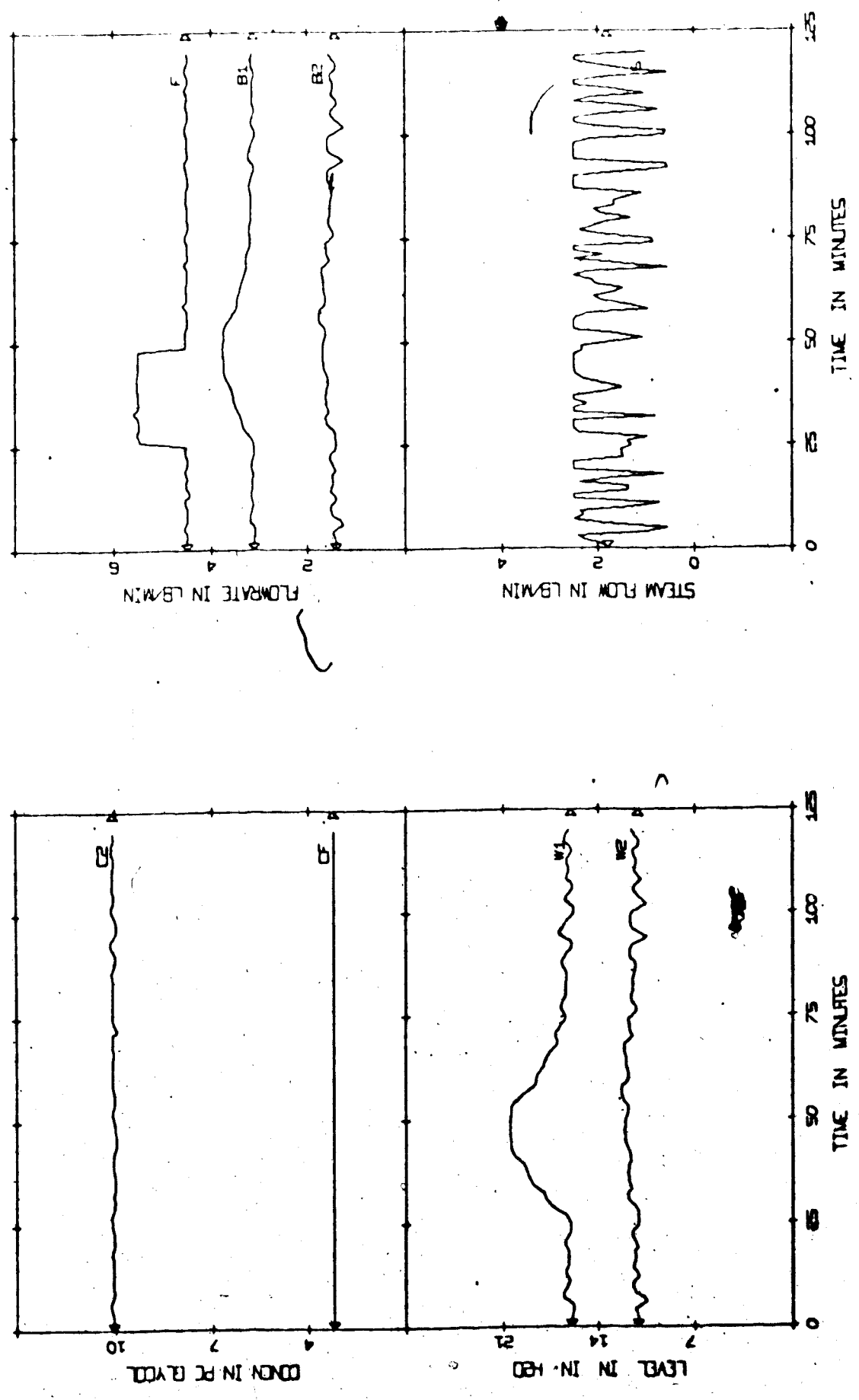


Figure 5.13 Evaporator response (EXP/+20% F, -20% F/STR),  $K_{W1} = 0.5$ ,  $K_{W2} = 3.0$

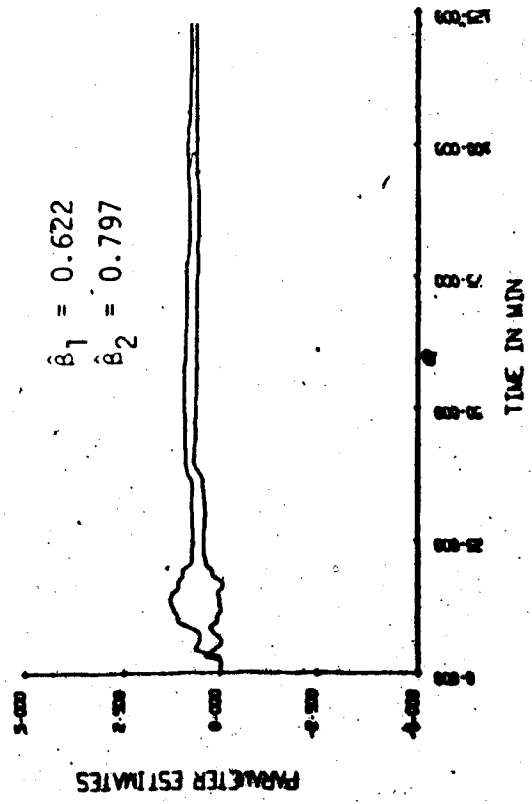
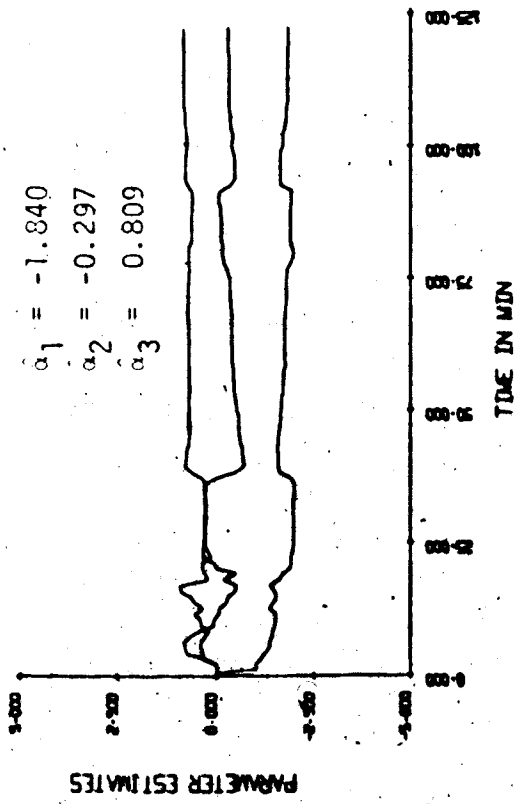


Figure 5.14 Parameter estimates (EXP/STR),  $K_{W1} = 0.5, K_{W2} = 3.0$

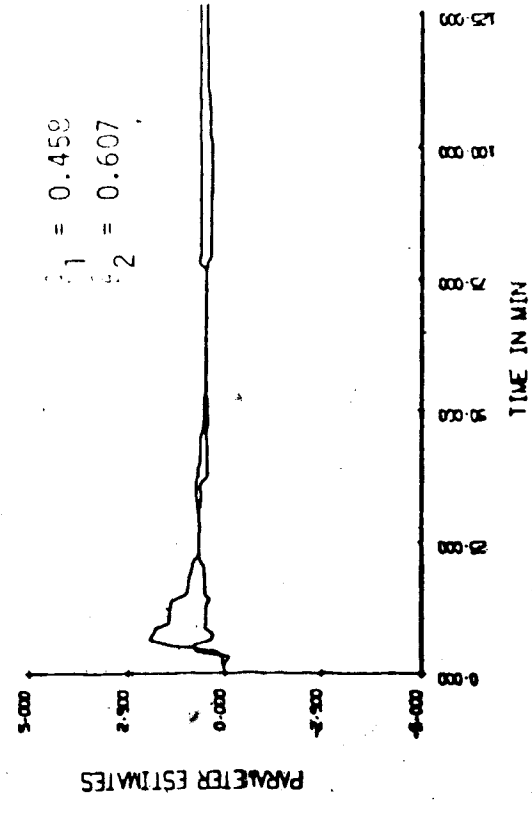
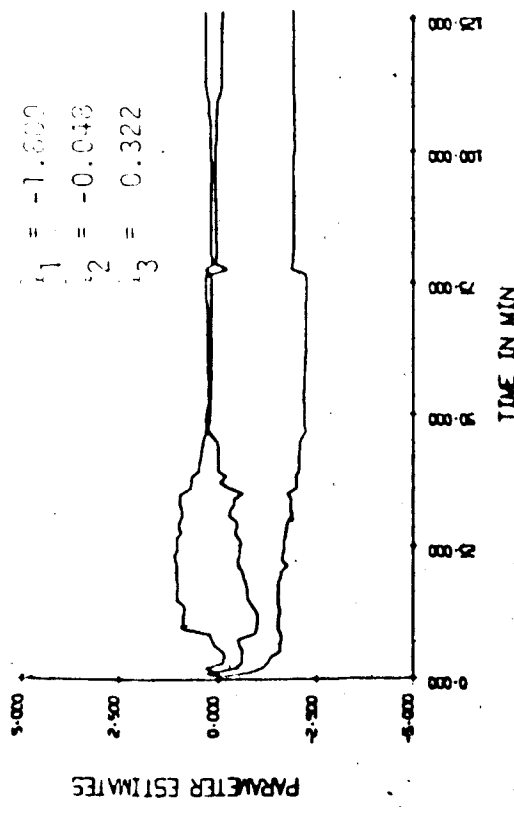


Figure 5.15 Parameter estimates (EXP/+20% F, -20% F/STR),  $K_{W1} = 0.5, K_{W2} = 3.0$

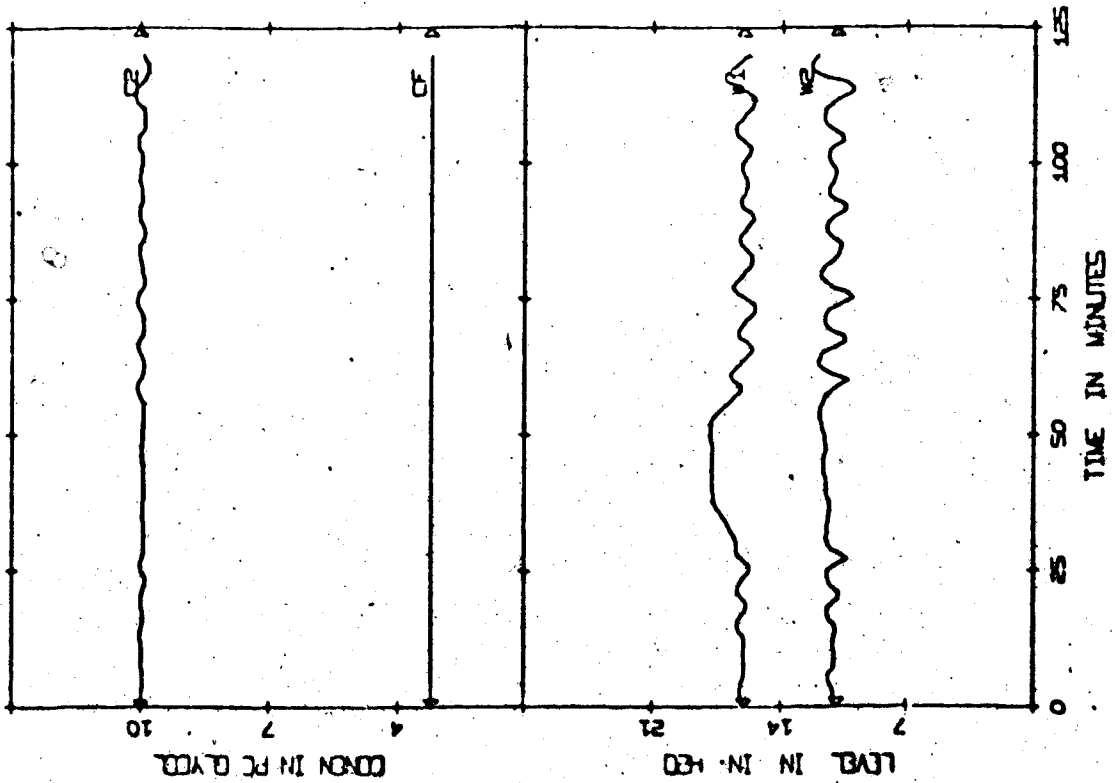
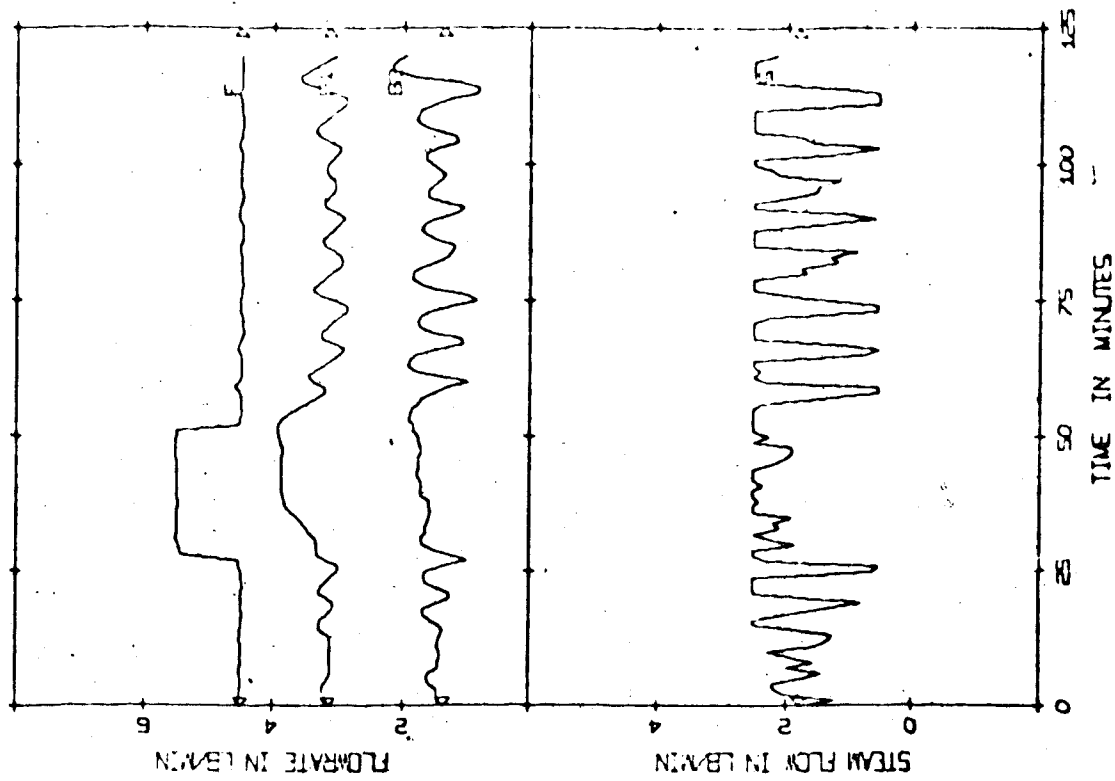


Figure 5.16 Evaporator response (EXP/+20% F, -20% F/STR)



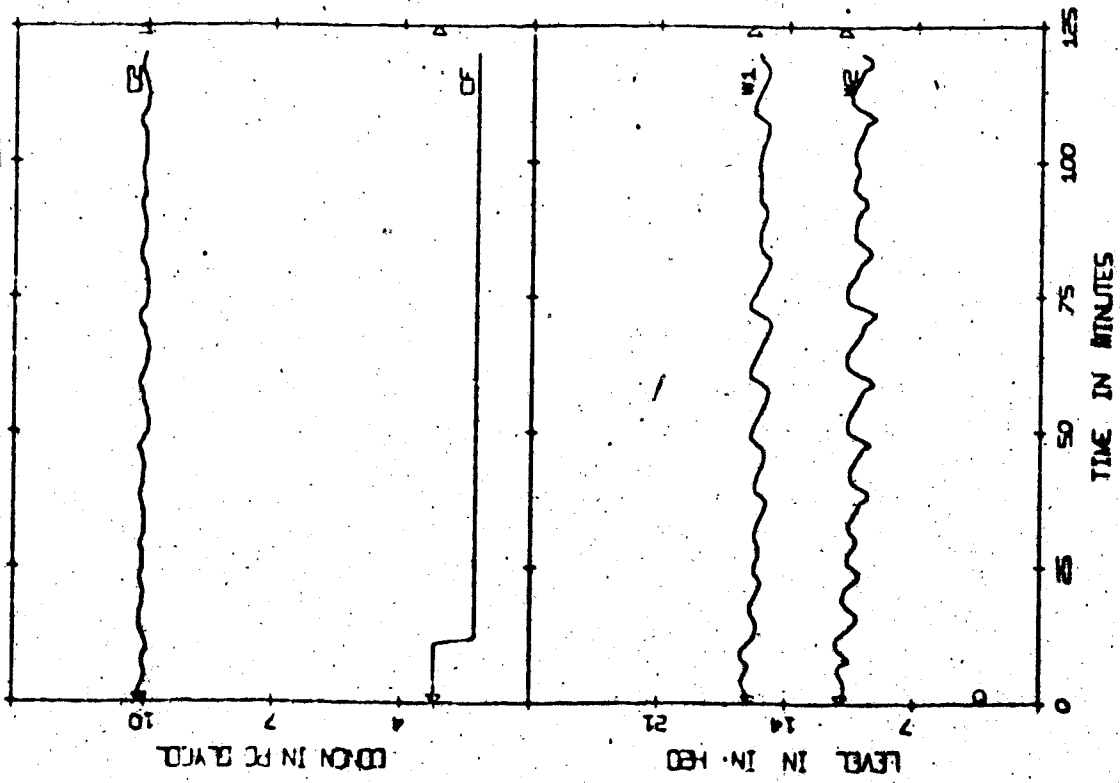
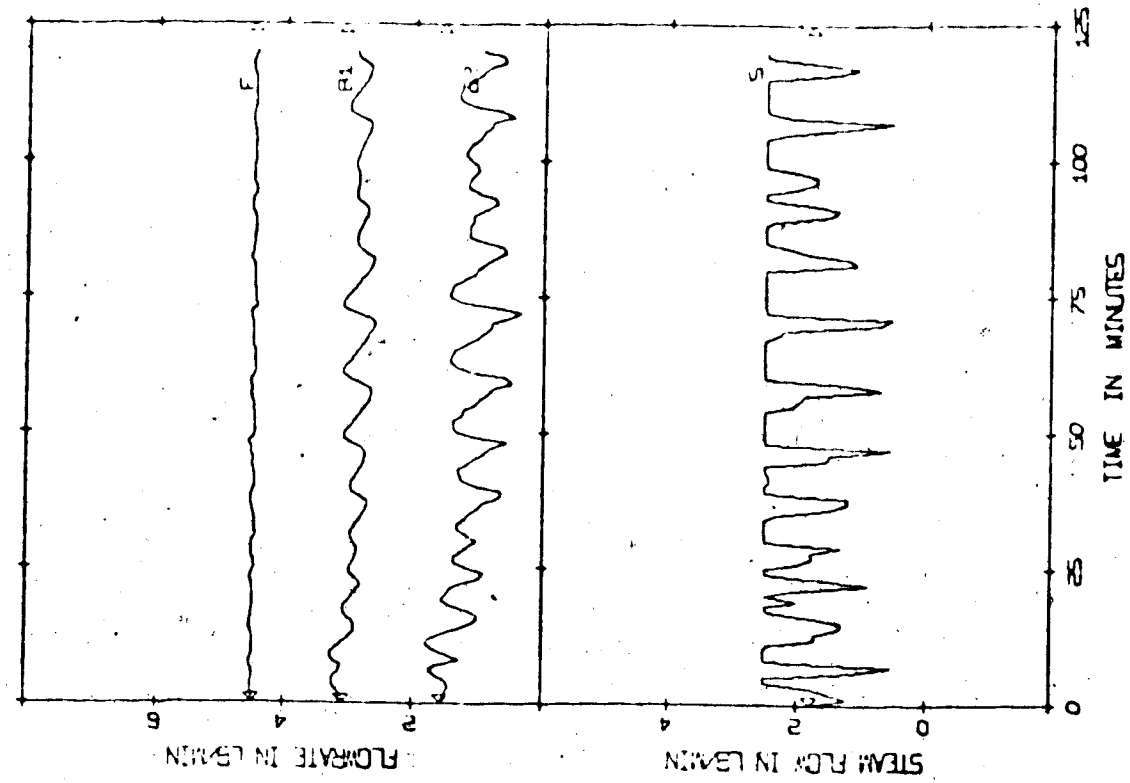


Figure 5.17 Evaporator response (EXP/-30% CF/STR)

ing parameter estimates are shown in Figures 5.18 and 5.19.

Figures 5.20 and 5.21 illustrate the effect of using values of  $\beta_0 = 0.1$  and  $\beta_0 = 0.001$  in the self-tuning algorithm. The characteristics of the steam signals are similar to those observed in the simulation study (see Figures 4.18 and 4.19). For the larger scaling factor of  $\beta_0 = 0.1$ , the steam signal exhibits similar small fluctuations initially but it eventually results in sustained oscillations. For the smaller scaling factor of  $\beta_0 = 0.001$ , the steam signals hit the constraints more frequently. The parameter estimates in Figures 5.22 and 5.23 show even a closer resemblance to those obtained in the simulation study. For  $\beta_0 = 0.1$ , the  $\{\hat{\alpha}_i\}$  have large fluctuations and the  $\{\hat{\beta}_i\}$  converge, while for  $\beta_0 = 0.001$ , the exact opposite can be observed.

Model orders of  $n = 2$  and  $n = 4$  were used in the self-tuning regulator and gave the results shown in Figures 5.24 and 5.25, respectively. Step disturbances in feed flow were applied to both runs and the control of C2 was good. For  $n = 2$ , the C2 performance was one of the best observed in the experimental study. The corresponding parameter estimates are shown in Figures 5.26 and 5.27, respectively.

Experimental runs using the self-tuning regulator in which all the parameters including  $\beta_0$  were estimated, proved to be unsuccessful as compared to those runs in the simulation study. The steam signal would drop to the lower limit and stayed there until the runs were terminated.

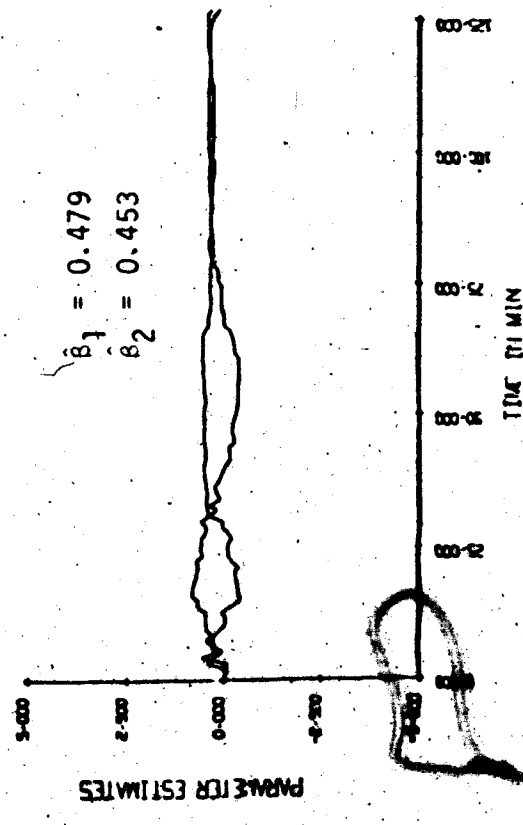
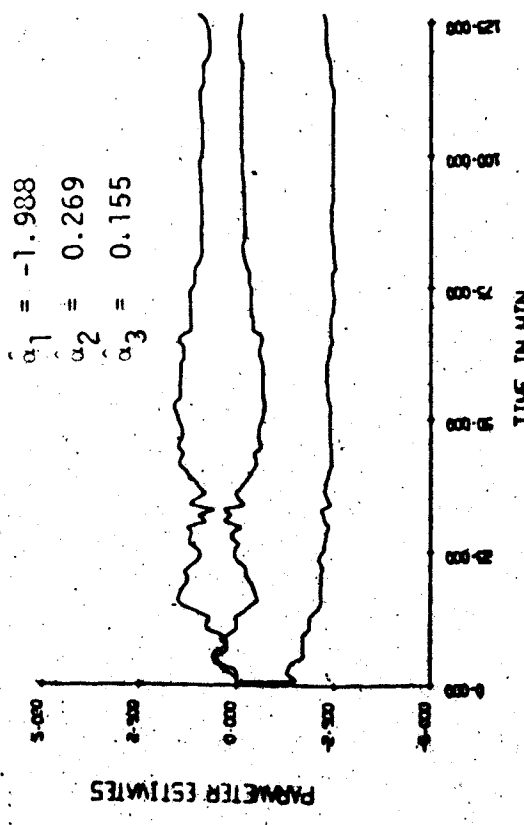


Figure 5.18 • Parameter estimates (EXP/-20% F, +20% F/STR)

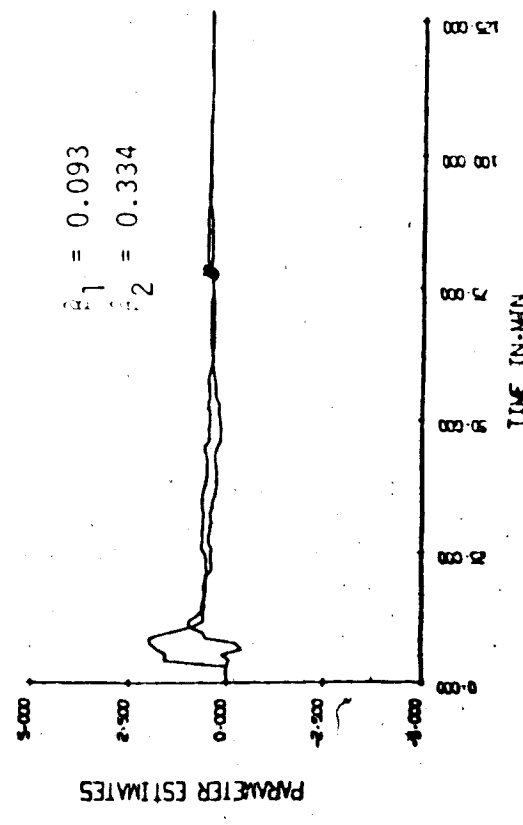
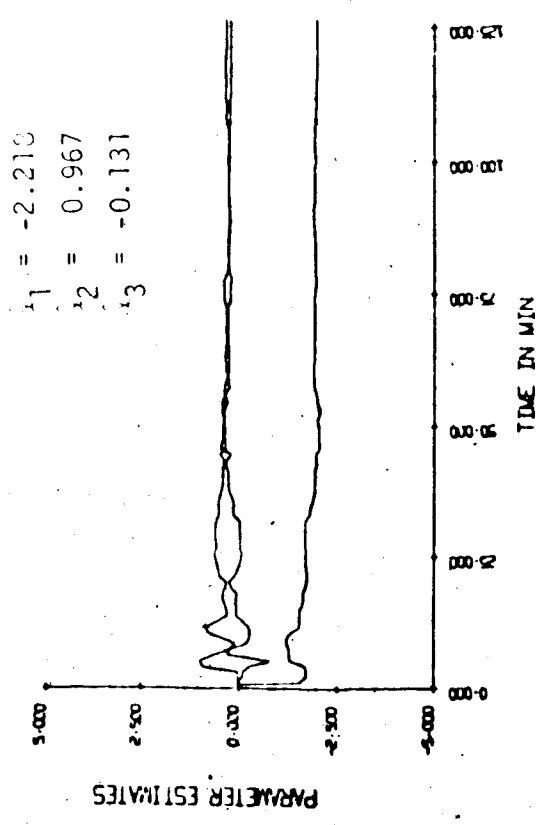


Figure 5.19 Parameter estimates (EXP/-30% CF/STR)

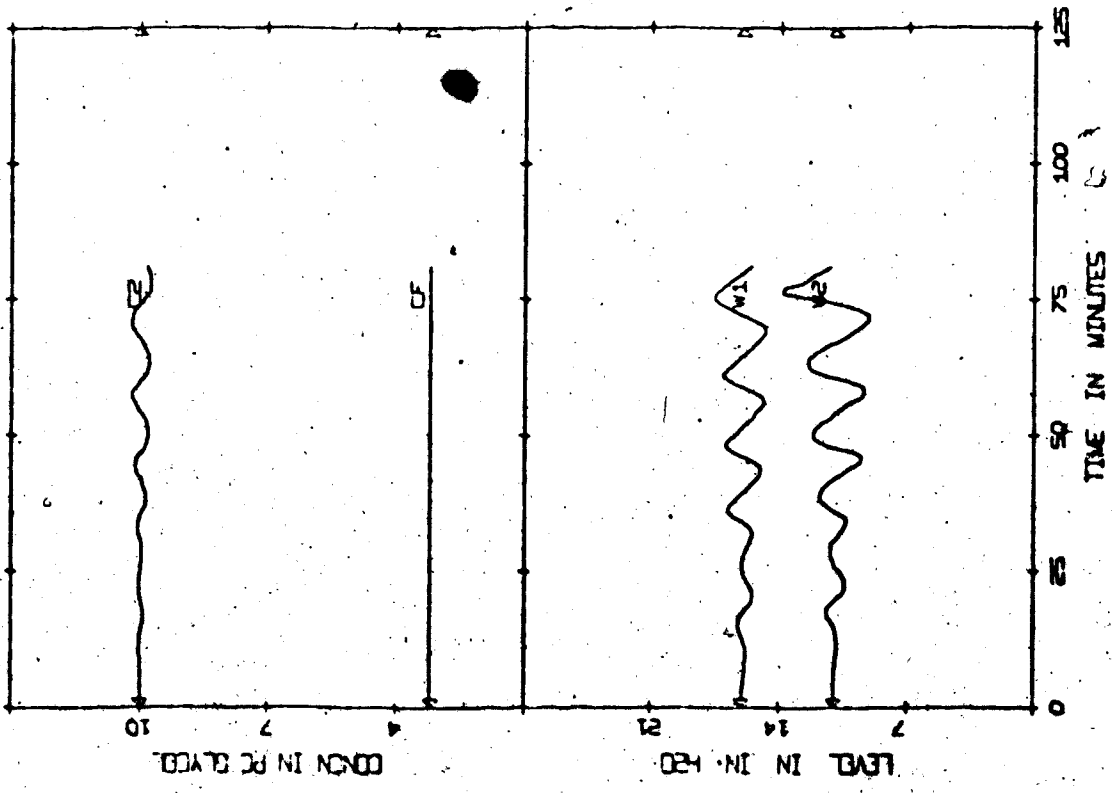
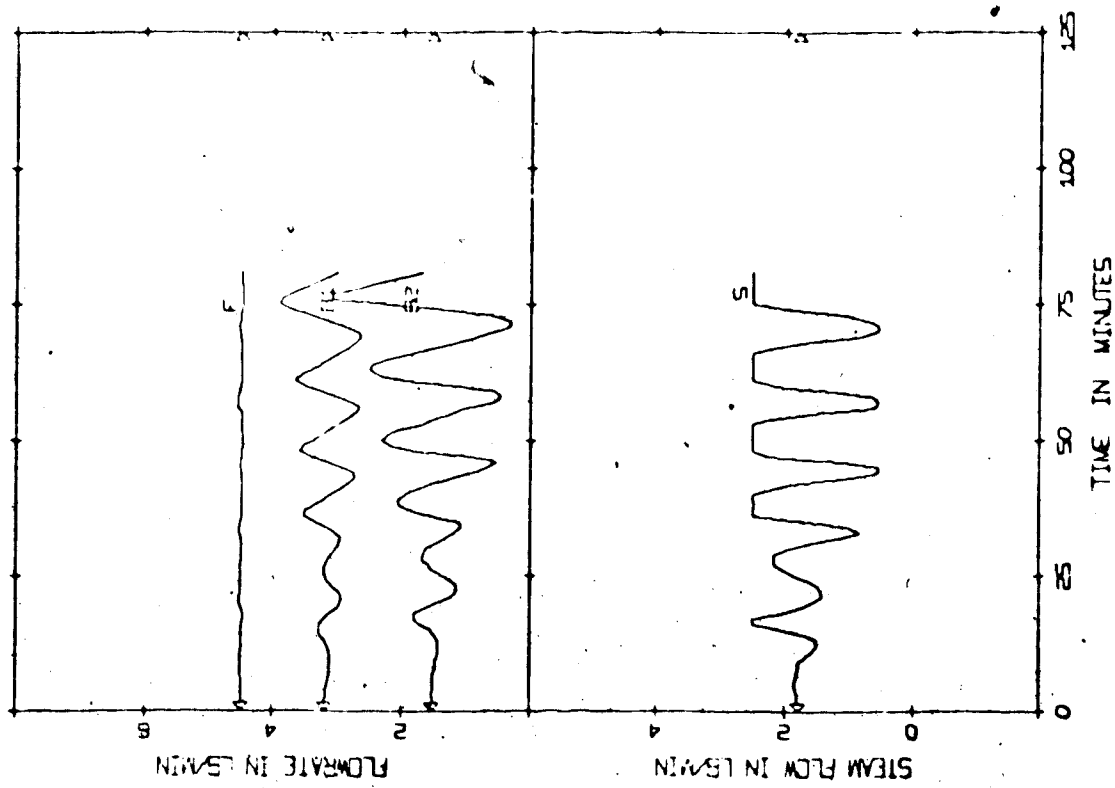


Figure 5.20 Evaporator response (EXP/STR),  $\beta_0 = 0.1$

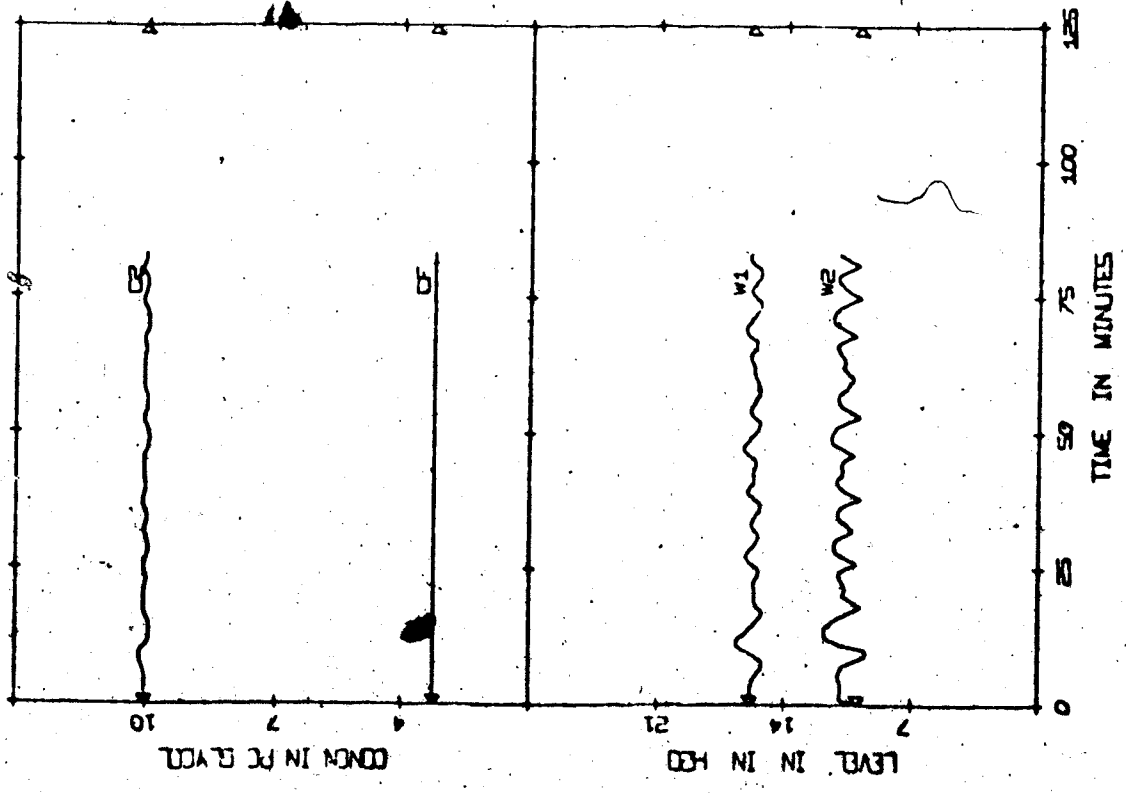
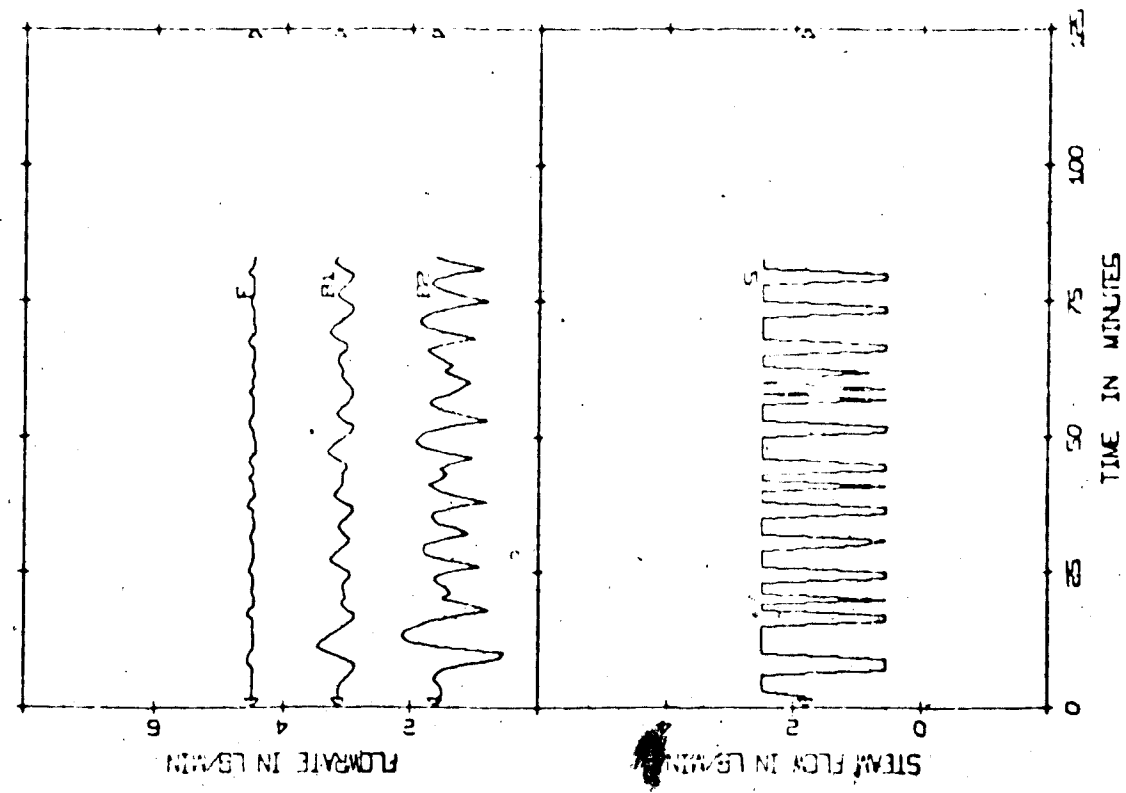


Figure 5.21 Evaporator response (EXP/STR),  $\beta_0 = 0.001$

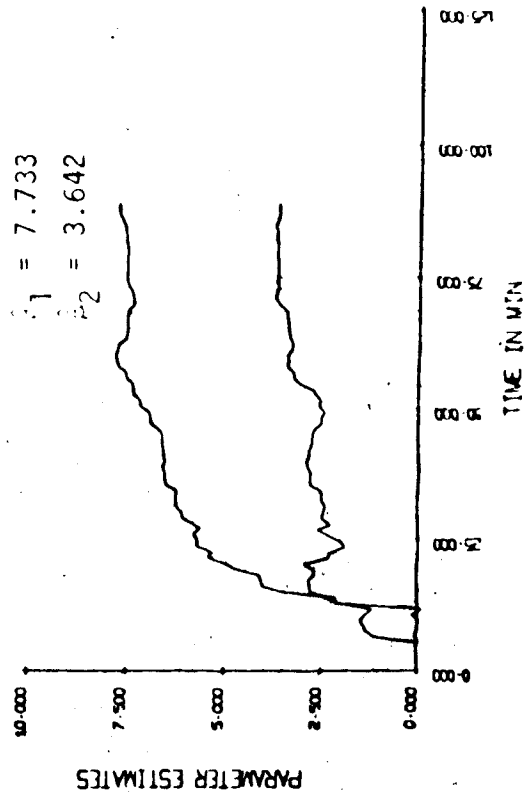
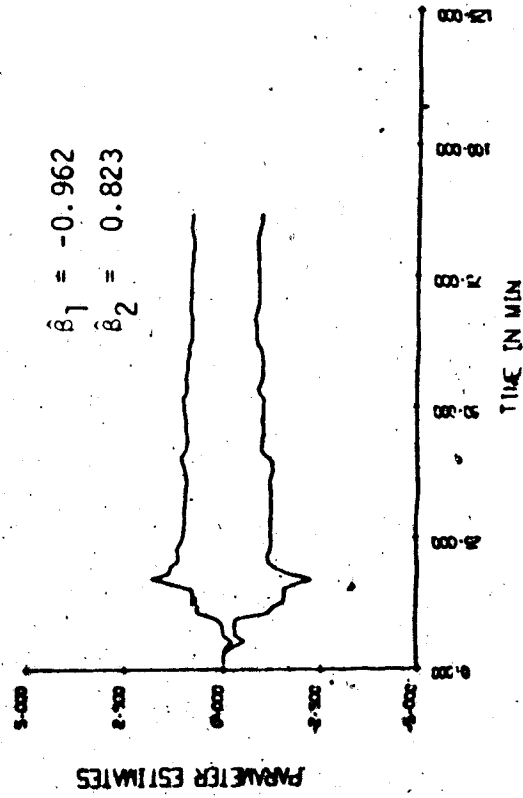
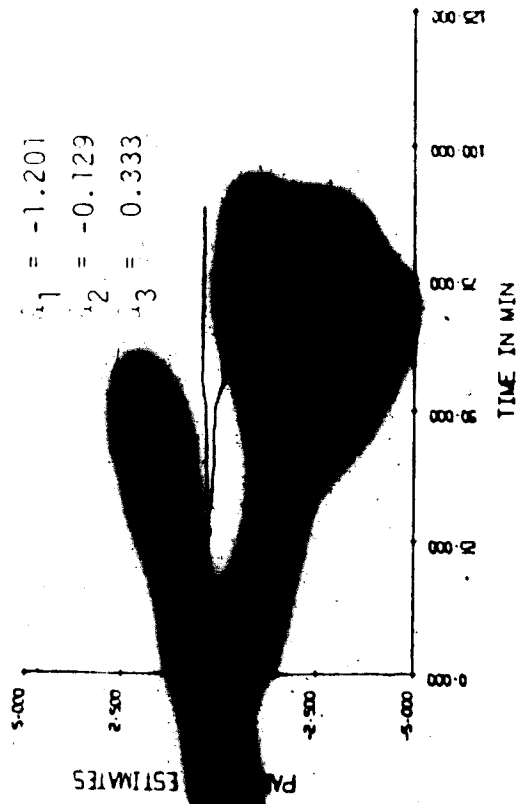
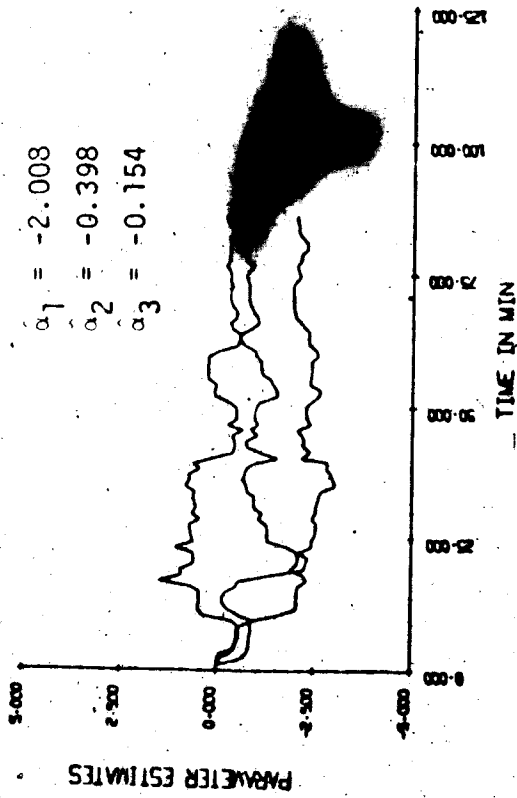


Figure 5.22 Parameter estimates (EXP/STR),  $\beta_0 = 0.1$

Figure 5.23 Parameter estimates (EXP/STR),  $\beta_0 = 0.001$

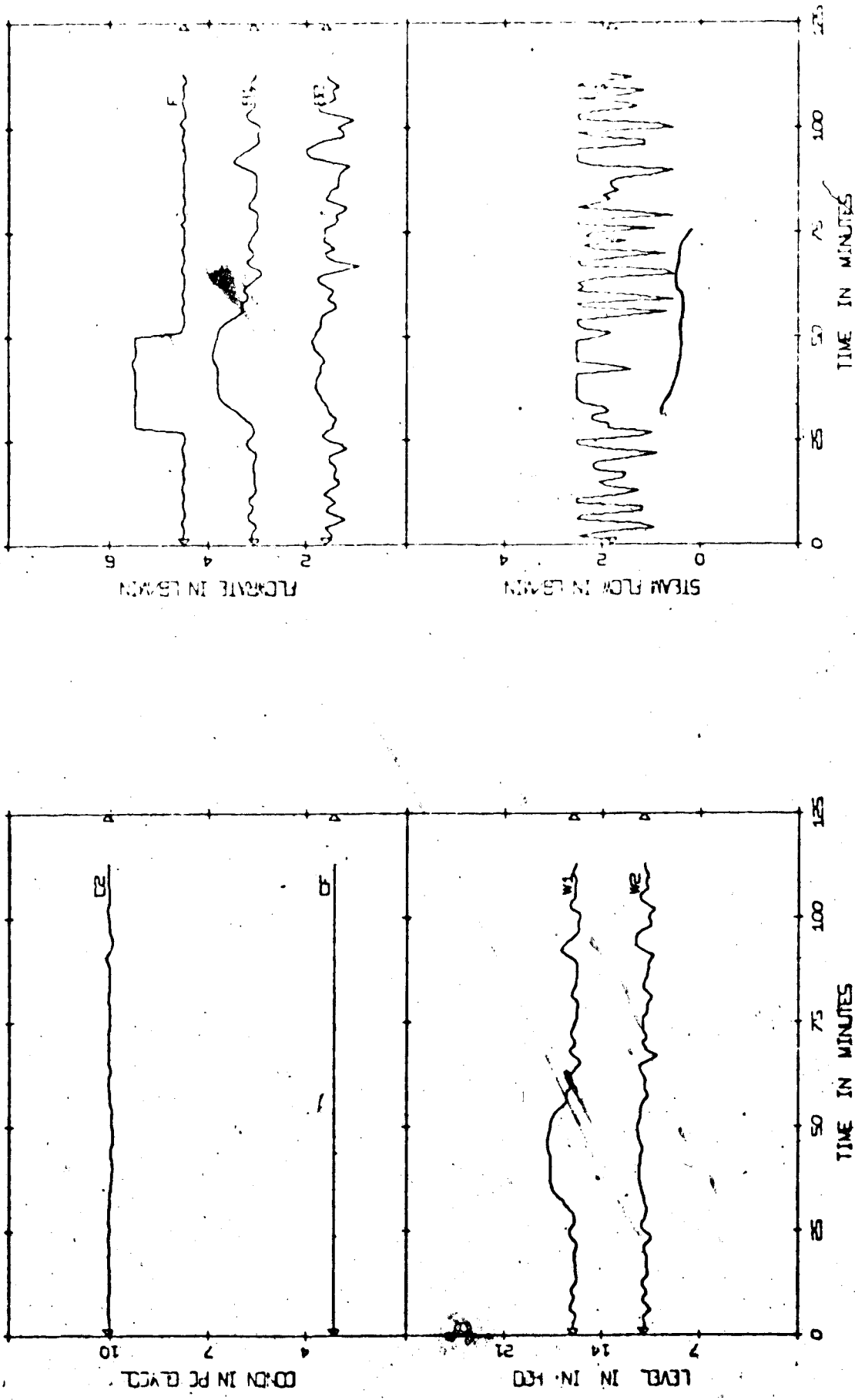


Figure 5.24 Evaporator response (EXP/+20% F, -20% F/STR); 2<sup>nd</sup> order model.

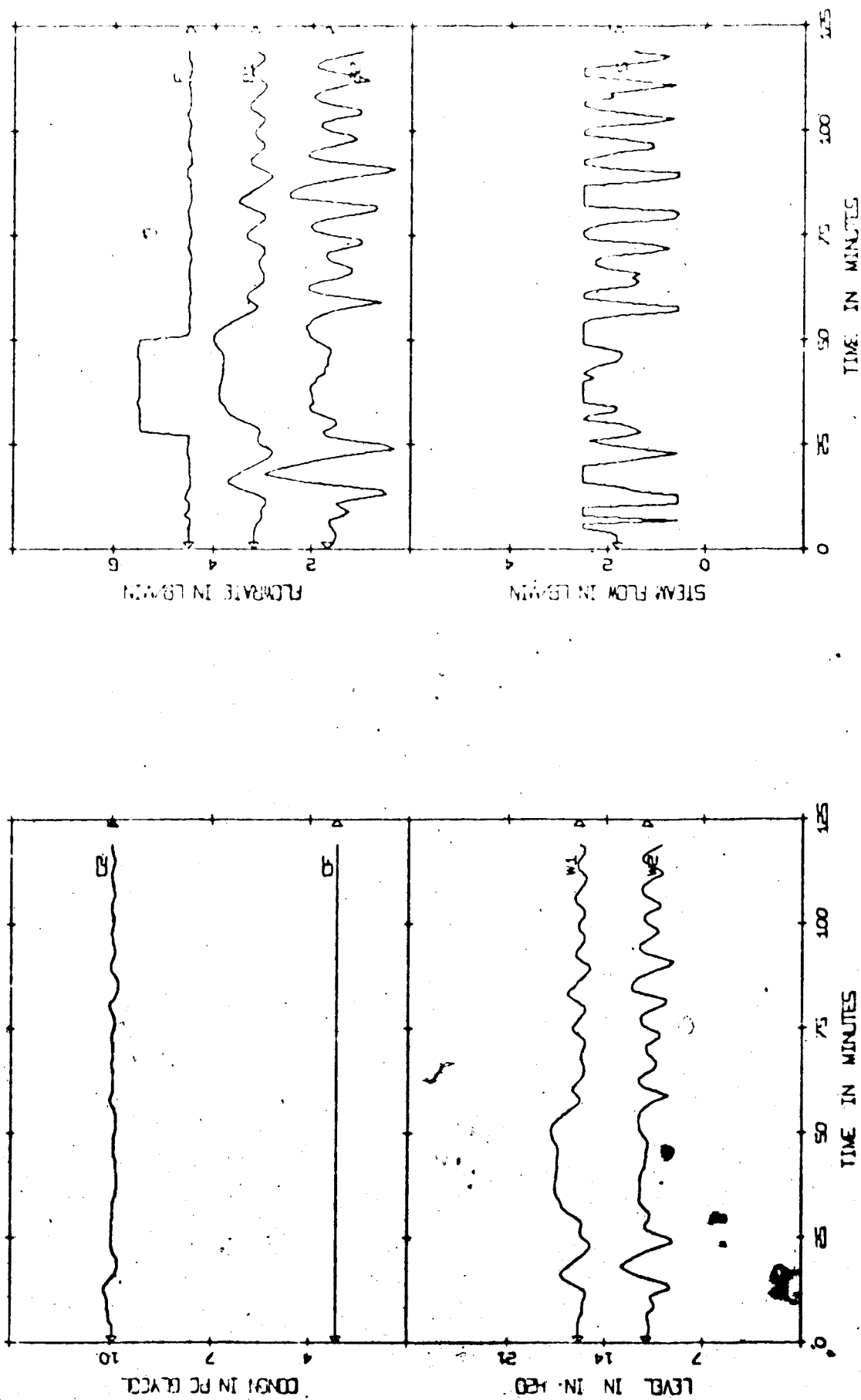


Figure 5.25 Evaporator response (EXP/+20% F, -20% F/STR), 4<sup>th</sup> order model



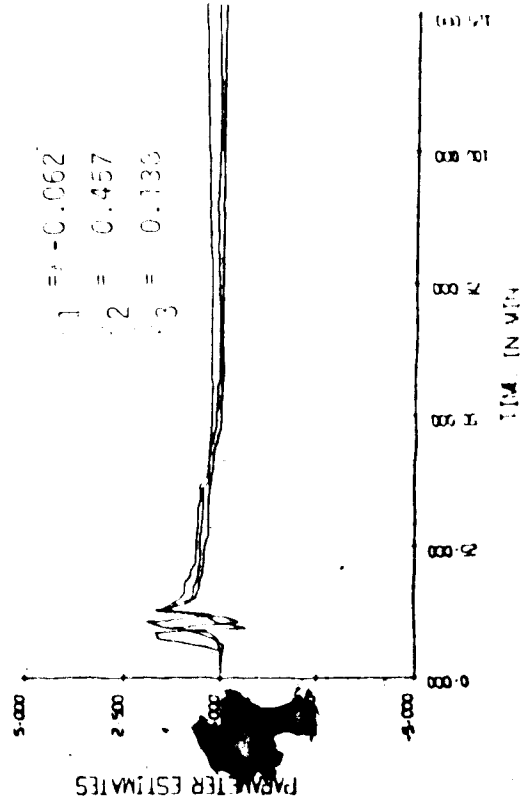
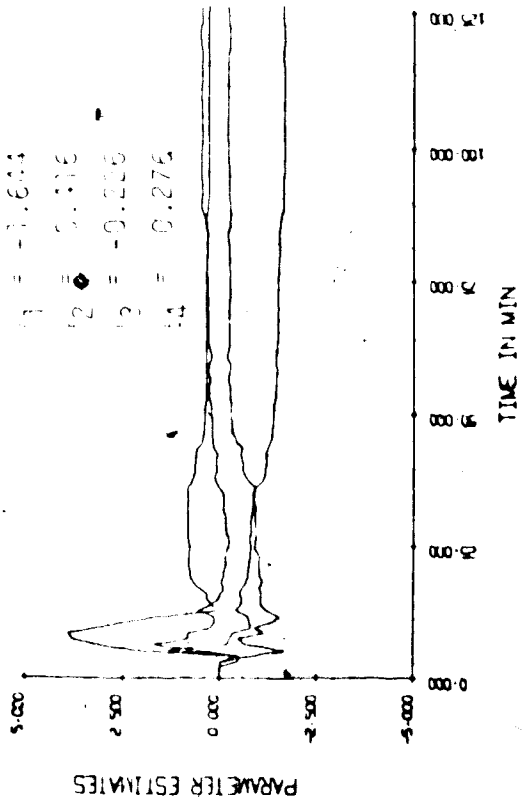
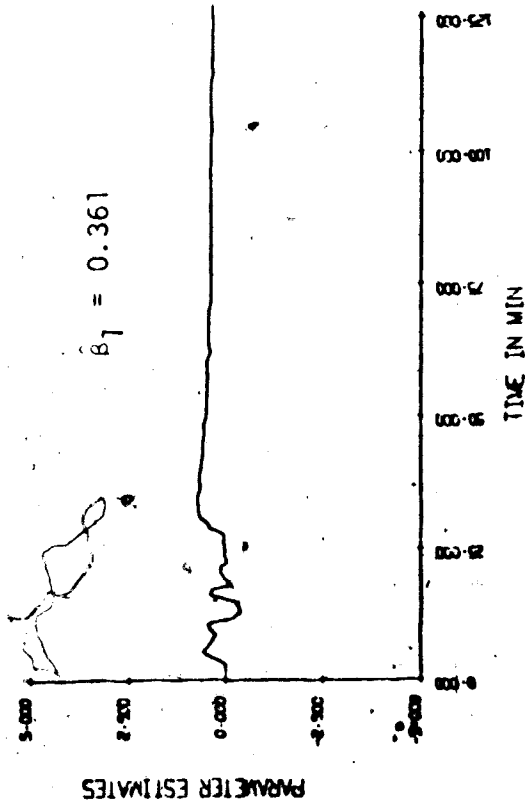
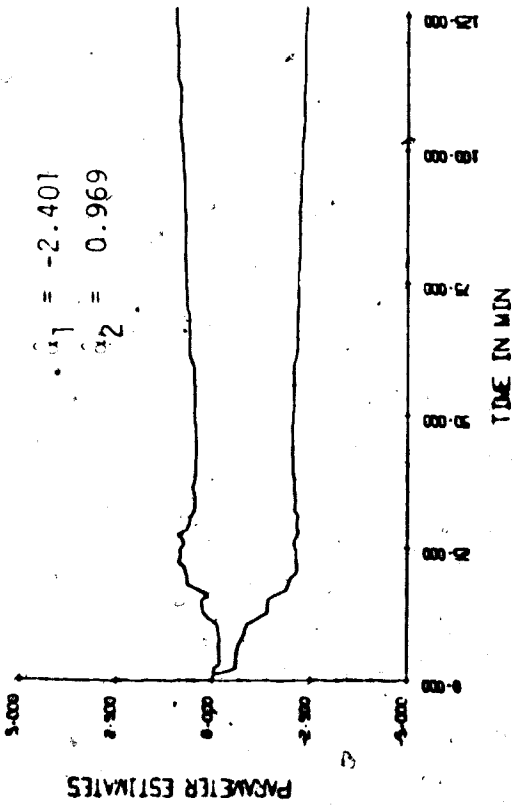


Figure 5.26 Parameter estimates (EXP/+20% F, -20% F/STR), 2nd order model

Figure 5.27 Parameter estimates (EXP/+20% F, -20% F), 4th order model

### 5.4.3 Practical Strategies for Implementing the Self-Tuning Regulator

Practical strategies for applications of the self-tuning regulator were considered in the simulation study of Section 4.5. In this section, two of these strategies were tried experimentally.

In Figure 5.28, the parameter estimates recorded at the end of the experimental run in Figure 5.14 were used as constant parameters in the control law of Equation (2.28). This constant parameter control law is the minimum variance controller for the empirically determined transfer function model. The satisfactory C2 response verifies that once good parameter estimates are obtained, the estimator can be bypassed and these constant parameters can be used in the control law until conditions warrant the use of the estimator again.

The strategy of using the estimator to estimate model parameters (except  $\beta_0$ ) while the evaporator was under conventional proportional control was also tried. The results are shown in Figure 5.29. The estimator was used for the first 24 minutes and the resulting parameter estimates were then used as the initial parameter estimates at  $t = 25$  minutes when the conventional controller was replaced by the self-tuning regulator. A scaling factor of  $\beta_0 = 0.02$  and an exponential forgetting factor of  $\mu = 0.995$  were used in this run.

The purpose of this strategy was to generate good parameter estimates before the self-tuning regulator is initiated. In the simulation run it was found that this method eliminated poor control during the transient period when the parameter estimates were adjusting (see Figure 4.44). In all the experimental runs, because of the lower process noise level, the control of C2 was satisfactory during the

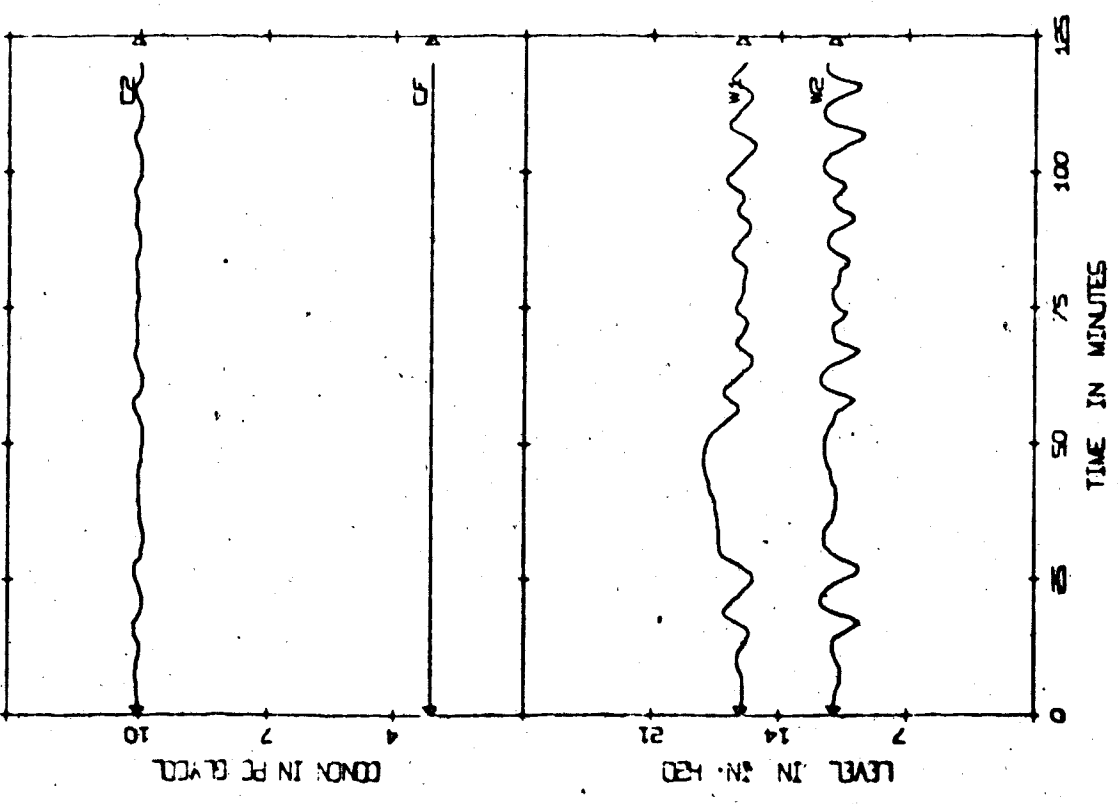
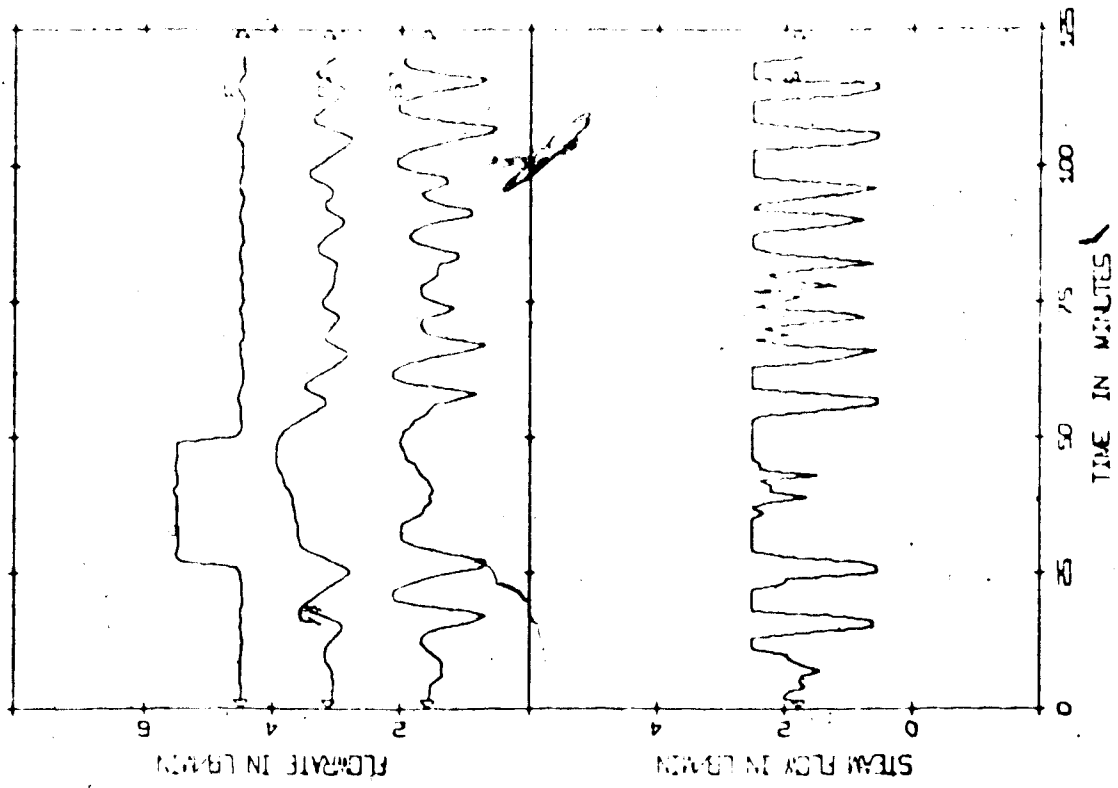


Figure 5.28 Evaporator response (EXP/+20% F, -20% F/STR), constant parameters

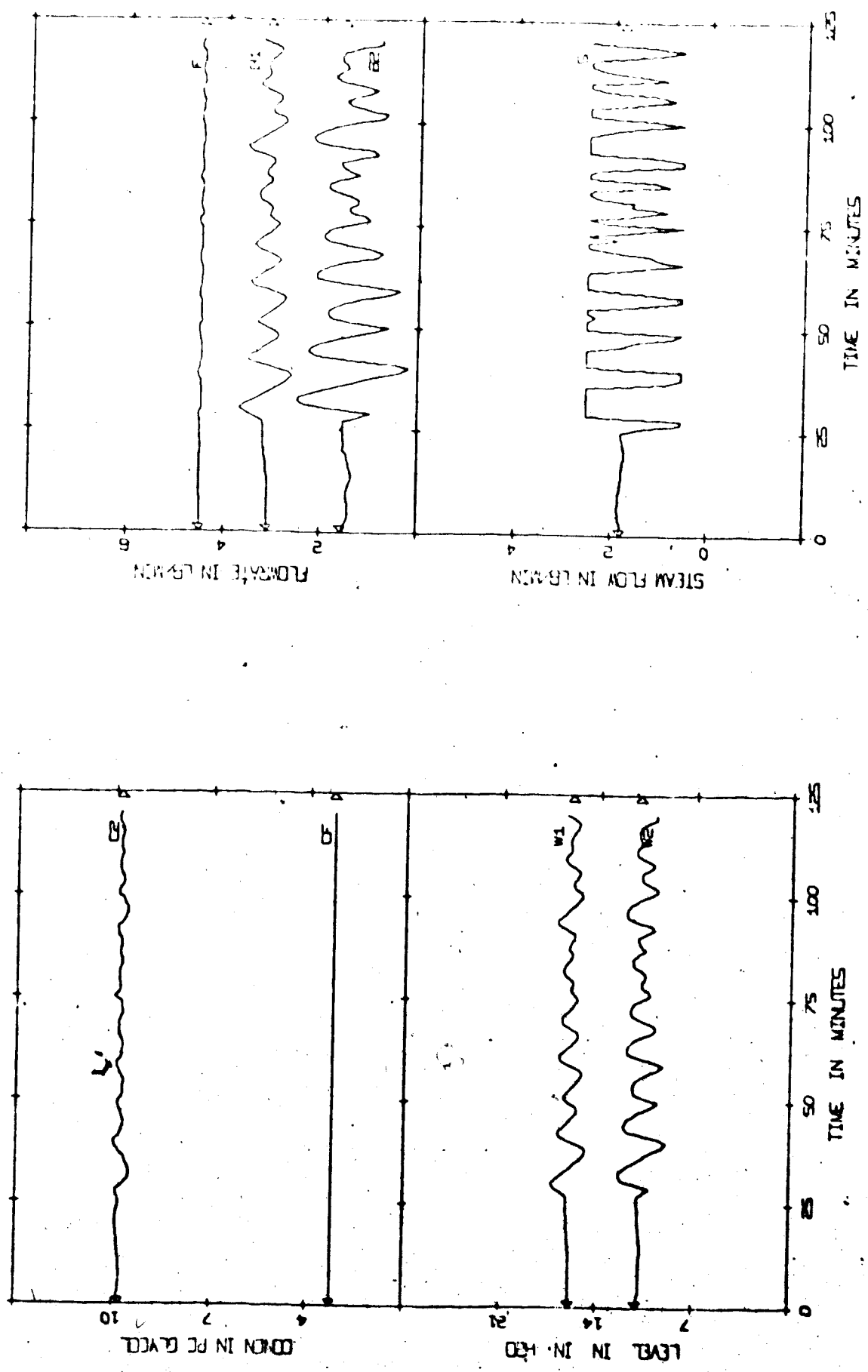


Figure 5.29 Evaporator response (EXP/ML prop. control & STR),  $\beta_0 = 0.02$ ,  $\mu = 0.995$

transient period, so the merit of using this strategy is not as apparent. The corresponding parameter estimates are shown in Figure 5.31.

A similar run was performed using the same large level loop gains that were used in the simulation study and the base case initial parameters in the self-tuning regulator. The results are shown in Figure 5.30. The C2 response was good for the major portion of the run, but towards the end, the high gains in the level loops again caused sustained oscillations in the control and output variables. The corresponding parameter estimates are shown in Figure 5.32.

## 5.5 Conclusions

For multi-loop proportional control, the experimental responses contained less fluctuations than those obtained in the simulation study. This was due to the lower process noise levels in the actual evaporator. The experimental results also show that the steady state control of C2 was fair and that C2 responses were satisfactory when step disturbances were applied. The standard DDC version of multi-loop proportional plus integral control gave slightly better control of C2, as expected, and the C2 response would probably be improved if there were looser control over the two effect levels (i.e., lower gains). All the conventional multi-loop control strategies that were applied gave much better C2 responses than those reported by Jacobson [30].

The experimental application of the self-tuning regulator for the base case conditions of the simulation study was unsuccessful. All of the control and output variables had sustained oscillations due to control loop interactions. However, when the gains in the level control loops were reduced by a factor of two the self-tuning regulator applica-

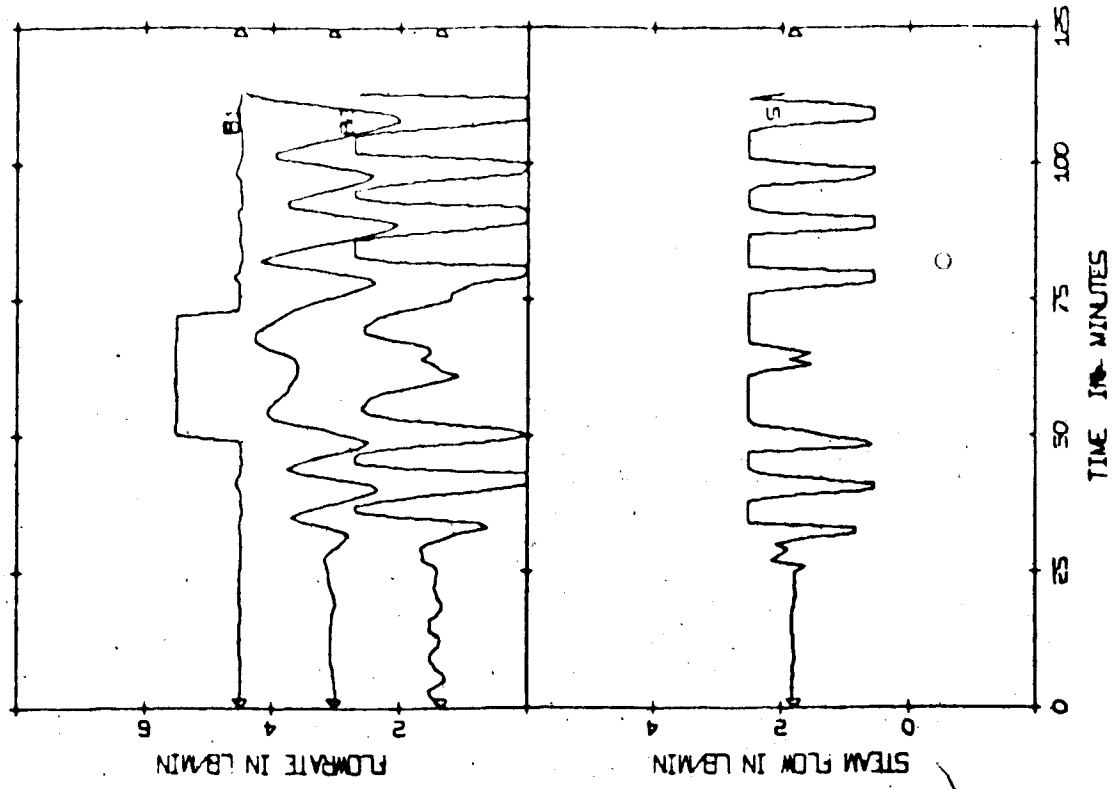
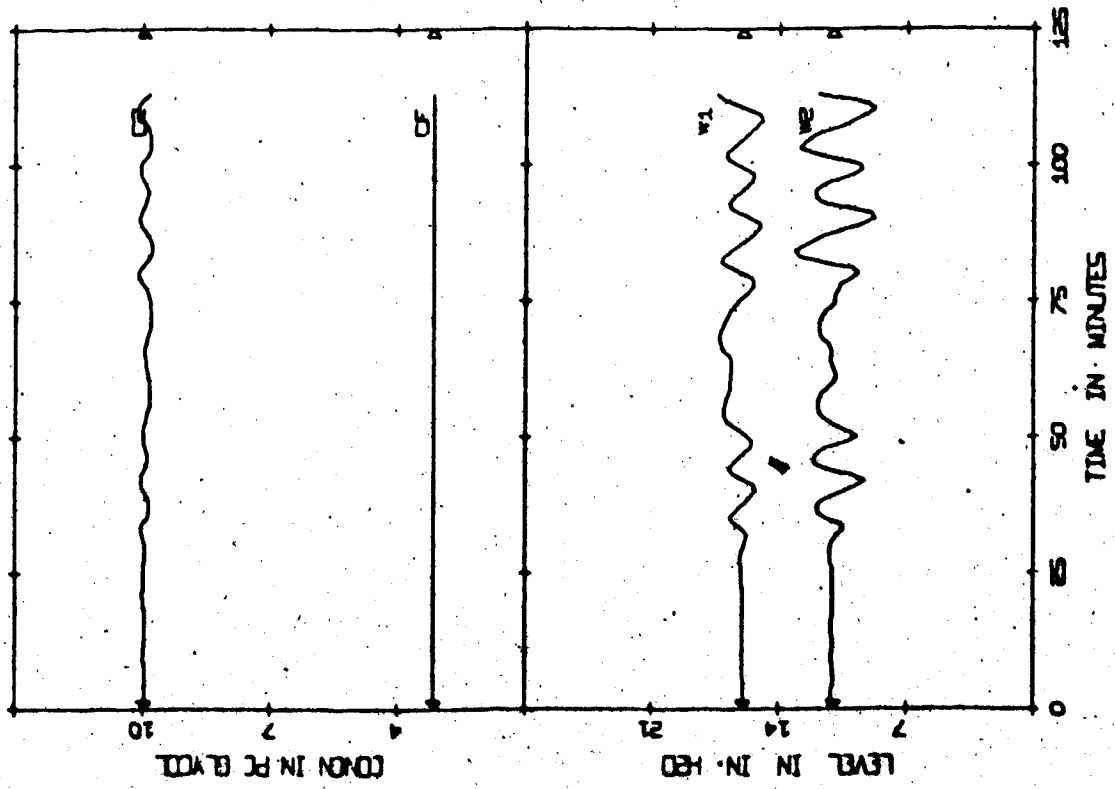


Figure 5.30 Evaporator response (EXP/+20% F, -20% F/ML prop. control & STR),  $K_{W1} = 3.52$ ,  $K_{W2} = 15.8$  [4]

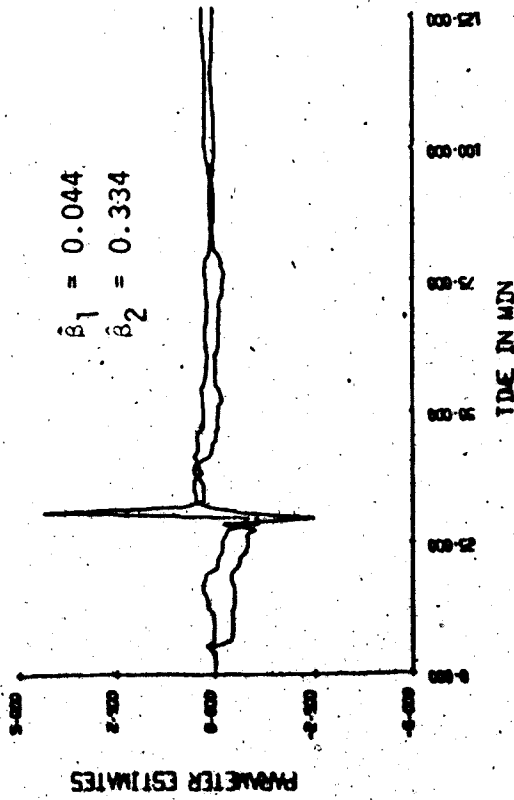
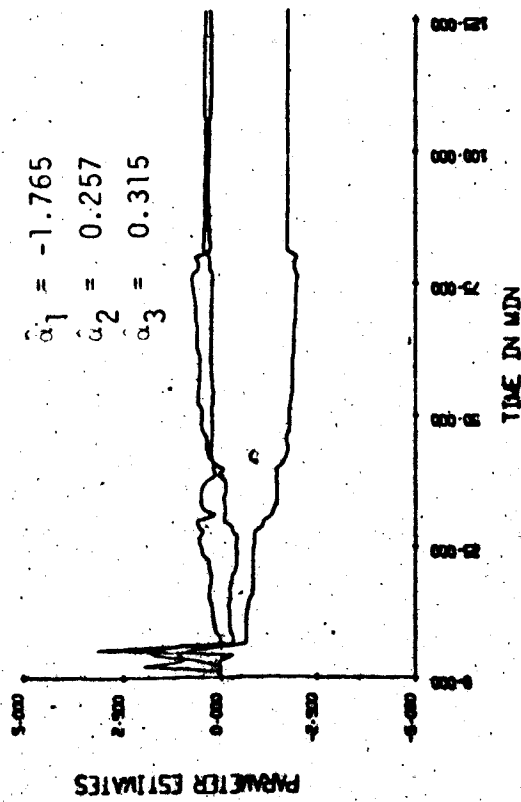


Figure 5.31 Parameter estimates (EXP/ML proportional control & STR).  $\hat{\theta}_0 = 0.02$ ,  $\mu = 0.995$

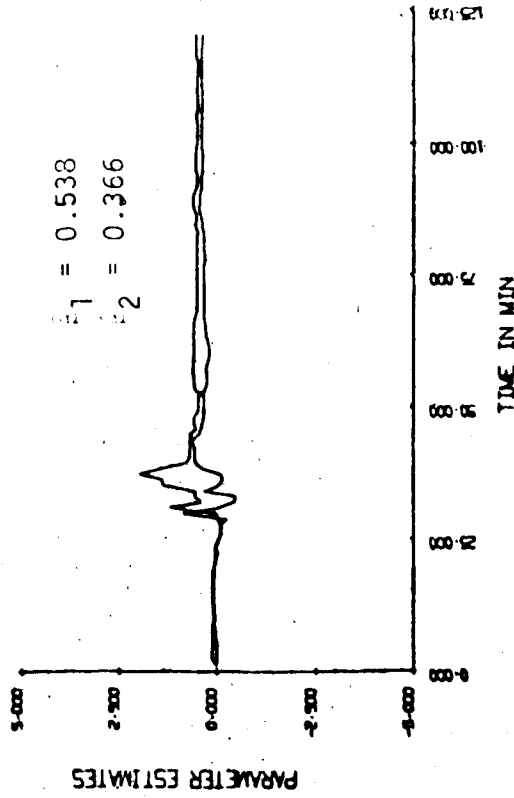
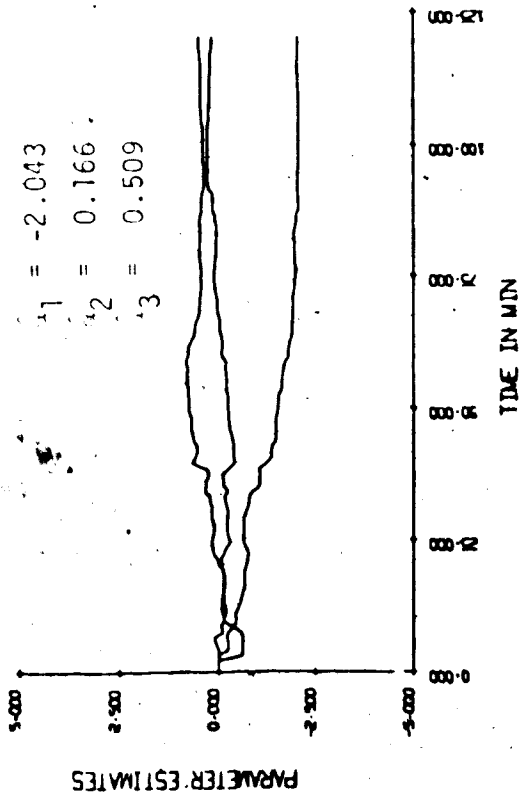


Figure 5.32 Parameter estimates (EXP/+20% F, -20% F/ML proportional control & STR),  $K_{W1} = 3.52$ ,  $K_{W2} = 15.8$

tion was successful. With the smaller proportional gains in the level control loop, good experimental results were obtained for base case conditions. A direct comparison of simulation and experimental runs could not be made, since the proportional gains of the level loops were different, the steam signals were constrained within narrower bounds, the actual process noise levels were lower, and output variables contain small measurement noise. In general, the performance of the self-tuning regulator was quite good and the characteristics of the regulator observed in the simulation study were verified in the experimental results. The corresponding parameter estimates did not converge as well as in the simulation runs but were still satisfactory.

Three different values of  $\beta_0$  were tried and the characteristic influence of  $\beta_0$  over the steam signal and the parameter estimates was similar to the simulation results. Different model order were tried ( $n = 2, 3$  and  $4$ ) and all gave satisfactory C2 responses. These experimental results verified the observation in the simulation study that the choice of model order was not critical.

It was also demonstrated that once a good set of parameter estimates have been obtained, these parameters could be held constant and used in the regulator until there were significant changes in process conditions. The proposed strategy of estimating the model parameters under conventional feedback control for a certain period before switching to the self-tuning regulator did not show any improvement for the actual evaporator system. This occurred because the evaporator was close to steady state during the estimation period, and with low process noise levels and little or no excitation in the steam signal, the estimator could not generate good estimates for use in the



self-tuning regulator.

Experimental runs in which all the parameters (including  $\beta_0$ ) were estimated were not successful in contrast to the successful simulation runs. In all of the unsuccessful runs, the steam signal would drop to the lower limit initially and remain there until the run was terminated. Thus it appears that attempting to estimate all the parameters in the self-tuning regulator results in non-identifiability of the parameters and poor control of C2. Consequently, one parameter should be fixed for the evaporator system as recommended by Aström and Wittenmark [1].

To summarize, the self-tuning regulator performed quite well even with an approximate set of initial parameters and handled unmeasured step disturbances quite well. In comparison with well-tuned P or PI controllers, the self-tuning regulator resulted in similar steady state control but better control when unmeasured step disturbances occurred. However, the merits of the self-tuning regulator were not fully demonstrated in this application due to the low process noise levels.

## CHAPTER SIX

## CONCLUSIONS

The purpose of this investigation was to provide a detailed evaluation of the self-tuning regulator and to investigate its performance in a practical application to a pilot plant, double effect evaporator. Simulation and experimental studies have demonstrated that the evaporator application was successful and have shown that the regulator works well for a relatively wide range of design parameters. The following design parameters were investigated: exponential forgetting factor, initial covariance matrix, initial parameter estimates, scaling factor, model order and system time delay. The self-tuning regulator was also evaluated for non-ideal operating conditions including different process noise and measurement noise levels, and unmeasured step disturbances.

The conclusions concerning the effects of the various design parameters can be summarized as follows:

1. Scaling factor  $\beta_0$ ; The scaling factor is the most difficult parameter to specify. In the simulation study a wide range of values ( $0.1 \geq \beta_0 \geq 0.00001$ ) gave satisfactory results when the control signal was constrained. This was reduced significantly when the control signal was unconstrained. An experimental run with  $\beta_0 = 0.1$  resulted in large fluctuations in the output indicating that only a smaller range of values can be used in practice. Both the simulation and experimental results show that smaller values of  $\beta_0$  produce significant fluctuations in  $(\hat{\beta}_i)$ , rapid convergence of

$\hat{\beta}_i$ , and large, frequent fluctuations in the control signal. The converse situation occurred for large values of  $\sigma_0$ . Here  $\{\hat{\beta}_i\}$  converged quickly,  $\{\hat{\alpha}_i\}$  fluctuated and the control signal was smoother.

2. Model order  $n$ ; The assumed order did not significantly affect the process responses. Except for the initial twenty minute transient, second, third and fourth order evaporator models gave practically the same simulated responses, but in the experimental study, underestimation of the model order ( $n = 2$ ) gave better control of the output.
3. System time delay  $k$ ; Overestimation of the process time delay by two sampling intervals (128 seconds) still resulted in satisfactory control in the simulation study. This factor was not investigated experimentally since the actual evaporator system has no time delay.
4. Initial covariance matrix  $\underline{P}(0)$ ; The selection of the initial covariance matrix and initial parameter estimates should be made together since the choice of the initial covariance matrix is based on the degree of confidence one has in the initial parameter estimates. If poor initial parameter estimates are used, then large diagonal elements in the initial covariance matrix should be assigned. Large diagonal elements in  $\underline{P}(0)$  produce large initial adjustments of the parameter estimates followed by fast convergence. During the initial transient large variations in the control signal occur and unless the control signal is bounded, this will produce undesirable results. Smaller diagonal elements in  $\underline{P}(0)$  produce a slower rate of convergence.

and smaller changes in the parameter estimates during the initial part of the response. In the simulation study, choosing  $\underline{P}(0) = 100 \underline{I}$  provided good convergence of the parameter estimates starting from zero initial values. However,  $\underline{P}(0) = 10,000 \underline{I}$  was used in most simulation runs and in all experimental runs to ensure fast convergence of the estimates to satisfactory values.

5. Initial parameter estimates  $\hat{\theta}(0)$ ; The self-tuning regulator worked well in the simulation study for a wide range of poor initial estimates including  $\hat{\theta}_i(0) = 0, -5, \text{ and } 10$ , when large diagonal elements were used in  $\underline{P}(0)$ . Zero initial parameter estimates were used in all experimental runs and rapid convergence of the parameter estimates occurred. Thus a priori knowledge of actual system parameters is not necessary for satisfactory performance of the self-tuning regulator.
6. Exponential forgetting factor  $\mu$ ; Values of  $\mu$  between 0.9 and 1.0 did not significantly affect the simulated responses but the parameter estimates fluctuated more for smaller values. A value of  $\mu = 1.0$  proved to be satisfactory in the experimental study.

In this application, it was found that the design parameters, particularly  $B_0$ ,  $\underline{P}(0)$ , and  $\mu$  can be adjusted on-line to give better values after examining the transient process response and the parameter estimates.

The simulation results showed that the self-tuning regulator can handle unmeasured step disturbances better than a digital proportional controller. The experimental runs confirmed this result but gave small oscillations around the steady state in some runs due to the

significant fluctuations in the manipulated variable. In the simulation study, the output variance increased as the process noise level increased and that the addition of 5% measurement noise resulted in large fluctuations in the controlled variable. It was found that estimating all of the parameters including the scaling factor was possible in the simulation study though the control of the output was not very good. However, this method did not work well in the experimental runs.

The interacting nature of the multi-input, multi-output evaporator system strongly affected the performance of the self-tuning regulator. This was clearly seen in the experimental results where the influence of other evaporator variables, such as the bottom flow rates, resulted in large sustained oscillations when normal proportional gains were used in the two level control loops. These interactions were significantly reduced by decreasing the gains in the level control loops but very small oscillations about the desired steady state still persisted in most runs.

In general, the self-tuning regulator performed well especially when a good set of initial parameters were used. The regulator is very simple to use and does not involve complex mathematical operations. It can take into account system time delays and can have different numbers of control parameters depending on the assumed system model. It can be used continuously so that it will automatically adjust control parameters on-line to suit changing operating conditions or process dynamics, or it can be used periodically for the purpose of tuning control parameters. A practical scheme for implementing the self-tuning regulator in which

a conventional controller is used initially before switching to the regulator has proved to be useful in this work and is recommended. The self-tuning regulator is probably best suited for stochastic processes with relatively high process noise levels and frequent unmeasured disturbances since its design is based on stochastic control theory. Its use is recommended especially if conventional control techniques are unable to provide good control for these conditions.

### 6.1 Future Work

The simulation and experimental studies in this thesis provide a detailed examination of the self-tuning regulator and general guidelines for its use. However, there are a number of areas that require further investigation and these will be discussed as follows.

1. The self-tuning algorithm can be extended to include feedforward control of a measured disturbance [7,22]. This extension can be applied to the evaporator system by using measurements of either feed flow rate or feed concentration. Although it has been shown that the self-tuning regulator can handle unmeasured disturbances well, this feedforward investigation may prove valuable for other systems.
2. The self-tuning regulator can also be modified to include setpoint control of the output variable [7]. This extension would increase the capability of the regulator.
3. The scaling factor in the regulator was normally assumed to be constant in this study. The effect of holding some other parameter constant instead of the scaling factor or the effect of fixing several parameters could also be studied.

4. Only a single self-tuning regulator was used for one particular control loop in the evaporator application. A logical extension would be to use self-tuning regulators in several control loops either sequentially or simultaneously.
5. In this study, the self-tuning regulator was used in an interacting multivariable system and the effects of interaction were not directly taken into account. However, from previous evaporator studies, it is known that the first effect bottom flow rate affects the product concentration to a significant extent. The influence of this control variable could be included in the self-tuning regulator by using a two input, one output process model. This extension may reduce the experimental difficulties caused by control loop interactions.
6. The self-tuning regulator is usually designed to minimize the output variance. Other performance indices that include control variable terms have been recently proposed [15,16,23] and should be evaluated. These modifications might reduce the relatively large magnitude fluctuations in the control variable.
7. The extension of the self-tuning type of control strategy to multi-input, multi-output systems is currently under investigation [21]. If successful, such an extension would certainly increase the flexibility of the control strategy and the evaporator would be an appropriate system for an application.

## NOMENCLATURE

a) Alphabetic

A	Polynomial in Åström - Bohlin model
$a_i$	Coefficient in polynomial A
B	Polynomial in Åström - Bohlin model
$b_i$	Coefficient in polynomial B
B1	First effect bottom flowrate
B2	Second effect bottom flowrate
C	Polynomial in Åström - Bohlin model
$c_i$	Coefficient in polynomial C
C1	First effect concentration
C2	Second effect concentration
CF	Feed concentration
D	Polynomial
$d_i$	Coefficient in polynomial D
<u>d</u>	Disturbance vector
E	Expectation operator
e	Random normal variable
F	Feed flow rate
G	Polynomial
$g_i$	Coefficient in polynomial G
<u>H</u>	Output coefficient matrix
H1	First effect enthalpy
HF	Feed enthalpy
<u>I</u>	Identity matrix
<u>K</u>	Gain vector



$k$	Time delay
$\ell$	Number of parameters
$M$	Polynomial
$m_i$	Coefficient in polynomial $M$
$N$	Normal distribution
$n$	Order of model
$O1$	Overhead from first effect
$O2$	Overhead from second effect
$\underline{P}$	Covariance matrix
$P1$	Pressure in first effect
$P2$	Pressure in second effect
$q^{-1}$	Backward shift operator
$R$	Covariance of noise variable
$S$	Steam flow rate
$T1$	Temperature in first effect
$T2$	Temperature in second effect
$TF$	Feed temperature
$t$	Sampling instant
$\underline{u}$	Control vector
$V$	Loss function
$\underline{w}$	Measurement noise vector
$W1$	First effect holdup
$W2$	Second effect holdup
$\underline{x}$	State vector
$\underline{y}$	Output vector
$Z$	Polynomial
$z_i$	Coefficient in polynomial $Z$

b) Greek

$\alpha$	Coefficient of predictive model
$\beta$	Coefficient of predictive model
$\beta_0$	Scaling factor
$\Gamma$	Process noise coefficient matrix
$\Delta$	Control coefficient matrix
$\epsilon$	Moving average process of driving noise $e$
$\theta$	Parameter vector
$\lambda$	Constant
$\mu$	Exponential forgetting factor
$\Pi$	Disturbance coefficient matrix
$\sigma$	Standard deviation
$\tau$	Information vector

c) Subscripts

$i$	$i^{\text{th}}$ element
$\underline{\quad}$	Vector
$\underline{\quad}$	Matrix
PN	Process noise
MN	Measurement noise
SS	Steady state

d) Superscripts

T	Matrix transpose
$^{-1}$	Matrix inverse

Estimated value

Perturbed variable

e) Abbreviations

adj	Matrix adjoint
det	Determinant
prop	Proportional
CC	Concentration controller
CR	Concentration recorder
FC	Flow controller
FR	Flow recorder
LC	Level controller
PC	Pressure controller
KP	Proportional constant
KI	Integral constant
PI	Proportional plus integral

f) Codes for Computer Plots

$\Delta, \nabla$	Denote time of step disturbance
$\blacktriangleleft, \blacktriangleright$	Denote initial steady state

Type of Run :

SIM	Simulated
EXP	Experimental

Disturbance (· / X% / XX):

+ , -	Positive or negative step
X%	Step size as percentage of steady state
XX	Process variable disturbed

Control Mode:

OL	Open loop
ML	Multi-loop conventional control
STR	Self-tuning regulator
PI	Proportional plus integral

## REFERENCES

1. Åström, K.J. and Wittenmark, B., "On Self-Tuning Regulators", *Automatica*, 9, pp. 185-199, 1973.
2. Åström, K.J. and Eykhoff, P., "System Identification, a Survey", *Automatica*, 7, pp. 123-162, 1971.
3. Nieman, R.E., Fisher, D.G. and Seborg, D.E., "A Review of Process Identification and Parameter Estimation Techniques", *Int. J. Control*, 13, pp. 209-264, 1971.
4. Gustavsson, I., "Survey of Applications of Identification in Chemical and Physical Processes", *Automatica*, 11, pp. 3-24, 1975.
5. Åström, K.J. and Bohlin, T., "Numerical Identification of Linear Dynamic Systems from Normal Operating Data", *Proc. 2nd IFAC Symp. on the Theory of Self-Adaptive Control Systems*, Teddington, pp. 96-111, Sept. 1965.
6. Peterka, V., "Adaptive Digital Regulation of Noisy Systems", Preprint of 2nd Prague IFAC Symp. on Identification and Process Parameter Estimation, Prague, paper no. 6.2, June 1967.
7. Wittenmark, B., "A Self-Tuning Regulator", Research Report 7311, Division of Automatic Control, Lund Institute of Technology, April 1973.
8. Åström, K.J. and Wittenmark, B., "Problems of Identification and Control", *Journal of Mathematical Analysis and Application*, 34, pp. 90-113, 1971.
9. Åström, K.J., Borisson, U., Ljung, L., and Wittenmark, B., "Theory and Application of Adaptive Regulators based on Recursive Parameter Estimation", Paper to be presented at the 6th IFAC World Congress, Boston, August, 1975.

10. Kalman, R.E., "Design of a Self-Optimizing Control System", Trans. ASME, 80, pp. 468-478, 1958.
11. Wittenmark, B., and Wieslander, J., "Identification and Process Parameter Estimation", Preprint of 2nd Prague IFAC Symp. on Identification and Process Parameter Estimation, Prague, paper no. 6.3, June 1967.
12. Sage, A.P., and Melsa, J.L., "System Identification", Academic Press, New York (1971).
13. Åström, K.J., "Introduction to Stochastic Control Theory", Academic Press, New York, 1970.
14. Cegrell, T., and Hedqvist, T., "A Self-Adjusting Regulator", ASEA LME Automation, Internal Report, 1973.
15. Clarke, D.W., and Gawthrop, P.J., "Generalization of the Self-Tuning Regulator", Electronics Letters, 11, pp. 40-41, Jan. 1975.
16. Clarke, D.W., and Gawthrop, P.J., "Simulation of a Generalized Self-Tuning Regulator", Electronics Letters, 11, pp. 41-42, Jan. 1975.
17. Ljung, L., and Wittenmark, B., "Asymptotic Properties of the Self-Tuning Regulator", Research Report 7404, Division of Automatic Control, Lund Institute of Technology, Feb. 1974.
18. Åström, K.J. and Wittenmark, B., "Analysis of Self-Tuning Regulator for Nonminimum Phase Systems", Research Report 7418 (c), Division of Automatic Control, Lund Institute of Technology, August 1974.
19. Turtle, D.P. and Phillipson, P.H., "Simultaneous Identification and Control", Automatica, 7, pp. 445-453, 1971.
20. Gustavsson, I., Ljung, L. and Söderström, T., "Identification of Linear Multivariable Process Dynamics Using Closed Loop Experiments",

- Research Report 7401, Division of Automatic Control, Lund Institute of Technology, Jan. 1974.
21. Peterka, V. and Åström, K.J., "Control of Multivariable System with Unknown but Constant Parameters", 3rd IFAC Symp. on Identification and System Parameter Estimation, Hague, pp. 535-544, June, 1973.
  22. Wittenmark, B. and Borisson, U., "An Industrial Application of a Self-Tuning Regulator", Research Report 7310, Division of Automatic Control, Lund Institute of Technology, April, 1973.
  23. Cegrell, T. and Hedqvist, T., "Successful Adaptive Control of Paper Machines", 3rd IFAC Symp. on Identification and System Parameter Estimation, Hague, pp. 485-491, June 1973. (Also published in *Automatica*, 11, pp. 53-59, 1975.)
  24. Clarke, D.W., "Generalized Least Squares Estimation of the Parameters of a Dynamic Plant", Preprints of 2nd IFAC Symp. on Identification in Automatic Control Systems, Prague, paper no. 3.17, June 1967.
  25. Sinha, N.K., "On-Line Identification of Continuous System from Sampled Data", 3rd IFAC Symp. on Identification and System Parameter Estimation, Hague, pp. 385-392, June 1973.
  26. Åström, K.J., "On the Achievable Accuracy in Identification Problems", Preprints of 2nd IFAC Symp. on Identification in Automatic Control Systems, Prague, paper no. 1.8, June 1967.
  27. Borisson, U. and Syding, R., "Self-Tuning Control of a Ore Crusher", IFAC Symp. on Stochastic Control, Budapest, 1974.
  28. Hamilton, J.C., "An Experimental Investigation of State Estimation in Multivariable Control Systems", M.Sc. Thesis, Department of Chemical Engineering, University of Alberta (1972).

29. Newell, R.B., "Multivariable Computer Control of an Evaporator", Ph.D. Thesis, Department of Chemical Engineering, University of Alberta (1971).
30. Jacobson, B.A., "Multi-Loop Computer Control of an Evaporator", M.Sc. Thesis, Department of Chemical Engineering, University of Alberta (1970).
31. Fisher, D.G., Wilson, R.G., and Agostinis, W., "Description and Application of a Computer Program for Control System Design", *Automatica*, 8, pp. 737-746, 1972.
32. Newell, R.B., and Fisher, D.G., "Plotting Evaporator Data", Research Report 701203, Department of Chemical Engineering, University of Alberta (1970).
33. Hamilton, J.C., and Seborg, D.E., "User Manual for Thesis Programs", Research Report 721101, Department of Chemical Engineering, University of Alberta (1972).
34. Oliver, W.K., "Model Reference Adaptive Control: Hybrid Computer Simulation and Experimental Verification", M.Sc. Thesis, Department of Chemical Engineering, University of Alberta (1972).
35. Wilson, R.G., "Model Reduction and the Design of Reduced-Order Control Laws", Ph.D. Thesis, Department of Chemical Engineering, University of Alberta (1974).
36. Newell, R.B. and Fisher, D.G., "User's Manual for Multivariable Control Programs", Research Report 701201, Department of Chemical Engineering, University of Alberta (1970).
37. King, B. and McNeill, J., "On-Line Tuning of a Composition Control Loop", Ch.E. 552 Report, Department of Chemical Engineering, University of Alberta (1975).



38. Hamilton, J.C. and Liesch, D.W., "Evaporator Operator's Manual", Internal Report, Department of Chemical Engineering, University of Alberta (1971).
39. Anonymous, "DDC Manual", 2<sup>nd</sup> edition, Internal Report, Department of Chemical Engineering, University of Alberta (1975).

## APPENDIX FOR CHAPTER THREE

(a) Normal Steady State Operating Conditionsx Five element state vector

W1	First effect holdup	46 lb (16.0 in)
C1	First effect concentration	4.59% glycol
H1	First effect solution enthalpy	190 BTU/lb
W2	Second effect holdup	42 lb (11.0 in)
C2	Second effect concentration	10.11% glycol

u Three element control vector

S	Steam flowrate to first effect	2.00 lb/min
B1	First effect bottoms flowrate	3.49 lb/min
B2	Second effect bottoms flowrate	1.58 lb/min

d Three element disturbance vector

F	Feed flow rate	5.0 lb/min
CF	Feed concentration	3.2% glycol
HF	Feed enthalpy	162 BTU/lb

$$\underline{y}^T = [W1, W2, C2]$$

(b) Matrices for the Discrete Evaporator Model (based on Steady State condition in (a) and a sampling interval of 64 seconds)

$$\Phi = \begin{bmatrix} 1.0 & -0.0008 & -0.0912 & 0 & 0 \\ 0 & 0.9223 & 0.0871 & 0 & 0 \\ 0 & -0.0042 & 0.4377 & 0 & 0 \\ 0 & -0.0009 & -0.1052 & 1.0 & 0.0001 \\ 0 & 0.0391 & 0.1048 & 0 & 0.9603 \end{bmatrix}$$

$$\Delta = \begin{bmatrix} -0.0119 & -0.0817 & 0 \\ 0.0116 & 0 & 0 \\ 0.1569 & 0 & 0 \\ -0.0137 & 0.0847 & -0.0406 \\ 0.0137 & -0.0432 & 0 \end{bmatrix}$$

$$\Gamma = \begin{bmatrix} 0.1182 & 0 & -0.0050 \\ -0.0351 & 0.0785 & 0.0049 \\ -0.0135 & -0.0002 & 0.0662 \\ -0.0012 & 0 & -0.0058 \\ -0.0019 & 0.0016 & 0.0058 \end{bmatrix}$$

$$H = \begin{bmatrix} 1 & 0 & 0 & 0 & 0 \\ 0 & 0 & 0 & 1 & 0 \\ 0 & 0 & 0 & 0 & 1 \end{bmatrix}$$

$$\Gamma = \begin{bmatrix} \Gamma \\ \Delta \end{bmatrix}$$

## APPENDIX FOR CHAPTER FIVE

The following is a listing of computer printouts containing information about the controllers and steady state condition of the evaporator that are collected at the start of a typical experimental run. The reader is referred to the User's Manual [38] for information on the computer programs used.

(a) Computer printout from program FLC32

\*\*\* SELF-TUNING CONTROL EXECUTIVE \*\*\*

INITIALIZATION DATA FOR RUN 12

DATA STORAGE INTERVAL(SEC)= 0  
 COUNTER INDICATOR= 0  
 CONTROL INTERVAL(SEC)= 64

JFLAG= 2 KFLAG=99

STD. DEV.(PROC. NOISE)= 0.10 STD. DEV.(MEAS. NOISE)= 0.00

KP(1)= -4.89 KP(2)= 1.50 KP(3)= 6.50

INITIAL CONSTANTS

B0=0.01400 M= 3 K= 0 Z= 1.000

INITIAL CONTROL PARAMETERS

0.00 0.00 0.00 0.00 0.00

INITIAL COVARIANCE MATRIX

10000.001	0.000	0.000	0.000	0.000	0.000
0.000	10000.001	0.000	0.000	0.000	0.000
0.000	0.000	10000.001	0.000	0.000	0.000
0.000	0.000	0.000	10000.001	0.000	0.000
0.000	0.000	0.000	0.000	10000.001	0.000
0.000	0.000	0.000	0.000	0.000	10000.001

STEADY STATE VALUES FOR XM, U, AND D

0.16060E 02	0.22140E 03	0.10930E 02	0.99899E-01
0.18009E 01	0.31480E 01	0.13580E 01	
0.45020E 01	0.32100E-01	0.18830E 03	

(b) Computer printout from program PVLOG

THE FOLLOWING IS A LISTING OF THE MEASURED VALUE FOR EACH LOOP RECORD SPECIFIED, WITH THE ASSOCIATED MEASUREMENT CONDITION CODES.

LOOP ID	MEASUREMENT	LOOP DESCRIPTION	15 APR 75 15/27 HRS			
			CONDITION CODES			
			GTU	ERR	PVR	MEAS
141	3.063 LB/MIN	FEED WATER FLOW	1	2	2	
139	1.433 LB/MIN	FEED SOL. FLOW	1	2	2	
149	4.494 LB/MIN	TOTAL FEED FLOW	1	2	2	
151	3.143 LB/MIN	B1	1	2	2	
152	1.439 LB/MIN	B2	1	2	2	
132	1.798 LB/MIN	STEAM FLOW	1	2	2	
150	1.540 LB/MIN	CONDENSATE FROM SECOND EFFECT	1	2	2	
126	1.385 LB/MIN	CONDENSER COND. FLOW	1	2	2	
133	48.590 LB/MIN	COOLING WATER FLOW	1	2	4	
136	16.070 IN H2O	FIRST EFFECT LEVEL	1	2	2	
137	11.000 IN H2O	SEPARATOR LEVEL	1	2	2	
125	5.000 IN H2O	CONDENSATE LEVEL	1	2	2	
135	4.810 PSIG	FIRST EFFECT PRESSURE	1	2	2	
134	17.960 IN HG	SECOND EFFECT PRESSURE	1	2	2	
142	190.000 DEG F	FEED WATER TEMPERATURE	1	2	2	
138	190.000 DEG F	FEED SOL. TEMPERATURE	1	2	2	
159	188.600 DEG F	TOTAL FEED TEMPERATURE	1	2	2	
143	0.032	FEED CONCENTRATION	1	1	1	
164	221.600 DEG F	FIRST EFFECT TEMPERATURE	1	2	2	
129	0.099	ACTUAL PRODUCT CONC.	1	2	2	

## MEASUREMENT CODES USED ARE

## GTU ERROR CODES

- 1 NO ERROR DETECTED
- 2 VALUE NOT IN LOOP RECORD
- 3 INVALID ID. LOOP NOT IN TABLE
- 4 INVALID DATA IN CALL GTU STATEMENT

## PROCESS VARIABLE RECORD (LOOP RECORD) CONDITION CODES:

- 1 LOOP OUT OF SERVICE
- 2 LOOP IN SERVICE

## MEASUREMENT VALUE CONDITION CODES

- 1 INPUT BAD
- 2 INPUT NORMAL
- 3 LOW ALARM LIMIT
- 4 HIGH ALARM LIMIT

(c) Computer printout from program BJ200

STEADY STATE TEMPERATURES<sup>v</sup>

MPX	TEMP. (F)	DESCRIPTION
-16318	219.9	TR20 - FIRST EFFECT, SOLUTION AT TOP OF DOWNCOMER
-16316	218.9	TR 3 - FIRST EFFECT, SOLUTION ABOVE THE TUBES.
-16314	154.8	TR14 - FIRST EFFECT, SOLUTION AT THE BOTTOM.
-16313	153.0	TR33 - SECOND EFFECT, CONDENSATE AFTER THE COOLER
-16312	162.2	TR 6 - SECOND EFFECT, SOLUTION AT THE BOTTOM.
-16311	219.2	TR32 - SECOND EFFECT, STEAM BLEED.
-16306	72.6	TR27 - STEAM, OUTLET OF THE FEED WATER HEATER.
-16305	160.9	TR34 - SECOND EFFECT, PRODUCT JUST BEFORE PUMP.
-16304	74.2	TR21 - SOLUTION TANK, INLET SOLUTION.
-16303	153.2	TR18 -
-16302	190.6	TT12 - FEED, TOTAL AFTER MIXING.
-16301	189.6	TT11 - FEED, WATER BEFORE MIXING.
-16300	189.3	TT10 - FEED, SOLUTION BEFORE MIXING.
-16299	85.5	TT13 - CONDENSER, CONDENSATE INSIDE.
-16298	298.3	TR15 - STEAM, TO FIRST EFFECT BEFORE ORIFICE.
-16297	253.1	TR13 - FIRST EFFECT, STEAM IN THE CHEST.
-16296	252.4	TR 5 - FIRST EFFECT, STEAM CONDENSATE.
-16295	221.4	TR19 - FIRST EFFECT, SOLUTION AT BOTTOM OF DOWNCOMER
-16294	218.3	TR 2 - FIRST EFFECT, VAPOUR LEAVING.
-16293	188.5	TR 7 - FIRST EFFECT, FEED AT INLET.
-16292	182.8	TR 4 - SECOND EFFECT, FEED AT INLET.
-16291	-33.1	TR16 - SECOND EFFECT, STEAM AT TOP OF CHEST.
-16290	172.9	TR 9 - SECOND EFFECT, SOLUTION AT TOP.
-16289	161.6	TR17 - SEPARATOR, SOLUTION LEAVING.
-16288	161.7	TR12 - SEPARATOR, VAPOUR LEAVING.
-16287	161.4	TR10 - SECOND EFFECT, STEAM AT INLET TO CHEST.
-16286	194.0	TR28 - SECOND EFFECT, STEAM CONDENSATE BEFORE COOLER

-16284	90.4	TR 1 - CONDENSER, COOLING WATER LEAVING.
-16283	90.4	TR30 - RUN DOWN TANK, COOLING WATER LEAVING.
-16282	90.1	TR31 - RUN DOWN TANK, LIQUID LEAVING.
-16281	86.0	TR11 - CONDENSER, CONDENSATE LEAVING.

(d) Computer printout from program HMBAL

15 APR 75  
15/28 HRS

ERROR OF CLOSURE  
INPUT-OUTPUT (PERCENTAGE)

## OVERALL BALANCES

TOTAL MASS BALANCE	0.177	LB/MIN	( 3.94 )
COMPONENT MASS BALANCE	-0.003	LB/MIN	( 2.29 )
HEAT BALANCE	0.120E 03	BTU/MIN	( 4.99 )

## FIRST EFFECT BALANCES

TOTAL MASS BALANCE	-0.216	LB/MIN	( -4.66 )
--------------------	--------	--------	-----------

## SECOND EFFECT AND CONDENSER BALANCES

TOTAL MASS BALANCE	0.387	LB/MIN	( 2.24 )
--------------------	-------	--------	----------